Augusto Akio Lucchezi Miyahara

Impactos do clima e da poluição do ar no desenvolvimento de árvores de *Tipuana tipu* (Benth.) Kuntze em diferentes tipologias urbanas.

Tese apresentada ao Instituto de Pesquisas Ambientais da Secretaria do Meio Ambiente, Infraestrutura e Logística, como parte dos requisitos exigidos para a obtenção do título de DOUTOR em BIODIVERSIDADE VEGETAL E MEIO AMBIENTE, na Área de Concentração de Plantas Vasculares em Análises Ambientais.

São Paulo

2025

Augusto Akio Lucchezi Miyahara

Impactos do clima e da poluição do ar no desenvolvimento de árvores de *Tipuana tipu* (Benth.) Kuntze em diferentes tipologias urbanas.

Tese apresentada ao Instituto de Pesquisas Ambientais da Secretaria do Meio Ambiente, Infraestrutura e Logística, como parte dos requisitos exigidos para a obtenção do título de DOUTOR em BIODIVERSIDADE VEGETAL E MEIO AMBIENTE, na Área de Concentração de Plantas Vasculares em Análises Ambientais.

São Paulo
2025

Augusto Akio Lucchezi Miyahara

Impactos do clima e da poluição do ar no desenvolvimento de árvores de *Tipuana tipu* (Benth.) Kuntze em diferentes tipologias urbanas.

Tese apresentada ao Instituto de Pesquisas Ambientais da Secretaria do Meio Ambiente, Infraestrutura e Logística, como parte dos requisitos exigidos para a obtenção do título de DOUTOR em BIODIVERSIDADE VEGETAL E MEIO AMBIENTE, na Área de Concentração de Plantas Vasculares em Análises Ambientais.

ORIENTADOR: DR. GIULIANO MASELLI LOCOSSELLI

CO-ORIENTADORA: DRA. MILENA GODOY-VEIGA

Ficha Catalográfica elaborada pelo SBMMAAI do Instituto de Pesquisas Ambientais

Miyahara, Augusto Akio Lucchezi
M677 Impactos do clima e da poluição do ar no desenvolvimento de árvore de Tipuana tipu (Benth.) Kuntze em diferentes tipologias urbanas / Augusto Akio Lucchezi Miyahara. - São Paulo, 2025

224.; il.

Tese (Doutorado) -- Instituto de Pesquisas Ambientais da Secretaria de Meio Ambiente, Infraestrutura e Logística, 2025.
.
Orientador: Giuliano Maselli Locosselli

Bibliografia.

1. Soluções baseadas na natureza. 2. Dendrocronologia. 3. Árvores urbanas. I. Título.

CDU: 551.6

Bibliotecária Arlete Alves Ferreira CRB-8/7646

BANCA EXAMINADORA

Dr. Giuliano Maselli Locosselli (Orientador)
Centro de Energia Nuclear em Agricultura - Universidade de São Paulo (CENA-USP)

Dra. Marisa Domingos
Núcleo de Ecologia - Instituto de Pesquisas Ambientais (NE-IPA)

Dr. Bruno Barçante Ladvocat Cintra
Birmingham Institute of Forest Research - University of Birmingham (BIFoR-UoB)

Dra. Aline Andréia Cavalari Corete
Departamento de Ecologia e Biologia Evolutiva - Universidade Federal do Estado de São Paulo (DEBE-UNIFESP)

Dra. Fernanda Mendes de Rezende
Instituto de Biociências - Universidade de São Paulo (IB-USP)

Aos meus pais, cujo amor e apoio foram fundamentais em minha trajetória.
Ao meu filho, que ilumina meu caminho e é minha principal fonte de alegria.
Aos meus amigos, cuja amizade sincera me fortaleceu em momentos desafiadores.

Ao estudar os anéis de crescimento das árvores, revelamos não apenas sua história, mas também a conexão que construímos com elas ao longo da pesquisa.

Agradecimentos

Agradeço ao Programa de Pós-Graduação em Biodiversidade Vegetal e Meio Ambiente do Instituto de Pesquisas Ambientais (IPA), por sediar o presente projeto de doutorado. À Coordenação de Aperfeiçoamento de Pessoal de Nível Superior (CAPES), pela concessão da bolsa de doutorado do Programa Nacional de Apoio e Desenvolvimento da Botânica (PNADB), que permitiu a execução do presente projeto. À CAPES, pela concessão da verba do Programa de Apoio à Pós-Graduação (PROAP), que permitiu a realização de trabalhos de campo e a participação em congressos. À Fundação de Amparo à Pesquisa do Estado de São Paulo (FAPESP), por financiar o Projeto Jovem Pesquisador intitulado "Florestas Funcionais", que abrigou a presente tese, e possibilitou a construção de uma rede internacional de pesquisadores de árvores urbanas, além de proporcionar os recursos para a extração de celulose e análise interanual de isótopos estáveis. À CAPES, pela concessão da bolsa do Programa de Doutorado-sanduíche no Exterior (PDSE), que promoveu a troca de experiências com pesquisadores estrangeiros, além do contato com a metodologia de última geração para a análise intra-anual em alta resolução de isótopos estáveis, por ablação a laser.

Agradeço ao orientador, Dr. Giuliano Maselli Locosselli, pelo excelente trabalho e dedicação à liderança da equipe de pesquisa, e por guiar o presente projeto de doutorado do início ao fim. Por estar sempre presente e disponível para direcionar, desde a coleta de amostras e análises em laboratório, até a interpretação dos resultados, redação de manuscritos e publicação de artigos em periódicos internacionais renomados. Inclusive, por propiciar o aprendizado em colaborações com pesquisadores de referência na área de pesquisa do presente projeto, tornando este estudo relevante na comunidade científica. Agradeço à co-orientadora, Dra. Milena Godoy-Veiga, que acompanhou de perto a execução deste projeto e cuja contribuição foi essencial para enriquecer e fortalecer o trabalho do orientador. Agradeço ao Dr. Marcos Silveira Buckeridge, pesquisador referência em botânica, que abriu as portas e incentivou a execução desse projeto ao indicar o Dr. Giuliano como orientador.

Agradeço aos colegas de Pós-graduação, Leticia Figueiredo Candido, Matheus Casarini Siqueira, Polari Batista Corrêa, e Ricardo Reale, pelo trabalho em equipe e por todas as experiências, que fortaleceram tanto as relações profissionais como pessoais.

Agradeço à Dra. Inês Cordeiro, que coordenou com excelência o Programa de Pós-Graduação em Biodiversidade Vegetal e Meio Ambiente do IPA durante a execução do presente projeto, e sempre se manteve acessível para sanar dúvidas e fornecer informações sobre os regimentos e normas do programa, garantindo o andamento desta pesquisa. Agradeço à Shirlei e à Iolane, do Departamento de Gestão do Conhecimento do Núcleo de Pós-Graduação do IPA, pelo suporte

à Dra. Inês e à equipe de pesquisa do presente projeto. Agradeço a todo o corpo docente, pela excelência em pesquisa e por todas as disciplinas ofertadas.

Agradeço à Secretaria do Verde e Meio Ambiente da Cidade de São Paulo, em especial Priscilla Cerqueira, Deborah Schmidt Neves dos Santos e Cyra Malta Olegario da Costa, por fortalecerem o presente projeto de pesquisa e apoiarem as coletas de amostras de madeira na Cidade de São Paulo.

Agradeço ao Dr. Marcos Silveira Buckerigde, da Universidade de São Paulo, por possibilitar a execução do estudo do Capítulo 1 da presente tese. Ao Dr. Paulo Renato Mesquita Pellegrino, da Universidade de São Paulo, por conectar a equipe de arquitetos e urbanistas ao estudo deste Capítulo. Ao Dr. Carlos Alberto da Silva Filho, da Secretaria do Verde e Meio Ambiente da Cidade de São Paulo, por representar o poder público do Município de São Paulo no estudo do Capítulo 1 desta tese. Ao Dr. Tom Wild, da Universidade de Sheffield, por trazer excelência em Soluções Baseadas na Natureza ao estudo do Capítulo 1. Agradeço ao GeoSampa, da Secretaria Municipal de Urbanismo e Licenciamento de São Paulo, e ao Centro de Gerenciamento de Emergências Climáticas (CGE) da Prefeitura de São Paulo, por disponibilizarem dados essenciais ao estudo dos Capítulos 1 e 4 desta tese.

Agradeço à Dra. Cristina Nabais, da Universidade de Coimbra, por coordenar o congresso Tree Rings in Archaeology, Climatology and Ecology (TRACE) 2023, onde foi apresentado o estudo do Capítulo 2 da presente tese.

Agradeço à Ana Julia Francisco, do Departamento de Arborização Urbana do Município de Lisboa, por auxiliar nas permissões para a coleta de amostras de madeira na Cidade de Lisboa e trazer as demandas do poder público em Soluções Baseadas na Natureza, permitindo a idealização do estudo do Capítulo 3 da presente tese. À Dra. Ana Paula Ramos e à pesquisadora Fillipa Maia, da Universidade de Lisboa, pela recepção e suporte aos trabalhos de campo em Lisboa, além da obtenção de outros dados complementares para o estudo do Capítulo 3 da presente tese. À Dra. Laia Andreu-Hayles, do Centro de Pesquisa Ecológica e Aplicações Florestais de Barcelona (CREAF), por trazer excelência em anéis de crescimento da madeira ao estudo do Capítulo 3 desta tese, além do apoio em trabalhos de campo em Barcelona, junto com a Dra. Clara Rodríguez-Morata (CREAF), para a coleta de amostras de madeira e contribuição na construção da rede internacional de pesquisadores de árvores urbanas. Ao Dr. Francisco J. Escobedo, do Departamento de Agricultura e Serviço Florestal dos Estados Unidos, por trazer excelência em arborização urbana ao estudo do Capítulo 3 da presente tese, além do apoio em trabalhos de campo em Los Angeles para a coleta de amostras, e contribuição na construção da rede internacional de pesquisadores de árvores urbanas. À pesquisadora Giulia

Nunes de Aguiar Souto, da Universidade de São Paulo, por colaborar com o tratamento e análise de amostras para o estudo do Capítulo 3 desta tese, e das amostras das outras cidades. Ao Dr. Mário Tomazello Filho, da Universidade de São Paulo, que colaborou com os estudos dos Capítulos 3 e 4 desta tese ao disponibilizar o laboratório para a análise de densidade da madeira. À doutoranda Gabriela Morais Olmedo, da Universidade de São Paulo, pelo suporte em laboratório para a análise de densidade da madeira para os estudos dos Capítulos 3 e 4. Ao Dr. William Francisco da Cruz Júnior, da Universidade de São Paulo, que colaborou com o estudo do Capítulo 3 desta tese ao disponibilizar o laboratório para a análise de isótopos estáveis. À técnica Natália da Silva Santos, da Universidade de São Paulo, pelo suporte em laboratório para a análise de isótopos estáveis para o estudo do Capítulo 3.

Agradeço ao Dr. Ariel Andrés Muñoz Navarro, da Pontifícia Universidade Católica de Valparaíso do Chile, por aceitar ser o co-orientador no exterior e possibilitar a execução do PDSE do presente projeto, além de colaborar com as análises de isótopos estáveis em alta resolução por ablação a laser para o estudo do Capítulo 4 da presente tese. Ao Dr. Francisco Javier Fernandoy Pedreros, da Universidade Adrés Bello de Viña del Mar, por disponibilizar o laboratório para a análise de isótopos estáveis por ablação à laser para o estudo do Capítulo 4 desta tese. Ao técnico Sebastián Alfredo Godoy Nuñez, da Pontifícia Universidade Católica de Valparaíso do Chile, pela recepção e suporte com as análises por ablação a laser para o estudo do Capítulo 4, além do auxílio na obtenção das permissões e trabalho de campo para a coleta de amostras de madeira em Santiago do Chile para a rede internacional de pesquisadores de arborização urbana. Ao técnico Luis Ignacio Muñoz Gaete e sua colega Francisca, da Universidade Andrés Bello de Viña del Mar, pelo suporte com as análises por ablação a laser e os cálculos de pós-processamento dos dados para o estudo do Capítulo 4 desta tese. À Companhia Ambiental do Estado de São Paulo (CETESB), por disponibilizar os dados de poluição do ar do município de São Paulo, que foi essencial para o estudo do Capítulo 4.

Agradeço ao Dr. Gregório Cardoso Tápias Ceccantini, da Universidade de São Paulo, por disponibilizar a xiloteca para a preparação das amostras de madeira. Ao Dr. Plínio Barbosa de Camargo, da Universidade de São Paulo, por disponibilizar espaço e ferramentas para preparação das amostras, e o laboratório para pesar e encapsular as amostras de celulose para a análise de isótopos estáveis. Agradeço ao Dr. Bruno Barcante Ladvocat Cintra, da Universidade de Birmingham, por disponibilizar o protocolo detalhado do método de extração de celulose, possibilitando a preservação das estruturas anatômicas dos anéis de crescimento nas amostras e, consequentemente, o sucesso em análises de isótopos estáveis por ablação a laser.

Agradeço a todas as pessoas que valorizam o papel das árvores urbanas e se dedicam à proteção do meio ambiente, representando a sociedade civil no desenvolvimento desta tese.

Agradeço ao meu filho, meus pais, e amigos, por estarem sempre comigo nessa jornada trazendo alegria e força.

RESUMO

A urbanização crescente vem intensificando os impactos das mudanças climáticas globais, pois é um processo diretamente associado à remoção da vegetação, à impermeabilização do solo e ao aumento das emissões de gases poluentes. Nesse contexto, as árvores urbanas desempenham um papel fundamental na promoção da resiliência climática e na provisão de serviços ecossistêmicos. No entanto, os ambientes urbanos impõem desafios específicos ao desenvolvimento das árvores, exigindo estratégias com embasamento técnico e científico para a implementação e o manejo das infraestruturas verdes. Esta tese investigou diferentes aspectos das soluções baseadas na natureza em ambientes urbanos, com ênfase no papel das árvores como elementos-chave para adaptar as cidades frente às mudanças climáticas globais. No primeiro capítulo, foi desenvolvido um modelo de classificação de "biomas urbanos", baseado em dados de clima e vegetação, com o objetivo de associar a heterogeneidade ambiental da cidade de São Paulo aos biomas naturais brasileiros mais semelhantes a cada região do município. Essa proposta visou fornecer embasamento teórico para apoiar as tomadas de decisões relacionadas à seleção de espécies vegetais mais compatíveis com as características específicas de cada microambiente urbano. O segundo capítulo teve como foco a dendrocronologia, o estudo dos anéis de crescimento da madeira, e seu uso como ferramenta para investigar o desenvolvimento e as respostas fisiológicas das árvores, contribuindo com subsídios teóricos para a implementação e manejo de infraestruturas verdes urbanas. Neste capítulo, foi conduzida uma revisão sistemática sobre o uso de isótopos estáveis em análises intra-anuais de anéis de crescimento, com o intuito de identificar o estado da arte dessa abordagem na dendrocronologia e discutir seu potencial para aplicações, inclusive em contextos urbanos. No terceiro capítulo, a dendrocronologia foi aplicada com o intuito de gerar conhecimento empírico a partir de um cenário urbano real. Foi conduzida uma abordagem *multiproxy* dos anéis de crescimento – incluindo medidas de largura, densidade e assinaturas isotópicas de carbono ($\delta^{13}C$) e oxigênio ($\delta^{18}O$) – para avaliar os efeitos da irrigação no crescimento de árvores urbanas da espécie *Tipuana tipu* (Benth.) Kuntze em uma praça central de Lisboa, Portugal. As árvores irrigadas dobraram sua taxa de crescimento, sem comprometer significativamente a resistência da madeira, destacando a condutância estomática como principal fator limitante ao crescimento. Este estudo atendeu às demandas do poder público para tomar decisões sobre práticas de manejo e implementação de infraestruturas verdes urbanas eficazes. O quarto capítulo apresenta um estudo aplicado de dendrocronologia, com uma abordagem *multiproxy* intra-anual focada em isótopos estáveis de carbono e densidade da madeira. Este estudo se baseou no conhecimento desenvolvido no segundo capítulo e aplicou a

técnica de ablação a laser para a análise de $\delta^{13}C$, superando limitações técnicas na escala intra-anual. O objetivo foi avaliar se os sinais de redução da poluição atmosférica durante os períodos de distanciamento social (*lockdowns*) impostos pela pandemia do COVID-19 foram registrados nos anéis de crescimento de árvores urbanas. A redução de $^{12}CO_2$ atmosférico levou a um aumento significativo no $\delta^{13}C$ dos segmentos intra-anuais formados durante o *lockdown*. Por outro lado, os efeitos no crescimento não foram evidentes, mas a densidade da madeira nos segmentos intra-anuais formados durante este período indica um ajuste na eficiência do uso da água em resposta às menores concentrações de CO_2 atmosférico. Em conjunto, os quatro estudos desta tese buscaram construir conhecimento para fortalecer a base científica voltada à implementação e ao manejo de soluções baseadas na natureza em contextos urbanos, investigando a apropriação dos métodos, e considerando tanto as condições ambientais quanto os mecanismos fisiológicos que influenciam a performance das árvores.

Palavras-chave: Soluções baseadas na natureza; dendrocronologia; isótopos estáveis; *Tipuana tipu*; árvores urbanas.

ABSTRACT

The ongoing process of urbanization has been exacerbating the impacts of global climate change, as it is directly associated with vegetation removal, soil sealing, and increased emissions of air pollutants. In this context, urban trees play a critical role in enhancing climate resilience and providing ecosystem services. However, urban environments pose specific challenges to tree development, requiring strategies grounded in technical and scientific knowledge for the implementation and management of green infrastructure. This dissertation investigated different aspects of nature-based solutions in urban settings, with an emphasis on the role of trees as key elements in supporting urban adaptation to global climate change. In the first chapter, an "urban biome" classification model was developed based on climate and vegetation data, aiming to associate the environmental heterogeneity of São Paulo with the Brazilian natural biomes that most closely resemble each region of the city. This approach was intended to provide theoretical foundations to support decision-making processes related to the selection of plant species that are better suited to the specific characteristics of each urban microenvironment. The second chapter focused on dendrochronology, the study of tree-ring formation in wood and its use as a tool to investigate tree development and physiological responses, thereby contributing theoretical support for the implementation and management of urban green infrastructure. A systematic review was conducted on the use of stable isotopes in intra-annual tree-ring analyses, aiming to identify the state of the art of this approach in dendrochronology and discuss its potential for application, including in urban contexts. In the third chapter, dendrochronology was applied to generate empirical knowledge from a real urban scenario. A multiproxy tree-ring approach – including measurements of ring width, wood density, and stable carbon ($\delta^{13}C$) and oxygen ($\delta^{18}O$) isotopic signatures – was conducted to assess the effects of irrigation on the growth of *Tipuana tipu* (Benth.) Kuntze trees in a central square in Lisbon, Portugal. Irrigated trees doubled their growth rate without significantly compromising wood strength, highlighting stomatal conductance as the main limiting factor for tree growth. This study met the demands of local authorities for decision-making regarding management practices and the implementation of effective urban green infrastructure. The fourth chapter presents an applied dendrochronological study using an intra-annual multiproxy approach focused on stable carbon isotopes and wood density. This study builds upon the knowledge developed in the second chapter and applies the laser ablation technique for $\delta^{13}C$ analysis, overcoming technical limitations at the intra-annual scale. The objective was to assess whether the signals of reduced air pollution during the COVID-19 lockdown periods were recorded in the growth rings of urban trees. The reduction in atmospheric $^{12}CO_2$ led to a significant increase of $\delta^{13}C$ in the intra-annual tree-ring segments formed during the lockdown.

Although the effects on growth are not evident, the wood density of the intra-annual segments formed during this period indicates an adjustment in water use efficiency in response to lower atmospheric CO_2 concentrations. Together, the four studies presented in this thesis aimed to build knowledge to strengthen the scientific basis for the implementation and management of nature-based solutions in urban contexts, by investigating the applicability of methods and considering both environmental conditions and physiological mechanisms that influence tree performance.

Keywords: Nature based solutions; dendrochronology; stable isotopes; *Tipuana tipu*; urban trees.

Lista de figuras

Capítulo 1

Capítulo 2

Capítulo 3

Capítulo 4

Lista de tabelas

Capítulo 1

Capítulo 2

Capítulo 3

Capítulo 4

SUMÁRIO

Introdução geral

Segundo dados da Organização das Nações Unidas (2019), mais da metade da população mundial vive atualmente em cidades, e as projeções indicam que esse número pode alcançar dois terços da população global até 2050 (Lee et al., 2023). Esse aumento populacional impulsiona significativamente os processos de urbanização, os quais estão diretamente associados à remoção da vegetação, à emissão de gases do efeito estufa e poluentes, à impermeabilização do solo e à alteração dos ciclos biogeoquímicos como do carbono e da água (Gong et al., 2020; Kaushal et al., 2014; Maher et al., 2013; Seto et al., 2011; Tiotiu et al., 2020). Consequentemente, a urbanização é um dos principais epicentros das mudanças climáticas globais atuais, impactando negativamente a qualidade de vida de bilhões de pessoas (Fletcher et al., 2024). Como uma alternativa ao ambiente urbano hostil, as soluções baseadas na natureza (SBN), que utilizam elementos "inspirados, apoiados, ou copiados da natureza" para enfrentar problemas ambientais, sociais e econômicos (Krull et al., 2015), têm se difundido e ganhado destaque entre os tomadores de decisões nas cidades.

Entretanto, estas alterações nas condições ambientais afetam diretamente o desenvolvimento das árvores, parte central das SBN, gerando limitações fisiológicas como a redução da condutância estomática e da fotossíntese (Fini et al., 2022; López et al., 2021; Matsumoto et al., 2022). Tais limitações comprometem o funcionamento e o desenvolvimento das árvores, as quais representam uma das principais ferramentas naturais para a promoção dos serviços ecossistêmicos e para o fortalecimento da resiliência urbana frente às mudanças climáticas globais (Elmqvist et al., 2015; Horvath et al., 2016; Kong et al., 2021). Ambientes urbanos são significativamente heterogêneos (Cadenasso et al., 2007) e diferem significativamente dos ambientes naturais de origem das árvores (Grimm et al., 2008), condições que representam um desafio ao desenvolvimento arbóreo. A exposição à altas concentrações de poluentes atmosféricos, as ilhas de calor, eventos extremos de temperatura e escassez hídrica, bem como a competição por espaço com infraestruturas urbanas, são exemplos desses desafios (Bieller, 1992; Gesualdo et al., 2019; Kendal et al., 2018; Locosselli et al., 2019). Portanto, ao plantar árvores nas cidades, é imprescindível selecionar as espécies mais adequadas, de modo que se desenvolvam e ofereçam os serviços ecossistêmicos à população, tais como o sequestro de carbono atmosférico, o conforto térmico, a redução do calor latente, a interceptação de poluentes atmosféricos, e o contato com a biodiversidade (Daba & Dejene, 2018; Escobedo et al., 2011; Lafortezza & Chen, 2016; Niemelä, 1999; Swaffield & McWilliam, 2013; Wei et al., 2021). Entre os principais debates sobre a seleção de espécies arbóreas para ambientes urbanos,

destaca-se a dicotomia entre espécies nativas e exóticas (Schlaepfer, 2018). Considerar a adequação das espécies aos locais de plantio é fundamental para o sucesso das políticas de arborização urbana, que visam implementar soluções baseadas na natureza eficazes.

Garantir o desenvolvimento apropriado das espécies arbóreas na heterogeneidade urbana é fundamental para a provisão de serviços ecossistêmicos, os quais estão diretamente relacionados ao seu crescimento e performance (Thomas et al., 2021). Existem diversos métodos para investigar o desenvolvimento das árvores, entre os quais a dendrocronologia, que é o estudo dos anéis de crescimento formados na madeira, se destaca como uma ferramenta valiosa para avaliar retrospectivamente a performance da árvore diante das condições ambientais (Fritts, 1971; McGinnies, 1963). A análise de diversos parâmetros dos anéis de crescimento (também conhecida como *multiproxy*) permite reconstruir o desenvolvimento passado das árvores, correlacionando-o com as condições ambientais do local e do período de formação de cada anel (Ortega Rodriguez et al., 2023; Römer et al., 2023). Além disso, aplicações da dendrocronologia em ambientes urbanos já demonstraram eficácia na geração de conhecimento e no suporte à tomadas de decisões nas cidades, por exemplo, no manejo de árvores, na avaliação de respostas à poluição ambiental, e na análise de riscos associados a condições climáticas (Miyahara et al., 2022).

Ainda dentro da abordagem *multiproxy* destacam-se os estudos da assinatura de isótopos estáveis de carbono ($\delta^{13}C$) e oxigênio ($\delta^{18}O$), por fornecerem informações sobre os impactos ambientais nos mecanismos fisiológicos associados ao crescimento (Gessler et al., 2014; Hartl-Meier et al., 2015; Miyahara & Locosselli, 2024; Treydte et al., 2014). As plantas C_3 discriminam os isótopos estáveis de carbono por meio da difusão do CO_2 pelos estômatos e por meio da afinidade da enzima rubisco, ambos os processos favorecendo a fixação do ^{12}C em detrimento do ^{13}C (McCarroll & Loader, 2004). De modo semelhante, os isótopos estáveis de oxigênio são discriminados com base na assinatura isotópica da água fonte, e por evapotranspiração preferencial de moléculas de água contendo ^{16}O, resultando no enriquecimento de ^{18}O nos tecidos vegetais (McCarroll & Loader, 2004). Compreender não apenas como as árvores respondem a determinado ambiente, mas também quais mecanismos fisiológicos estão associados a essas respostas – como condutância estomática e assimilação de carbono – apresenta potencial significativo para apoiar decisões mais eficientes relacionadas à implementação e ao manejo de infraestruturas verdes nas cidades (Locosselli et al., 2020, 2024; Miyahara et al., 2022).

Uma análise dendrocronológica *multiproxy* pode ser aplicada com a finalidade de gerar conhecimento empírico em cenários urbanos reais para atender às demandas do poder público.

Um problema recorrente para as árvores urbanas é o acesso das raízes à água subterrânea (Cregg, 1995; Smith et al., 2024), principalmente devido à impermeabilização e compactação do solo urbano (Bouma, 1991; Mullaney et al., 2015). Uma prática de manejo consolidada e amplamente adotada é a irrigação, cujo objetivo é promover o desenvolvimento adequado da vegetação exposta a condições não naturais (Gimpel et al., 2021; Livesley et al., 2021; Rambhia et al., 2023; Vico et al., 2014). A irrigação favorece a manutenção do sistema hidráulico da madeira, promovendo a evapotranspiração e a assimilação de carbono (Ibsen et al., 2023; López et al., 2021; Luketich et al., 2019), auxiliando no desenvolvimento das árvores e na provisão de serviços ecossistêmicos (Dobbertin et al., 2010; Vessella et al., 2010; Xi et al., 2021). Apesar de diversas evidências demonstrarem os benefícios da irrigação para o crescimento arbóreo, também há registros de redução na densidade da madeira associada a crescimentos acelerados (Arsić et al., 2021; Medina et al., 2024; Wimmer & Downes, 2003). Essa redução na densidade pode tornar as árvores mais suscetíveis a falhas mecânicas e infestações por patógenos (Larjavaara & Muller-Landau, 2010; Martinez-Meier et al., 2008; Niklas & Spatz, 2010; van Duong et al., 2023). Estudos dendrocronológicos com análises de diferentes parâmetros – como largura, densidade, e assinaturas isotópicas – ao comparar períodos anteriores e posteriores ao início da irrigação, permitem compreender os impactos da irrigação a fim de gerar evidências sobre seus efeitos nas árvores.

Outro fator potencial que afeta o desenvolvimento das árvores nas cidades é a emissão de poluentes atmosféricos. Há evidências na literatura de diversos efeitos desses poluentes no crescimento das árvores (Winner & Atkinson, 1986), incluindo reduções de crescimento de até 30% (Locosselli et al., 2019). Grande parte do conhecimento sobre os impactos do aumento da concentração de poluentes no ar urbano está relacionada a mudanças de longo prazo (Pozzer et al., 2023), enquanto pouco se sabe sobre os efeitos de variações abruptas nessas concentrações. Alterações rápidas na composição atmosférica normalmente estão associadas a desastres ambientais, mas recentemente, cidades ao redor do mundo passaram por uma experiência sem precedentes: a redução temporária das emissões de poluentes em decorrência das medidas restritivas (*lockdowns*) adotadas para conter o avanço da pandemia de COVID-19 (Sannigrahi et al., 2021). Essas alterações pontuais na concentração de poluentes dificilmente são detectadas em estudos dendrocronológicos de resolução anual (Camarero et al., 2025). No entanto, a dendrocronologia, além de possibilitar reconstruções anuais – já que os anéis de crescimento são formados uma vez por ano – também permite análises intra-anuais, nas quais cada anel pode ser subdividido em diferentes segmentos, possibilitando compreender como o desenvolvimento da árvore variou ao longo do mesmo ano (Helle & Schleser, 2004; Monson et al., 2018). Entender como os poluentes atmosféricos afetam o crescimento das árvores é de grande

interesse para os tomadores de decisão, visto que as florestas urbanas são consideradas soluções baseadas na natureza para mitigar a poluição do ar nas cidades, dado o seu potencial de absorver e acumular material particulado (Monaci & Baroni, 2025; Wang et al., 2024).

Na presente tese, foi explorado o tema das soluções baseadas na natureza, amplamente estudado e cada vez mais presente nas tomadas de decisões em cidades, como estratégia para mitigar os efeitos das mudanças climáticas globais. No primeiro capítulo, foi conduzido um estudo com base em dados secundários de clima e vegetação para desenvolver um modelo de classificação de "biomas urbanos", utilizando o município de São Paulo como estudo de caso. Partindo da premissa de que ambientes urbanos são heterogêneos, buscou-se associar as diferentes condições ambientais encontradas na cidade aos biomas naturais mais semelhantes, com o objetivo de utilizá-los como critério na seleção de espécies vegetais para a implementação de infraestruturas verdes na cidade. No segundo capítulo, foi realizada uma revisão sistemática sobre dendrocronologia, com foco em análises intra-anuais de isótopos estáveis. O objetivo deste estudo foi compilar os trabalhos científicos com essa abordagem, a fim de verificar o estado da arte nesse campo da dendrocronologia e propor perspectivas para suas aplicações, incluindo aquelas de interesse desta tese. No terceiro capítulo, foi conduzido um estudo prático de dendrocronologia em parceria com a Câmara Municipal de Lisboa, com o intuito de aplicar esse conhecimento para dar suporte às decisões sobre o manejo de infraestruturas verdes, mais especificamente sobre a implementação de irrigação em árvores da espécie *Tipuana tipu* (Benth.) Kuntze, localizadas na Praça Duque de Saldanha, no centro urbano de Lisboa. No quarto capítulo, foi desenvolvido um estudo de dendrocronologia com análise intra-anual de alta resolução de densidade da madeira, e isótopos estáveis de carbono por ablação a laser. Esta análise de isótopos envolve uma tecnologia de ponta altamente sofisticada, identificada na revisão sistemática do segundo capítulo como a mais promissora para superar as limitações envolvendo a grande quantidade de amostras intra-anuais e o número de anéis de crescimento a serem analisados. O objetivo deste quarto capítulo foi avaliar a possibilidade de identificar alterações no funcionamento de árvores urbanas em resposta às variações na concentração de poluentes atmosféricos na cidade de São Paulo, durante os eventos de restrição de atividades (*lockdowns*) implementados para conter a pandemia do COVID-19. Os *lockdown* que coincidiram com as estações de crescimento das árvores – período em que se formam os anéis – tiveram duração relativamente curta, limitada a poucas semanas. Nesse contexto, a análise de isótopos de carbono por ablação a laser apresentou-se como a melhor ferramenta, por oferecer a resolução espacial necessária para detectar possíveis sinais dos efeitos ambientais dos *lockdowns* nos anéis de crescimento.

Objetivos gerais

A presente tese teve como objetivo principal contribuir com o avanço do conhecimento científico e prático relacionado às soluções baseadas na natureza em ambientes urbanos, com foco no papel das árvores para a mitigação dos efeitos das mudanças climáticas globais e na promoção de resiliência urbana. Para isso, foram desenvolvidos quatro estudos complementares com os seguintes destaques:

- Classificar as condições de clima e vegetação da cidade de São Paulo para identificar quais biomas naturais brasileiros mais se assemelham às características observadas na cidade; criar um modelo de classificação dos biomas urbanos da cidade estudada, para oferecer apoio ao poder público para implementar soluções baseadas na natureza.
- Realizar uma revisão sistemática da literatura voltada à análise intra-anual de isótopos estáveis em anéis de crescimento da madeira, uma ferramenta promissora para as tomadas de decisões sobre soluções baseadas na natureza, visando: compreender o estado da arte desta abordagem; mapear suas limitações e avanços; propor perspectivas futuras.
- Utilizar a dendrocronologia como ferramenta para atender às demandas do poder público em manejo de infraestruturas verdes urbanas, trazendo evidências sobre as práticas de manejo relacionadas à irrigação, e respostas sobre seus efeitos no funcionamento e desenvolvimento de árvores urbanas.
- Avaliar o potencial da análise intra-anual de alta resolução de densidade da madeira por Raio-X, associada à análise de isótopos estáveis de carbono por ablação a laser para detectar alterações no funcionamento de árvores urbanas em resposta à redução da poluição atmosférica durante eventos de curta duração, como os *lockdowns* durante a pandemia d COVID-19 com comprovada redução na poluição do ar.

Bibliografia

Arsić, J., Stojanović, M., Petrovičová, L., Noyer, E., Milanović, S., Světlík, J., Horáček. P., & Krejza, J. (2021). Increased wood biomass growth is associated with lower wood density in *Quercus petraea* (Matt.) Liebl. saplings growing under elevated CO_2. *PloS One*, 16(10).

Bieller, J. A. (1992). Utility and Municipal Competition for Space in the Urban Environment. *Arboriculture & Urban Forestry*, *18*(2), 76–78.

Bouma, J. (1991). Influence of Soil Macroporosity on Environmental Quality. In D. L. Sparks (Ed.), *Advances in Agronomy* (46), 1–37.

Cadenasso, M. L., Pickett, S. T. A., & Schwarz, K. (2007). Spatial heterogeneity in urban ecosystems: Reconceptualizing land cover and a framework for classification. *Frontiers in Ecology and the Environment*, *5*(2), 80–88.

Camarero, J. J., Rubio-Cuadrado, Á., de Andrés, E. G., Valeriano, C., Sánchez, P., & Querejeta, J. I. (2025). A tale of two cities: Impacts of the COVID-19 lockdown on growth and wood chemistry of urban trees. *Science of The Total Environment*, 974, 179252.

Cregg, B. (1995). Plant moisture stress of green ash trees in contrasting urban sites. *Arboriculture & Urban Forestry*, 21(6), 271–276.

Daba, M. H., & Dejene, S. W. (2018). The role of biodiversity and ecosystem services in carbon sequestration and its implication for climate change mitigation. *Environmental Sciences and Natural Resources*, 11(2), 1–10.

Dobbertin, M., Eilmann, B., Bleuler, P., Giuggiola, A., Graf Pannatier, E., Landolt, W., Schleppi, P., & Rigling, A. (2010). Effect of irrigation on needle morphology, shoot and stem growth in a drought-exposed *Pinus sylvestris* forest. *Tree Physiology*, *30*(3), 346–360.

Elmqvist, T., Setälä, H., Handel, S., van der Ploeg, S., Aronson, J., Blignaut, J., Gómez-Baggethun, E., Nowak, D., Kronenberg, J., & de Groot, R. (2015). Benefits of restoring ecosystem services in urban areas. *Current Opinion in Environmental Sustainability*, *14*, 101–108.

Escobedo, F. J., Kroeger, T., & Wagner, J. E. (2011). Urban forests and pollution mitigation: Analyzing ecosystem services and disservices. *Environmental Pollution*, *159*(8–9), 2078–2087.

Fini, A., Frangi, P., Comin, S., Vigevani, I., Rettori, A. A., Brunetti, C., Moura, B. B., & Ferrini, F. (2022). Effects of pavements on established urban trees: Growth, physiology, ecosystem services and disservices. *Landscape and Urban Planning*, *226*, 104501.

Fletcher, C., Ripple, W. J., Newsome, T., Barnard, P., Beamer, K., Behl, A., Bowen, J., Cooney, M., Crist, E., Field, C., Hiser, K., Karl, D. M., King, D. A., Mann, M. E., McGregor, D. P., Mora, C., Oreskes, N., & Wilson, M. (2024). Earth at risk: An urgent call to end the age of destruction and forge a just and sustainable future. *PNAS Nexus*, *3*(4), 106.

Fritts, H. C. (1971). Dendroclimatology and dendroecology. *Quaternary Research*, 1(4), 419–449.

Gessler, A., Ferrio, J. P., Hommel, R., Treydte, K., Werner, R. A., & Monson, R. K. (2014). Stable isotopes in tree rings: Towards a mechanistic understanding of isotope fractionation and mixing processes from the leaves to the wood. *Tree Physiology*, *34*(8), 796–818.

Gesualdo, G. C., Oliveira, P. T., Rodrigues, D. B. B., & Gupta, H. V. (2019). Assessing water security in the São Paulo metropolitan region under projected climate change. *Hydrology and Earth System Sciences*, *23*(12), 4955–4968.

Gimpel, H., Graf-Drasch, V., Hawlitschek, F., & Neumeier, K. (2021). Designing smart and sustainable irrigation: A case study. *Journal of Cleaner Production*, *315*, 128048.

Gong, P., Li, X., Wang, J., Bai, Y., Chen, B., Hu, T., Liu, X., Xu, B., Yang, J., Zhang, W., & Zhou, Y. (2020). Annual maps of global artificial impervious area (GAIA) between 1985 and 2018. *Remote Sensing of Environment*, *236*, 111510.

Grimm, N. B., Faeth, S. H., Golubiewski, N. E., Redman, C. L., Wu, J., Bai, X., & Briggs, J. M. (2008). Global change and the ecology of cities. *Science*, *319*(5864), 756–760.

Hartl-Meier, C., Zang, C., Büntgen, U., Esper, J., Rothe, A., Göttlein, A., Dirnböck, T., & Treydte, K. (2015). Uniform climate sensitivity in tree-ring stable isotopes across species and sites in a mid-latitude temperate forest. *Tree Physiology*, *35*(1), 4–15.

Helle, G., & Schleser, G. H. (2004). Beyond CO_2-fixation by Rubisco – an interpretation of $^{13}C/^{12}C$ variations in tree rings from novel intra-seasonal studies on broad-leaf trees. *Plant, Cell & Environment*, *27*(3), 367–380.

Horvath, Z. (2016). Transforming our world-new agenda and goals for sustainable development. *Hungarian YB Int'l L. & Eur. L.*, 167.

Ibsen, P. C., Santiago, L. S., Shiflett, S. A., Chandler, M., & Jenerette, G. D. (2023). Irrigated urban trees exhibit greater functional trait plasticity compared to natural stands. *Biology Letters*, 19(1), 20220448.

Kaushal, S. S., McDowell, W. H., & Wollheim, W. M. (2014). Tracking evolution of urban biogeochemical cycles: past, present, and future. *Biogeochemistry*, *121*(1), 1–21.

Kendal, D., Dobbs, C., Gallagher, R. V., Beaumont, L. J., Baumann, J., Williams, N. S. G., & Livesley, S. J. (2018). A global comparison of the climatic niches of urban and native tree populations. *Global Ecology and Biogeography*, *27*(5), 629–637.

Kong, X., Zhang, X., Xu, C., & Hauer, R. J. (2021). Review on urban forests and trees as Nature-Based Solutions over 5 Years. *Forests*, 12(11), 1453.

Krull, W., Berry, P., Bauduceau, N., Cecchi, C., Elmqvist, T., Fernandez, M., Hartig, T., Mayerhofer, E., Naumann, S., & Noring, L. (2015). Towards an EU research and innovation policy agenda for nature-based solutions & re-naturing cities. *Final report of the Horizon 2020 expert group on nature-based solutions and re-naturing cities.*

Lafortezza, R., & Chen, J. (2016). The provision of ecosystem services in response to global change: Evidences and applications. *Environmental Research*, *147*, 576–579.

Larjavaara, M., & Muller-Landau, H. C. (2010). Rethinking the value of high wood density. *Functional Ecology*, *24*(4), 701–705.

Lee, H., Calvin, K., Dasgupta, D., Krinner, G., Mukherji, A., Thorne, P., Trisos, C., Romero, J., Aldunce, P., & Barrett, K. (2023). Climate change 2023: Synthesis report. Contribution of working groups I, II and III to the sixth assessment report of the intergovernmental panel on climate change. *The Australian National University*.

Livesley, S. J., Marchionni, V., Cheung, P. K., Daly, E., & Pataki, D. E. (2021). Water smart cities increase irrigation to provide cool refuge in a climate crisis. *Earth's Future*, *9*(1), e2020EF001806.

Locosselli, G. M., de Camargo, E. P., Moreira, T. C. L., Todesco, E., de Fátima Andrade, M., de André, C. D. S., de Andre, P. A., Singer, J. M., Ferreira, L. S., & Saldiva, P. H. N. (2019). The role of air pollution and climate on the growth of urban trees. *Science of the Total Environment*, *666*, 652–661.

Locosselli, G. M., Brienen, R. J., de Souza Martins, V. T., Gloor, E., Boom, A., de Camargo, E. P., Saldiva, P. H. N., & Buckeridge, M. S. (2020). Intra-annual oxygen isotopes in the tree rings record precipitation extremes and water reservoir levels in the Metropolitan Area of São Paulo, Brazil. *Science of the Total Environment*, *743*, 140798.

Locosselli, G. M., Cintra, B. B. L., Ferreira, L. S., da Silva-Luz, C. L., Miyahara, A. A. L., Brienen, R. J. W., Gloor, E., Boom, A., Grandis, A., & Buckeridge, M. S. (2024). Stress-tolerant trees for resilient cities: Tree-ring analysis reveals species suitable for a future climate. *Urban Climate*, *55*, 101964.

López, J., Way, D. A., & Sadok, W. (2021). Systemic effects of rising atmospheric vapor pressure deficit on plant physiology and productivity. *Global Change Biology*, *27*(9), 1704–1720.

Luketich, A. M., Papuga, S. A., & Crimmins, M. A. (2019). Ecohydrology of urban trees under passive and active irrigation in a semiarid city. *PloS One*, 14(11), e0224804.

Maher, B. A., Ahmed, I. A., Davison, B., Karloukovski, V., & Clarke, R. (2013). Impact of roadside tree lines on indoor concentrations of traffic-derived particulate matter. *Environmental Science & Technology*, *47*(23), 13737–13744.

Martinez-Meier, A., Sanchez, L., Pastorino, M., Gallo, L., & Rozenberg, P. (2008). What is hot in tree rings? The wood density of surviving Douglas-firs to the 2003 drought and heat wave. *Forest Ecology and Management*, *256*(4), 837–843.

Matsumoto, M., Kiyomizu, T., Yamagishi, S., Kinoshita, T., Kumpitsch, L., Kume, A., & Hanba, Y. T. (2022). Responses of photosynthesis and long-term water use efficiency to ambient air pollution in urban roadside trees. *Urban Ecosystems*, *25*(4), 1029–1042.

McCarroll, D., & Loader, N. J. (2004). Stable isotopes in tree rings. *Quaternary Science Reviews*, *23*(7), 771–801.

McGinnies, W. G. (1963). Dendrochronology. *Journal of Forestry*, *61*(1), 5–11.

Medina, M., Flores, M. P., Ritter, L. J., Goya, J. F., Campanello, P. I., & Arturi, M. F. (2024). Wood density and leaf traits independently relate to growth rate of naturally regenerated tree species in *Araucaria angustifolia* plantations in the Atlantic Forest, Argentina. *Canadian Journal of Forest Research*, *54*(1), 1–11.

Miyahara, A. A. L., & Locosselli, G. M. (2024). Challenges and advances in intra-annual tree-ring stable isotope research, a systematic review. *Dendrochronologia*, *85*, 126218.

Miyahara, A. A. L., Paixão, C. P., dos Santos, D. R., Pagin-Cláudio, F., da Silva, G. J., Bertoleti, I. A. F., de Lima, J. S., da Silva, J. L., Candido, L. F., & Siqueira, M. C. (2022). Urban dendrochronology toolkit for evidence-based decision-making on climate risk, cultural heritage, environmental pollution, and tree management–A systematic review. *Environmental Science & Policy*, *137*, 152–163.

Monaci, F., & Baroni, D. (2025). Leaves and tree rings as biomonitoring archives of atmospheric mercury deposition: an ecophysiological perspective. *Plants*, 14(9), 1275.

Monson, R. K., Szejner, P., Belmecheri, S., Morino, K. A., & Wright, W. E. (2018). Finding the seasons in tree ring stable isotope ratios. *American Journal of Botany*, *105*(5), 819–821.

Mullaney, J., Lucke, T., & Trueman, S. J. (2015). A review of benefits and challenges in growing street trees in paved urban environments. *Landscape and Urban Planning*, *134*, 157–166.

Niemelä, J. (1999). Ecology and urban planning. *Biodiversity & Conservation*, *8*, 119–131.

Niklas, K. J., & Spatz, H.-C. (2010). Worldwide correlations of mechanical properties and green wood density. *American Journal of Botany*, *97*(10), 1587–1594.

Ortega Rodriguez, D. R., Sánchez-Salguero, R., Hevia, A., Granato-Souza, D., Cintra, B. B. L., Hornink, B., Andreu-Hayles, L., Assis-Pereira, G., Roig, F. A., & Tomazello-Filho, M. (2023). Climate variability of the southern Amazon inferred by a multi-proxy tree-ring approach using *Cedrela fissilis* Vell. *Science of The Total Environment*, *871*, 162064.

Rambhia, M., Volk, R., Rismanchi, B., Winter, S., & Schultmann, F. (2023). Supporting decision-makers in estimating irrigation demand for urban street trees. *Urban Forestry & Urban Greening*, *82*, 127868.

Pozzer, A., Anenberg, S. C., Dey, S., Haines, A., Lelieveld, J., & Chowdhury, S. (2023). Mortality attributable to ambient air pollution: A review of global estimates. *GeoHealth*, 7(1), e2022GH000711.

Römer, P., Reinig, F., Konter, O., Friedrich, R., Urban, O., Čáslavský, J., Pernicová, N., Trnka, M., Büntgen, U., & Esper, J. (2023). Multi-proxy crossdating extends the longest high-elevation tree-ring chronology from the Mediterranean. *Dendrochronologia*, *79*, 126085.

Sannigrahi, S., Kumar, P., Molter, A., Zhang, Q., Basu, B., Basu, A. S., & Pilla, F. (2021). Examining the status of improved air quality in world cities due to COVID-19 led temporary reduction in anthropogenic emissions. *Environmental research*, *196*, 110927.

Schlaepfer, M. A. (2018). Do non-native species contribute to biodiversity? *PloS Biology*, *16*(4), e2005568.

Seto, K. C., Fragkias, M., Güneralp, B., & Reilly, M. K. (2011). A Meta-Analysis of Global Urban Land Expansion. *PloS One*, *6*(8), e23777.

Smith, I. A., Templer, P. H., & Hutyra, L. R. (2024). Water sources for street trees in mesic urban environments. *Science of The Total Environment*, *908*, 168411.

Swaffield, S. R., & McWilliam, W. J. (2013). Landscape aesthetic experience and ecosystem services. *School of Landscape Architecture, Lincoln University*, *2.6*, 349–362.

Thomas, E., Jansen, M., Chiriboga-Arroyo, F., Wadt, L. H. O., Corvera-Gomringer, R., Atkinson, R. J., Bonser, S. P., Velasquez-Ramirez, M. G., & Ladd, B. (2021). Habitat quality differentiation and consequences for ecosystem service provision of an amazonian hyperdominant tree species. *Frontiers in Plant Science*, *12*, 621064.

Tiotiu, A. I., Novakova, P., Nedeva, D., Chong-Neto, H. J., Novakova, S., Steiropoulos, P., & Kowal, K. (2020). Impact of air pollution on Asthma outcomes. *International journal of environmental research and public health*, 17(17), 6212.

Treydte, K., Boda, S., Graf Pannatier, E., Fonti, P., Frank, D., Ullrich, B., Saurer, M., Siegwolf, R., Battipaglia, G., Werner, W., & Gessler, A. (2014). Seasonal transfer of oxygen isotopes from

precipitation and soil to the tree ring: source water versus needle water enrichment. *New Phytologist*, *202*(3), 772–783.

UN, D. (2019). Department of Economic and Social Affairs, Population Division. World Population Prospects: *The 2019 Revision, Highlights. New York*.

van Duong, D., Schimleck ,Laurence, & and Lam Tran, D. (2023). Variation in wood density and mechanical properties of *Acacia mangium* provenances planted in Vietnam. *Journal of Sustainable Forestry*, *42*(5), 518–532.

Vessella, F., Parlante, A., Schirone, A., Sandoletti, G., Bellarosa, R., Piovesan, G., Santi, L., & Schirone, B. (2010). Irrigation regime as a key factor to improve growth performance of *Quercus suber* L. *Scandinavian Journal of Forest Research*, *25*(S8), 68–74.

Vico, G., Revelli, R., & Porporato, A. (2014). Ecohydrology of street trees: design and irrigation requirements for sustainable water use. *Ecohydrology*, *7*(2), 508–523.

Wang, M., Qin, M., Xu, P., Huang, D., Jin, X., Chen, J., Dong, D., & Ren, Y. (2024). Atmospheric particulate matter retention capacity of bark and leaves of urban tree species. *Environmental Pollution*, *342*, 123109.

Wei, J., Li, H., Wang, Y., & Xu, X. (2021). The cooling and humidifying effects and the thresholds of plant community structure parameters in urban aggregated green infrastructure. *Forests*, *12*(2), 111.

Wimmer, R., & Downes, G. M. (2003). Temporal variation of the ring width–wood density relationship in Norway spruce grown under two levels of anthropogenic disturbance. *Iawa Journal*, *24*(1), 53–61.

Winner, W. E., & Atkinson, C. J. (1986). Absorption of air pollution by plants, and consequences for growth. *Trends in Ecology & Evolution*, *1*(1), 15-18.

Xi, B., Clothier, B., Coleman, M., Duan, J., Hu, W., Li, D., Di, N., Liu, Y., Fu, J., Li, J., Jia, L., & Fernández, J.-E. (2021). Irrigation management in poplar (*Populus* spp.) plantations: a review. *Forest Ecology and Management*, *494*, 119330.

Capítulo 1

Developing and classifying urban biomes as a basis for nature-based solutions

In collaboration with: Dr. Tom Wild, Dra. Adriana Sandre, Dr. Paulo Renato Mesquita Pellegrino, Dr. Carlos Alberto da Silva Filho & Dr. Marcos Silveira Buckeridge.

Manuscript published in *Urban Climate* 45 (2022) 101251.

https://doi.org/10.1016/j.uclim.2022.101251

Highlights

1. Laws and regulations often promote the use of species from the local biome for Nature-based Solutions (NbS).
2. They are usually considered the best adapted to regional environmental conditions.
3. We evaluated the extant conditions of the green infrastructure across São Paulo city.
4. 47% of São Paulo has conditions similar to the non-local but adjacent woody savannas.
5. The definition of urban biomes may leverage informed decision-making on urban forests.

Abstract

Urbanization is a major driver of environmental change, which calls for multifunctional and comprehensive actions such as Nature-based Solutions (NbS). They are "inspired and supported by nature… and must benefit biodiversity and support the delivery of a range of ecosystem services". But what nature should one aim for? We tested the hypothesis that local vegetation may not always be the best source of inspiration, as environmental changes impact both extant conditions and species suitability for restored ecosystems. We analyzed the megacity of São Paulo, where laws promote the use of species from the local Atlantic Forest biome. We trained a Linear Discriminant Analysis to classify the Brazilian biomes and predicted the biomes' correspondence considering city's vegetation cover and climate. With 80% accuracy, the model predicted correspondence with the Atlantic Forest in 57% of the city, while 43% is better represented by the Cerrado, a dense Tropical Savanna biome. Cerrado species are naturally adapted to higher insolation, temperature and more seasonal precipitation, and they can parallel the ecosystem services from the Atlantic Forest. To help guide NbS implementation, we consider four "urban biomes": Atlantic Forest, Seasonally Flooded Atlantic Forest, Cerrado, and the Seasonally Flooded Cerrado, and discuss possible examples of NbS.

Keywords: Green Infrastructure, Blue Infrastructure, Urban forests, Machine Learning, NDVI.

1. Introduction

The world is rapidly urbanizing, with changes in land use and management practices altering natural vegetation cover and environmental quality, which affects cities' functioning, the health of citizens and their well-being (Goldstein, 1990; Seto et al., 2011). Impacts include poor thermal comfort; low air humidity; high air, water, and soil pollution; increased noise pollution; high vulnerability to flooding events and drought; high cityscape oppressiveness; low biodiversity; to name a few (Lehner et al., 2006; Asgarzadeh et al., 2010; Oleson et al., 2015; Elmqvist et al., 2016; Jariwala et al., 2017; Liang et al., 2019). Tackling these environmental issues can be challenging, and many cutting-edge engineering solutions have been proposed in the past. They are often planned and built as monofunctional solutions that frequently lead to other issues including landscape degradation (Brink et al., 2016). These limited solutions may gradually become unsuitable in modern cities as they grow in complexity, and instead multifunctional solutions, policies, and strategies may be required to address current environmental, social and economic problems (Ghafouri and Weber, 2020).

Nature-based Solutions (NBS) - actions "inspired by, supported by, or copied from nature" to tackle environmental, social and economic problems - arose as a multifunctional approach based on natural mechanisms (ECDG, 2015) that have been carefully evolving for thousands to millions of years as a part of Earth's biodiversity evolution (Mace et al., 2012). Biodiversity may provide tools to promote effective green and blue infrastructures and nature-based responses promoting benefits to human populations and helping them to adapt to ongoing environmental changes (van den Bosch and Sang, 2017; Anderson et al., 2019; Wild et al., 2020). However, an outstanding question for the implementation of NbS in different urban contexts is around "What nature should be used as a source of support and inspiration?".

The disputed debate on the use of native and non-native species underlies this question (Schlaepfer 2018). Not only because decisions on the urban green infrastructure of cities are oftentimes culturally and historically oriented (Whitney and Adams 1980), but also because managing urban forests requires pragmatic decisions related to the availability of seedlings in local nurseries (Almas and Conway 2016) and how species perform under the altered urban environment (Locosselli et al 2019). Native species available for urban reforestation may be naturally limited in regions characterized by low biodiversity, and non-native species present a renowned potential to add to the urban ecosystem development (*e.g.* Zerbe et al 2003, Schlaepfer et al 2020). Nonetheless, the availability of native species and associated environmental conditions exponentially increases across the latitudinal biodiversity gradient

peaking at the tropics (Pianka 1966, Willig et al 2003), where native biodiversity may leverage urban ecosystem's function.

The use of native species finds strong support in the scientific literature, local laws and regulations (*e.g.* Alvey, 2006; Özgüner et al 2007, Ordóñez and Duinker, 2013; Ramage et al., 2013; Zhang and Jim, 2014; Almas and Conway, 2016) and in urban environmental activism worldwide (*e.g.* Krasny and Tidball 2012, Silva et al., 2019). The main argument holds that native species are better adapted to local environmental conditions, offering improved prospects for their deployment, development and growth to leverage ecosystem services (McPherson et al., 1994; Sydnor and Subburayalu, 2011; Mullaney et al., 2015). The addition of the clause to the European Commission's original definition of NBS that they "*must benefit biodiversity and support the delivery of a range of ecosystem services*" (Wild et al., 2020) may be viewed as underlining this point, if one subscribes to the view that biodiversity and native species are inextricably linked. Nonetheless, environmental change impacts from urbanization are now affecting these prospects and perspectives in most cities.

In addition to habitats' fragmentation and degradation during urbanization (Seto et al., 2011), climate has significantly changed in the cities largely affecting the potential use of some species in urban forests (Esperon-Rodriguez et al 2019). Heat islands are an emblematic issue in the cities worldwide (Manoli et al 2019). The replacement of green cover with grey infrastructure causes significant reduction in the turbulent convection, evaporative cooling, and albedo while enhancing heat retention and emissions (Oke 1982, Arnfield 2003). Such changes in the energy balance in the cities further affect the convective activities that shift precipitation regimes across cities (Marengo et al., 2020). Thus, both changes in vegetation and climate lead to altered extant local conditions found within cities.

Because substantial variations in vegetation and climate conditions define biomes (Conradi et al., 2020), cities are now considered as a new unique world biome (Pincetl, 2015). But, classifying an entire city as the unique urban biome (Pincetl, 2015) is limiting and does not aid NbS decision-making or action because cities are heterogeneous. Such heterogeneity of urban environments has long been studied and debated (*e.g.* Grimm et al., 2000) and classification systems have been proposed to aid integrated urban planning and governance in relation to ecosystem restoration. For instance, biotopes have been long used to characterize the heterogeneity of urban vegetation for green infrastructure plans and implementations, attesting the importance of the clear understanding of vegetation structure across the city (*e.g.* Sukkop and Weiler, 1988; Stewart et al., 2009; Yilmaz et al., 2010). But this approach fails to account for the broad variability in climate conditions within the city (Steenberg et al., 2015) and new

classification systems are needed that account for intra-urban variation of both vegetation structure and climatic conditions. If carefully analyzed, vegetation and climate conditions may vary within cities perimeter in a similar magnitude to that observed among natural biomes.

While local native species may still fully grow and provide optimum ecosystem services in many urban settings, unfavorable conditions to the development, growth and longevity of local native species may jeopardize their potential role as a solution for local environmental problems (Kendal et al., 2018; Burley et al., 2019; Gesualdo et al., 2019; Locosselli et al., 2020; Marengo et al., 2020; Hanley et al., 2021). We propose that the urban environment should not be considered as single biome (Pincetl, 2015), rather, the variability of the urban conditions may be evaluated in terms of regional biomes, to define corresponding "urban biomes" and associated habitat types as a source of support and inspiration for the implementation of urban NbS. Towards that goal, we analyzed the current climate and vegetation cover of the megacity of São Paulo as a case study to test the following hypotheses: I) there is a significant variation in vegetation cover, precipitation, and temperature in the city; II) the variation of vegetation and climate is similar to that observed among natural surrounding biomes; III) the current distribution of vegetation cover and climate values give support to the use of natural elements from biomes other than the one found before urbanization. Here we refer to plant species including herbs, shrubs, and trees, their associations, and how they related to the physical environment, as "elements of nature" that can be used in NbS.

2. Material and Methods

2.1 The city of São Paulo

The city of São Paulo is one of the largest megacities in the world (United Nations, 2018), with more than 11.25 million people and a demographic density of 7398.26 people per square kilometer (IBGE, 2010). This population faces an urban territory with highly unequal environmental conditions ranging from districts with no street trees or green spaces to large protected urban forest patches (Silva et al., 2019). Overall, 75% of the residences are on roads that hold street trees whose density increases towards the city center (Silva et al., 2019). In addition, the city of São Paulo has large private green areas such as education centers, sports centers, cemeteries, to name but a few, plus 107 parks under the responsibility of the municipality, and some larger State parks, including one of the largest urban rainforests in the world (Negreiros et al., 1974).

The city of São Paulo is located within a Tropical/Subtropical Moist Broadleaf Forest biome, according to Olson's classification (Figure 1, Olson et al., 2001), or Atlantic Forest according to the official Brazilian biome classification (IBGE, 2004). This vegetation is associated with the subtropical humid / temperate summer climate, according to Köppen's classification (Alvares et al., 2014), with a strong influence from the Southern Atlantic Ocean. The Atlantic Forest domain is considered a "hotspot" of biodiversity (Myers et al., 2000), with more than 3,000 tree species (Zappi et al., 2015), of which 577 may still be found in the city of São Paulo (Biodiversity Inventory of the City of São Paulo, 2016). These native species belong to the "Serra do Mar Coastal Forest" ecoregion (Olson et al., 2001) that used to represent most of the vegetation before the urbanization (Figure S1). This ecoregion borders the "Alto do Paraná Atlantic Rainforests" that are the semi-deciduous forest formations of the plateau, and the "Cerrado" that corresponds to the Tropical/Subtropical Grasslands, Savannas, and Shrublands biome (Olson et al., 2001), another world "hotspot" of biodiversity (Myers et al., 2000). Studies from the early 20th century reported patches of Cerrado in the city, mostly grasslands and shrublands, immersed in the matrix of the Atlantic Forest. The genesis of these grasslands, however, is still debated and may be less natural, but related to past anthropogenic fires that changed soils' compositions (Usteri, 1911; Joly, 1950; Garcia and Pirani, 2003).

Because the city lies in the domain of the Atlantic Forest, municipal laws and strategic plans regarding street trees, green spaces, and protected areas promote (to some extent) the restoration of ecosystems based on the structure and composition of this specific biome. For instance, the municipal laws 15.428/2011 and 16.050/2014 promote urban reforestation with native species that contribute to a better environmental quality and chosen based on scientific and technical studies (see Silva et al., 2019 for further details). Activists working in the city largely agree with the current municipal regulation, by promoting urban reforestation mainly using species from the previously found forest biome, based on the argument that such species are the best adapted to the local conditions (Silva et al., 2019).

2.2 Vegetation data

Since vegetation structure (such as leaf structure and deciduousness) is a key factor to characterize biomes (Woodward et al., 2004), the vegetation found in the Brazilian biomes and across the city of São Paulo was characterized using the Normalized Difference Vegetation Index (NDVI) products from MODIS, with 250 meters spatial resolution (MYD13Q1v006 product, United States Geological Service, Earth Explorer platform). Although NDVI is a

measure of greenness (Tucker 1979), it is largely dependent on leaf status and biomass, and thus can be used as an indirect measure of vegetation structure related to crown closure and leaf area index (Ren et al 2017), and thus it has been long used for monitoring vegetation across different environments, cities included (*e.g.* Gallo et al 1993, Yuan F, Bauer ME 2006 Bilgili et al 2013, Wong et al 2019 Aabeyir et al 2022). MODIS images have been used before for the evaluation of the cities' heterogeneities with great success (*e.g.* Engel-Cox et al., 2004; Tomlinson et al., 2010; Ferreira and Duarte, 2019; Mishara et al., 2019), and this spatial resolution represents about 4 blocks in the city which is sufficiently fine-grained for the large-scale biome approach used in this study. The use of the same MODIS products to characterize the natural Biomes of Brazil and the "urban biomes" of São Paulo greatly reduced any bias related to mixing imaging periods and potentially different satellite sources, atmospheric corrections for different areas of the country and the city, and further data corrections and analyses.

We obtained NDVI images for all of Brazil to characterize vegetation during wet and dry seasons from 2013 to 2019. We then calculated the mean NDVI value for the entire period to characterize the vegetation structure, the maximum NDVI, and the mean ratio of the NDVI (max NDVI / min NDVI) to characterize vegetation seasonality (Figures S2 and S3). For the city of São Paulo, we only used the images from 2013 and 2017, because other years were strongly influenced by clouds during the wet season (Figure S3). Finally, we compared the distribution of the values of NDVI variables from São Paulo and the Brazilian biomes using density plots.

2.3 Climate data

To characterize the climate, we used spatially interpolated bioclimatic variables at 30" spatial resolution from WorldClim V2 (Fick and Hijmans, 2017), which are based on local records of temperature and precipitation. We selected bioclimatic variables over regular climate variables for having more biological and ecological meaning. The spatial coherence of the interpolated data was calibrated using local observations of precipitation and temperature obtained from 28 climate stations from the Emergency Management Center of São Paulo (CGE-SP, Figure 1). Ten-minute frequency measurements were obtained from automatic stations covering the period between 2013 to 2019. We calculated the monthly values of temperature and precipitation to then estimate the 19 bioclimatic variables for each climate station using the 'Dismo' package in R (Booth et al., 2014). The distribution of the values of precipitation and

temperature variables were then compared for the São Paulo and Brazil-wide biomes, using density plots.

2.4 Characterization of the Brazilian biomes

We trained a classification algorithm based on the values of the bioclimatic and NDVI variables from protected areas with distinct levels of disturbance in Brazil. This step allowed us to characterize the natural vegetation of each biome other than the surrounding matrix of vegetation cover mostly related to different crops like soybean, sugarcane, cotton, and pastures that cover most of the former natural areas. We calculated the centroid for the polygon of 550 protected areas (Figure S4), including 303 protected areas in the Atlantic Forest (Tropical Moist Broadleaf Forest biome), 130 in the Cerrado (Tropical Grasslands and Savannas biome, considering both Cerrado and Pantanal as Savanna biomes, Olson et al., 2001), 79 in the Amazon Forest (Tropical Moist Broadleaf Forest biome) and 79 in the Caatinga (Tropical Desert and Xeric Shrublands biome), using QGIS software. We used the coordinates of the centroids of the protected areas to obtain the values of bioclimate variables and NDVI variables.

We then used these variables to train a Linear Discriminant Analysis (LDA, Venables and Ripley, 2002) that is a learning method (Araújo et al 2021) to classify the Brazilian biomes. We used the following three steps for the variables' selection. Firstly, we selected the least collinear variables based on a Hierarchical Clustering Analysis that group the variables according to their linear association (Figure S5, Chavent et al., 2017). In this step, we selected variables that represent annual and seasonal values of NDVI, temperature, and precipitation. Secondly, we validated the spatial variation of the chosen interpolated bioclimatic data using the data from the 28 climate stations in São Paulo (Figure 1, two climate stations were removed for presenting unusual behavior for temperature, Figure S6). Thirdly, we looked for the combination of vegetation and climate variables that resulted in the highest model accuracy. We then calculated the Kappa coefficient for that model using the package 'e1071' (Meyer et al., 2019) in R. For the Linear Discriminant Analysis, we standardized the data using z-scores and then used 80% of the data of the protected area to calibrate the discriminant model and the remaining 20% to validate it in R.

2.5 Characterization of the urban biomes of São Paulo

Once we established appropriate variables to classify the Brazilian biomes, the same variables were sampled across the city of São Paulo. A grid with 30,426 points across the city was built, excluding areas covered by two large water reservoirs, with an approximate spatial resolution of 250 m, to match the spatial resolution of the climate and NDVI data. For each point, NDVI and climatic values were obtained. We then used the dataset obtained with the grid of points to predict each corresponding urban biome in the city using the previously trained Linear Discriminant model. We used the same standardization parameters used in the model training to predict the corresponding "urban biomes". A raster file was built in QGIS (V.3.12) with the spatial distribution of the corresponding "urban biomes" of São Paulo. We further validated the application of the trained linear discriminant model in the city by testing the accuracy in the biome classification of São Paulo's Atlantic Rainforest remnants (GEOSAMPA).

We also investigated the role of green cover across the whole city in the classification of the urban biomes. We first focused on the green spaces (GEOSAMPA) of the city larger than 62,500 m^2, which is equivalent to the spatial resolution of the urban biome analysis. These spaces include public parks, sports centers, education centers, cemeteries, large extension private lands, restored landfills. We then focus on characterizing four summarized green cover types (GEOSAMPA) – including grass and shrubs, low tree density, medium tree density, and forest patches. We also characterized the composition of the green cover outside the largest green areas but across the urban fabric using the same grid of points used for the urban biome classification to understand how green cover types influenced the classification of the urban Cerrado and Mata Atlântica. Principal component analyses were used to evaluate the composition of green cover of the different urban biomes at both spatial scales.

In addition, to gain further insights into aquatic and wetland ecosystem types, flood extents were mapped, corresponding with each urban biome. A raster file was generated using flooding datasets from GEOSAMPA to infer the locations of the seasonally flooded sites in the city, and thereby to infer terrestrial c.f. aquatic and riparian ecosystems. Main flood areas were checked using city flood events datasets (Fundação Centro Tecnológico de Hidráulica - FCTH - Poli-USP).

3. Results

A wide variety of vegetation structure and climate conditions were observed in the city of São Paulo (Figure 2, S6). Vegetation structure varied considerably in the city, from highly vegetated areas in the south and north, represented by mean NDVI values higher than 0.7, to areas almost entirely lacking vegetation cover, represented by mean NDVI values lower than 0.25. Climate also varies consistently across the city. Current annual mean temperature varies between 16.46˚C and 21.69˚C across the city, while the mean temperature of the warmest quarter varies between 19.28 and 24.64˚C. Precipitation presented a two-fold variation both in terms of total annual precipitation volume (1366 to 2724 mm / year), precipitation of the driest month (53 to 112 mm / month), and three-fold variation during the coldest quarter (118 to 368 mm / month). These interpolated values showed consistent spatial variability with the calculated values based on the data from the local climate stations. Correlation between interpolated and observed annual values are statistically significant for temperature ($r = 0.75$, $p < 0.05$, Figure S7), as well as for the selected precipitation variables ($r = 0.41$ to 0.80, $p < 0.05$, Figure S7).

The spatial variability of the vegetation structure and climate conditions across the city of São Paulo (Figure 2) paralleled that of the Brazilian biomes (Figure 3). Overall, the vegetation density as measured by the NDVI across the city of São Paulo ranges from that observed in the dense Atlantic Forest and Amazon, to that observed in the Cerrado and Caatinga, to the complete absence of vegetation. On the other hand, the distribution of temperature and precipitation within the city of São Paulo falls mainly within the climate envelope of the Atlantic Rain Forest and the Cerrado.

Because of these similarities in the vegetation structure and climate conditions between the city of São Paulo and some of the Brazilian biomes, we trained a Linear Discriminant Analysis to classify the four main Official Brazilian biomes in terms of natural coverage. According to the criteria of variables selection for this model described in section 2.4 (Figure 4) the most accurate model incorporated the following variables: mean NDVI; the ratio of summer NDVI: winter NDVI; annual mean temperature (Bioclim 1); mean temperature of the warmest quarter (Bioclim 10); annual precipitation (Bioclim 12); precipitation of the driest month (Bioclim 14); and precipitation of the coldest quarter (Bioclim 19). This model showed 80% accuracy (95% confidence interval) in predicting official Brazilian biomes according to the mentioned variables, with a Kappa coefficient of 0.66. The misclassified biomes coincided with protected areas in the transition between different biomes, especially between Cerrado and Atlantic Forest (Table S2). The mean temperature of the warmest quarter, annual precipitation, and annual

mean temperature are the main variables in the first linear discriminant (LD1) that comprises 62% of the data variability (Table 1). Mean temperature of the warmest quarter, annual precipitation, and mean NDVI are the main variables in the second linear discriminant (LD2) that comprises 30% of the data variability. Annual precipitation, precipitation of the driest month, and annual temperature are the main variables in the third linear discriminant (LD3) that comprises 8% of the data variability. In a second round of the model validation, this model accurately classified 99.92% of the area of São Paulo's Atlantic Rainforest remnants (Figure S8).

According to this Linear Discriminant Model, 57% of the city has vegetation structure and climate conditions that correspond to the Atlantic Forest biome according to the classification model (Figure 5). It is continuously distributed in the north and south, with a fragmented distribution in the west and at the extreme east. The other 43% of the city has vegetation structure and climate conditions that were classified as Cerrado. These conditions are mainly found in the central and eastern areas of São Paulo, whilst the Cerrado biome type is highly fragmented in the west.

Out of São Paulo's 165 green spaces with more than 62,500 m^2, 48 were classified as Cerrado and 117 were classified as Mata Atlântica regardless of the land use (Figure 5A, B and C). According to the PCA (Tables S3-S6), the main difference between the classification of the green spaces classified is the higher proportion of forest cover in those classified as Mata Atlantica, with almost any influence from other vegetation cover types (Figure 5E). This pattern is still consistent when vegetation cover is evaluated outside the largest green spaces where the presence of even small forest patches across the urban fabric results in the Mata Atlântica category (Figure 5F). Overall, green cover is consistently lower in the areas classified as Cerrado, and 9.36% of the city of São Paulo has less than 5% of green cover (Figure 6).

In addition, about 5% of the city is under the influence of seasonal floods (Figure S9). These aquatic and riparian habitats were thus classified as Seasonally Flooded Atlantic Forest (1%) and Seasonally Flooded Cerrado (4%), thus resulting in a total of four urban biomes in the city of São Paulo (Figure 6).

4. Discussion

Nature-based Solutions are planned to tackle environmental, social, and economic challenges through actions supported by nature (van den Bosch and Sang, 2017). But, what nature should be used as a source of support and inspiration? Municipal laws, regulations, and activists of São Paulo prioritize the use of tree species from the local Atlantic Forest (Silva et al., 2019). The main argument is built around the long adaptation of this vegetation to the local environmental conditions (Silva et al., 2019). However, the local conditions that used to support this vegetation may no longer be found across the entire city, because land-use change resulted in a significant increase in mean temperature (Silva et al., 2019), and changes in convective activities and precipitation patterns (Marengo et al., 2020).

To evaluate if such environmental changes have the potential to affect the source of inspiration of NbS, we trained a Linear Discriminant model to classify the Brazilian Biomes. The final model showed an 80% accuracy, equivalent to other classification models for the Brazilian biomes (Miranda et al., 2018), and a moderate to substantial Kappa coefficient (McHugh, 2012). The biomes' discrimination depends mostly on the local climate conditions and to a certain extent on the vegetation cover as assessed using NDVI, which is an expected result given the importance of climate and vegetation in this broad classification system (Conradi et al., 2020). When validated at the city level, the discriminant model yielded an accuracy of 99.92% in the classification of the Atlantic Rainforest remnants pointing to its reliable use in the city despite potential reflectance noise from atmospheric pollution and deposition of particulate matter on the surface of leaves. Despite the evidence of model robustness, a careful evaluation must be taken in areas with extremely low vegetation cover where the model may fail to properly find a meaningful correspondence with the natural biomes based on greenness derived from NDVI values (dashed areas of Figure 6). Significant uncertainties where also found in the transitions between Atlantic Forest and Cerrado, so that it may not be as accurate in the limits of these two biomes either in the natural or urban environments.

According to this model, 57% of the city may be classified as Atlantic Rainforest. It corresponds to the actual large patches of Atlantic Forest in northern and southern São Paulo and adjacent districts, and the so-called green districts characterized by a dense vegetation cover. The model results also point to 43% of the city with a better correspondence to the Cerrado, a Tropical Grassland, Savanna, and Shrublands biome (Olson et al., 2001) that is characterized by the combination of grasses, shrubs, and relatively dense tree cover (Coutinho, 1978). The predicted Cerrado areas in the city correspond to large green spaces with lower proportion of forest cover,

and densely urbanized but still sparsely vegetated parts of São Paulo. Interestingly, they include former areas of anthropogenic savannas long described by Usteri (1911) at the early 20th century at the city center, where most of the early urbanization took place. Thus, we propose the classification of the city of São Paulo in two main "urban biomes" according to its current environmental conditions, the Urban Atlantic Forest and the Urban Cerrado, or the Urban Moist Broadleaf Forest and Urban Savanna for international use, respectively.

We then characterized the urban biomes according to the occurrence of floods given their significant geographical extension in the city and overall severity of impacts (Gu et al., 2015; Haddad and Teixeira, 2015). Seasonally flooded areas require interventions based on elements from nature that are adapted to a humid phase (Scharenbroch et al., 2016; Yuan et al., 2017) a fact that led us to define the seasonally flooded urban biomes. The urban seasonally flooded Atlantic Forest would require elements from the swamp forests locally known as "Florestas Paludosas", which are characterized by various plant species adapted to seasonal flood (Figure 7, Teixeira and Assis, 2005, 2009; Reis et al., 2009). Whereas the seasonally flooded Cerrado requires elements from the wet grasslands locally known as "Campos Húmidos" (Figure 6, Ruggiero et al., 2006; Tannus et al., 2006; Rossato et al., 2008), or riparian forests for larger watercourses. These are likely the best sources for suitable species to the specific conditions found in rain gardens, detention / retention basins, wetlands, and bioswales, to name few devices related to Green and Blue Infrastructure. These sustainable drainage systems are needed in at about 5% of the entire city of São Paulo to make room for water storage and regeneration, and in the rest of the watersheds for control and treatment of the runoff.

Two questions remain to be answered. Does the Cerrado truly holds more resilient species? Can it equal or surpass the ecosystem services provided by the species from the Atlantic Forest? Based on studies currently limited to natural areas, trees from the Cerrado are naturally adapted to high temperatures and seasonally restricting precipitation conditions (Cabral et al., 2015, Loram-Lourenço, 2020), similar to that found in parts of São Paulo. Because the dry season length is expected to increase by two or three months in the upcoming decades (Gesualdo, 2019), Cerrado' species may also be considered future proof in terms of environmental changes increasing the resilience of the green infrastructure. Their deep root systems (Coutinho, 1978, 2016; Oliveira et al., 2005) may also represent an adaptation advantage useful to cope with the lowering of water tables resulting from climate extremes, construction work, extensive soil impermeabilization, excessive water pumping, and reduction in the vegetation cover (*e.g.* Hirata and Conicelli, 2012; Mohanavelu et al., 2020; Yadav et al., 2020; Nath, 2021). Their adaptation to the high metal concentrations in the soil (Coutinho, 1978, 2016) likely make them

also adapted to the diffuse urban metal pollution (Moreira et al., 2018) that severely restricts tree growth and development (Locosselli et al., 2019). Thus, these species have advantages in terms of growth that may increase the prospects for long-term of ecosystem services delivery urban environment.

In terms of ecosystem services quality, again based on the current literature limited to the natural environment, Atlantic Forest species have a greater potential to control temperature since taller and densely arranged trees may provide better thermal comfort (Abreu-Harbich et al., 2015) but only if the natural structure and conditions of the Atlantic Forest can be replicated along the urban infrastructure. For the most compact urban areas, the often-shorter Cerrado species will still promote thermal comfort through shading (Bowler et al., 2010; Abreu-Harbich et al., 2015) and evaporative cooling (Bowler et al., 2010, Moss et al., 2019) sustained by their deep root systems (Coutinho, 1978, 2016; Oliveira et al., 2005). Likewise, the carbon sink potential of the Atlantic Forest can be higher than in the Cerrado if the vegetation structure, longevity and recruitment of trees are replicated in the city (David et al., 2017). Otherwise, Cerrado trees often present higher growth rate at early stages of life (Locosselli et al., 2017) favoring the establishment of young trees especially in open spaces, and higher investment of carbon in below ground organs (Castro and Kauffman, 1998; Ribeiro et al., 2011) and overall wood density (Chave et al., 2009). The thick and rough barks of the Cerrado trees (Loram-Lourenço, 2020) may represent an additional advantage in terms of adsorption of particulate air pollution (Moreira et al., 2018) and rainfall interception (Oliveira et al., 2015; Tonello et al., 2021), that is on par or even higher to that observed in the mature Atlantic Forest (Junior et al., 2019). Although restricted to natural areas, these observations could inform their potential roles in the deployment of ecosystem services in urban areas.

The implementation of Cerrado inspired NbS would further benefit from the often-neglected ecosystem services provided by grasses and shrubs (Deletic et al 2006, Ryan et al 2016). Consideration of other vegetation assemblages (and supporting substrates) is required if cities are to make use of all the tools in the toolkit of NbS to become more resilient to climate change, and to address other urgent challenges such as wellbeing, pollution, biodiversity, and inclusion. When integrated into NbS, grasslands and shrublands can provide improvements in thermal comfort (vaz Monteiro et al., 2016), rainfall-runoff response (Davis et al., 2021) and air quality (Escobedo et al., 2008), water pollution remediation (*e.g.* Urbonas et al., 1989; Clary et al., 2017), and biodiversity support (Sala and Maestre, 2014).

Both the natural Atlantic Forest and the Cerrado have a long and dynamic history of contraction and expansion, and they often co-exist as mosaics in the ecotones nowadays. Such dynamics

are naturally controlled by changes in the climate conditions and by major disturbance forces like fire (Silva and Bates, 2002). The natural co-existence of these two biomes in the ecotones evidence a potential balanced co-existence in the cities, where their dynamics will likely be controlled by changes in the climate condition from climate change, urbanization, and implementation of NbS, and by major disturbance forces such as the anthropogenic activities undertaken in the cities. The urban ecosystem restoration could benefit from such natural and dynamic processes in which the Cerrado could act as a transient urban biome in the way of restoring the urban forests through soil horizon development and species succession followed by the densification of the vegetation whenever this planting scheme is possible. The urban Cerrado could also act as a permanent urban biome in appropriate areas of the city where dense vegetation cover is not possible, likely without compromising the ecosystem services delivery including biodiversity support.

The diversity of challenges faced by cities in becoming more resilient can therefore be considered as being addressed by a range of different interventions drawing on the diverse, valuable properties of natural processes, such as infiltration, evapotranspiration, pollination, and so on. Our findings present an important piece of the jigsaw puzzle, by providing a more nuanced and fine-grained appreciation of extant environmental conditions and appropriate ecologies from which to draw inspiration for the retrofitting of green elements back into the urban fabric. If NbS are to be successful in how they are 'locally adapted, resource-efficient and systemic' (EC, 2021), cities urgently need to know which types and combinations of vegetation may thrive when planted. They also need better spatial data on the supporting environmental conditions that will enable that flourishing of vegetation, so that these locally 'attuned' NbS may effectively deliver their intended ecosystem services.

5. Conclusions

We show that the use of elements of nature inspired by the local biome to improve the quality of the urban environment, as supported by laws and regulations, may not always be the best practice in the entire city. Because of changes in vegetation structure and climate conditions, 47% of the city of São Paulo has conditions that may better support elements inspired in the Cerrado, a Tropical Grassland, Savanna, and Shrubland biome, instead of the Atlantic Forest, a Tropical Moist Broadleaf Forest biome originally found there. This shift towards low vegetation coverage, high temperature, and changes in precipitation regime are expected outcomes of urbanization in many cities of the world, and thus, the use of elements from

adjacent biomes may bring resilience to the urban green infrastructure, while also acting as transition steps. These transitions among urban biomes may occur as local conditions change with the implementation of NbS, and the results point to the effectiveness of increasing the vegetation density wherever possible. The implementation of NbS inspired by different natural biomes such as proposed here may leverage the biodiversity in cities and its benefits to the population.

Acknowledgement

We thank Ligia Vizeu Barroso and Angélica Resende for the valuable early discussion on the methods of this study, Stefan Krottenthaler for providing the data of the protected areas of Brazil, and the Emergency Management Center of the City of São Paulo (CGE / PMSP) for providing the climate data for the 28 climate stations in São Paulo. We also thank the financial support of FAPESP (2017/50341-0, 2019/08783-0, 2020/09251-0). The authors also wish to acknowledge the support of colleagues in the CONEXUS project, funded by the European Commission through its Horizon 2020 Research & Innovation programme, under grant agreement no. 867564.

References

Aabeyir, R., Peprah, K., & Hackman, K. O. (2022) Spatio-temporal pattern of urban vegetation in the central business district of WA municipality of Ghana. *Trees, Forests and People* 8:100261.

Abreu-Harbich, L. V., Labaki, L. C., & Matzarakis, A. (2015). Effect of tree planting design and tree species on human thermal comfort in the tropics. *Landscape & Urban Planning* 138, 99-109.

Almas, A. D., & Conway, T. M. (2016). The role of native species in urban forest planning and practice: a case study of Carolinian Canada. *Urban Forestry & Urban Greening* 17, 54–62.

Alvares, C. A., Stape, J. L., Sentelhas, P. C., Gonçalves, J. L. M., & Sparovek, G. (2014). Köppen's climate classification map for Brazil. *Meteorologische Zeitschrift* 22(6), 711-728.

Alvey, A. A. (2006). Promoting and preserving biodiversity in the urban forest. *Urban Forestry & Urban Greening* 5, 195-201.

Araújo, H. C. L., Martins, F. S., Cortese, T. T. P., & Locosselli, G. M. (2021) Artificial intelligence in urban forestry – A systematic review. *Urban Forestry & Urban Greening* 66: 127410.

Arnfield, A. J. (2003) Two decades of urban climate research: a review of turbulence exchanges of energy and water, and the urban heat island. *International Journal of Climatology* 23: 1-26.

Asgarzadeh, M., Koga, T., Yoshizawa, N., Munakata, J., & Hirate, K. (2010). Investigating green urbanism; building oppressiveness. *Journal of Asian Architecture & Building Engineering* 9(2), 555-562.

Bilgili, B. C., Satir, O., & Müftüoglu, V. (2013) Using NDVI values for comparing parks in different scales. *Journal of Food, Agriculture & Environment* 11: 2451-2457.

Biodiversity Inventory of the City of São Paulo (2016). *Diário Oficial da Cidade de São Paulo*. 61(241), dia 24 de dezembro.

Booth, T. H., Nix, H. A., Busby, J. R., & Hutchinson, M. F. (2014). BIOCLIM: the first species distribution modelling package, its early applications and relevance to most current MAXENT studies. *Diversity & Distributions* 20(1), 1-9.

van den Bosch, M., & Sang, A. O. (2017). Urban natural environments as nature-based solutions for improved public health – A systematic review of reviews. *Environmental Research* 158, 373-384.

Bowler, D. E., Buyung-Ali, L., Knight, T. M., & Pullin, A. S. (2010). Urban greening to cool towns and cities: a systematic review of the empirical evidence. *Landscape & Urban Planning* 97, 147-155.

Brink, E., Aalders, T., Ádám, D., Feller, R., Henselek, Y., Hoffmann, A., Ibe, K., Matthey-Doret, A., Meyer, M., Negrut, N. L., Rau, A-L., Riewerts, B., van Schuchmann, L., Törnros, S., von Wehrden, H., Abson, D. J., & Wamsler, C. (2016). Cascades of green: a review of ecosystem-based adaptation in urban areas. *Global Environmental Change* 36, 111-123.

Burley, H., Beaumont, L. J., Ossola, A., Baumgarterns, J. B., Gallargher, R., Laffan, S., Esperon-Rodriguez, M., Manea, A., & Leishman, M. R. (2019). Substantial declines in urban tree habitat predicted under climate change. *Science of Total Environment* 685, 451-462.

Cabral, O. M. R., Rocha, H. R., Gash, J. H., Freitas, H. C., & Ligo, M. A. V. (2015). Water and energy fluxes from a woodland savanna (Cerrado) in southeast Brazil. *Journal of Hydrology: Regional Studies* 4, 22-40.

Castro, E. A., & Kauffman, J. B. (1998). Ecosystem structure in the Brazilian Cerrado: a vegetation gradient of aboveground biomass, root mass and consumption by fire. *Journal of Tropical Ecology* 14, 263–283.

Chave, J., Coomes, D., Jansen, S., Lewis, S. L., Swenson, N. G., & Zanne, A. E. (2009). Towards a worldwide wood economics spectrum. *Ecology Letters* 12, 351-366.

Chavent, M., Kuentz-Simonet, V., Liquet, B., & Saracco, J. (2017). *ClustOfVar: Clustering of Variables, R package version 1.1.*

Clary, J., Jones, J., Leisenring, M., Hobson, P., & Strecker E. (2017). International Stormwater BMP Database 2016 summary statistics. *Water Environment & Reuse Foundation*. Alexandria, Virginia.

Conradi, T., Sligsby, J. A., Midgley, G. F., Nottebrock, H., Schweiger, A. H., & Higgins, S. I. (2002). An operational definition of the biome for global change research. *New Phytologist* 227, 1294-1306.

Coutinho, L. M. (1978). O conceito de Cerrado. *Revista Brasileira de Botânica* 1, 17-23.

Coutinho, L. M. (2016). Os biomas brasileiros. *Oficina de Textos*, São Paulo, Brasil.

David, H. C., Araújo, E. J. G., Morais, V. A., Scolforo, J. R. S., Marques, J. M., Netto, S. P., & MacFarlane, D. W. (2017). Carbon stock classification for tropical forests in Brazil: understanding the effect of stand and climate variables. *Forest Ecology & Management* 404, 241-250.

Davis, A. P., Stagge, J. H., Jamil, E., & Kim, H. (2012). Hydraulic performance of grass swales for managing highway runoff. *Water Research*, 46(20), 6775-6786.

Deletic, A., & Fletcher, T. D. (2006). Performance of grass filters used for stormwater treatment—a field and modelling study. *Journal of Hydrology*, 317(3-4), 261-275.

ECDG (2015). *Towards an EU Research and Innovation Policy Agenda for Nature-Base Solutions & Re-Naturing Cities Final Report of the Horizon 2020 Expert Group on Nature-Based Solutions and Re-Naturing Cities*. Luxembourg.

Elmqvist, T., Zipperer, W. C., & Güneralp, B. (2016). Urbanization, habitat loss, biodiversity decline: solution pathways to break the cycle. In *The Routledge handbook of urbanization and global environmental change* (139-151). Routledge.

Seto K. C., Solecki, W., & Griffith, C. (Eds.). (2016). *The Routledge Handbook of Urbanization and Global Environmental Change*. New York: Routledge, 139-151.

Engel-Cox, J. A., Holloman, C. H., Countant, B. W., Hoff, R. M. (2004). Qualitative and quantitative evaluation of MODIS satellite sensor data for regional and urban scale air quality. *Atmospheric Environment*, 38(16), 2495-2509.

Escobedo, F. J., Wagner, J. E., Nowak, D. J., de la Maza, C. L., Rodriguez, M, Crane, D. E. (2008). Analyzing the cost effectiveness of Santiago, Chile's policy of using urban forests to improve air quality. *Journal of Environmental Management*, 1;86(1), 148-57.

Esperon-Rodriguez, M., Power, S. A., Tjoelker, M. G., Beaumont, L. J., Burley, H., Caballero-Rodriguez, D., & Rymer, P. D. (2019). Assessing the vulnerability of Australia's urban forests to climate extremes. *Plants, People, Planet*, 1(4), 387-397.

Ferreira, L. S., & Duarte, D. H. S. (2019). Exploring the relationship between urban form, land surface, temperature and vegetation indices in a subtropical megacity. *Urban Climate*, 27, 105-23.

Fick, S. E., & Hijmans, R. J. (2017). WorldClim 2: new 1km spatial resolution climate surfaces for global land areas. *International Journal of Climatology*, 37(12), 4302-4315.

Gallo, K. P., McNab, A. L., Karl, T. R., Brown, J. F., Hood, J. J., & Tarpley, J. D. (1993). The use of vegetation index for assessment of urban heat island effect. *Remote Sensing*, 14: 2223-2230.

Garcia, R. J. F., & Pirani, J. R. (2003). Revisão sobre o diagnóstico e caracterização da vegetação campestre junto à crista de serras no Parque Estadual da Serra do Mar, São Paulo, SP, Brasil. *Hoehnea,* 30(3), 217-241.

Gesualdo, G. C., Oliveira, P. T., Rodrigues, D. B. B., & Gupta, H. V. (2019). Assessing water security in the São Paulo metropolitan region under projected climate change. *Hydrology and Earth System Sciences*, 23(12), 4955-4968.

Ghafouri, A., & Weber, C. (2020). Multifunctional urban spaces a solution to increase the quality of urban life in dense cities. *Manzar, The Iranian Academic Open Access Journal of Landscape*, 12(51), 34-45.

Goldstein, G. (1990). Urbanization, health and well-being: a global perspective. *Journal of the Royal Statistical Society. Series D (The Statistician)*, 39(2), 121-133.

Grimm, N. B., Grove, G., Pickett, S. T. A., & Redman, C. L. (2000). Integrated approaches to long-term studies of urban ecological systems. *Bioscience*, 50(7), 571-584.

Gu, D., Gerland, P., Pelletier, F., & Cohen, B. (2015). Risks of exposure and vulnerability to natural disasters at the city level: a global overview. *United Nations, Technical Paper* N°2015/2.

Haddad, E. A., & Teixeira, E. (2015). Economic impacts of natural disasters in megacities: the case of floods in São Paulo Brazil. *Habitat International,* 45, 106-113.

Hanley, P. A., Arndt, S. K., Livesley, S. J., & Szota, C. (2021). Relating the climate envelopes of urban tree species to their drought and thermal tolerance. *Science of the Total Environment,* 753, 142012.

Hirata, R., & Conicelli, B. P. (2012). Groundwater resources in Brazil: a review of possible impacts caused by climate change. *Anais da Academia Brasileira de Ciências*, 84(2), 297-312.

IBGE (2004). Mapa de biomas do Brasil, escala 1: 5.000. 000. Rio de Janeiro: IBGE.

IBGE (2010). Censo demográfico. Características gerais da população. Resultado geral da amostra, 5(19), 2016.

Jariwala, H. J., Syed, H. S., Pandya, M. J., & Gajera, Y. M. (2017). Noise pollution & human health: a review. *Noise and Air Pollutions: Challenges and Opportunities*; LD College of Engineering: Ahmedabad, India.

Joly, A. B. (1950). Estudo fitobiogeográfico dos campos do Butantã. Boletim de Botânica 8, 18-68.

Junior, J. A. J., Mello, C. R., Mello, J. M., Scolforo, H. F., Beskow, S., & McCarter, J. (2019). Rainfall partitioning measurement and rainfall interception modelling in a tropical semi-deciduous Atlantic Forest remnant. *Agricultural & Forest Meteorology*, 275, 170-183.

Kendal, D., Dobbs, C., Gallagher, R. V., Beaumont, L. J., Baumann, J., Williams, N. S. G., & Livesley, S. J. (2018). A global comparison of the climatic niches of urban and native tree populations. *Global Ecology & Biogeography*, 27(5), 629-637.

Krasny, M. E., & Tidball, K. G. (2012). Civic ecology: a pathway for Earth Stewardship in cities. *Frontiers in Ecology and the Environment*, 10(5): 267-273.

Lehner, B., Döll, P., Alcamo, J., Henrichs, T., & Kaspar, F. (2006). Estimating the impact of global change on flood and drought risks in Europe: a continental, integrated analysis. *Climatic Change*, 75(3), 273-299.

Lenoir, J., Hattab, T., & Pierre, G. (2017). Climatic microrefugia under anthropogenic climatic change: implications for species redistribution. *Ecography*, 40(2), 253-266.

Liang, L., Wang, Z., & Li, J. (2019). The effect of urbanization on environmental pollution in rapidly developing urban agglomerations. *Journal of Cleaner Production*, 237, 117649.

Locosselli, G. M., Krottenthaler, S., Pitsch, P., Anhuf, D., Ceccantini, G. (2017). Age and growth rate congeneric tree species (*Hymenaea spp*. - Leguminosae) inhabiting different tropical biomes. *Erdkunde*, 71, 45-57.

Locosselli, G. M., Camargo, E. P., Moreira, T. C. L., Todesco, E., Andrade, M. F., André, C. D. S., André, P. A., Singer, J. M., Ferreira, L. S., Saldiva, P. H. N., & Buckeridge, M. S. (2019). The role of air pollution and climate on the growth of urban trees. *Science of the Total Environment*, 666, 652-661.

Locosselli, G. M., Brienen, R. J. W., Leite, M. S., Gloor, M., Krothenthaler, S., Oliveira, A. A., Barichivich, J., Anhuf, D., Ceccantini, G., Schöngart, J., & Buckeridge, M. S. (2020). Global tree-ring analysis reveals rapid decrease in tropical tree longevity with temperature. *Proceedings of the National Academy of Sciences*, 117(52), 33358-33364.

Loram-Lourenço, L., Farnese, F. S., Souza, L. F., Alves, R. D. F. B., Andrade, M. C. P., Almeida, S. E. S., Moura, L. M. F., Costa, A. C., Silva, F. G., Galmés, J., Cochard, H., Franco, A. C., & Menezes-Silva, P. E. (2020). A structure shaped by fire, but also water: ecological consequences of the variability in bark properties across 31 species from the Brazilian Cerrado. *Frontiers in Plant Science*, 10, 1718.

Mace, G. M., Norris, K., & Fitter, A. H. (2012). Biodiversity and ecosystem services: a multilayered relationship. *Trends in Ecology & Evolution*, 27(1), 19-26.

Manoli, G., Fatichi, S., Schläpfer, M., Yu, K., Crowther, T. W., Meili, N., Burlando, P., Katul, G. G., & Bou-Zeid, E. (2019) Magnitude of heat islands largely explained by climate and population. *Nature*, 573: 55-60.

Marengo, J. A., Alves, L. M., Ambrizzi, T., Young, A., Barreto, N. J. C., & Ramos, M. R. (2020). Trends in extreme rainfall and hydrometeorological disasters in the Metropolitan Area of São Paulo: a review. *Annals of the New York Academy of Sciences*, 1472(1), 5-20.

McHugh, M. L. (2012). Interrater reliability: the kappa statistic. *Biochemia Medica*, 22, 276-282.

McPherson, E. G., Nowak, D. J., & Rowntree, R. A. (1994). *Chicago's urban forest ecosystem: results of the Chicago urban forest climate project* (Vol. 186). US Department of Agriculture, Forest Service, Northeastern Forest Experiment Station.

Meyer, D., Dimitriadou, E., Hornik, K., Weingessel, A., Leisch, F., Chang, C. C., & Lin, C. C. (2019). e1071: Misc Functions of the Department of Statistics, Probability Theory Group (Formerly: E1071), TU Wien, *R package version,* 1.7–3.

Miranda, P. L. S., Oliveira-Filho, A. T., Pennington, R. T., Neves, D. M., Baker, T. R., & Dexter, K. G. (2018). Using tree species inventories to map biomes and assess their climatic overlaps in lowland tropical South America. *Global Ecology & Biogeography*, 27, 899-912.

Mishara, B., Sandifer, J., Gyawali, R. B. (2019). Urban heat island in Kathmandu, Nepal: evaluating the relationship between NDVI and LST from 2000 to 2018. *International Journal of Environment,* 8(1), 17-29.

Mohanavelu, A., Kasiviswanathan, K. S., Mohanasundaram, S., Ilampooranan, I., He, J, Pigale, S. M., Soundharajan, R-S., & Mohaideen, M. M. D. (2020). Trends and non-stationarity in groundwater level changes in rapidly developing Indian cities. *Water,* 12, 3209.

Vaz Monteiro, M., Doick, K. J., Handley, P., & Peace, A. (2016). The impact of greenspace size on the extent of local nocturnal air temperature cooling in London. *Urban Forestry & Urban Greening,* 16, 160-169.

Moreira, T. C., Amato-Lourenco, L. F., da Silva G. T., Saldiva de Andre, C. D., de Andre, P. A., Barrozo. L. V., Singe, J., Saldiva, P. H. N., Saiki, M., & Locosselli, G. M. (2018). The use of tree barks to monitor traffic related air pollution: a case study in São Paulo–Brazil. *Frontiers in Environmental Science,* 6, 72.

Moss, J. L., Doick, K. J., Smith, S., & Shahrestani, M. (2019). Influence of evaporative cooling by urban forests on cooling demand in cities. *Urban Forestry & Urban Greening*, 37, 65-73.

Mullaney, J., Lucke, T., & Trueman, S. J. (2015). A review for benefits and challenges in growing street trees in paved environments. *Landscape & Urban Planning*, 134, 157–166.

Myers. N., Mittermeier, R. A., Mittermeier, C. G., Fonseca, G. A. B., & Kent, J. (2000). Biodiversity hotspots for conservation priorities. *Nature*, 403, 853-858.

Nath, B., Ni-Meister, W., & Choudhury, R. (2021). Impact of urbanization on land use and land cover change in Guwahati city, India, and its implication on declining groundwater level. *Groundwater for Sustainable Development*, 12, 100500.

Negreiros, O. C., Carvalho, C. T., Cesar, S. F., Duarte, F. R., Deshler, W. O., & Thelen, K. D. (1974). Plano de manejo para o Parque Estadual da Cantareira. *Boletim Técnico do Instituto Florestal*, 10, 1–58.

Oke, T. R. (1982) The energetic basis of the urban heat-island. *Quarterly Journal of the Royal Meteorological Society*, 108: 1-24

Oleson, K. W., Monaghan, A., Wilhelmi, O., Barlage, M., Brunsell, N., Feddema, J., Hu, L., & Steinhoff, D. F. (2015). Interactions between urbanization, heat stress, and climate change. *Climatic Change*, 129(3-4), 525-541.

Oliveira, P. T. S., Wendland, E., Nearing, M. A., Scott, R. L., Rosolem, R., & Rocha, H. R. (2015). The water balance components of undisturbed tropical woodlands in the Brazilian Cerrado. *Hydrology & Earth System Sciences*, 19, 2899-2910.

Oliveira, R. S., Bezerra, L., Davidson, E. A., Pinto, F., Klink, C. A., Nepstad D. C., & Moreira, A. (2005). Depp root function in soil water dynamics in Cerrado savannas of central Brazil. *Functional Ecology*, 19(4), 574-581.

Olson, D. M., Dinerstein, E., Wikramanayake, E. D., Burgess, N. D., Powell, G. V., Underwood, E. C., D'amico, J. A., Itoua, I., Strand, H. E., Morrison, J. C., Loucks, C. J., Allnutt, T. F., Ricketts, T. H., Kura, Y., Lamoreux, J. F., Wettengel, W. W., Hedao, P., & Kassem, K. R. (2001). Terrestrial Ecoregions of the World: A New Map of Life on Earth. A new global map of terrestrial ecoregions provides an innovative tool for conserving biodiversity. *BioScience*, 51(11), 933-938.

Ordóñez, C., & Duinker, P. N. (2013). An analysis of urban forest management plans in Canada: implications for urban forest management. *Landscape & Urban Planning*, 116, 36-47.

Özgüner, H., Kendle, A. D., & Bisgrove, R. J. (2007) Attitudes of landscape professionals towards naturalistic versus formal urban landscape in the UK. *Landscape & Urban Planning*, 81(1-2), 34-45.

Peng, S., Piao, S., Ciais, P., Friedlingstein, P., Ottle, C., Bréon, F-M., Nan, H., Zhou, L., & Myneni, R. B. (2012). Surface urban heat island across 419 global big cities. *Environmental Science & Technology*, 46, 696-703.

Pianka, E. R. (1966) Latitudinal gradients in species diversity: a review of concepts. *The American Naturalist*, 100: 33-46.

Pincetl, S. (2015). Cities as novel biomes: recognizing urban ecosystem services as anthropogenic. *Frontiers in Ecology & Evolution*, 3, 140.

Ramage, B. S., Roman, L. A., & Dukes, J. S. (2013). Relationships between urban tree communities and the biomes in which they reside. *Applied Vegetation Science*, 16, 8-20.

Ryan, C. M., Pritchard, R., McNicol, I., Owen, M., Fisher, J. A., & Lehman, C. (2016) Ecosystem services from southern African woodlands and their future under global change. *Philosophical Transactions of the Royal Society B*, 371, 20150312

Reis, C. A. F., Souza, A. M., Mendonça, E. G., Gonçalvez, F. R., Melo, R. M. G., & Carvalho, D. (2009). Diversidade e estrutura genética espacial de *Calophyllum brasiliense* Camb. (Clusiaceae) em uma floresta paludosa. *Revista Árvore*, 33(2), 265-275.

Ren, Z., Pu, R., Zheng, H., Zhang, D., & He, X. (2017) Spatiotemporal analyses of urban vegetation structural attributes using multitemporal Landsat TM data and field measurements. *Annals of Forest Science*, 74: 54.

Ribeiro, S. C., Fhrmann, L., Soares, C. P. B., Jacovine, L. A. G., Kleinn, C., & Gaspar, R. O. (2011). Above- and belowground biomass in a Brazilian Cerrado. *Forest Ecology & Management*, 262, 491-499.

Richardson, D. M., Pysek, P., Rejmánek, M., Barbour, M. G., Panetta, F. D., & Wet, C. J. (2000). Naturalization and invasion of alien plants: concepts and definitions. *Diversity & Distribution*, 6, 93-107.

Ruggiero, P. G. C., Pivello, V. R., Sparovek, G., Teramoto, E., & Neto, A. G. P. (2006). Relação entre solo, vegetação e topografia em área de Cerrado (Parque Estadual de Vassununga, SP): como se expressa em mapeamentos? *Acta Botanica Brasilica*, 20(2), 383-394.

Rossatto, D. R., Toniato, M. T. Z., & Durigan, G. (2008). Flora fanerogâmica não-arbórea do cerrado na Estação Ecológica de Assis, Estado de São Paulo. *Brazilian Journal of Botany,* 31, 409-424.

Sala, O. E., & Maestre, F. T. (2014). Grass-woodland transitions: determinants and consequences for ecosystem functioning and provision of services. *Journal of Ecology*, 102, 1357-1362.

Scharenbroch, B. C., Morgenroth, J., & Maule, B. (2016). Tree species suitability to bioswale and impact on the urban water budget. *Journal of Environmental Quality* 45, 199-206.

Schlaepfer, M. A., Guinaudeau, B. P., Martins, P., & Wyler, N. (2020). Quantifying the contributions of native and non-native trees to a city's biodiversity and ecosystem services. *Urban Forestry & Urban Greening*, 56: 126861.

Schlaepfer, M. A. (2018). Do non-native species contribute to biodiversity? *PloS Biology*, 16(4): e2005568.

Seto, K. C., Fragkias, M., & Güneralp, B. (2011). A meta-analysis of global urban land expansion. *Plos One*, 6, e23777.

Silva, E. M. F. D., Bender, F., Monaco, M. L. D. S. D., Smith, A. K., Silva, P., Buckeridge, M. S., Elbl, P. M., & Locosselli, G. M. (2019). Um novo ecossistema: florestas urbanas construídas pelo Estado e pelos ativista. *Estudos Avançados*, 33(97), 81-102.

Silva, J. M. C., & Bates, J. M. (2002). Biogeographic patterns and conservation in the South America Cerrado: a tropical savanna hotspot. *BioScience*, 52(3), 225-233.

Steenberg, L. W. N., Millward, A. A., Duinker, P. N., Nowak, D. J., & Robinson, P. J. (2015). Neighborhood-scale urban forest ecosystem classification. *Journal of Environmental Management*, 163, 134-145.

Stewart, G. H., Meurk, C. D., Ignatieva, M. E., Buckley, H. L., Magueur, A., Case, B. S., Hudson, M., & Parker, M. (2009). Urban biotopes of Aotearoa New Zealand (URBANZ) II: Floristics, biodiversity and conservation values of urban residential and public woodlands, Christchurch. *Urban Forestry & Urban Greening*, 8, 149-162.

Sukkop, H., & Weiler, S. (1988). Biotope mapping and nature conservation strategies in urban areas of the Federal Republic of Germany. *Landscape & Urban Planning*, 15, 39-58.

Sydnor, T. D., & Subburayalu, S. K. (2011). Should we consider expected environmental benefits when planting larger or smaller tree species. *Arboriculture & Urban Forestry*, 37(4), 167-172.

Tannus, J. L. S., Assis, M. A., & Morellato, L. P. (2006). Reproductive phenology in dry and wet grassland in an area of Cerrado at Southeastern Brazil, Itirapina-SP. *Biota Neotropica*, 6(3), 00.

Teixeira, A. P., & Assis, M. A. (2005). Caracterização florística e fitossociologia do componente arbustivo-arbóreo de uma floresta paludosa no Município de Rio Claro (SP), Brasil. *Revista Brasileira de Botânica*, 28(3), 467-476.

Teixeira, A. P., & Assis, M. A. (2009). Relação entre heterogeneidade ambiental e distribuição de espécies em uma floresta paludosa no Município de Cristais Paulista, SP, Brasil. *Acta Botânica Brasilica,* 23(3), 843-853.

Tomlinson, C. J., Chapman, L., Thornes, J. E., & Baker, C. J. (2010). Derivation of the Birmingham's summer surface urban heat island from MODIS satellite images. *International Journal of Climatology,* 32, 214-224.

Tonello, K. C., Stan II, J. T. V., Rosa, A. G., Balbinot, L., Pereira, L. C., & Bramorski, J. (2021). Stemflow variability across tree stem and canopy traits in the Brazilian Cerrado. *Agricultural & Forest Meteorology*, 308-309, 108551.

Tucker, C. J. (1979). Red and photographic infrared linear combinations for monitoring vegetation. *Remote Sensing of Environment*, 8: 127-150.

United Nations, Department of Economic and Social Affairs, Population Division (2018). *The world's cities in 2018* – Data Booklet (ST/ESA SER.A/417).

Venables, W. N., Ripley, B. D. (2002). *Modern applied statistics with S-PLUS.* Springer Science & Business Media.

Urbonas, B., Guo, J. C. Y., & Tucker, L. S. (1989). Sizing Capture Volume for Stormwater Quality Enhancement. *Flood Hazard News*, 19(1), 1-9.

Usteri, A. (1911). *Flora der umgebung der Stadt São Paulo in Brasilien*, Verlag von Gustav Fischer Jena, 271.

Vitousek, P. M., D'antonio, C. M., Loope, L. L., Rejmanek, M., & Westbrooks, R. (1997). Introduced species: a significant component of human-caused global change. *New Zealand Journal of Ecology*, 1-16.

Yadav, B., Gupta, P. K., Patidar, N., & Himanshu, S. K. (2020). Ensemble modelling framework for groundwater level prediction in urban areas of India. *Science of the Total Environment*, 712, 135539.

Yilmaz, B., Gülez, S., Kaya, G. (2010). Mapping of biotopes in urban areas: a case study of the city of Bartin and its environs, Turkey. *Scientific Research & Essays*, 5(4), 352-365.

Yuan, F., & Bauer, M. E. (2006). Comparison of impervious surface area and normalized difference vegetation index as indicator of surface urban heat island effects in Landsat imagery. *Remote Sensing of Environment*, 17, 3071-3076.

Yuan, J., Dunnett, N., & Stovin, V. (2017). The influence of vegetation on rain garden hydrological performance. *Urban Water Journal*, 14(10), 1083-1089.

Whitney, G. G., & Adams, S. D. (1980). Man as maker of new plant communities. *Journal of Applied Ecology*, 17, 431-448.

Wilcove, D. S., Rothstein, D., Dubow, J., Phillips, A., & Losos, E. (1998). Quantifying threats to imperilled species in the United States. *BioScience*, 48(8), 607-615.

Wild, T., Freitas, T., & Vandewoestijne, S. (2020) *Nature-based Solutions: state of the art in EU-funded projects.* Publications Office of the European Union.

Willig, M. R., Kaufman, D. M., & Stevens, R. D. (2003) Latitudinal gradients of biodiversity. *Annual Review of Ecology, Evolution and Systematics*, 34: 273-309.

Wong, M. M. F., Fung, J. C. H., & Yeung, P. S. (2019) High-resolution calculation of the urban vegetation fraction in the Pearl River Delta from the Sentinel-2 NDVI for urban climate parametrization. *Geoscience Letters*, 6, 2.

Woodward, F. I., Lomas, M. R., & Kelly, C. K. (2004). Global climate and the distribution of plant biomes. *Philosophical Transactions of the Royal Society of London. Series B: Biological Sciences*, 359(1450), 1465-1476.

Zappi, D. C., Filardi, F. L. R., Leitman, P., Souza, V. C., Walter, B. M., Pirani, J. R., ..., Forzza, R. C. (2015). Growing knowledge: an overview of seed plant diversity in Brazil. *Rodriguésia,* 66(4), 1085-1113.

Zerbe, S., Maurer, U., Schmitz, S., & Sukopp, H. (2003) Biodiversity in Berlin and its potential for nature conservation. *Landscape and Urban Planning*, 62: 139-148.

Zhang, H., & Jim, C. Y. (2014). Contributions of landscape trees in public housing estates to urban biodiversity in Hong Kong. *Urban Forestry & Urban Greening*, 13(2), 272-284.

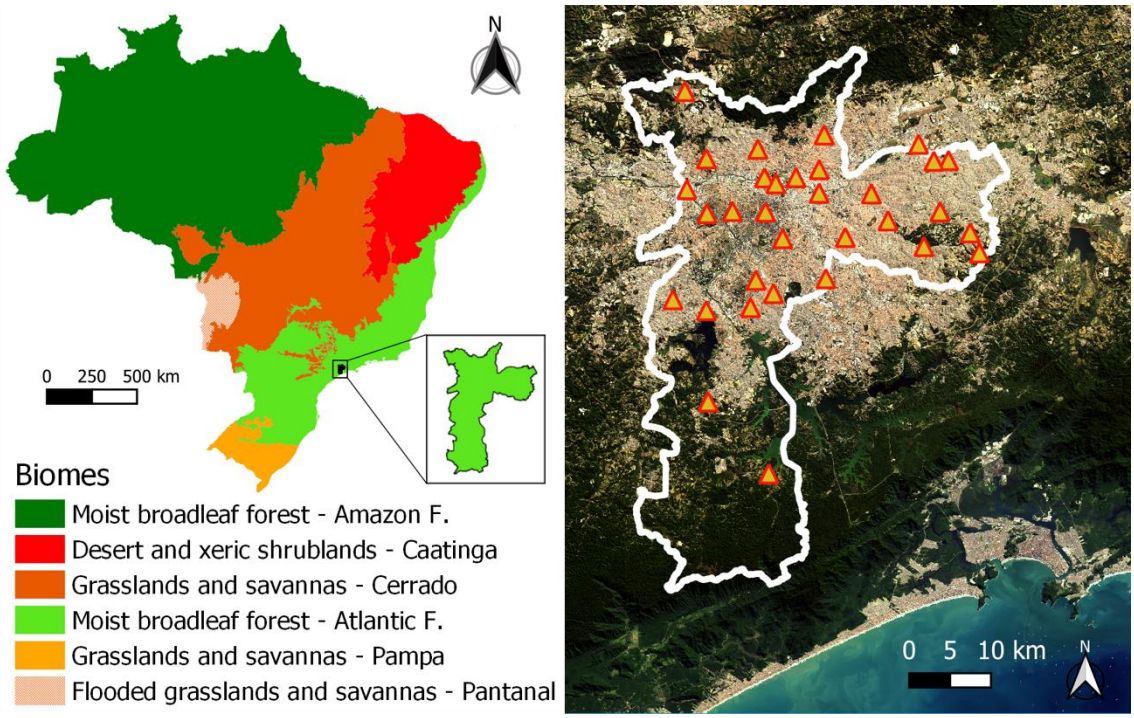

Figure 1: The left panel shows the Official Brazilian Biomes and the location of the city of São Paulo in the Atlantic Forest biomes, a Tropical Moist Broadleaf Forest according to the international biome's classification (Olson et al., 2001). The right panel shows a detail of the city of São Paulo (white outline) on a panchromatic satellite imagery (Landsat 8) with the 28 climate stations of the Emergency Management Center of the City of São Paulo used in the validation of the spatially interpolated climate variables.

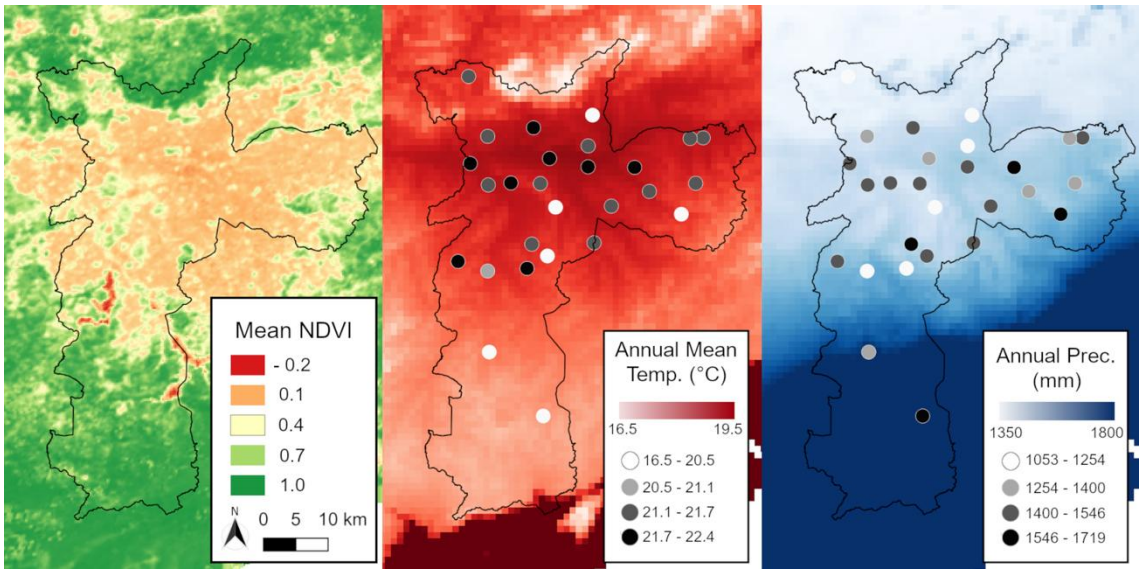

Figure 2: Spatial distribution of variables related to the vegetation structure and climate in the city of São Paulo (black outline). Vegetation structure is represented by the mean NDVI ratio, while the seasonality of the vegetation structure is represented by the ratio of the NDVI values between the summer (wet season) and the winter (dry season). Climate spatial variability is represented here by the annual mean temperature and the total annual precipitation values. For the seasonal NDVI, precipitation and temperature, refer to Figure S6). The circles represent the climate stations from the Center of Emergency Management of São Paulo (CGE). Shades of gray indicate the values of the respective climate variables in each of the stations (refer to Figure S7 for the linear association between the interpolated data and the data from the CGE stations).

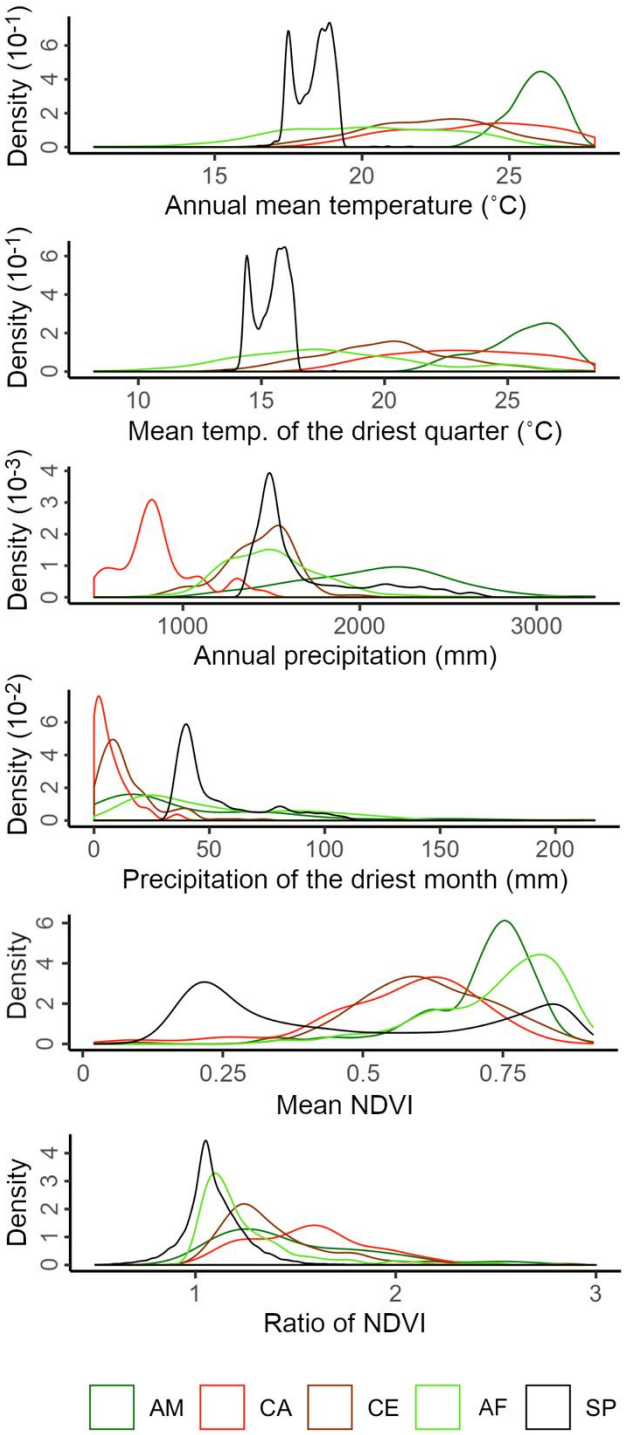

Figure 3: Density plots showing the distribution of the vegetation and climate variables used the Linear Discriminant Analysis. Distribution of the values are show for the main Official Brazilian Biomes (AM: Amazon Forest – Tropical Moist Broadleaf Forest, CA: Caatinga - Tropical Deserts and Xeric Shrublands, CE: Cerrado – Tropical Grassland and Savanna, and MA: Atlantic Forest – Tropical Moist Broadleaf Forest) and the city of São Paulo.

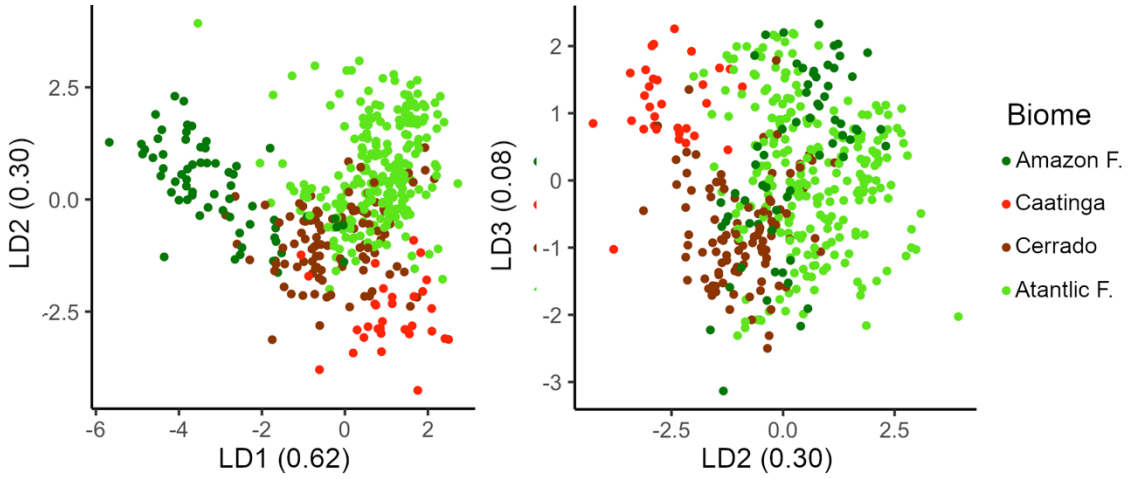

Figure 4: Scatterplot of the Linear Discriminant Analysis used to classify the main Brazilian biomes. Proportion of the explained variability is given for each Linear Discriminant axes (LD). This discriminant model has an accuracy of 80%.

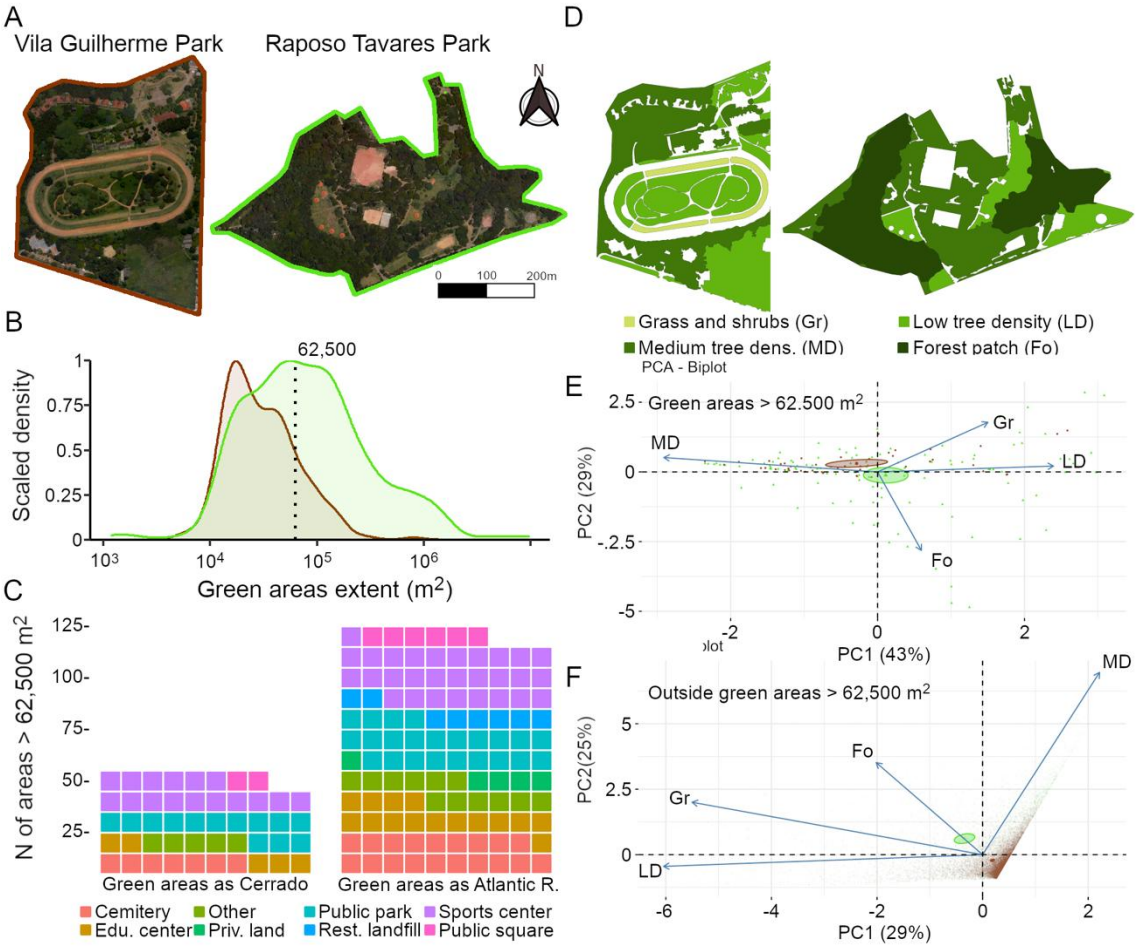

Figure 5: Detailed evaluation of the green spaces from the city of São Paulo, A) with two examples of Public Parks classified as Cerrado (brown outline) and Mata Atlantica (green outline). B) The distribution of green spaces extent is displayed in the density plot, C) whose land use are described for areas larger than 62.500 m^2. D) An example of the distribution of four types of green cover in two Public Parks, E) and the Principal Component Analyses of the proportion of green cover in green spaces with more than 62,500 m^2 (ellipses indicate 95% confidence interval), and F) of the proportion of green cover outside the green spaces but across the urban fabric (ellipses indicate 95% confidence interval).

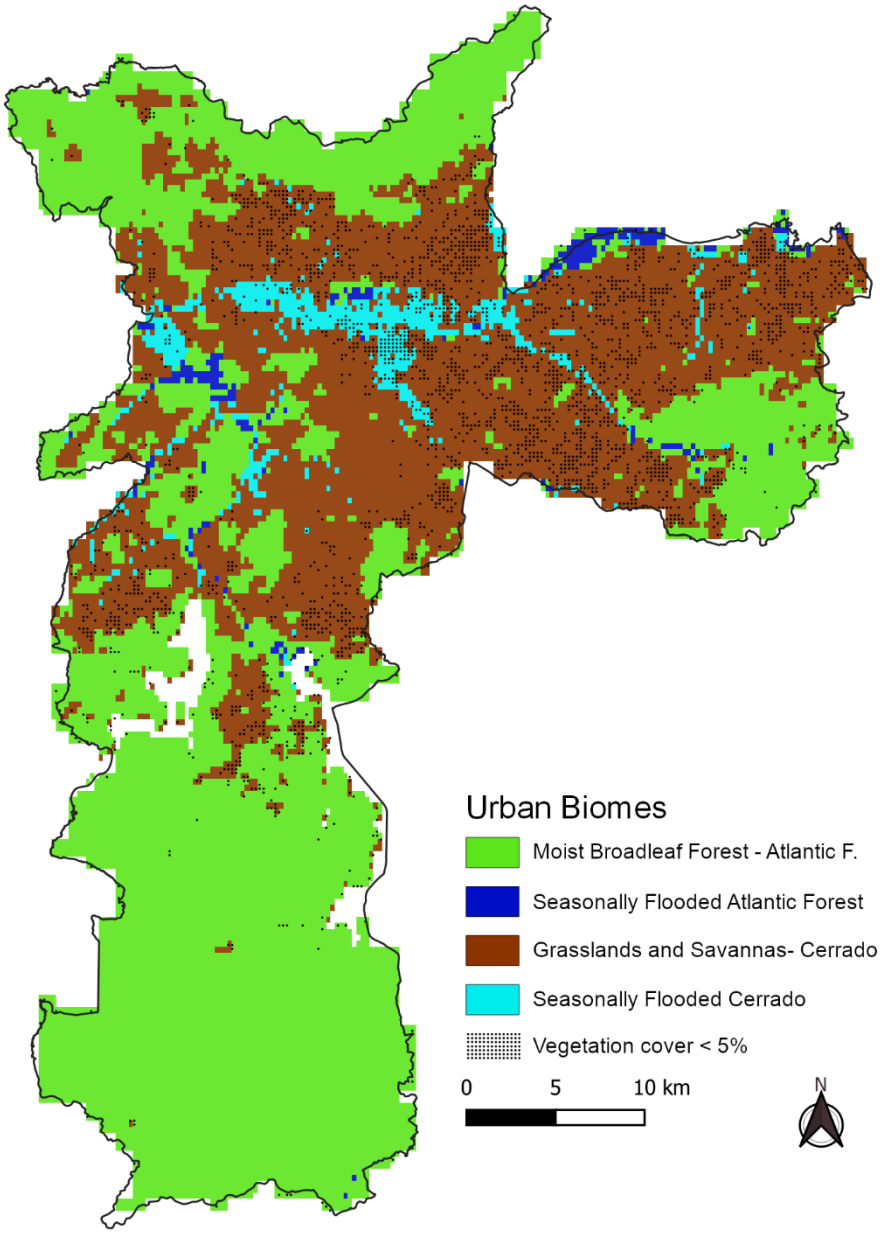

Figure 6: Classification of the city of São Paulo in the Urban Biomes (refer to Figure 1), according to the extant climate conditions and vegetation structure. Seasonally flooded areas in each biome are based on the overlaying naturally flooding areas of the main rivers in the city (Flood Areas map from GeoSampa).

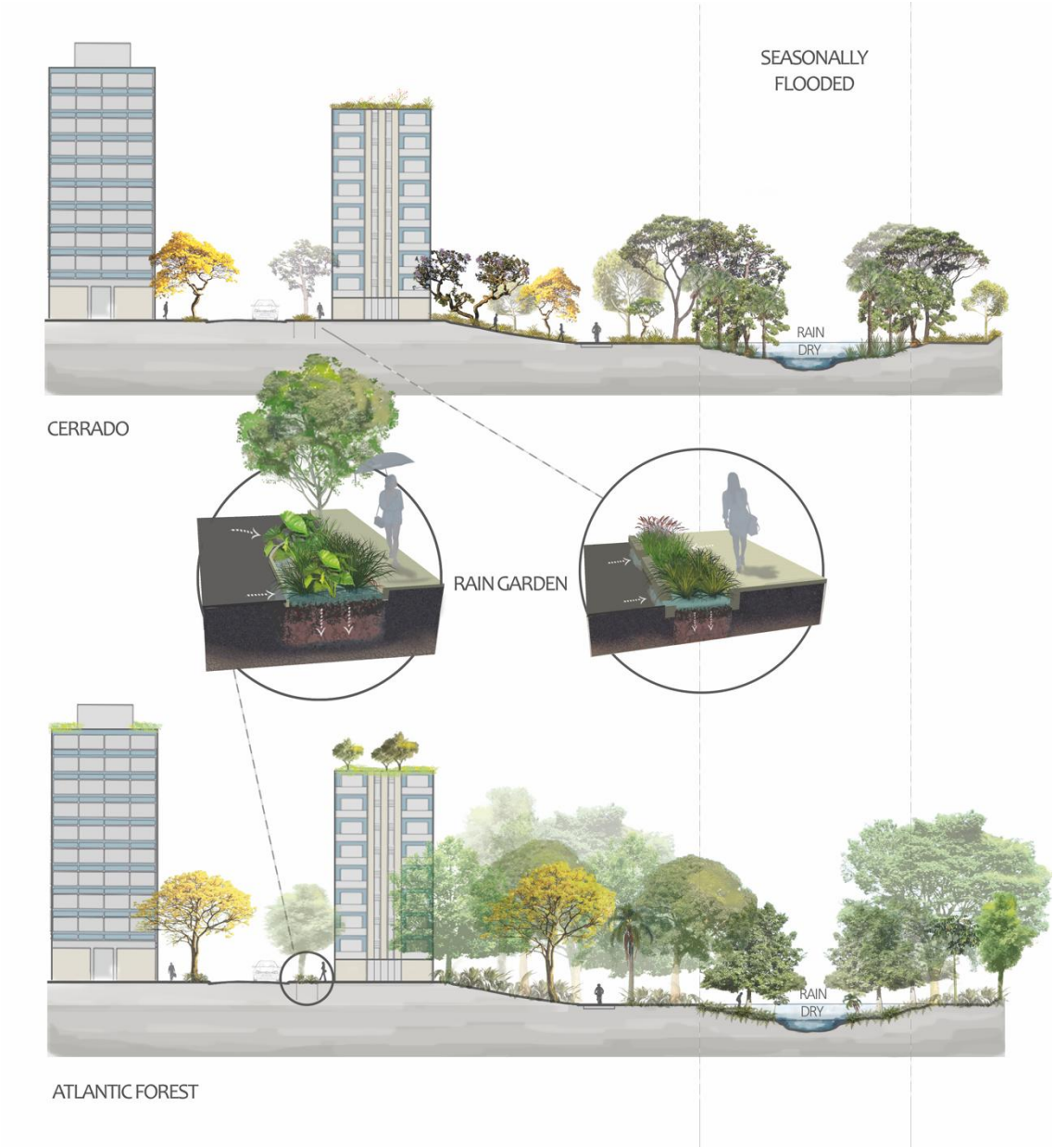

Figure 7: Examples of possible interventions of green infrastructure according to the four Urban Biomes in the city of São Paulo.

Table 1: Coefficients of the Linear Discriminant Analysis used to classify the Official Brazilian Biomes.

Variables	LD1	LD2	LD3
Mean NDVI	-0.13	0.48	0.38
Ratio NDVI (max NDVI / min NDVI)	-0.09	-0.24	0.25
Annual mean temperature	0.92	0.42	-0.84
Mean temp. of the warmest quarter	1.58	2.13	-0.83
Annual precipitation	-1.20	0.80	-1.16
Precipitation of the driest month	0.26	-0.37	0.84
Precipitation of the coldest quarter	0.01	0.42	0.75

Supplementary material

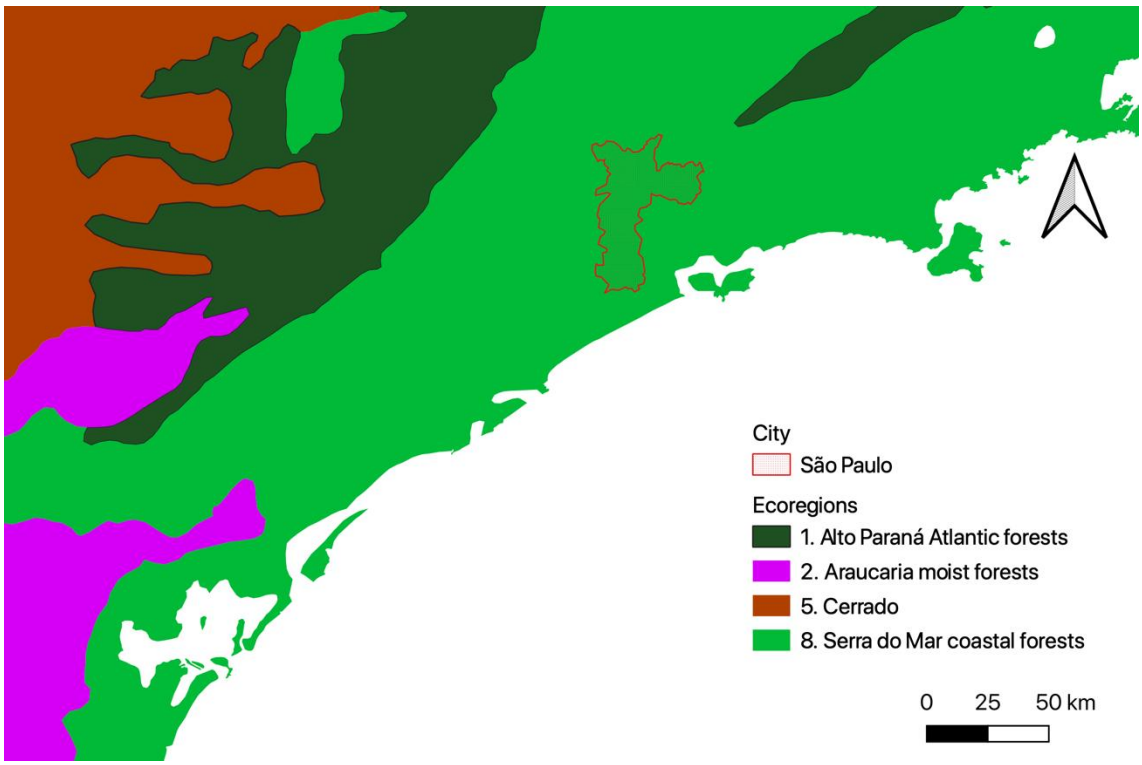

Figure S1: Location of São Paulo in the Serra do Mar coastal forest ecoregion in Brazil.

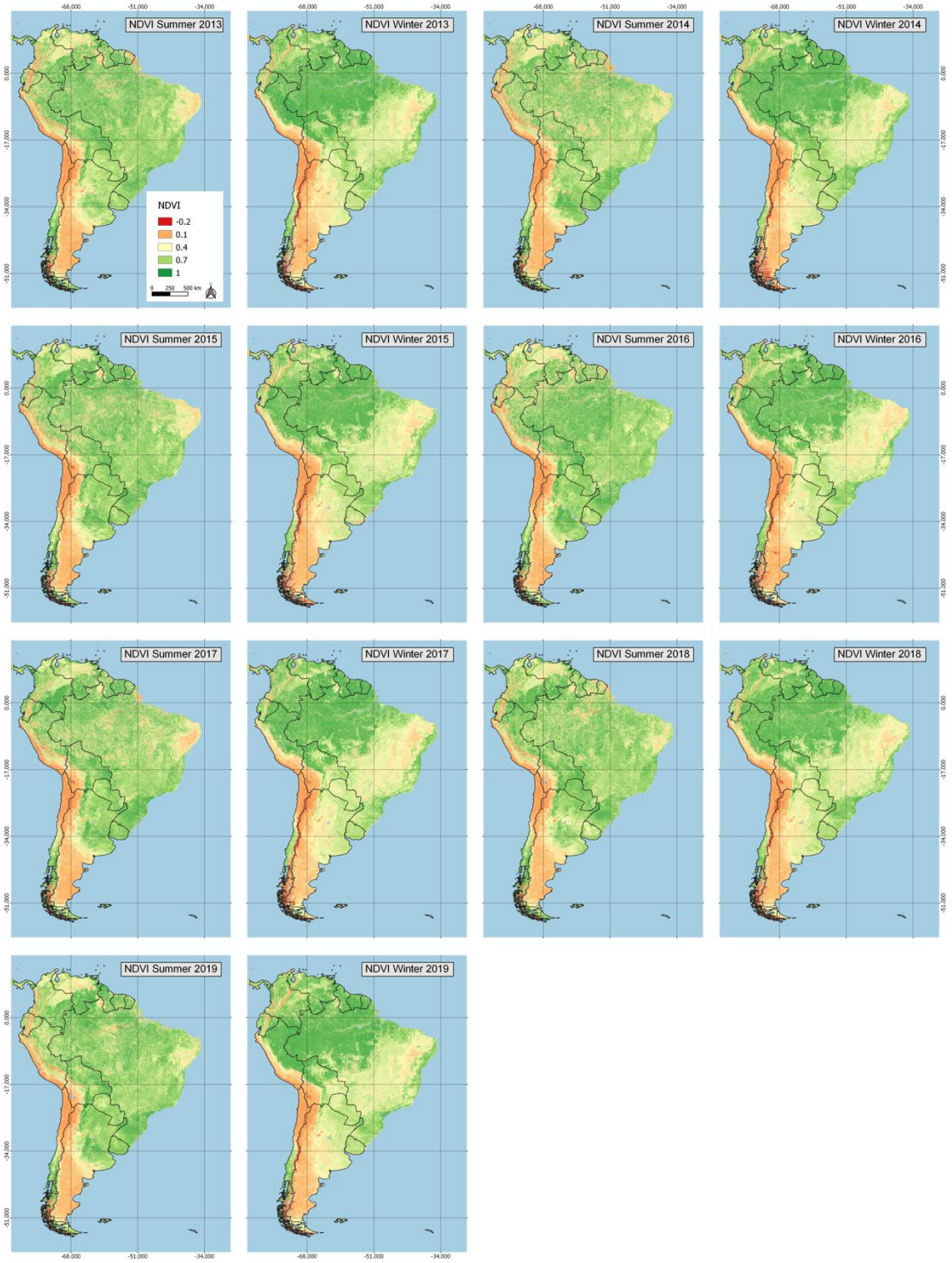

Figure S2: Example of the spatial and temporal variability of the NDVI over South America and Brazil.

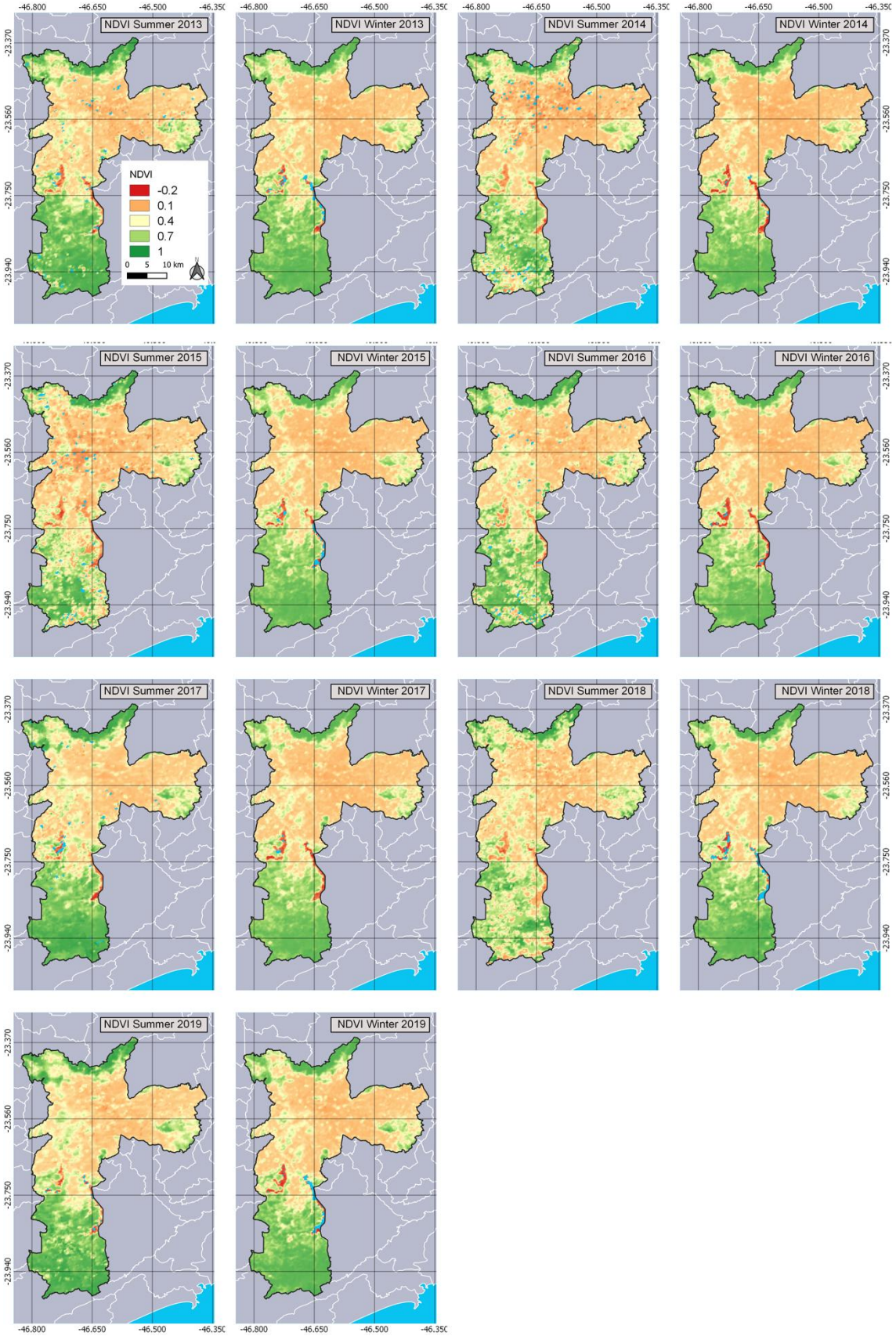

Figure S3: Temporal and spatial variability of the NDVI across the city of São Paulo between the summer and winter from 2013 to 2019.

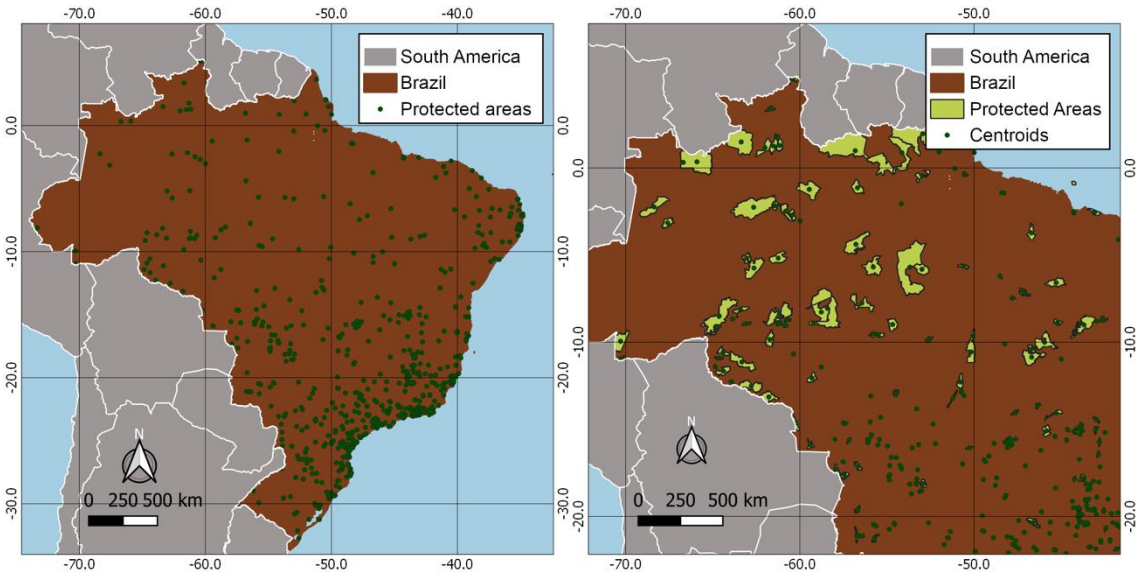

Figure S4: Map with all the protected areas used in this study to characterize the main Brazilian Biomes. Data for the characterization of the Biomes were obtained at the centroids of the polygon of each protected area.

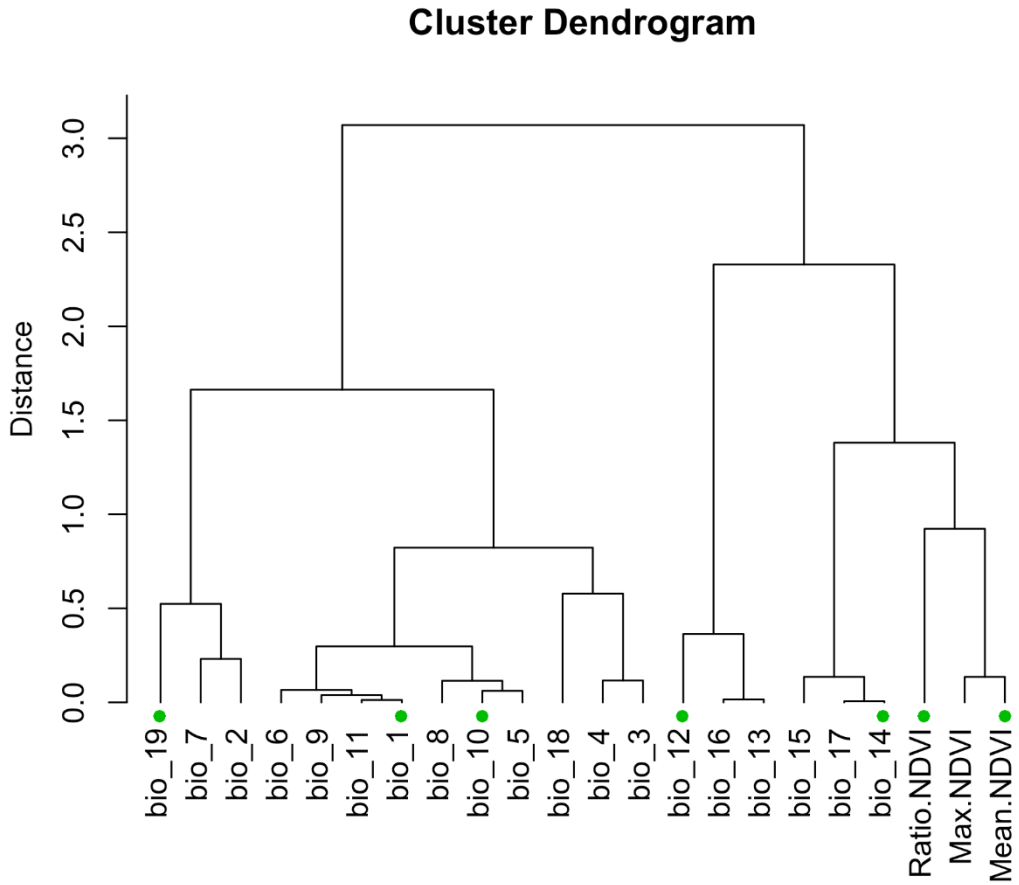

Figure S5: Result of the Hierarchical Clustering Analysis using all bioclimatic and NDVI variables initially used in this study. Lower distance between variables indicates higher collinearity. We used these variables to run the Linear Discriminant Analysis for characterizing the Brazilian Biomes. The best model in terms of accuracy uses the variables indicated by the green circles.

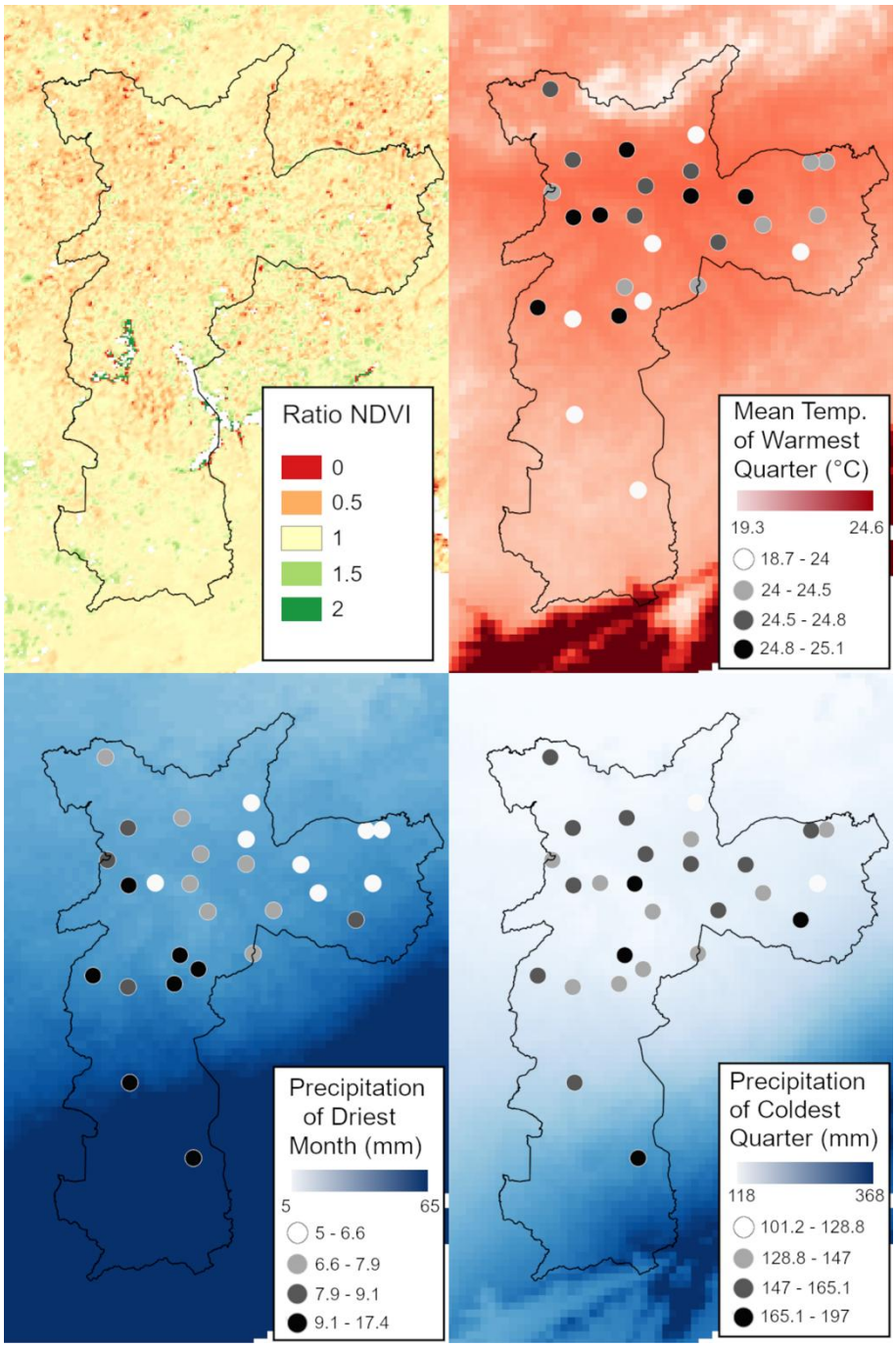

Figure S6: Spatial distribution of variables related to the vegetation structure and climate in the city of São Paulo (black outline), variables related to the climate and vegetation structure in the city of SP, in addition to that shown in Figure S3. The circles represent the climate stations from the Center of Emergency Management of São Paulo (CGE). Shades of gray indicate the values of the respective climate variables in each of the stations (refer to Figure S7 for the linear association between the interpolated data and the data from the CGE stations).

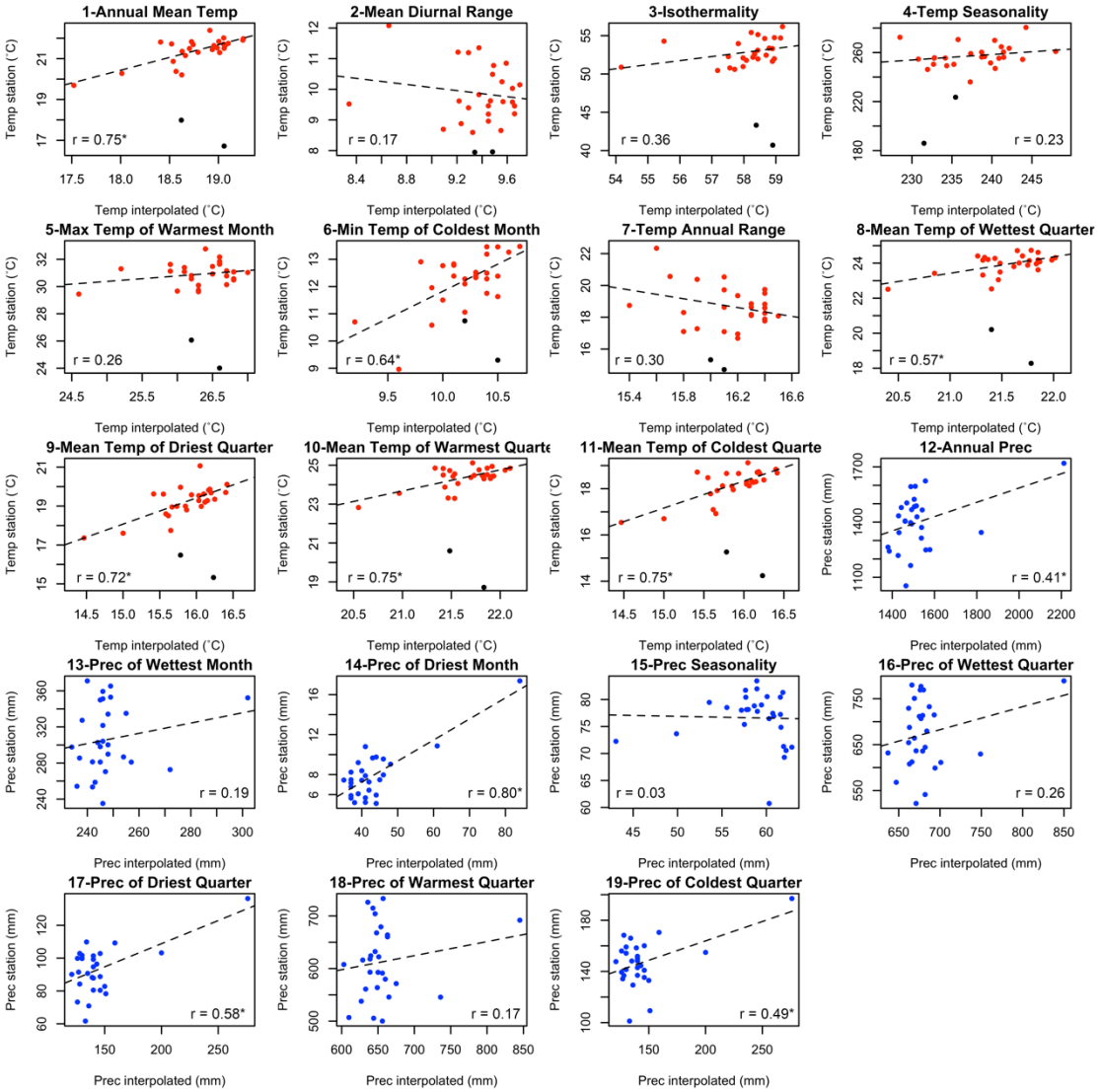

Figure S7: Linear relationship between the bioclimate variables from the interpolated WordClim Data and the same variables calculated with the data from the local meteorological stations.

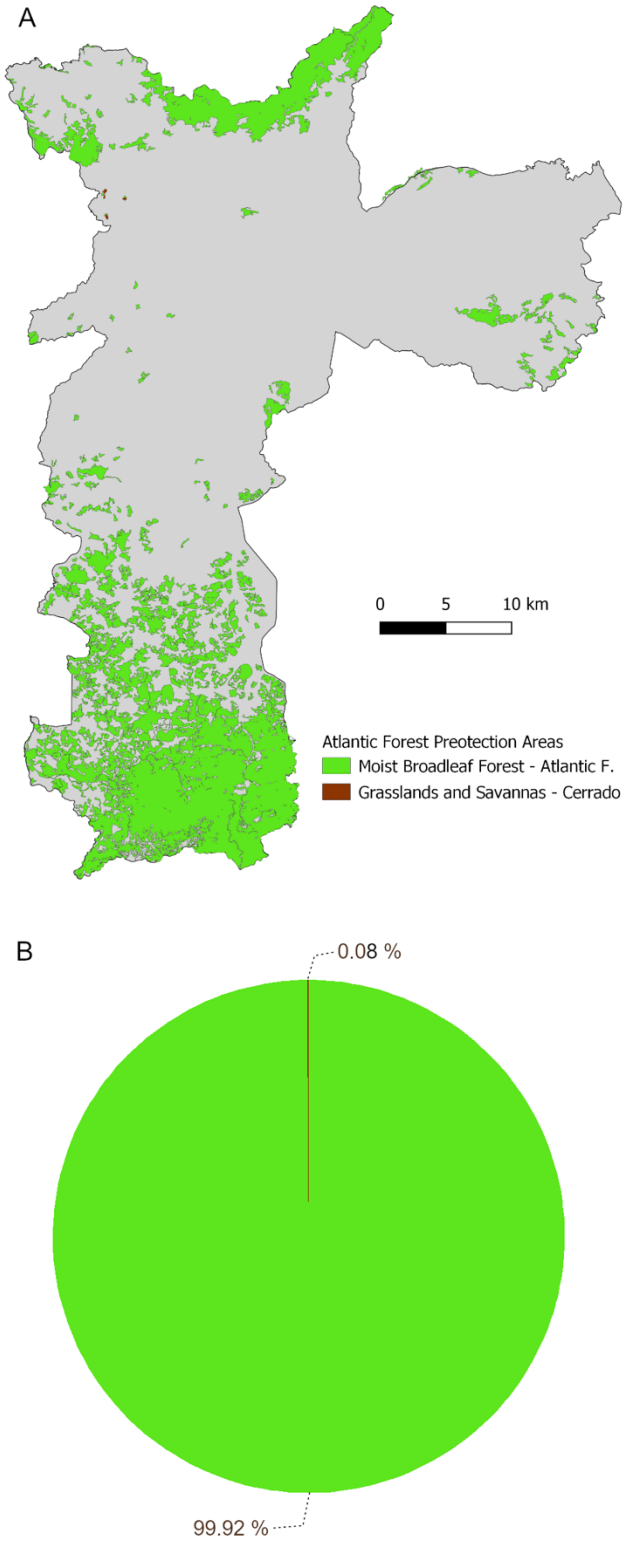

Figure S8: Validation of the discriminant model in the city through the classification of the Atlantic Rainforest remnants of São Paulo.

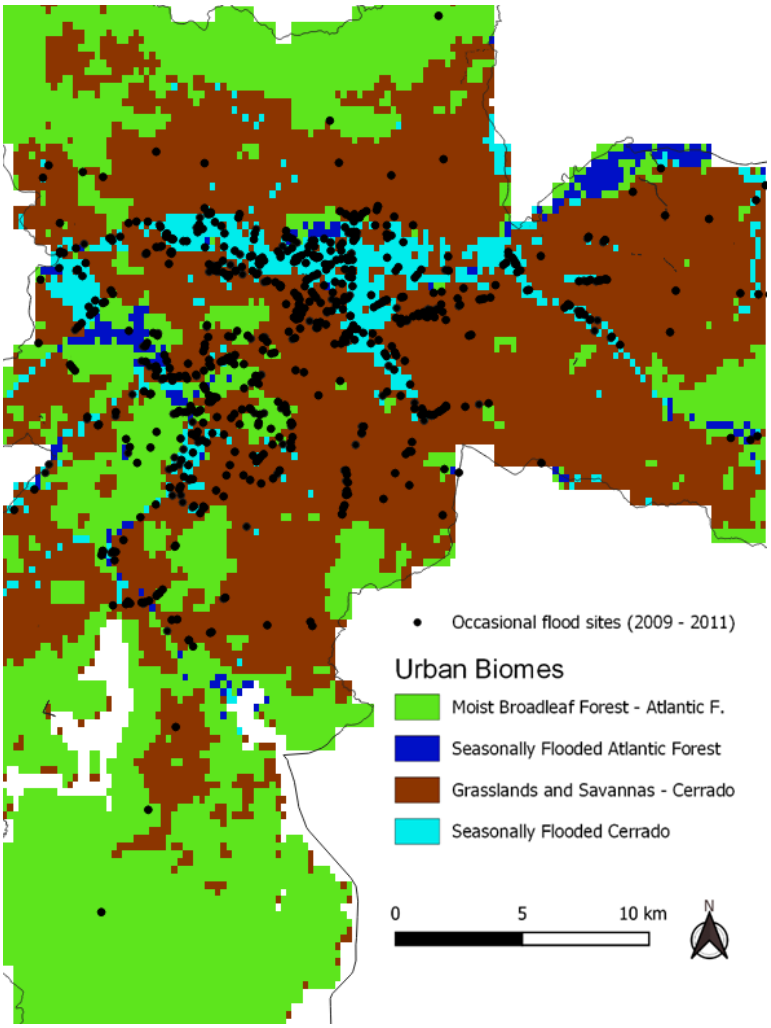

Figure S9: Similarity between the spatial distribution of the estimated seasonally flooded urban biomes and the occurrence of floods in the city between the years of 2009 and 2011 (Data from: FCTH / USP).

Table S1: Mean values of the standardized variables of vegetation index (NDVI), precipitation (P.) and temperature (T.), used to classify the Official Brazilian Biomes (AM: Amazon Forest, CA: Caatinga, CE: Cerrado, AR: Atlantic Forest) with the Linear Discriminant Analysis.

Biome	Mean NDVI	Ratio NDVI	Annual T.	T. warmest quarter	Annual P.	P. driest month	P. coldest quarter
AM	0.12	0.52	1.27	1.10	1.39	0.12	1.22
CA	-1.02	0.54	0.67	0.54	-1.70	-0.87	-0.41
CE	-0.61	0.20	0.16	0.02	-0.22	-0.69	-0.59
AF	0.36	-0.29	-0.48	-0.37	-0.06	0.37	-0.02

Table S2: Confusion matrix for the linear discriminant analysis of the main Official Brazilian Biomes in extension (AM: Amazon, CA: Caatinga, CE: Cerrado, AF: Atlantic Forest).

Prediction	AM	CA	CE	AF
AM	11	0	3	0
CA	0	5	1	1
CE	0	0	19	7
AF	2	0	7	51

Table S3: Rotation values of the variable in the PCA based on the data of the green spaces with more than 62,500m^2.

	PC1	PC2	PC3	PC4
Grass	0.37	0.53	-0.68	0.35
Low	0.58	0.06	0.62	0.51
Medium	-0.71	0.15	0.09	0.68
Forest	0.15	-0.83	-0.37	0.38

Table S4: Absolute and cumulative proportion of the variance explained by each of the four principal components of the green spaces with more than 62,500m^2.

Importance of components	PC1	PC2	PC3	PC4
Standard deviation	1.31	1.08	0.95	0.47
Proportion of variance	0.43	0.29	0.23	0.05
Cumulative proportion	0.43	0.72	0.95	1.00

Table S5: Rotation values of the variable in the PCA based on the data outside the green spaces with more than 62,500m^2.

	PC1	PC2	PC3	PC4
Grass	-0.63	0.25	0.35	0.64
Low	-0.69	-0.06	0.09	-0.71
Medium	0.25	0.86	0.34	-0.27
Forest	-0.23	0.44	-0.87	0.08

Table S6: Absolute and cumulative proportion of the variance explained by each of the four principal components outside the green spaces with more than 62,500m^2.

Importance of components	PC1	PC2	PC3	PC4
Standard deviation	1.08	1.00	0.99	0.92
Proportion of variance	0.29	0.25	0.25	0.21
Cumulative proportion	0.29	0.54	0.79	1.00

Capítulo 2

Challenges and advances in intra-annual tree-ring stable isotope research, a systematic review

Manuscript published in *Dendrochronologia* 85 (2024) 126218.

https://doi.org/10.1016/j.dendro.2024.126218

Abstract

The intra-annual stable isotope approach emerged in the 1970s as a cornerstone in dendrochronology temporal resolution. Despite the recent progress, it still grapples with methodological and interpretation hurdles that limit its potential. Aiming at stepping forward and envisaging the systematization of the intra-annual approach, we systematically reviewed the literature using a search expression on SCOPUS that resulted in 132 eligible studies. From each study, we gathered data on sampling sites, stable isotopes, studies' goals, sampling methods, and results interpretation. This review points to geographical biases reflecting the early dendrochronological development in temperate sites, disbelief in tropical tree rings, and the eventual limited access to high-end methods in developing countries. Although methods like laser microdissection and ablation-combustion open new research avenues, cheap razor blades are the primary sampling tool. If sampling is not the bottleneck, the number of analyses is because of the trade-off between the number of intra-annual samples and the chronology length observed in the studies. Dendroecological studies rely on dozens of intra-annual samples obtained across short tree-ring series, whereas dendroclimatological studies assess a few segments, often earlywood and latewood, over a hundred-year-long series. We also identified two main approaches in the analyses of the intra-annual data, either the studies obtained intra-ring samples and analyzed them on an interannual basis using long-established dendrochronological methods to address common question in dendroclimatology and dendroecology, or they analyzed the seasonal variability of the intra-annual stable isotopes using novel statistical approaches addressing new research questions. These questions range from the potential to reconstruct short-term extreme climate events to a detailed evaluation of the responses of trees to environmental stress. Based on the analyses of these studies, we bring five propositions for methodological advances and discuss future research avenues. These prospects and propositions are a starting point for systematizing the intra-annual stable isotope approach and fostering research.

Keywords: Carbon isotopes, Oxygen Isotopes, Deuterium, Dendroecology, Dendroclimatology, Methodological advances.

1. Introduction

Stable isotopes emerged in dendrochronology by the 1950s as a source of potential progress in geochemistry and plant physiology (Craig, 1954). After decades of successful research on an interannual basis, tree-ring stable isotopes studies naturally evolved to the intra-annual scale as a cornerstone in dendrochronology temporal resolution (Andreu-Hayles et al, 2022; Kagawa and Battipaglia, 2022; Ogle and McCormac, 1994), holding the promise of a more refined method for dendrochronological reconstructions (Wilson and Grinsted, 1975; Wilson and Grinsted, 1977; Tans and Mook, 1980; Leavitt and Lone, 1991). Despite this high promise, many challenges and achievements have been reported over the last decades of intra-annual stable isotope research. These advances are yet to be systematized.

There is no question that one of the main challenges in such high-resolution studies is to sample intra-annual segments. Taking samples at high spatial, and thus temporal, resolution can be time-consuming and a labor-intensive task (Li et al, 2011). Tackling this challenge has pushed forward the development of new sampling methods to meet the precision requirements, oftentimes at a very high cost (Belmecheri et al, 2022; Kagawa and Battipaglia, 2022; Giraldo et al, 2022; Ohashi et al, 2009). Microtomes (Helle and Schleser, 2004; Martínez-Sancho et al, 2022), robotic micro-milling (Dodd et al, 2008; Poussart et al, 2004), laser microdissection (Schollaen et al, 2014; Schollaen et al, 2017) and laser ablation (Schulze et al, 2004; De Micco et al, 2012, Saurer et al, 2023) are all high-end equipment and methods used for precisely producing intra-annual samples. As the need for precision increases, expensive cutting-edge technology and sophisticated techniques are required (Helle et al, 2022), eventually limiting the access of a broader scientific community to this approach.

Higher resolution analyses also mean more intra-annual samples to be handled and analyzed. The number of segments reported by the studies in this field varies from two (*e.g.* Marshall and Monserud, 1996; An et al, 2012; Tepley et al, 2020), usually earlywood and latewood, to dozens of samples (*e.g.* Ogle and McCormac, 1994; Gessler et al, 2009; Treydte et al, 2014) according to the studies goals. There are still caveats in the methodological choices and currently no standard definition in the sampling design. Including if sampling should follow a similar segment width across various tree rings, producing a distinct number of intra-annual samples per tree ring (*e.g.* Leavitt, 1993; Cintra et al, 2019; Xu et al, 2020), or if the number of intra-annual samples should remain constant across distinct tree rings (*e.g.* Sheu et al, 1996; Leavitt, 2002; Locosselli et al, 2020a). In addition, the oftentimes used multiple isotopes approach in interannual studies (Roden et al, 2022) poses increasing complexity at the intra-annual scale,

as the multiplication effect manifests in terms of labor, time, and resources needed (Dodd et al, 2008; Nabeshima et al, 2018; Giraldo et al, 2022). Therefore, these decisions currently come down to the parsimony among the requirements of each study's goal, and the availability of time and financial resources to produce and analyze the samples.

Having decided on the sampling methods, one must face the challenge of analyzing and interpreting the high-resolution data. Because dendrochronology has traditionally relied on annual datasets, dividing the tree rings into intra-annual segments but analyzing them on a year-to-year basis is a straightforward way to use the set of standard dendrochronological methods put together throughout decades. This annual approach of the intra-annual segments can offer significant advances in dendrochronology, like isolating the strongest climate signal for reliable climate reconstruction. Recovering stronger climate signals using intra-annual segments is possible because the tree-ring stable isotopes depend not only on the source signal but also on endogenous and exogenous factors that modulate fractionation processes throughout the growing season (Leavitt and Roden, 2022). We are aware of these endogenous and exogenous factors acting along the growing season because of studies devoted to the analysis of the intra-annual variability of stable isotopes - that brings information on a daily, weekly, and monthly basis (Barbour et al, 2002; Berkelhammer et al, 2009; Sarris et al, 2013; Belmecheri et al, 2022). It is based on such high-resolution measurements that allocation and mobilization of carbon during the growing season has been described in certain species and site conditions (Jäggi et al, 2002; Kimak and Leuenberger, 2015; Nabeshima et al, 2018). These metabolic strategies can result in recurrent trends of $\delta^{13}C$ (Leavitt and Lone, 1991) like the decreasing trend from the early- to the latewood attributed to the use of carbon reserves during the onset of the growing season.

These applications point to the potential of the intra-annual approach in investigating climate, environmental conditions, and tree physiology at a high temporal resolution. Despite holding such a high promise, this approach is still surrounded by methodological and interpretation challenges that can limit its full potential. We performed the first systematic review to evaluate the current state-of-art of this approach to propose future directions for further development in this field. A handful of questions guided our review, namely: I) Is there any geographical bias worldwide driven by the accessibility to the means of this approach? II) What are the main methods used for intra-annual sampling and their advantages and disadvantages? III) What are the main intra-annual sampling designs used in these studies and is it possible to systematize them to promote consistent and comparable results across future studies? IV) Is there any consistent interpretation narrative of intra-annual isotope series across all the studies? V) What

are the main scientific advances supported by the intra-annual approach? We believe this systematic review is a starting point for the systematization of the intra-annual approach to support future development in the field.

2. Material and Methods

2.1 Study design

We used PRISMA 2020 framework (Page et al, 2021) to guide the survey, data acquisition, analysis, and narrative building regarding the state-of-art in intra-annual tree-ring stable isotopes. We built a search expression (see Supplementary material) comprising three primary groups of keywords and their potential synonyms. The first group of keywords refers to the "intra-annual" resolution, including potential synonyms like "high-resolution", "within-rings", and "seasonal", to name a few. The second group of keywords relates to the specific parameter under examination in this systematic review, which is "stable isotopes", including "$\delta^{13}C$", "$\delta^{18}O$", and "deuterium". We chose not to include $\delta^{15}N$ in this review due to the complexity of the N cycle in trees, involving translocations between leaves, stems, roots, and even between tree rings. In addition, external factors such as anthropogenic emissions of reactive N, and the activity of dinitrogen-fixing microbes in the soil can influence the $\delta^{15}N$ ratio in plant materials (Savard and Siegwolf, 2022). The amount of sample required for $\delta^{15}N$ analysis in tree rings is also significantly higher than $\delta^{13}C$ or $\delta^{18}O$, for the naturally low concentration of N in the wood (Savard and Siegwolf, 2022). Such low concentrations potentially limit the application of intra-annual analysis using $\delta^{15}N$. Still, we only found one study about the intra-annual $\delta^{15}N$ (Reimchen and Arbellay, 2018) by adapting the original search expression to include this isotope.

We employed the original search expression to the Title, Abstract, and Keywords, to research articles published up to April 2022. We obtained a total of 333 studies on Scopus and assessed them by reading all the abstracts, removing those failing the inclusion criteria (Figure S1), including those focused on natural archives like: speleothems, corals, ice cores, and sediments, or conducted interannual tree-ring analyses. From this sample, 149 studies were initially considered eligible for this systematic review. After a full-text evaluation, 47 were removed for not meeting one or more inclusion criteria, resulting in a sample of 102 studies. We conducted a second round of surveys to identify studies not captured by the initial search expression. This step was undertaken by checking the references of the 105 studies sample. An additional 350

potential studies were selected, however, 65 of them had already been included during the first round of screening. Therefore, the abstract of 285 new studies was assessed, and 62 of them initially met the inclusion criteria (Figure S1). Two additional studies that match the inclusion criteria, but were not found in the steps mentioned above, were included for analysis. This new sample of 64 studies was assessed for eligibility by a full-text reading, and only 30 were included in this review. The survey resulted in a final sample of 132 studies. Any additional study that has been published after the limit date of the literature survey, but that may represent a significant step in terms of tackling the challenges of the intra-annual approach, was not included in the analysis to allow the reproductivity of this systematic review but was brought to the discussion to support the definition of prospects.

2.2 Data acquisition and analysis

2.2.1. Geographical patterns and temporal trends

We assessed the global distribution of intra-annual stable isotope studies to determine whether this approach exhibits a geographical bias across tropical or extra-tropical countries. We refer to the tropics all land between 30˚N and 30˚S, including the subtropics (Corlett, 2013). And we refer to the extra-tropics, all land outside this rage. In this analysis, the coordinates of all sampling sites or experiments conducted for each study were documented and plotted on a map created using the QGIS software. We also evaluated the temporal trends of the studies across the tropics and extra-tropics and among the three stable isotopic pairs. We plotted this data using a stacked area graph.

2.2.2. Methodological characteristics

We also grouped the studies into three major categories and respective subcategories according to their applications, based on their main objectives and interpretation of the results: I) Dendroclimatology, II) Dendroecology, and III) Methodological Advances. The criteria for defining these categories are described in Table 1. To assess whether there is a discernible preference of tree species for intra-annual stable isotope studies, we quantified all the species sampled and categorized them as conifer or broadleaf species. The global distribution of conifer and broadleaf aligns with patterns related to tropical and extra-tropical regions (Condamine et al, 2020), aiding the discussion of the potential species across different climate zones. The

species sampled in two or more studies were compiled in a heatmap. These species were grouped by stable isotopic pairs and the main category of application goals, using a cluster analysis (Ward method).

Given the significance of selecting the isotopic pairs for the intended analysis and the importance of deciding whether to use multiple isotopes or not to achieve the research objectives, we build an UpSet plot to quantify the use of each isotope and their combinations. We also quantified the use of each isotope type per studies' goals as discriminated in Table 1 to find any associations between these categories and the preferred isotopes as sources of information.

We also gathered data on species' types of habits, classifying them as trees, shrubs, or lianas. The sample sites were categorized as either field-based or experimental (including field experiments such as irrigation or fertilization). We also noted whether pulse labeling was used or not. The sample materials were assessed, including the use of whole-wood, cellulose, or lignin as well as the intra-ring sampling method, whether by blade, micro-milling, or laser. We also assessed how sampling was designed, either by segment with equal width or mass, and if there is any trade-off between the number of intra-annual segments in the tree rings and the number of tree rings in the studies.

2.2.3. Data interpretation

To assess how the intra-annual stable-isotope results have been interpreted by each study, we first characterized the intra-annual patterns reported for the $\delta^{13}C$ for its consistent patterns across growing conditions (Leavitt and Lone et al, 1991). We characterized the overall $\delta^{13}C$ patterns described in the studies as follows: I) decreasing trend; II) bell-shape, in which the value is lower at the beginning, increases by the middle of the tree ring, and then decreases; III) u-shape, in which the values are high at the beginning, decrease by the middle of the tree ring, and increase again by the end; IV) increasing trend; and V) stable. We based our classification on the description of the intra-annual trends by the authors, or we defined the major patterns based on the study's graphics whenever the authors failed to provide it in the text. We did not predefine the patterns for the $\delta^{18}O$ and $\delta^{2}H$ for their high variability trends reported in the studies.

We listed the physiological and environmental factors that influenced intra-ring stable isotope trends for each sample site in all studies based on the authors' interpretation of the data. We

established primary categories of influences on physiology and the environment to consolidate the overall influences and facilitate data interpretation. The main categories of influences, the inclusion criteria, and all the reported influences in all 132 studies are given in detail in Table S2. The relationship between isotopes, patterns, and influences was summarized using a Sankey chart.

3. Results and discussion

3.1 Global overview of the intra-annual studies

This systematic review yielded a sample size of 132 studies (Table S1). The final dataset pervades 49 countries across six continents (Figure 1). The United States (32 studies), China (11), France (9), Italy (9), Russia (7), Germany (6), and Switzerland (6) hold the highest number of studies in descending order, respectively (Figure 1). The geographical distribution and historical trends in intra-annual tree-ring research follow the historical development of dendrochronology itself, pioneered by Dr Andrew Douglas in the US in the early 20th century (Stokes and Smiley, 1996), followed by a rapid expansion and application in Europe and elsewhere. Nonetheless, the onset of intra-annual studies only took place in the 1970s (Figure 2A) likely for requirements in basic science investment and technological advances common to the global north. Thus, North American and European tree species dominate in the intra-annual stable isotope studies as the most commonly used species, including *Pinus ponderosa*, *Pinus sylvestris*, *Pinus strobus*, *Pseudotsuga menziesii*, and *Quercus petrea*, to mention a few (Figure S2). China disrupts these historical trends likely due to unprecedented scientific development during the recent decades (Woolston et al, 2023).

Conversely, research on tropical countries consistently lagged behind (Figure 2B). It began in the early 2000s not only because of the early disbelief in the annual nature of tropical tree rings due to the lack of significant temperature seasonality (Bijaksana et al, 2007) but also because of the delayed implementation of the costly isotopic research in developing countries that tend to have limited investment in science (Figure 2B). Thailand is a tropical country that stands out in terms of the number of studies (6 studies) because of the focus on the local *Tectona grandis* (Figure S2), a broadleaf species renowned for its qualities in dendrochronology such as the formation of clearly distinct ring porous wood and sensitive tree rings (Bijaksana et al, 2007). These are early arguments in favor of using a more laborious and expensive method on tropical tree species.

Nonetheless, decades of tropical tree-ring research demonstrated the annual formation of tree rings under seasonal drought, flooding, and soil salinity (van der Sleen et al, 2022) and even in seemly ever-wet sites (Giraldo et al 2022). The intra-annual stable isotopes supported evidence on favor of growth seasonality in challenging tropical and eventually extratropical species including those with unclear tree-ring boundaries, such as in *Carapa guianensis, Cordia sp., Dipterocarpus intricatus, Dipterocarpus tuberculatus, Eusideroxylon zwageri, Goupia glabra, Hyeronima alchorneoides, Miliusa velutina, Ocotea tenera, Samanea saman, Quercus kerrii, Shorea henryana, Shorea johorensis, Shorea superba, Shorea obtuse* and *Styrax tonkinensis* (Evans and Schrag, 2004; Poussart et al, 2004; Poussart and Schrag, 2005; Verheyden et al, 2006; Anchukaitis et al, 2008; Ohashi et al, 2009; Ballantyne et al, 2011; Loader et al, 2011; Pons and Helle, 2011; Xu et al, 2014; Ohashi et al, 2016).

In the surveyed studies, the stable carbon isotopes stand out not only as one of the first isotopes employed on an intra-annual basis in the 1970s (Wilson and Grinsted, 1975; Figure 2A) but also as the main isotopic approach in our study sample (Figure 3). The use of carbon isotopes consolidated the intra-annual analysis as a valuable approach during the 1990s. From the 2000s onward, the number of intra-annual studies displayed a substantial increase fostered not only by studies based on carbon stable isotopes but also on oxygen (Figure 2), with a significant share of them applying the dual-isotope approach (Scheidegger et al, 2000). These historical trends reveal almost two decades of methodological development and validation in intra-annual stable isotope research before its ample use.

The late use of the intra-annual $\delta^{18}O$ likely reflects the more sophisticated and costly procedures like pyrolysis instead of the combustion used for the carbon analysis. However, the advent of the $\delta^{18}O$ allowed more comprehensive studies to take place using not only the carbon isotopes as a source of valuable information but also the $\delta^{18}O$, whose interpretation challenges will be discussed in the next section. Still, using two isotopes is rather common in the literature (Figure 3), and eventually, a triple approach is also possible by adding the $\delta^{2}H$, but at the cost of multiplying the challenges in sampling intra-annual segments, storing, and analyzing them.

3.2 Methodological advances

Other than the choice of the isotopic pairs, one must also decide on the study target and where it will take place. By far, trees sampled at their natural location (Figure 4B; 92.4% of the surveyed studies) are the main target of intra-annual studies. Still, other habits of wooden

species showed up in our survey, like shrubs (*e.g.* Battipaglia et al, 2010; de Micco et al, 2012; Battipaglia et al, 2014; He et al, 2021) and lianas (*e.g.* Verheyden et al, 2006). This ample application of the intra-annual approach proves its potential for species with remarkably low growth rates such as the dwarf shrubs common to high latitudes (Schweingruber et al, 2013) or at altitudes (Dolezal et al, 2016), expanding the potential of intra-annual isotope approach for natural areas without favorable conditions for tree development (Büntgen et al, 2014). In addition to the lianas with their cambial variants that result in complex and diverse morphological stem architectures, especially in the tropics (Brandes et al, 2022), which represents an alternative niche in tropical woodlands and an important element of the ecosystem functioning (Brandes et al, 2022).

Regarding the material to be analyzed, not every study relies on cellulose extraction for the intra-annual stable isotope analysis (Figure 4C). Cellulose and other constitutes of the wood like lignin can, at least in theory, hold distinct isotopic signals because of the different metabolic pathways and deposition during cell-wall synthesis and xylogenesis (Locosselli and Buckeridge, 2017). It is true for the interannual $\delta^{13}C$ signal as observed in past studies (Wilson and Grinsted, 1977) since lignin is more depleted than the cellulose (Helle et al, 2022). However, this difference may not be substantial when analyzing the intra-annual $\delta^{13}C$ signature since both cellulose and lignin can display a similar intra-annual pattern of $\delta^{13}C$ values (Schulze et al, 2004). Thus, in theory, intra-annual stable isotopes in the whole wood can still suite for some applications like climate reconstruction (Tans and Mook, 1980; Jahren and Sternberg, 2008; Schubert and Timmermann, 2015; Vornlocher et al, 2021), assessment of climate signal (Fichtler et al, 2010; Treydte et al, 2014; Baton et al, 2017; Landshuter et al, 2020), methodological advances in sample preparation (Verheyden et al, 2005; Li et al, 2011), xylogenesis (de Micco et al, 2012), and for species with indistinct growth rings (Verheyden et al, 2004; Loader et al, 2011; Pons and Helle, 2011).

3.2.1. Intra-annual sampling methods

Dividing the tree rings into sub-annual segments is one of the main methodological bottlenecks in intra-annual studies. There is a clear predominance of the use of all sorts of blades in dividing the tree rings (86.3% of the studies) regardless of the material: either whole wood, cellulose, or lignin. Razor blades are commonly employed in intra-annual studies likely for their sharpness and low cost. Disposable microtome blades are a shaper and likely a more robust alternative, that comes at a higher cost. Still, in both cases, the delimitation of the exact area of the tree ring

to be cut is visual and, therefore, not entirely precise. Vessel patterns may help to delimit the segment outline, usually aided by scanned images of the polished wood surface as a guide to support the segmentation of cellulose cross-sections (Kagawa et al, 2015; Schollaen et al, 2015). For more precise intra-annual sampling, microtomes may be used to produce segments with even width in whole-wood samples that may or not be subject to cellulose extraction. Micro-milling and micro-drilling are alternative methods that can also be employed for intra-annual sampling (Dodd et al, 2008). They allow sampling several centimeters along the tree-ring circumference at a high-spatial precision while homogenizing each intra-annual segment, reducing circumferential variations, and producing a more representative isotopic signature (Dodd et al, 2008). This approach produces wood-powder samples that can directly meet the requirements for the whole-wood analyses, bypassing the grinding step, or for cellulose extraction protocols based on wood powder.

Even higher precision and productivity may be achieved by using powerful laser sources. Laser microdissection offers an ultrahigh dissection precision to the micrometer scale (Schollaen et al, 2014). These virtues come at a significant cost when compared to a rotary microtome that can also reach high precision levels. Still, only the laser microdissection will allow one to obtain precise samples with an outline other than straight lines, a valuable feature for delimiting specific tree-ring anatomical structures like fibers and vessels, sampling tree rings close to the pith, or for species with asymmetrical stem growth (Schollaen et al, 2014). One of the downsides of the laser microdissection is that the samples still must be placed into labeled containers for later weighting and packing inside silver or tin caps.

The laser ablation-combustion allows by-passing the latter steps by directly producing a nanoparticle aerosol from the sample surface that is carried out to the mass spectrometer for the determination of the isotopic ratio (Schulze et al, 2004). It is a considerable step forward in terms of spatial precision and productivity, although an extension of the laser ablation system to analyze $\delta^{18}O$ is still missing (Saurer et al, 2023). Despite all the advances and benefits of using laser ablation, it is still an inaccessible technology for most laboratories due to its high cost representing only 6.47% of the studies. The diversity of high-resolution sampling methods available (figure 4C) offers a different balance between cost and benefits, and the choice of which method to employ must be based on the goals and available resources.

3.2.2. Intra-annual sampling design

The sample size is another constraint in intra-annual stable isotope studies, as any other limitation scales up rapidly depending on the number of segments and tree rings to be studied. This constraint is represented by the trade-off between the number of tree rings and the number of intra-annual segments (Figure 5). Because the whole sample preparation and analyses are laborious and expensive, one must decide between a higher temporal resolution or a longer span (Figure 5) unless cost and time are no constraints in the study (which seems to be the case for Pons and Helle, 2011; Zhu et al, 2012; Xu et al, 2020).

On one side of this spectrum, studies focused on methodological advances as a proof of concept of the use of intra-annual segments (*e.g.* Ogle and McCorman, 1994; Ogée et al, 2009; de Micco et al, 2012; Schollaen et al, 2014) and studies on dendroecology trying to unveil the climate effect on plant's endogenous responses (*e.g.* Macfarlane and Adams, 1998; Barbour et al, 2002; Eilmann et al, 2010) have divided only very few tree rings into dozens to more than a hundred segments for a fine analysis of stable isotope variation and related fractionation processes. On the other end of the spectrum, studies focused on the validation of this approach for paleoclimate assessment and actual climate reconstruction for hundreds of years only rely on two segments per ring, usually splitting it into earlywood and latewood (*e.g.* Miller et al, 2006; An et al, 2012; Labotka et al, 2016; Szejner et al, 2020). Arguably, the laser ablation coupled to the mass spectrometer is the only sampling method that has the potential to overcome this trade-off by producing a high number of intra-annual samples in multiple tree rings (*e.g.* Skomarkova et al, 2006; Battipaglia et al, 2010; Soudant et al, 2016; Fonti et al, 2018).

There is no question that the higher number of intra-annual samples will increase the temporal resolution and the information retrieved from the tree rings (Figure 6A), but it can be tricky to tear apart the actual information from noise as one significantly increases the number of segments in the tree rings (Figure 6A). Even in studies that divided the tree ring into more than a hundred samples, the actual gain in information is very limited and may only work as a proof of concept (*e.g.* Fichtler et al, 2010; Eilmann et al, 2010). Another decision is either to divide all tree rings into an equal number of segments or not (Figure 6B). 51.4% of the surveyed studies produced an unequal number of segments per ring. This approach is acceptable for studies focusing on characterizing the intra-annual patterns of the stable isotopes, but it increases the complexity when trying to statistically analyse the dataset. One way of comparing intra-annual patterns among tree rings with an unequal number of segments is not to present the data in terms of absolute position within the tree ring, but in relative terms, like percentage of

the tree-ring width (Figure 6B). This approach is commonly employed by many studies and partially supports visual insights (*e.g.* Cintra et al, 2019). Conversely, dividing the tree rings into equal numbers of segments aids the statistical analysis for having a paired dataset across the tree rings (Leavitt, 2002). In addition, one may test and correct for shifts in the onset and end of the growing season among trees in the same population. These mismatches in the intra-annual series (Figure 6C) are likely expected in sites where the phenology of trees is not perfectly synchronized, as for the tropics (Vogado et al, 2016). Shifting the intra-annual series one position to the left or to the right may improve the synchrony between the series (Figure 6C; Locosselli et al, 2020a; Guimarães et al, 2024), a feature that can be measured by calculating the GLK (Gleichläufigkeit; Bura and Wilmking, 2015).

3.2.3. Space-for-time conversion

Although achieving a high spatial resolution in the tree rings is possible through various techniques, the identification of time intervals that correspond to each spatial unit within the tree ring is still challenging (Pérez-de-Lis et al, 2022). Monitoring the growth of the trees is probably one of the most reliable ways to attribute the period of intra-annual segment formation. In our sample of studies, the authors employed two methods to define this period of segment formation. High-resolution dendrometers allow one to build a seasonal growth curve that can be expressed by, for instance, a sigmoidal function that is used to integrate the growth and define the moment of formation of each segment (*e.g.* Barbour et al, 2002; Skomarkova et al, 2006; Offermann et al, 2011). Other studies used microcores to assess the moment of each segment formation (*e.g.* Leavitt, 2002). Despite being successfully employed, these approaches are limited to tree rings monitored during the study period, whereas assigning the time of formation of segments from past tree rings is trickier, if ever possible.

The most used sampling design, dividing the tree rings into segments of the same width (Figure 4D), can pose additional uncertainty in the space-for-time conversion for past tree rings because tree-ring growth is non-linear and the deposition of structural biomass during wood formation varies in time decoupling and overlapping of cell expansion and cell-wall thickening, resulting into segments that can represent different lengths of time (Pérez-de-Lis et al, 2022). Some authors have utilized generalized additive mixed models to calculate the kinetics of each cell and convert the segment's width into time (Martínez-Sancho et al, 2022). As an alternative for space-for-time conversion by segment's width, some authors proposed intra-annual sample preparation by segments with the same mass instead of width (Locosselli et al, 2020a; Sargeant

and Singer, 2016; Vornlocher et al, 2021). The use of segment mass to prepare intra-annual samples considers the wood density instead of the segment's width, a simplistic strategy of space-for-time conversion that considers the processes of xylogenesis. The main argument holds that wood density represents more closely the cambium activity than the width because higher wood density can reflect into periods of slower radial growth, mainly during the end of the growing season.

3.3. Scientific advances

This systematic review revealed two basic approaches in intra-annual analyses to answer questions related to dendroclimatology and dendroecology (Figure 7). 33.3% of the studies assessed the variability in the stable isotope values of each intra-annual segment on an interannual basis (Figure 7). It is an expected approach that builds upon long-used standard dendrochronological methods to answer overall well-established research questions on climate variability and ecology of trees. These studies usually sought for more refined information analyzed over decades to centuries on a year-to-year basis. Although building upon established fields is a common path in science, it was rather surprising to find that 56.4% of studies attempted to assess the seasonal variation of tree-ring stable isotopes (Figure 7), from the visual evaluation of the intra-annual trends to more complex experimental designs. These scientific advances will be discussed through the lens of these two approaches in the sections below.

3.3.1. Inter-annual analysis

3.3.1.1. In dendroclimatology

The climate signal/effect assessment predominates in the studies surveyed by this systematic review (63.3%). Water-related parameters like precipitation and air humidity are the main interpretation of environmental factors influencing the intra-annual signature observed in the tree rings (Figure 8) for carbon, oxygen, and deuterium. Studies based on the use of the intra-annual segments evaluated on an interannual basis usually aim at a more refined and reliable climate signal retreieved from the tree rings (45.2% of the studies). It is the case for dendroclimatological studies that look for the strongest climate signal for past reconstructions. Dividing the tree rings into earlywood and latewood is a basic approach, with some studies producing over 400-year-long chronologies for past climate reconstructions in the United States

(Labotka et al, 2016). Eventually, neither earlywood nor latewood positions record the strongest climate signal, but the position in between, depending on species and local conditions (Johnstone et al, 2013). These differences in the climate signal come down to how the isotopic ratios are modulated along the growth season, ranging from a pure metabolic and physiological signal to a predominance of the climate signal (Skomarkorva, 2006; Michelot, 2011).

Because the climate signal may not be constant along the tree-ring segments, in other words, along the growing season, the intra-annual analysis can further provide valuable insights into the phases of important climate modes, like the monsoon systems (*e.g.* Managave et al, 2010, Figure 8A). Monsoon systems are characterized by a seasonal oscillation in precipitation volume driven by the periodic shifts in the directions of atmospheric circulations between continents and oceans (Yihui and Chan, 2005), which can get imprinted in the tree-ring $\delta^{18}O$. For instance, tree-ring $\delta^{18}O$ records the onset of the Asian summer monsoon precipitation season over the Tibetan Plateau in the first intra-annual segment of *Abies georgei*, reaching strong association with the precipitation during the mature phase of the monsoon in the intra-annual positions two to four, the latter being the closest to the tree-ring boundary ($r = -0.81$, Xu et al, 2020). The distinction between early phases and the middle/peak of the upstream Indian Summer Moonson have also been reported in the earlywood and latewood, respectively, of *Tsuga chinesis* tree rings in the Himalayas (An et al, 2019), all valuable insights into the atmospheric circulation and moisture origin.

Some studies on dendroclimatology stand out by producing a substantial number of intra-annual segments on relatively long tree-ring series. Such a high-resolution intra-annual approach allowed them to step forward and retrieve detailed information on past climate variability by not only analyzing the absolute values of the stable isotopes in the intra-annual segments but also their variability within the tree rings. The use of the maximum and minimum oxygen values, and eventually the delta between them (Figure 7B), brings significant advances in the comprehension of the climate signal in the tree rings and past climate variability, especially for those invested in studying extreme events (Zhu et al, 2012; Xu et al, 2020; Schubert and Timmermann, 2015).

It is not only the oxygen isotopes that can retrieve valuable information about climate extremes. Detecting early signs of megadroughts like the one in place in the Southwestern United States is challenging. Whereas $\delta^{18}O$ and tree-ring width series of *Pinus ponderosa* failed to record the organizational phase of this megadrought, the $\delta^{13}C$ content of the early-wood and late-wood increased in the two decades before the drought, indicating an increase in the water-use efficiency in the driest-edge of this species' distribution (Szejner et al, 2021; Figure 8A).

3.3.1.2. In dendroecology

The advances in dendroecology supported by the interannual analysis of the intra-annual segments are overall less notable. The assessment of the effect of climate variability on the stable isotopes remains quite similar to standard inter-annual studies using tree-ring stable isotopes, many of them assessing how climate modulates the fractionation processes in different periods of the growing season (*e.g.* Livingston and Spittlehouse, 1996; Koretsune et al, 2009; Fu et al, 2017). The analysis of the Intra-annual Density Fluctuations (IADF) is probably one of the main advances in these studies invested in evaluating the climate influence on tree's functioning (Zalloni et al, 2018). Some of these studies focus on the direct impact of drought frequency on trees' functioning and try to report the presence of any drought legacies (Szejner et al, 2020). Climate legacies can be especially determined by correlating the stable isotope values between the earlywood of current rings and the previous latewood likely (Szejner et al, 2018). This comparison stems from the largely reported use of previously stored non-structural carbohydrates on the onset of the earlywood formation (Figure 7E). Such post-photosynthetic studies represent most of the scientific advances in the year-to-year intra-annual approach applied to dendroecology.

3.3.2. Seasonal analysis

The visual assessment of the intra-annual cycles was one of the first steps in the evaluation of the intra-annual stable isotopes on a seasonal basis (Tans and Mook, 1980; Wilson and Grinsted, 1975; Wilson and Grinsted, 1977; Nakatsuka et al, 2004; Schollaen, 2013; Helle and Scheleser, 2004; Sheu et al, 1996). The early evidence of intra-annual cycles was the initial motor for the remarkable development in this field. Some studies still rely on the visual assessment only as a sufficient approach to prove the annual nature of tree rings or to define annual growth cycles in ringless species, quite often in the tropics (Ohashi et al, 2016; Xu et al, 2014; Pons and Helle, 2011; Ohashi et al, 2009; Verheyden et al, 2004; Poussart et al, 2004; Anchukaits et al, 2008; Evans and Schrag, 2004). The visual evaluation of the intra-annual cycles is also common in studies combining the interannual and seasonal approaches, as a way of first describing the intra-annual trends in detail, to plan the sampling design and discuss the results of the interannual analysis (*e.g.* Leavitt, 2007).

3.3.2.1. In dendroclimatology

In dendroclimatology, the seasonal analysis not only provides a stronger climate signal than standard dendrochronological approaches (Xu et al, 2016), but also a better understanding of climate systems. Defining the precipitation volume and moisture source of the Asian monsoon system has been a natural application of intra-annual stable isotopes. Because the monsoon is the principal mode of atmospheric circulation and moisture redistribution in South-eastern Asia, many studies have successfully employed intra-annual $\delta^{18}O$ analysis to define the sources of moisture along the growth season (*e.g.* Managave et al, 2011; Zeng et al, 2016; Figure 7A). Studies conducted in Thailand deserve special attention in this context for their key geographical position where the moisture from the Indian and the Western Pacific monsoon systems converge (Wang and LinHo, 2002; Wei et al, 2018). Whereas the annual $\delta^{18}O$ series of *Tectona grandis* from northern Thailand is associated with the rainfall amount, intra-annual $\delta^{18}O$ values display a bimodal trend from contrasting influences from the moisture originating in the Indian and Pacific originating sources (Muangsong et al, 2016; 2020). Moisture sources have also been studied in the western flanks of tropical Andes, in Ecuador. Based on a climatological study supported by an intra-annual series of $\delta^{18}O$ from *Bursera graveolens*, Landshuter et al (2020) demonstrate that this region received moisture from the Atlantic and Pacific Oceans, and revealed an increasing contribution from the Pacific over the course of the last decade. These studies point to the potential of using $\delta^{18}O$ intra-annual series to disentangle moisture sources along past climate conditions.

Because of this potential to record detailed climate modes, intra-annual stable isotopes have been used to retrieve past climate variability from fossil wood samples (Figure 7C). Wood samples analyzed in such studies date back to the Eocene (ca. 45 Ma), as the study by Jahren and Sternerg (2008) with *Metasequoia* from the Artic. Based on carbon isotopes, the study revealed evidence of significant deciduousness in the trees associated with the marked decreasing trend in the $\delta^{13}C$ values from the beginning to the end of the tree ring likely from the use of stored NSC to support the onset of the growing season, an issue further discussed below. Leaf deciduousness is likely driven by the marked seasonal variability in moisture and temperature as revealed by the intra-annual $\delta^{18}O$ trends. The interpretation of these intra-annual trends becomes more reliable whenever compared with the trends observed in modern wood samples. It is the case for the studies conducted by Vornlocher et al (2021) that show seasonal monsoon-like precipitation in East Asia during the Oligocene, as well as the study by Olson et

al (2020) that provide strong evidence of the decreasing water availability and increasing seasonality in the Atacama Desert during the early- to late- Holocene period.

3.3.2.2. In dendroecology

Dendroecology was the main subject of 51.7% of the studies conducting a seasonal analysis of the intra-annual tree-ring stable isotopes (Figure 7). The intra-annual trends of the stable isotopes have been used to compare trees' responses (Figure 7D): to wet and dry years (Sarris et al, 2013), distinct site conditions, and forest stands (Battipaglia et al, 2010; Leavitt et al, 1993; de Micco et al, 2012), in years with distinct climates across a variety of site conditions (Managave et al, 2017), between healthy and declining trees (Michelot-Antalik, 2019), and across a spectrum of growth rate of trees in a population (Vaganov et al, 2009). This array of applications based on $\delta^{13}C$ and $\delta^{18}O$ demonstrates the remarkable possibilities of the seasonal analysis.

Interpreting these differences in the tree-ring stable isotope signatures can be challenging. This is probably why most studies refrain from striving for interpretations related to endogenous processes (Figure 8). For those studies invested in understanding physiological and metabolic processes, the interpretation of the results of $\delta^{13}C$ in terms of assimilation and stomatal conductance relies on Farquahr's discrimination equation. These theoretical considerations support most discussions on these endogenous parameters, meaning that these studies lean towards a more speculative discussion of the results. Having real elements to prove the influence of certain physiological processes requires careful monitoring of the stable isotopes along different compartments of trees (*e.g.* Klein et al, 2005; Offermann et al, 2011; Rinne et al, 2015), or pulse-labeling experiments using $^{13}CO_2$ (*e.g.* Kagawa et al, 2006; Krepkowski et al, 2013; He et al, 2021; Figure 8E) to precisely understand the magnitude of the carry-over effects and post-photosynthetic processes, during translocation, storage, and remobilization of photoassimilates. Pulse-labeling techniques for oxygen and hydrogen isotopes have only been recently employed, and they might contribute to improving the single-substrate model that explains intra-annual fluctuations of $\delta^{18}O$ (*e.g.* Kagawa and Battipaglia, 2022).

Because of this consistent modulation of the stable isotopes, especially for $\delta^{13}C$, some authors have already reported recurrent intra-annual trends (*e.g.* Kitagawa and Wada, 1993; Sheu et al, 1996; Vaganov et al, 2009). We confirm these recurrent patterns reported by the intra-annual studies surveyed here, which we systematized into five trends: I) decreasing trend; II) bell-shape, in which the value is lower at the beginning, increases by the middle of the tree ring, and

then decreases; III) u-shape, in which the values are high at the beginning, decrease by the middle of the tree ring, and increase again by the end; IV) increasing trend; and V) stable. The bell-shaped intra-annual trend is the most reported by the studies which usually associate it with temperature constraints in the middle of the growing season (Soudant et al, 2016; Belmecheri et al, 2018). The decreasing trend is the second most reported in the literature, and the highest values of $\delta^{13}C$ at the beginning are often associated with the use of carbon reserves during the onset of the growth season (Jäggi et al, 2002; Kimak and Leuenberger, 2015). Both bell-shaped and decreasing trends are the most common ones independently of climate zone and high taxonomic groups (Figure 9), implying that differences may results from local climate conditions in lower taxonomic levels like genus or species. Such recurrent patterns are less expected for the $\delta^{18}O$ trends, and usually only occur in sites under the influence of well-defined regional-scale circulation systems like the monsoons (Zeng et al, 2016).

4. Prospects on intra-annual stable isotope research

4.1. Methodological propositions

The progress undertaken in the field of intra-annual stable isotopes in the last decades points to the value of this approach in clarifying questions related to the ecology of trees and the climate. Many challenging obstacles arose along this long path that required technological advances, theoretical improvements, and a touch of creativity. The solutions to these challenges have been developed across different research groups, many of which are valuable steps into systematizing the intra-annual stable isotope research. Based on this review, we bring five methodological propositions:

Proposition 1: Although much has been achieved using simple razor blades for sampling, still intra-annual studies are bound to the trade-off between the number of intra-annual segments and the number of tree rings, because sampling is labor intensive, and analyses are costly. Until now, laser ablation seems to be the only method that can disrupt this trade-off for allowing an online analysis of the stable isotopes in the tree rings for optimizing most of the processes. Thus, there is a need for investment in laser ablation systems to increase the availability including in collaboration terms to reduce the costs.

Proposition 2: Having comparable datasets is fundamental in intra-annual stable isotopes research. There are clear advantages in producing an even number of intra-annual samples among tree rings. This strategy helps with the statistical analyses and data interpretation.

Regarding the number of intra-annual samples, this choice comes down to the goals of the study. Still, the average of ten segments calculated in this survey seems to produce quite detailed intra-annual trends. For instance, in a five-month growing season, each segment would represent roughly information on a two-week basis. The gains of dividing the tree ring into more than ten segments are still unclear, as it is hard to disentangle the actual information from noise.

Proposition 3: Synchronizing the intra-annual series is still an underused tool in intra-annual analysis. This may be a necessary step in sites where trees display low growth synchrony that results in lagged intra-annual series. Only then, intra-annual series could be averaged without introducing noise from misaligned series. The GLK (gleichwertigkeit) could be used as a measure of the synchronization quality.

Proposition 4: The so-called space-for-time conversion has received some attention from the literature, which proposed, for instance, using generalized additive mixed models to calculate the cell kinetics and corresponding space-for-time conversion. Other than these fundamental but complex approaches, there is a need for further evaluation of the differences in obtaining samples with the same width or producing them with the same mass per segment, which would be a shortcut to the space-for-time conversion. It may not fully clarify the representativeness of the intra-annual samples in terms of time during the growing season, but it may strengthen the analyses by allowing the comparison of segments representing a similar time length.

Proposition 5: There is still room for future development in the statistical analysis specifically designed for the intra-annual series to properly analyze the datasets on a seasonal basis.

4.2. Future research avenues

The scientific advances supported by the intra-annual stable isotopes in the tree rings are remarkable both in dendroclimatology and dendroecology. However, these studies only cover limited geographical distribution and diversity of species, not comparable with the coverage of standard tree-ring studies (Locosselli et al, 2020b; Zuidema et al, 2022) and those using tree-ring stable isotopes (Huang et al, 2024). This discrepancy points to the still unexplored potential of using the intra-annual approach across climate conditions and plant species, including woody plants from other habitats like the underexplored lianas.

In dendroclimatology, despite the proven gains in using this higher-resolution approach, most studies on paleoclimatology relied on few intra-annual segments, except for those studies analyzing floating chronologies from fossil wood samples. For all other reconstructions, the

analysis of multiple intra-annual segments can provide valuable insights into important short-term extreme events like flash floods, heatwaves, and summer droughts that can disrupt the environmental functioning and directly or indirectly impact humans' lives. A step forward has been taken by some studies that analyzed the intra-ring maximum and minimum values of the stable isotopes, and their delta, in relatively long stable isotope series. Further combining these high-resolution tree-ring records with other natural archives like speleothems (*e.g.* Stríkis et al, 2024), just as one example, can provide a more comprehensive understanding of climate systems and climate change.

If the studies lean towards understanding trees' functioning, there is a wealth of possibilities in applying the intra-annual resolution approach. We indeed gained valuable knowledge based on standard tree-ring methods, like on the climate effects on the growth of trees and the eventual presence of climate legacies, how trees responded to natural and anthropogenic disturbances, how trees display or not early signals of senescence, just to name a few applications. All these applications can benefit from more detailed information about tree development during the growing season, and using the intra-annual isotopes will push forward our current knowledge.

On top of these consolidated research questions in dendroecology, there are new research questions associated with the allocation and mobilization of carbohydrates to support tree growth, that still have only a handful of studies. A detailed understanding of how trees use the NSC stored to support early growth, or growth during less than favorable conditions, either under controlled conditions eventually using labeled compounds, or even under natural conditions still lagged. The use of the dual-isotope approach largely used in standard dendrochronology can also help understand how trees modulate the physiology and eventually partitioning of carbon allocation and mobilization during the growth season (Roden et al, 2022).

Finally, by standardizing the methods of the intra-annual analyses in both dendroclimatological and dendroecological studies, a whole new avenue of opportunities will open by combining global datasets similar to what has been done with tree-ring width data (Brienen et al, 2020; Locosselli et al, 2020b; Zuidema et al, 2022; Bose et al, 2024). Such re-analyses usually result in ground-breaking insights and knowledge on the functioning of climate systems and responses of trees to global changes in climate conditions and environmental stresses. By putting this effort into the high-resolution analysis perspective, one can strive for detailed sub-annual information on key processes governing the atmospheric circulation and the modulation of the responses of trees during the growing season.

5. Conclusions

In summary, this review put together challenges and proposed solutions for the intra-annual analysis. Having them scrutinized can allow researchers worldwide to follow comparable steps for more comprehensive studies fostering the development of the tree-ring intra-annual stable isotope research. As stated before, the role of this systematic review was not to provide full guidelines for the systematization of this research field but to be a starting point to aid further development.

Acknowledgement

The authors thanks Dr. Bruno Barçante Ladvocat Cintra for providing the dataset used in Figure 6. The authors also thank FAPESP (FAPESP 2017/50085-3, 2017/50341-0, 2019/08783-0, 2020/09251-0), CNPq (311854/2022-2), and CAPES (88887.715354/2022-00) for financial support.

References

An, W., Liu, X., Leavitt, S., Ren, J., Sun, W., Wang, W., Wang, Y., Xu, G., Chen, T., & Qin, D. (2012). Specific climatic signals recorded in earlywood and latewood $\delta^{18}O$ of tree rings in southwestern China. *Tellus B: Chemical and Physical Meteorology*, 64(1), 18703.

An, W., Xu, C., Liu, X., Tan, N., Sano, M., Li, M., Shao, X., Nakatsuka, T. & Guo, Z. (2019). Specific response of earlywood and latewood $\delta^{18}O$ from the east and west of Mt. Qomolangma to the Indian summer monsoon. *Science of the total environment*, 689, 99-108.

Anchukaitis, K. J., Evans, M. N., Wheelwright, N. T., & Schrag, D. P. (2008). Stable isotope chronology and climate signal calibration in neotropical montane cloud forest trees. *Journal of Geophysical Research: Biogeosciences*, 113(G3).

Andreu-Hayles, L., Lévesque, M., Guerrieri, R., Siegwolf, R. T., & Körner, C. (2022). Limits and strengths of tree-ring stable isotopes. In *Stable isotopes in tree rings: inferring physiological, climatic and environmental responses* (pp. 399-428). Cham: Springer International Publishing.

Ballantyne, A. P., Baker, P. A., Chambers, J. Q., Villalba, R., & Argollo, J. (2011). Regional differences in South American monsoon precipitation inferred from the growth and isotopic composition of tropical trees. *Earth Interactions*, 15(5), 1-35.

Barbour, M. M., Walcroft, A. S., & Farquhar, G. D. (2002). Seasonal variation in $\delta^{13}C$ and $\delta^{18}O$ of cellulose from growth rings of *Pinus radiata*. *Plant, Cell & Environment*, 25(11), 1483-1499.

Baton, F., Tu, T. T. N., Derenne, S., Delorme, A., Delarue, F., & Dufraisse, A. (2017). Tree-ring $\delta^{13}C$ of archaeological charcoals as indicator of past climatic seasonality. A case study from the Neolithic settlements of Lake Chalain (Jura, France). *Quaternary international*, 457, 50-59.

Battipaglia, G., De Micco, V., Brand, W. A., Linke, P., Aronne, G., Saurer, M., & Cherubini, P. (2010). Variations of vessel diameter and $\delta^{13}C$ in false rings of *Arbutus unedo* L. reflect different environmental conditions. *New Phytologist*, 188(4), 1099-1112.

Battipaglia, G., De Micco, V., Brand, W. A., Saurer, M., Aronne, G., Linke, P., & Cherubini, P. (2014). Drought impact on water use efficiency and intra-annual density fluctuations in *Erica arborea* on Elba (Italy). *Plant, Cell & Environment*, 37(2), 382-391.

Belmecheri, S., Wright, W. E., Szejner, P., Morino, K. A., & Monson, R. K. (2018). Carbon and oxygen isotope fractionations in tree rings reveal interactions between cambial phenology and seasonal climate. *Plant, Cell & Environment*, 41(12), 2758-2772.

Belmecheri, S., Wright, W. E., & Szejner, P. (2022). Sample collection and preparation for annual and intra-annual tree-ring isotope chronologies. In *Stable isotopes in tree rings: inferring physiological, climatic and environmental responses* (pp. 103-134). Cham: Springer International Publishing.

Berkelhammer, M., & Stott, L. D. (2009). Modeled and observed intra-ring $\delta^{18}O$ cycles within late Holocene Bristlecone Pine tree samples. *Chemical Geology*, 264(1-4), 13-23.

Bijaksana, S., Ngkoimani, L. O., D'Arrigo, R., Krusic, P., Palmer, J., Sakulich, J., & Zulaikah, S. (2007). Status of tree-ring research from teak (*Tectona grandis*) for climate studies. *Jurnal Geofisika*, 2, 1-7.

Bose, A. K., Doležal, J., Scherrer, D., Altman, J., Ziche, D., Martínez-Sancho, E., Bigler, C., Bolte, A., Colangelo, M., Dorado-Liñán, I., Drobyshev, I., Etzold, S., Fonti, P., Gessler, A., Kolář, T., Koňasová, E., Korznikov, K. A., Lebourgeois, F., Lucas-Borja, M. E., Menzel, A., Neuwirth, B., Nicolas, M., Omelko, A. M., Pederson, N., Petritan, A. M., Rigling, A., Rybníček, M., Scharnweber, T., Schröder, J., Silla, F., Sochová, I., Sohar, K., Ukhvatkina, O. N., Vozmishcheva, A. S., Zweifel, R. & Camarero, J. J. (2024). Revealing legacy effects of extreme

droughts on tree growth of oaks across the Northern Hemisphere. *Science of The Total Environment*, 172049.

Brandes, A. F. N., Rizzieri, Y. C., Tamaio, N., Pace, M. R., & Barros, C. F. (2022) A global review on wood growth rings in lianas. *Dendrochronologia*, 71: 125920

Brienen, R. J., Caldwell, L., Duchesne, L., Voelker, S., Barichivich, J., Baliva, M., Ceccantini, G., Di Filippo, A., Helama, S., Locosselli, G. M., Lopez, L., Piovesan, G., Schöngart, J., Villalba, R., & Gloor, E. (2020). Forest carbon sink neutralized by pervasive growth-lifespan trade-offs. *Nature communications*, 11(1), 4241.

Büntgen, U., Psomas, A., & Schweingruber, F. H. (2014). Introducing wood anatomical and dendrochronological aspects of herbaceous plants: applications of the Xylem Database to vegetation science. *Journal of Vegetation Science*, 25(4), 967-977.

Bura, A., & Wilmking, M. (2015) Correcting the calculation of the Gleichläufigkeit. *Dendrochronologia*, 34: 29-30.

Cintra, B. B. L., Gloor, M., Boom, A., Schöngart, J., Locosselli, G. M., & Brienen, R. (2019). Contrasting controls on tree ring isotope variation for Amazon floodplain and terra firme trees. *Tree physiology*, 39(5), 845-860.

Condamine, F. L., Silvestro, D., Koppelhus, E. B., & Antonelli, A. (2020) The rise of angiosperms pushed conifers to decline during global cooling. *Proceedings of the National Academy of Sciences*, 117: 28867-28875.

Corlett, R. T. (2013) Where are the subtropics? *Biotropica*, 45: 273-275.

Craig, H. (1954). Carbon-13 variations in Sequoia rings and the atmosphere. *Science*, 119(3083), 141-143.

de Micco, V., Battipaglia, G., Brand, W. A., Linke, P., Saurer, M., Aronne, G., & Cherubini, P. (2012). Discrete versus continuous analysis of anatomical and $\delta^{13}C$ variability in tree rings with intra-annual density fluctuations. *Trees*, 26, 513-524.

Dodd, J. P., Patterson, W. P., Holmden, C., & Brasseur, J. M. (2008). Robotic micromilling of tree-rings: a new tool for obtaining subseasonal environmental isotope records. *Chemical Geology*, 252(1-2), 21-30.

Dolezal, J., Leheckova, E., Sohar, K., Dvorsky, M., Kopecky, M., Chlumska, Z., Wild, J., & Altman, J. (2016). Annual and intra-annual growth dynamics of *Myricaria elegans* shrubs in arid Himalaya. *Trees*, 30, 761-773.

Eilmann, B., Buchmann, N., Siegwolf, R., Saurer, M., Cherubini, P., & Rigling, A. (2010). Fast response of Scots pine to improved water availability reflected in tree-ring width and $\delta^{13}C$. *Plant, Cell & Environment*, 33(8), 1351-1360.

Evans, M. N., & Schrag, D. P. (2004). A stable isotope-based approach to tropical dendroclimatology. *Geochimica et Cosmochimica Acta*, 68(16), 3295-3305.

Fichtler, E., Helle, G., & Worbes, M. (2010). Stable-carbon isotope time series from tropical tree rings indicate a precipitation signal. *Tree-ring research*, 66(1), 35-49.

Fonti, M. V., Vaganov, E. A., Wirth, C., Shashkin, A. V., Astrakhantseva, N. V., & Schulze, E. D. (2018). Age-effect on intra-annual $\delta^{13}C$-variability within Scots pine tree-rings from Central Siberia. *Forests*, 9(6), 364.

Fu, P. L., Grießinger, J., Gebrekirstos, A., Fan, Z. X., & Bräuning, A. (2017). Earlywood and latewood stable carbon and oxygen isotope variations in two pine species in southwestern China during the recent decades. *Frontiers in plant science*, 7, 230776.

Gessler, A., Brandes, E., Buchmann, N., Helle, G., Rennenberg, H., & Barnard, R. L. (2009). Tracing carbon and oxygen isotope signals from newly assimilated sugars in the leaves to the tree-ring archive. *Plant, Cell & Environment*, 32(7), 780-795.

Giraldo, J. A., del Valle, J. I., González-Caro, S., & Sierra, C. A. (2022). Intra-annual isotope variations in tree rings reveal growth rhythms within the least rainy season of an ever-wet tropical forest. *Trees*, 36(3), 1039-1052.

Guimarães, K. S., Marimon, B. S., Locosselli, G. M., Brienen, R., Cintra, B. B. L., Boom, A., Araújo, I., Marimon-Junior, B. H., Ceccantini, G., da Cruz, W. J. A., & Phillips, O. L. (2024) Intra-annual stable isotopes in the tree rings of *Hymenaea courbaril* as a proxy for hydroclimate variations in southern Amazonia. *Dendrochronologia, 83, 126151.*

He, M., Bräuning, A., Rossi, S., Gebrekirstos, A., Grießinger, J., Mayr, C., Peng, C., & Yang, B. (2021). No evidence for carryover effect in tree rings based on a pulse-labelling experiment on *Juniperus communis* in South Germany. *Trees*, 35, 493-502.

Helle, G., & Schleser, G. H. (2004). Beyond CO_2-fixation by Rubisco–an interpretation of $^{13}C/^{12}C$ variations in tree rings from novel intra-seasonal studies on broad-leaf trees. *Plant, Cell & Environment*, 27(3), 367-380.

Helle, G., Pauly, M., Heinrich, I., Schollän, K., Balanzategui, D., & Schürheck, L. (2022). Stable isotope signatures of wood, its constituents and methods of cellulose extraction. In *Stable Isotopes in Tree Rings: Inferring Physiological, Climatic and Environmental Responses* (pp. 135-190). Cham: Springer International Publishing.

Huang, R., Xu, C., Grießinger, J., Feng, X., Zhu, H., & Bräuning, A. (2024). Rising utilization of stable isotopes in tree rings for climate change and forest ecology. *Journal of Forestry Research*, 35(1), 13.

Jäggi, M., Saurer, M., Fuhrer, J., & Siegwolf, R. (2002). The relationship between the stable carbon isotope composition of needle bulk material, starch, and tree rings in *Picea abies*. *Oecologia*, 131, 325-332.

Jahren, A. H., & Sternberg, L. S. (2008). Annual patterns within tree rings of the Arctic middle Eocene (ca. 45 Ma): Isotopic signatures of precipitation, relative humidity, and deciduousness. *Geology*, 36(2), 99-102.

Johnstone, J. A., Roden, J. S., & Dawson, T. E. (2013). Oxygen and carbon stable isotopes in coast redwood tree rings respond to spring and summer climate signals. *Journal of Geophysical Research: Biogeosciences*, 118(4), 1438-1450.

Kagawa, A., Sugimoto, A., & Maximov, T. C. (2006). $^{13}CO_2$ pulse-labelling of photoassimilates reveals carbon allocation within and between tree rings. *Plant, Cell & Environment*, 29(8), 1571-1584.

Kagawa, A., Sano, M., Nakatsuka, T., Ikeda, T., & Kubo, S. (2015). An optimized method for stable isotope analysis of tree rings by extracting cellulose directly from cross-sectional laths. *Chemical Geology*, 393, 16-25.

Kagawa, A., & Battipaglia, G. (2022). Post-photosynthetic carbon, oxygen and hydrogen isotope signal transfer to tree rings—how timing of cell formations and turnover of stored carbohydrates affect intra-annual isotope variations. In *Stable isotopes in tree rings: inferring physiological, climatic and environmental responses* (pp. 429-462). Cham: Springer International Publishing.

Kimak, A., & Leuenberger, M. (2015). Are carbohydrate storage strategies of trees traceable by early–latewood carbon isotope differences?. *Trees*, 29, 859-870.

Kitagawa, H., & Wada, H. (1993). Seasonal and secular $\delta^{13}C$ variations in annual growth rings of a Japanese cedar tree from Mt. Amagi, Izu Peninsula, Central Japan. *Geochemical Journal*, 27(6), 391-396.

Klein, T., Hemming, D., Lin, T., Grünzweig, J. M., Maseyk, K., Rotenberg, E., & Yakir, D. (2005). Association between tree-ring and needle $\delta^{13}C$ and leaf gas exchange in *Pinus halepensis* under semi-arid conditions. *Oecologia*, 144, 45-54.

Krepkowski, J., Gebrekirstos, A., Shibistova, O., & Bräuning, A. (2013). Stable carbon isotope labeling reveals different carry-over effects between functional types of tropical trees in an Ethiopian mountain forest. *New Phytologist*, 199(2), 431-440.

Koretsune, S., Fukuda, K., Chang, Z., Shi, F., & Ishida, A. (2009). Effective rainfall seasons for interannual variation in $\delta^{13}C$ and tree-ring width in early and late wood of Chinese pine and black locust on the Loess Plateau, China. *Journal of forest research*, 14(2), 88-94.

Labotka, D. M., Grissino-Mayer, H. D., Mora, C. I., & Johnson, E. J. (2016). Patterns of moisture source and climate variability in the southeastern United States: a four-century seasonally resolved tree-ring oxygen-isotope record. *Climate dynamics*, 46, 2145-2154.

Landshuter, N., Mölg, T., Grießinger, J., Bräuning, A., & Peters, T. (2020). 10-year characteristics of moisture source regions and their potential effect on seasonal isotopic signatures of $\delta^{18}O$ in tropical trees of southern Ecuador. *Frontiers in Earth Science*, 8, 604804.

Leavitt, S. W., & Lone, A. (1991) Seasonal stable-carbon isotope variability in tree rings: possible paleoenvironmental signals. *Chemical Geology: Isotope Geoscience section*, 87: 59-70.

Leavitt, S. W. (1993). Seasonal $^{13}C/^{12}C$ changes in tree rings: species and site coherence, and a possible drought influence. *Canadian Journal of Forest Research*, 23(2), 210-218.

Leavitt S. W. (2002) Prospects for reconstruction of seasonal environment from tree-ring $\delta^{13}C$: baseline findings from the Great Lakes area, USA. *Chemical Geology*, 192: 47-58.

Leavitt, S. W. (2007). Regional expression of the 1988 US Midwest drought in seasonal $\delta^{13}C$ of tree rings. *Journal of Geophysical Research: Atmospheres*, 112(D6).

Leavitt, S. W., & Roden, J. (2022). Isotope Dendrochronology: Historical Perspective. In *Stable Isotopes in Tree Rings: Inferring Physiological, Climatic and Environmental Responses* (pp. 3-20). Cham: Springer International Publishing.

Li, Z. H., Labbé, N., Driese, S. G., & Grissino-Mayer, H. D. (2011). Micro-scale analysis of tree-ring $\delta^{18}O$ and $\delta^{13}C$ on α-cellulose spline reveals high-resolution intra-annual climate variability and tropical cyclone activity. *Chemical Geology*, 284(1-2), 138-147.

Livingston, N. J., & Spittlehouse, D. L. (1996). Carbon isotope fractionation in tree ring early and late wood in relation to intra-growing season water balance. *Plant, Cell & Environment*, 19(6), 768-774.

Loader, N. J., Walsh, R. P. D., Robertson, I., Bidin, K., Ong, R. C., Reynolds, G., McCarroll, D., Gagen, M., & Young, G. H. F. (2011). Recent trends in the intrinsic water-use efficiency of

ringless rainforest trees in Borneo. *Philosophical Transactions of the Royal Society B: Biological Sciences*, 366(1582), 3330-3339.

Locosselli, G. M., & Buckeridge, M. S. (2017). Dendrobiochemistry, a missing link to further understand carbon allocation during growth and decline of trees. *Trees*, 31(6), 1745-1758.

Locosselli, G. M., Brienen, R. J., de Souza Martins, V. T., Gloor, E., Boom, A., de Camargo, E. P., Saldiva, P. H. N., & Buckeridge, M. S. (2020a). Intra-annual oxygen isotopes in the tree rings record precipitation extremes and water reservoir levels in the Metropolitan Area of São Paulo, Brazil. *Science of the Total Environment*, 743, 140798.

Locosselli, G. M., Brienen, R. J., Leite, M. D. S., Gloor, M., Krottenthaler, S., Oliveira, A. A. D., Barichivich, J., Anhuf, D., Ceccantini, G., Schöngart, J., & Buckeridge, M. (2020b). Global tree-ring analysis reveals rapid decrease in tropical tree longevity with temperature. *Proceedings of the National Academy of Sciences*, 117(52), 33358-33364.

Macfarlane, C., & Adams, M. A. (1998). $\Delta^{13}C$ of wood in growth-rings indicates cambial activity of drought-stressed trees of *Eucalyptus globulus*. *Functional Ecology*, 12(4), 655-664.

Marshall, J. D., & Monserud, R. A. (1996). Homeostatic gas-exchange parameters inferred from $^{13}C/^{12}C$ in tree rings of conifers. *Oecologia*, 105, 13-21.

Martínez-Sancho, E., Treydte, K., Lehmann, M. M., Rigling, A., & Fonti, P. (2022). Drought impacts on tree carbon sequestration and water use–evidence from intra-annual tree-ring characteristics. *New Phytologist*, 236(1), 58-70.

Michelot-Antalik, A., Granda, E., Fresneau, C., & Damesin, C. (2019). Evidence of a seasonal trade-off between growth and starch storage in declining beeches: assessment through stem radial increment, non-structural carbohydrates and intra-ring $\delta^{13}C$. *Tree Physiology*, 39(5), 831-844.

Michelot, A., Eglin, T., Dufrene, E., Lelarge-Trouverie, C., & Damesin, C. (2011). Comparison of seasonal variations in water-use efficiency calculated from the carbon isotope composition of tree rings and flux data in a temperate forest. *Plant, cell & environment*, 34(2), 230-244.

Miller, D. L., Mora, C. I., Grissino-Mayer, H. D., Mock, C. J., Uhle, M. E., & Sharp, Z. (2006). Tree-ring isotope records of tropical cyclone activity. *Proceedings of the National Academy of Sciences*, 103(39), 14294-14297.

Managave, S. R., Sheshshayee, M. S., Borgaonkar, H. P., & Ramesh, R. (2010). Past break-monsoon conditions detectable by high resolution intra-annual $\delta^{18}O$ analysis of teak rings. *Geophysical Research Letters*, 37(5).

Managave, S. R., Sheshshayee, M. S., Bhattacharyya, A., & Ramesh, R. (2011). Intra-annual variations of teak cellulose $\delta^{18}O$ in Kerala, India: implications to the reconstruction of past summer and winter monsoon rains. *Climate dynamics*, 37, 555-567.

Managave, S. R., Shimla, P., Borgaonkar, H. P., Bhattacharyya, A., & Ramesh, R. (2017). Regional differences in the carbon isotopic compositions of teak from two monsoonal regimes of India. *Dendrochronologia*, 44, 203-210.

Muangsong, C., Cai, B., Pumijumnong, N., Hu, C., & Lei, G. (2016). Intra-seasonal variability of teak tree-ring cellulose $\delta^{18}O$ from northwestern Thailand: a potential proxy of Thailand summer monsoon rainfall. *The Holocene*, 26(9), 1397-1405.

Muangsong, C., Pumijumnong, N., Cai, B., Buajan, S., Lei, G., Wang, F., Li., M. & Payomrat, P. (2020). Effect of changes in precipitation amounts and moisture sources on inter-and intra-annual stable oxygen isotope ratios ($\delta^{18}O$) of teak trees from northern Thailand. *Agricultural and Forest Meteorology*, 281, 107820.

Nabeshima, E., Nakatsuka, T., Kagawa, A., Hiura, T., & Funada, R. (2018). Seasonal changes of δD and $\delta^{18}O$ in tree-ring cellulose of *Quercus crispula* suggest a change in post-photosynthetic processes during earlywood growth. *Tree Physiology*, 38(12), 1829-1840.

Nakatsuka, T., Ohnishi, K., Hara, T., Sumida, A., Mitsuishi, D., Kurita, N., & Uemura, S. (2004). Oxygen and carbon isotopic ratios of tree-ring cellulose in a conifer-hardwood mixed forest in northern Japan. *Geochemical Journal*, 38(1), 77-88.

Offermann, C., Ferrio, J. P., Holst, J., Grote, R., Siegwolf, R., Kayler, Z., & Gessler, A. (2011). The long way down—are carbon and oxygen isotope signals in the tree ring uncoupled from canopy physiological processes? *Tree Physiology*, 31(10), 1088-1102.

Ogée, J., Barbour, M. M., Wingate, L., Bert, D., Bosc, A., Stievenard, M., Lambrot, C., Pierre, M., Bariac, T., Loustau, D., & Dewar, R. C. (2009). A single-substrate model to interpret intra-annual stable isotope signals in tree-ring cellulose. *Plant, Cell & Environment*, 32(8), 1071-1090.

Ogle, N., & McCormac, F. G. (1994). High-resolution $\delta^{13}C$ measurements of oak show a previously unobserved spring depletion. *Geophysical Research Letters*, 21(22), 2373-2375.

Ohashi, S., Okada, N., Nobuchi, T., Siripatanadilok, S., & Veenin, T. (2009). Detecting invisible growth rings of trees in seasonally dry forests in Thailand: isotopic and wood anatomical approaches. *Trees*, 23, 813-822.

Ohashi, S., Durgante, F. M., Kagawa, A., Kajimoto, T., Trumbore, S. E., Xu, X., Ishizuka, M., & Higuchi, N. (2016). Seasonal variations in the stable oxygen isotope ratio of wood cellulose reveal annual rings of trees in a Central Amazon terra firme forest. *Oecologia*, 180, 685-696.

Olson, E. J., Dodd, J. P., & Rivera, M. A. (2020). Prosopis sp. tree-ring oxygen and carbon isotope record of regional-scale hydroclimate variability during the last 9500 years in the Atacama Desert. *Palaeogeography, palaeoclimatology, palaeoecology*, 538, 109408.

Page, M. J., McKenzie, J. E., Bossuyt, P. M., Boutron, I., Hoffmann, T. C., Mulrow, C. D., Shamseer, L., Tetzlaff, J. M., Akl, E. A., Brennan, S. E., Chou, R., Glanville, J., Grimshaw, J. M., Hróbjartsson, A., Lalu, M. M., Li, T., Loader, E. W., Mayo-Wilson, E., McDonald, S., McGuinness, L. A., Stewart, L. A., Thomas, J., Tricco, A. C., Welch, V. A., Whiting, P., & Moher, D. (2021). The PRISMA 2020 statement: an updated guideline for reporting systematic reviews. *International journal of surgery*, 88, 105906.

Pérez-de-Lis, G., Rathgeber, C. B., Fernández-de-Uña, L., & Ponton, S. (2022). Cutting tree rings into time slices: how intra-annual dynamics of wood formation help decipher the space-for-time conversion. *New Phytologist*, 233(3), 1520-1534.

Pons, T. L., & Helle, G. (2011). Identification of anatomically non-distinct annual rings in tropical trees using stable isotopes. *Trees*, 25(1), 83-93.

Poussart, P. F., Evans, M. N., & Schrag, D. P. (2004). Resolving seasonality in tropical trees: multi-decade, high-resolution oxygen and carbon isotope records from Indonesia and Thailand. *Earth and Planetary Science Letters*, 218(3-4), 301-316.

Poussart, P. F., & Schrag, D. P. (2005). Seasonally resolved stable isotope chronologies from northern Thailand deciduous trees. *Earth and Planetary Science Letters*, 235(3-4), 752-765.

Reimchen, T. E., & Arbellay, E. (2018). Intra-annual variability in isotopic and total nitrogen in tree rings of old growth *Sitka spruce* from coastal British Columbia. *Botany*, 96(12), 851-857.

Rinne, K. T., Saurer, M., Kirdyanov, A. V., Loader, N. J., Bryukhanova, M. V., Werner, R. A., & Siegwolf, R. T. W. (2015). The relationship between needle sugar carbon isotope ratios and tree rings of larch in Siberia. *Tree Physiology*, 35(11), 1192-1205.

Roden, J., Saurer, M., & Siegwolf, R. T. (2022). Probing Tree Physiology Using the Dual-Isotope Approach. In *Stable Isotopes in Tree Rings: Inferring Physiological, Climatic and Environmental Responses* (pp. 463-479). Cham: Springer International Publishing.

Sargeant, C. I., & Singer, M. B. (2016). Sub-annual variability in historical water source use by Mediterranean riparian trees. *Ecohydrology*, 9(7), 1328-1345.

Sarris, D., Siegwolf, R., & Körner, C. (2013). Inter-and intra-annual stable carbon and oxygen isotope signals in response to drought in Mediterranean pines. *Agricultural and Forest Meteorology*, 168, 59-68.

Saurer, M., Sahlstedt, E., Rinne-Garmston, K. T., Lehmann, M. M., Oettli, M., Gessler, A., & Treydte, K. (2023). Progress in high-resolution isotope-ratio analysis of tree rings using laser ablation. *Tree Physiology*, 43(5), 694-705.

Savard, M. M., & Siegwolf, R. T. (2022). Nitrogen isotopes in tree rings—Challenges and prospects. *Stable Isotopes in Tree Rings: Inferring Physiological, Climatic and Environmental Responses*, 361-380.

Scheidegger, Y., Saurer, M., Bahn, M., & Siegwolf, R. (2000) Linking stable oxygen and carbon isotopes with stomatal conductance and photosynthetic capacity: a conceptual model. *Oecologia*, 125:350-357.

Schollaen, K., Heinrich, I., Neuwirth, B., Krusic, P. J., D'Arrigo, R. D., Karyanto, O., & Helle, G. (2013). Multiple tree-ring chronologies (ring width, $\delta^{13}C$ and $\delta^{18}O$) reveal dry and rainy season signals of rainfall in Indonesia. *Quaternary Science Reviews*, 73, 170-181.

Schollaen, K., Heinrich, I., & Helle, G. (2014). UV-laser-based microscopic dissection of tree rings–a novel sampling tool for $\delta^{13}C$ and $\delta^{18}O$ studies. *New Phytologist*, 201(3), 1045-1055.

Schollaen, K., Baschek, H., Heinrich, I., & Helle, G. (2015). An improved guideline for rapid and precise sample preparation of tree-ring stable isotope analysis. *Biogeosciences Discussions*, 12(14), 11587-11623.

Schollaen, K., Baschek, H., Heinrich, I., Slotta, F., Pauly, M., & Helle, G. (2017). A guideline for sample preparation in modern tree-ring stable isotope research. *Dendrochronologia*, 44, 133-145.

Schulze, B., Wirth, C., Linke, P., Brand, W. A., Kuhlmann, I., Horna, V., & Schulze, E. D. (2004). Laser ablation-combustion-GC-IRMS—a new method for online analysis of intra-annual variation of $\delta^{13}C$ in tree rings. *Tree Physiology*, 24(11), 1193-1201.

Schweingruber, F. H., Hellmann, L., Tegel, W., Braun, S., Nievergelt, D., & Büntgen, U. (2013). Evaluating the wood anatomical and dendroecological potential of Arctic dwarf shrub communities. In *Wood Structure in Plant Biology and Ecology* (pp. 157-169). Brill.

Sheu, D. D., Kou, P., Chiu, C. H., & Chen, M. J. (1996). Variability of tree-ring $\delta^{13}C$ in Taiwan fir: growth effect and response to May–October temperatures. *Geochimica et Cosmochimica Acta*, 60(1), 171-177.

Schubert, B. A., & Timmermann, A. (2015). Reconstruction of seasonal precipitation in Hawai'i using high-resolution carbon isotope measurements across tree rings. *Chemical Geology*, 417, 273-278.

Skomarkova, M. V., Vaganov, E. A., Mund, M., Knohl, A., Linke, P., Boerner, A., & Schulze, E. D. (2006). Inter-annual and seasonal variability of radial growth, wood density and carbon isotope ratios in tree rings of beech (*Fagus sylvatica*) growing in Germany and Italy. *Trees*, 20, 571-586.

Stokes, M. A., & Smiley, T. L. (1996). *An introduction to tree-ring dating*, 2nd ed.; The University of Arizona Press: Tucson, AZ, USA.

Stríkis, N. M., Buarque, P. F. S. M., Cruz, F. W., Bernal, J. P., Vuille, M., Tejedor, E., Santos, M. S., Shimizu, M. H., Ampuero, A., Du, W., Sampaio, G., Sales, H. dos R., Campos, J. L., Kayano, M. T., Apaèstegui, J., Fu, R. R., Cheng, H., Edwards, R. L., Mayta, V. C., Francischini, D. da S., Arruda, M. A. Z. & Novello, V. F. (2024). Modern anthropogenic drought in Central Brazil unprecedented during last 700 years. *Nature Communications*, 15(1), 1728.

Soudant, A., Loader, N. J., Bäck, J., Levula, J., & Kljun, N. (2016). Intra-annual variability of wood formation and $\delta^{13}C$ in tree-rings at Hyytiälä, Finland. *Agricultural and Forest Meteorology*, 224, 17-29.

Szejner, P., Wright, W. E., Belmecheri, S., Meko, D., Leavitt, S. W., Ehleringer, J. R., & Monson, R. K. (2018). Disentangling seasonal and interannual legacies from inferred patterns of forest water and carbon cycling using tree-ring stable isotopes. *Global change biology*, 24(11), 5332-5347.

Szejner, P., Belmecheri, S., Ehleringer, J. R., & Monson, R. K. (2020). Recent increases in drought frequency cause observed multi-year drought legacies in the tree rings of semi-arid forests. *Oecologia*, 192, 241-259.

Szejner, P., Belmecheri, S., Babst, F., Wright, W. E., Frank, D. C., Hu, J., & Monson, R. K. (2021). Stable isotopes of tree rings reveal seasonal-to-decadal patterns during the emergence of a megadrought in the Southwestern US. *Oecologia*, 197, 1079-1094.

Tans, P. P., & Mook, W. G. (1980). Past atmospheric CO_2 levels and the $^{13}C/^{12}C$ ratios in tree rings. *Tellus*, 32(3), 268-283.

Tepley, A. J., Hood, S. M., Keyes, C. R., & Sala, A. (2020). Forest restoration treatments in a ponderosa pine forest enhance physiological activity and growth under climatic stress. *Ecological Applications*, 30(8), e02188.

Treydte, K., Boda, S., Graf Pannatier, E., Fonti, P., Frank, D., Ullrich, B., Saurer, M., Siegwolf, R., Battipaglia, G., Werner, W., & Gessler, A. (2014). Seasonal transfer of oxygen isotopes from precipitation and soil to the tree ring: source water versus needle water enrichment. *New Phytologist*, 202(3), 772-783.

Vaganov, E. A., Schulze, E. D., Skomarkova, M. V., Knohl, A., Brand, W. A., & Roscher, C. (2009). Intra-annual variability of anatomical structure and $\delta^{13}C$ values within tree rings of spruce and pine in alpine, temperate and boreal Europe. *Oecologia*, 161, 729-745.

van der Sleen, P., Zuidema, P. A., & Pons, T. L. (2022). Stable Isotopes in Tree Rings of Tropical Forests. In *Stable Isotopes in Tree Rings: Inferring Physiological, Climatic and Environmental Responses* (pp. 631-649). Cham: Springer International Publishing.

Verheyden, A., Helle, G., Schleser, G. H., Dehairs, F., Beeckman, H., & Koedam, N. (2004). Annual cyclicity in high-resolution stable carbon and oxygen isotope ratios in the wood of the mangrove tree Rhizophora mucronata. *Plant, Cell & Environment*, 27(12), 1525-1536.

Verheyden, A., Roggeman, M., Bouillon, S., Elskens, M., Beeckman, H., & Koedam, N. (2005). Comparison between $\delta^{13}C$ of α-cellulose and bulk wood in the mangrove tree Rhizophora mucronata: implications for dendrochemistry. *Chemical Geology*, 219(1-4), 275-282.

Verheyden, A., Helle, G., Schleser, G. H., & Beeckman, H. (2006). High-resolution carbon and oxygen isotope profiles of tropical and temperate liana species. *Schr Forsch Jülich Reihe Umw*, 61, 31-35.

Vogado, N. O., Camargo, M. G. G., Locosselli, G. M., & Morelatto, L. P. C. (2016) Edge effects on the phenology of the Guamirim, *Myrcia guianensis* (Myrtaceae), a cerrado tree, Brazil. *Tropical Conservation Science*, *9:* 291-312.

Vornlocher, J. R., Lukens, W. E., Schubert, B. A., & Quan, C. (2021). Late Oligocene precipitation seasonality in East Asia based on $\delta^{13}C$ profiles in fossil wood. *Paleoceanography and Paleoclimatology*, 36(4), e2021PA004229.

Wang, B.; & LinHo (2002). Rainy season of the Asian–Pacific summer monsoon. *Journal of Climate*, 15(4), 386-398.

Wei, Z., Lee, X., Liu, Z., Seeboonruang, U., Koike, M., & Yoshimura, K. (2018). Influences of large-scale convection and moisture source on monthly precipitation isotope ratios observed in Thailand, Southeast Asia. *Earth and Planetary Science Letters*, 488, 181-192.

Wilson, A. T., & Grinsted, M. J. (1975). Palaeotemperatures from tree rings and the D/H ratio of cellulose as a biochemical thermometer. *Nature*, 257(5525), 387-388.

Wilson, A. T., & Grinsted, M. J. (1977). $^{12}C/^{13}C$ in cellulose and lignin as palaeothermometers. *Nature*, 265(5590), 133-135.

Woolston, C. (2023) China tops Nature Index: what a new milestone means for science. *Nature,* 620: S2-S5.

Xu, C., Sano, M., Yoshimura, K., & Nakatsuka, T. (2014). Oxygen isotopes as a valuable tool for measuring annual growth in tropical trees that lack distinct annual rings. *Geochemical Journal*, 48(4), 371-378.

Xu, C., Xi, X. C., Zheng, Z. H., Nakatsuka, T., Sano, M., Li, Z., & Ge, J. (2016). Inter and intra-annual tree-ring cellulose oxygen isotope variability in response to precipitation in Southeast China. *Trees - Structure and Function*, (2016): 785-794.

Xu, G., Liu, X., Sun, W., Szejner, P., Zeng, X., Yoshimura, K., & Trouet, V. (2020). Seasonal divergence between soil water availability and atmospheric moisture recorded in intra-annual tree-ring $\delta^{18}O$ extremes. *Environmental Research Letters*, 15(9), 094036.

Yihui, D., & Chan, J. C. (2005). The East Asian summer monsoon: an overview. *Meteorology and Atmospheric Physics*, 89(1), 117-142.

Zalloni, E., Battipaglia, G., Cherubini, P., Saurer, M., & De Micco, V. (2018). Contrasting physiological responses to Mediterranean climate variability are revealed by intra-annual density fluctuations in tree rings of *Quercus ilex* L. and *Pinus pinea* L. *Tree physiology*, 38(8), 1213-1224.

Zeng, X., Liu, X., Evans, M. N., Wang, W., An, W., Xu, G., & Wu, G. (2016). Seasonal incursion of Indian Monsoon humidity and precipitation into the southeastern Qinghai–Tibetan Plateau inferred from tree ring $\delta^{18}O$ values with intra-seasonal resolution. *Earth and Planetary Science Letters*, 443, 9-19.

Zhu, M., Stott, L., Buckley, B., Yoshimura, K., & Ra, K. (2012). Indo-Pacific Warm Pool convection and ENSO since 1867 derived from Cambodian pine tree cellulose oxygen isotopes. *Journal of Geophysical Research: Atmospheres*, 117(D11).

Zuidema, P. A., Babst, F., Groenendijk, P., Trouet, V., Abiyu, A., Acuña-Soto, R., ... & Zhou, Z. K. (2022). Tropical tree growth driven by dry-season climate variability. *Nature Geoscience*, 15(4), 269-276.

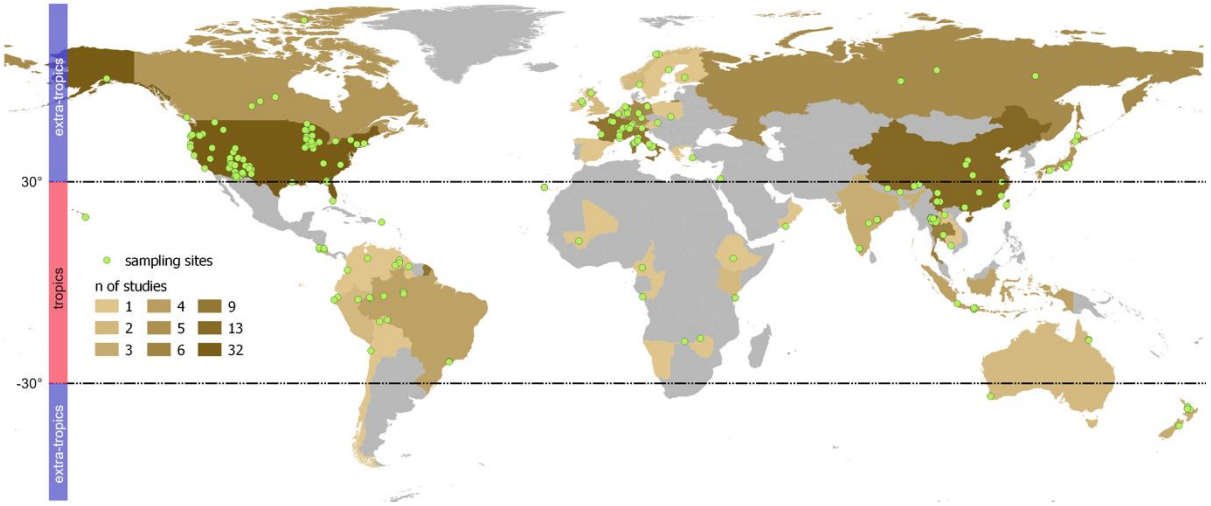

Figure 1: Geographical distribution of sampling sites of the tree-ring intra-annual stable isotope studies surveyed in this systematic review. The gradient color among the countries represents the number of studies. The sampling site coordinates are marked with green circles. The dashed lines delimit tropical and extra-tropical regions, according to Corlett (2013).

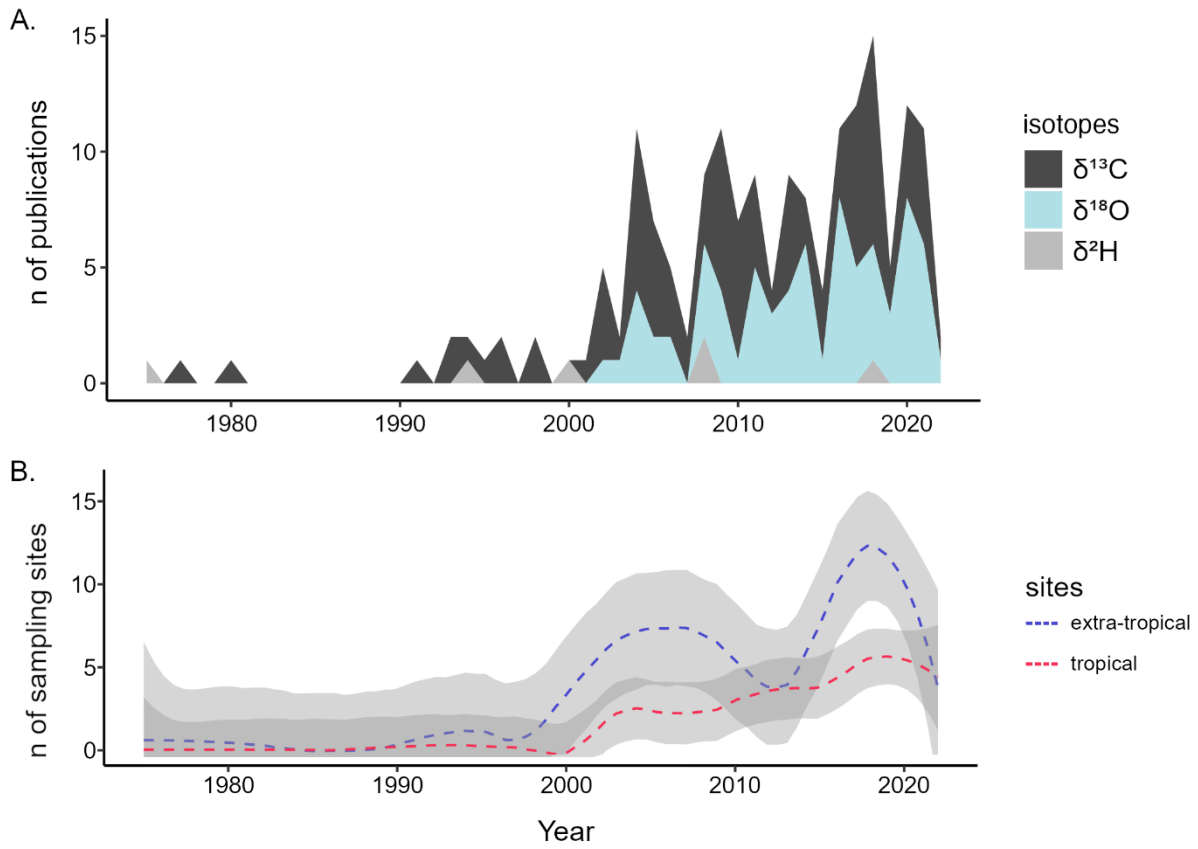

Figure 2: A) The historical trends of publications for each isotope type are represented by the shaded areas, and B) the evolution in the number of sampling sites both in the tropics and extra-tropics represented by a LOESS fit.

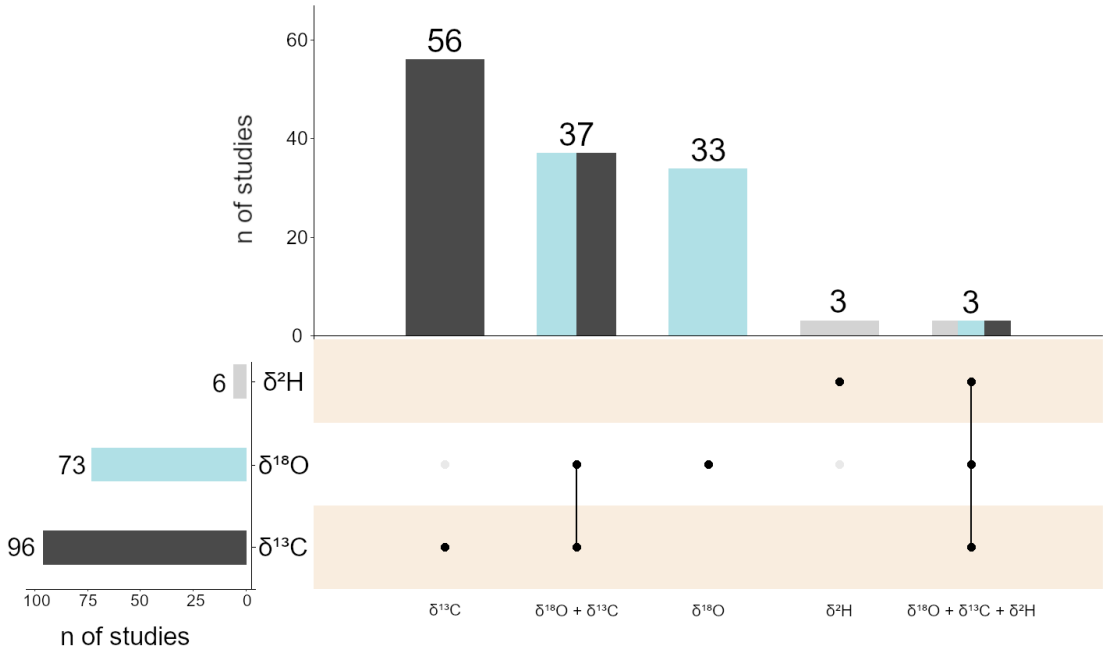

Figure 3: Number of studies using each stable isotope independently and number of studies using a combination of stable isotopes to reach their goals.

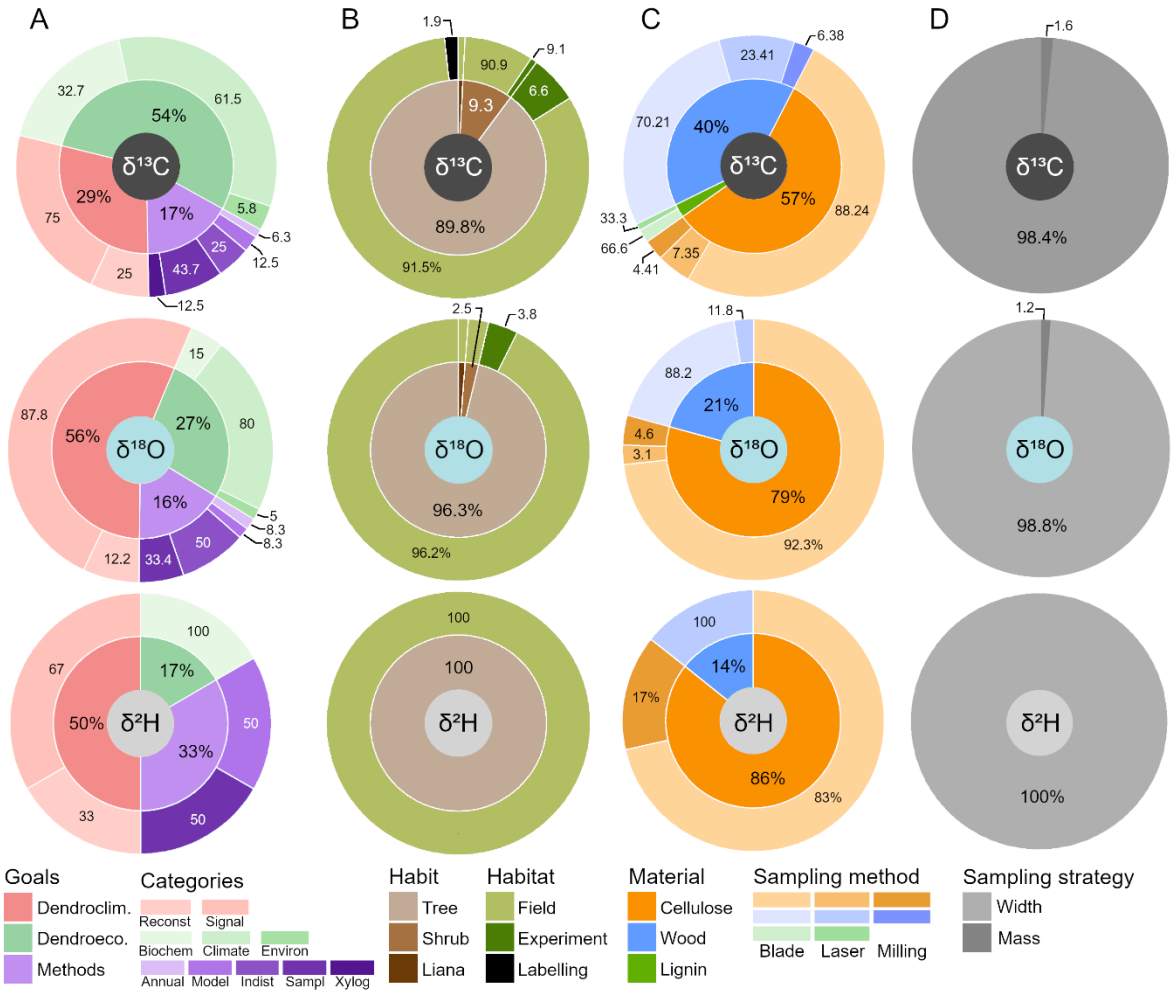

Figure 4: Characterization of the studies' goals and the methodological choices for each stable isotope, namely $\delta^{13}C$, $\delta^{18}O$, and $\delta^{2}H$. (A) the categories and subcategories of studies' goals; (B) the habit of sampled species and the sampling sites (we considered labeling experiments as an extra category for discussion purposes); (C) sample material and the intra-annual sampling methods; (D) categories of intra-annual sampling strategy to space-for-time conversion.

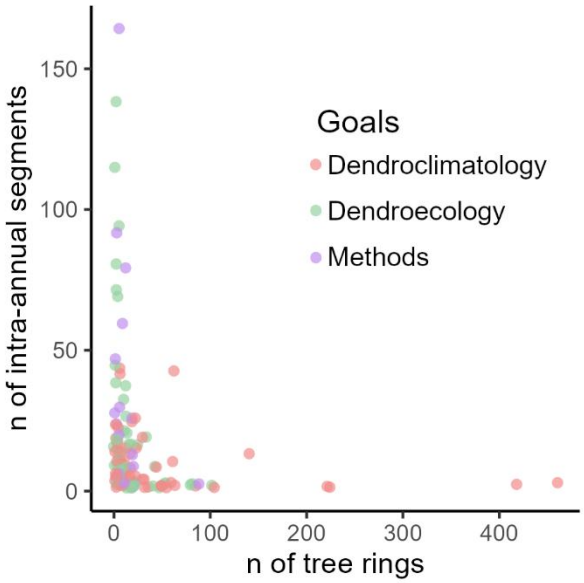

Figure 5: The trade-off between the number of intra-annual segments and number of tree rings used in the design of each study.

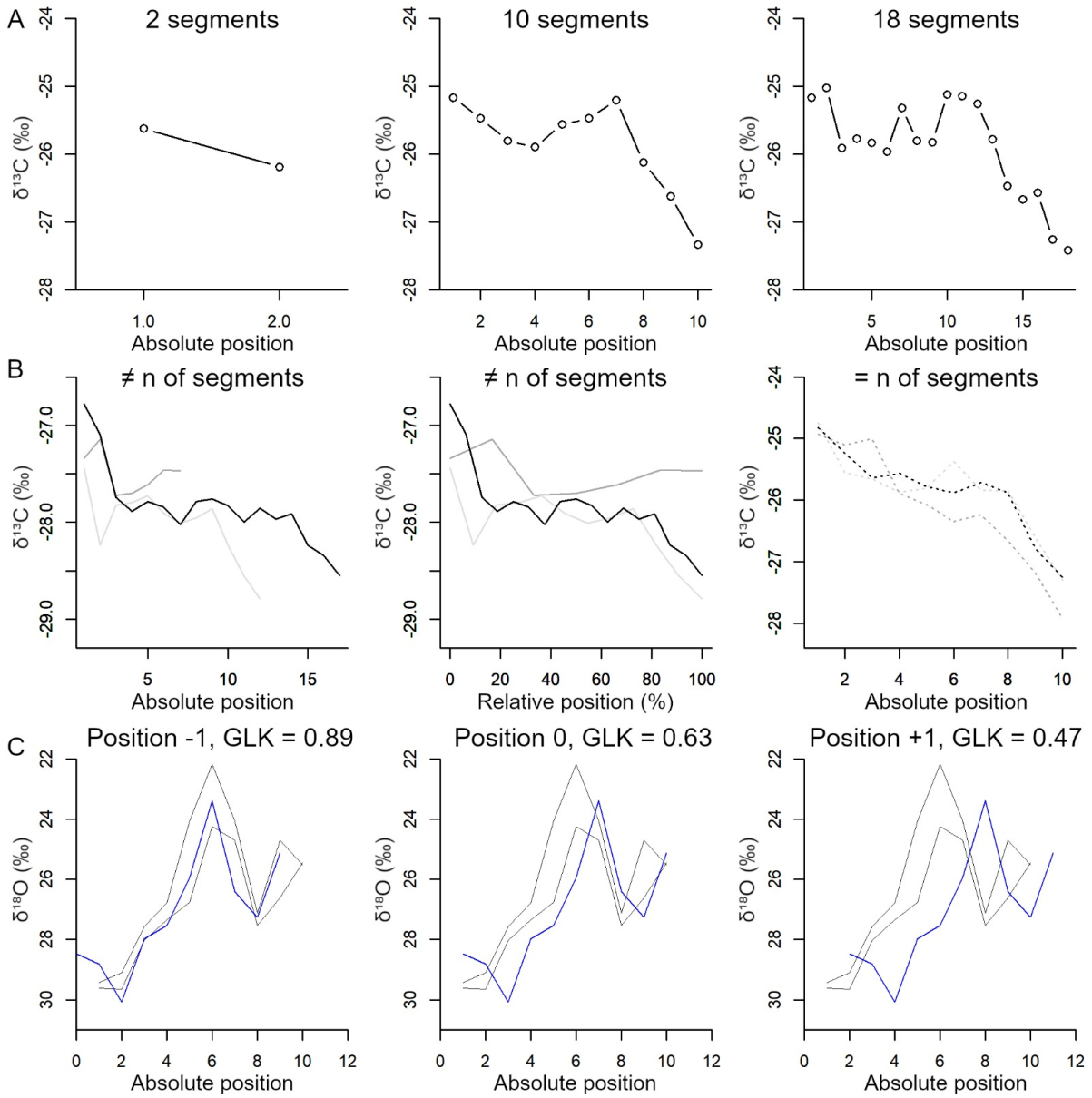

Figure 6: Examples of how the decision on the choice of the number of segments, use of distinct or equal segments, and synchronization of intra-annual series matters in the analyses and interpretation of the results. A) Visual comparison of the information brought by using two, ten, and eighteen segments of the same tree ring of a Tipuana tipu tree (data from Locosselli et al, 2020a). B) A visual comparison between the choice of using a distinct number of segments plotted by absolute intra-annual position, and how data visualization improves by using the relative position within the tree ring for the same dataset (data of Cedrela odorata from Cintra et al, 2019), and the choice of using an equal number of intra-annual segments (data of Tipuana tipu, from Locosselli et al, 2020a). C) Synchronization of intra-annual series of three trees of Tipuana tipu growing in the city of São Paulo during the year 2010 (modified from Locosselli et al, 2020a). The blue series represents the intra-annual series of one individual, and the grey lines represent the data from another two individuals. Position 0 represents the data as produced by dividing the tree rings into 10 segments. The blue line is shifted one position to the left

(position -1) or to the right (position +1) to improve the synchronization, measured by the GLK values.

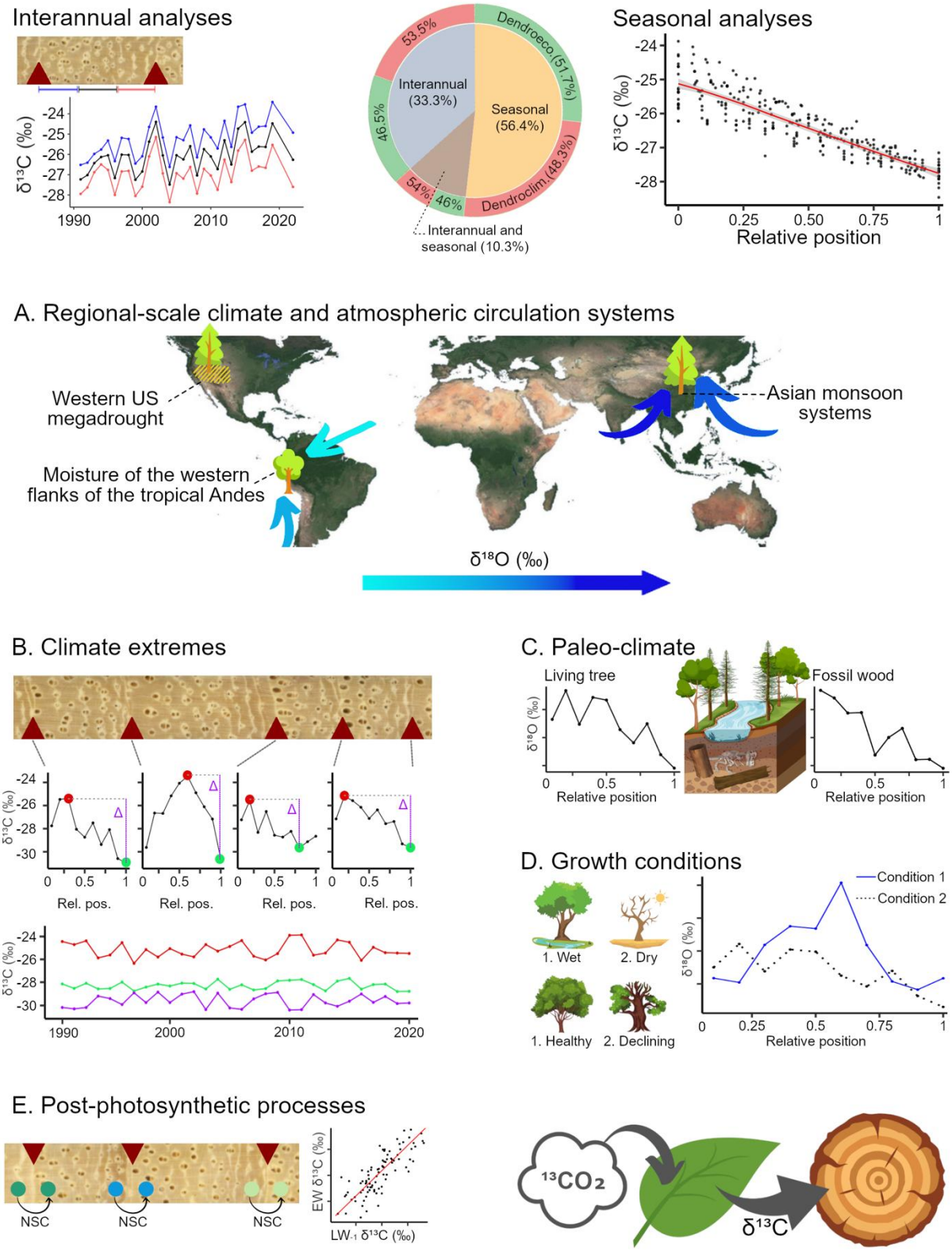

Figure 7: Examples of the application of the two basic approaches used in the intra-annual stable isotope studies, namely: interannual analysis and seasonal analysis. The interannual analysis of the intra-annual segments, that uses the intra-ring segments on a year-to-year basis, and the seasonal analysis that is more focused on the intra-ring variability of the stable isotopes. A) the regional scale climate and atmospheric circulation systems can be evaluated by the

means of these two approaches, as well as E) the assessment of post-photosynthetic processes. B) the evaluation of climate extremes using new metrics like the maximum, minimum and delta values of the stable isotopes allows creating highly informative annual series for climate reconstruction, whereas C) the use of fossil samples in combination with living trees allow striving past climate conditions at a high temporal resolution. Seasonal analyses can also be employed to assess growth strategies among distinct conditions.

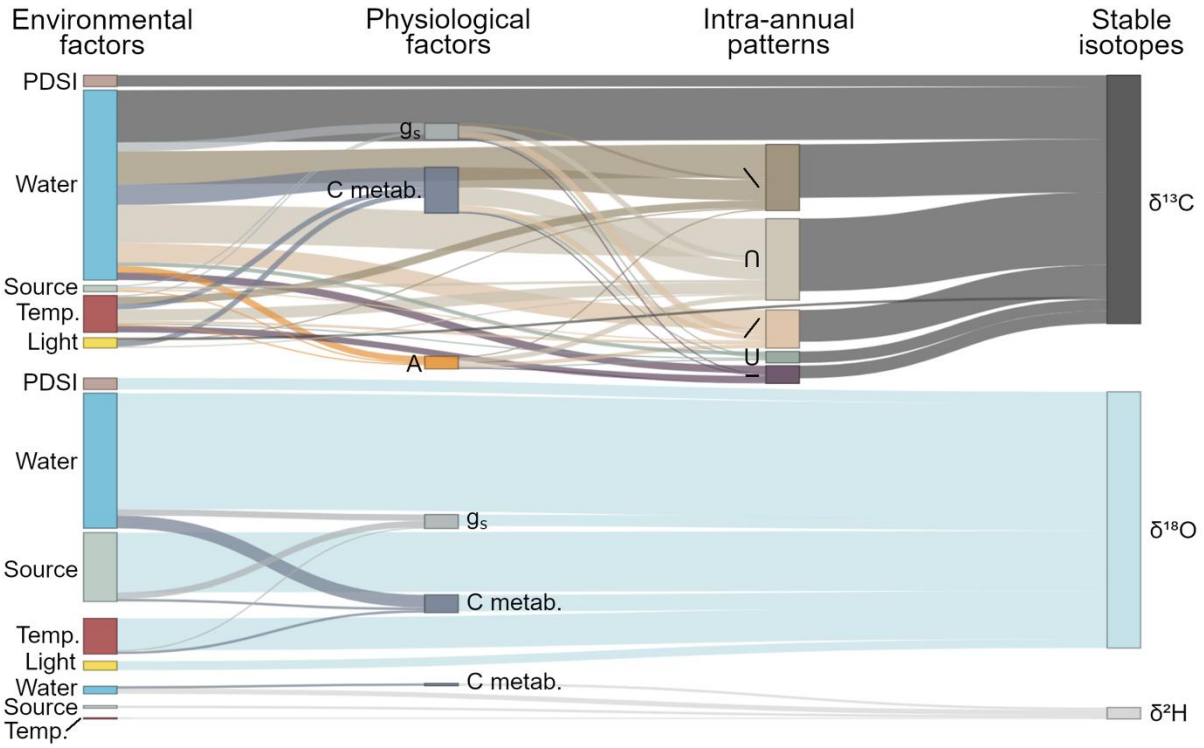

Figure 8: Sankey graphic showing how the results of each population across all studies were interpreted in terms of intra-annual patterns of stable isotope signatures in tree rings. Especially for $\delta^{13}C$, the observed recurrence of five intra-annual patterns led to the categorization of them according to the shape of $\delta^{13}C$ variation during the growth season (decreasing trend, bell-shaped, increasing trend, u-shaped, and flat). The factors that influence this oscillation of intra-annual isotope signatures, and consequently responsible for the observed patterns, were compiled, categorized in environmental or physiological, and subcategorized in groups (see Table S2 for further details).

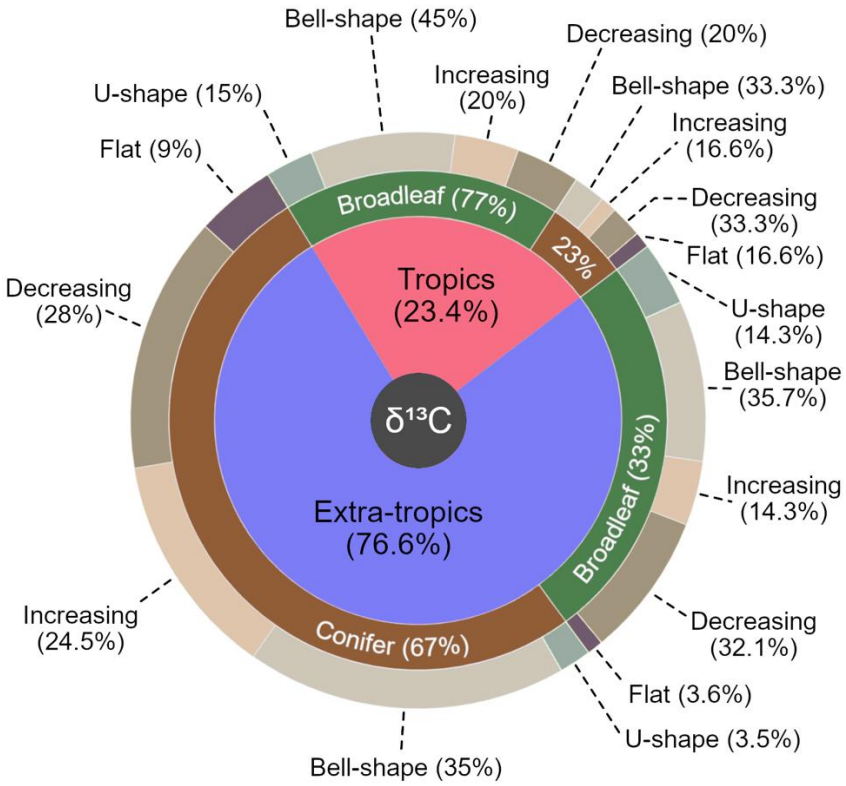

Figure 9: Distribution of the five recurrent intra-annual $\delta^{13}C$ trends described by the studies, and how these patterns change according to provenance and taxonomic groups.

Table 1: Main categories of the intra-annual stable-isotope studies goals based on the potential of their applications in dendrochronology

Goals	Inclusion criteria	Subcategories	Inclusion criteria
Dendroclimatology	Focus on paleoclimate reconstruction, or potential of climate influences on intra-ring isotope signatures	Climate reconstruction	Reconstruction of climate for periods without instrumental measurements.
		Climate signal	Recognize correlation of climate and isotopic signals for potential reconstruction.
Dendroecology	Assess the stable isotope across different species, populations, and environmental conditions, and eventually discuss it in terms of physiological mechanisms behind the observed patterns.	Biochemical effect	Focus on metabolic and physiological processes of trees.
		Climate effect	Evaluate the climate effects on tree functioning.
		Environmental effect	Assess the impact of distinct environmental conditions on trees.
Methodological advances	Test, improve or develop new methos for intra-ring stable isotopes analyses. Test the efficiency of new species for these studies.	Annuality	Verify the annual formation of tree rings based on isotopic signals.
		Modelling	Develop models to predict the isotopic signals.
		Indistinct rings	Identify seasonal wood formation in species with indistinct tree rings.
		Sample preparation	Enhancement of methods for intra-annual sampling.
		Xylogenesis	Elucidate wood formation processes by isotopic fractionation.

Supplementary material:

Search expression

("intra-annual" AND "stable isotope$" AND "tree ring$") OR ("intra-annual" AND "stable isotope$" AND "dendrochronology") OR ("high-resolution" AND "stable isotope$" AND "tree ring$") OR ("high-resolution" AND "stable isotope$" AND "dendrochronology") OR ("within-ring$" AND "stable isotope$" AND "tree ring$") OR ("within-ring$" AND "stable isotope$" AND "dendrochronology") OR ("sub-annual" AND "stable isotope$" AND "tree ring$") OR ("sub-annual" AND "stable isotope$" AND “dendrochronology”) OR ("intra-seasonal" AND "stable isotope$" AND "tree ring$") OR ("intra-seasonal" AND "stable isotope$" AND “dendrochronology”) OR ("seasonal" AND "stable isotope$" AND "tree ring$") OR ("seasonal" AND "stable isotope$" AND “dendrochronology”) OR ("intra-annual" AND "δ18O" AND "tree ring$") OR ("intra-annual" AND "δ18O" AND “dendrochronology”) OR ("high-resolution" AND "δ18O" AND "tree ring$") OR ("high-resolution" AND "δ18O" AND dendrochronology) OR ("within-ring$" AND "δ18O" AND "tree ring$") OR ("within-ring$" AND "δ18O" AND dendrochronology) OR ("sub-annual" AND "δ18O" AND "tree ring$") OR ("sub-annual" AND "δ18O" AND “dendrochronology”) OR ("intra-seasonal" AND "δ18O" AND "tree ring$") OR ("intra-seasonal" AND "δ18O" AND “dendrochronology”) OR ("seasonal" AND "δ18O" AND "tree ring$") OR ("seasonal" AND "δ18O" AND “dendrochronology”) OR ("intra-annual" AND "δ13C" AND "tree ring$") OR ("intra-annual" AND "δ13C" AND “dendrochronology”) OR ("high-resolution" AND "δ13C" AND "tree ring$") OR ("high-resolution" AND "δ13C" AND “dendrochronology”) OR ("within-ring$" AND "δ13C" AND "tree ring$") OR ("within-ring$" AND "δ13C" AND “dendrochronology”) OR ("sub-annual" AND "δ13C" AND "tree ring$") OR ("sub-annual" AND "δ13C" AND “dendrochronology”) OR ("intra-seasonal" AND "δ13C" AND "tree ring$") OR ("intra-seasonal" AND "δ13C" AND “dendrochronology”) OR ("seasonal" AND "δ13C" AND "tree ring$") OR ("seasonal" AND "δ13C" AND “dendrochronology”) OR ("intra-annual" AND "δD" AND "tree ring$") OR ("intra-annual" AND "δD" AND “dendrochronology”) OR ("high-resolution" AND "δD" AND "tree ring$") OR ("high-resolution" AND "δD" AND “dendrochronology”) OR ("within-ring$" AND "δD" AND "tree ring$") OR ("within-ring$" AND "δD" AND “dendrochronology”) OR ("sub-annual" AND "δD" AND "tree ring$") OR ("sub-annual" AND "δD" AND “dendrochronology”) OR ("intra-seasonal" AND "δD" AND "tree ring$") OR ("intra-seasonal" AND "δD" AND “dendrochronology”) OR ("seasonal" AND "δD" AND "tree ring$") OR ("seasonal" AND "δD" AND “dendrochronology”) OR ("intra-

annual" AND "deuterium" AND "tree ring$") OR ("intra-annual" AND "deuterium" AND "dendrochronology") OR ("high-resolution" AND "deuterium" AND "tree ring$") OR ("high-resolution" AND "deuterium" AND "dendrochronology") OR ("within-ring$" AND "deuterium" AND "tree ring$") OR ("within-ring$" AND "deuterium" AND dendrochronology) OR ("sub-annual" AND "deuterium" AND "tree ring$") OR ("sub-annual" AND "deuterium" AND "dendrochronology") OR ("intra-seasonal" AND "deuterium" AND "tree ring$") OR ("intra-seasonal" AND "deuterium" AND dendrochronology) OR ("seasonal" AND "deuterium" AND "tree ring$") OR ("seasonal" AND "deuterium" AND "dendrochronology").

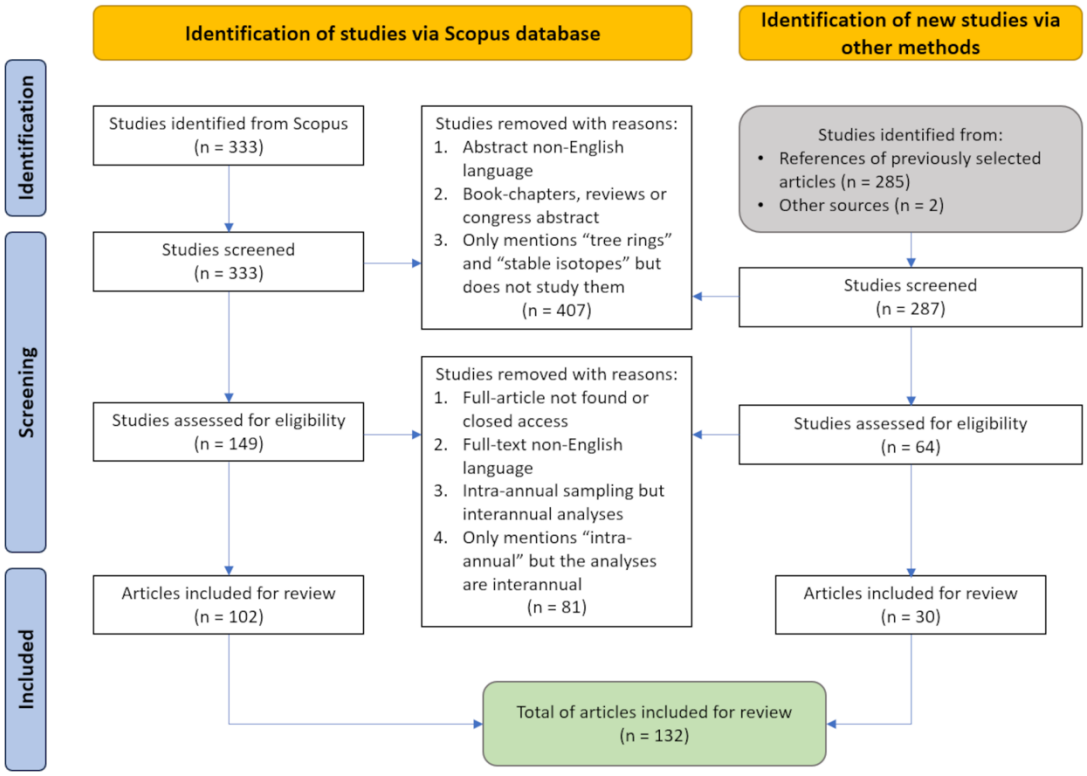

Figure S1: PRISMA 2020 flow diagram detailing the criteria used for screening the studies to be assessed for eligibility and the number of studies included or excluded in each step.

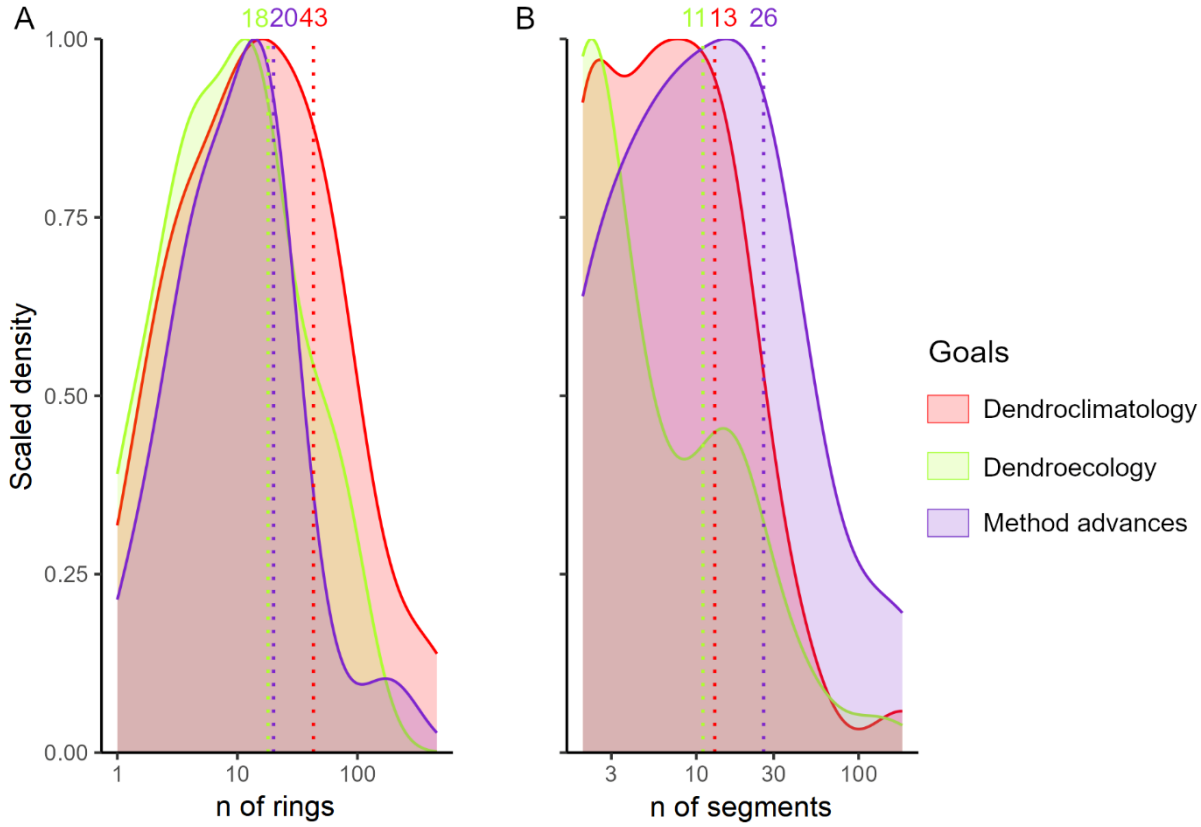

Figure S2: Density plots showing the distribution of the number of trees, tree rings and segments per ring for each intra-annual stable isotope studies, and respective average values.

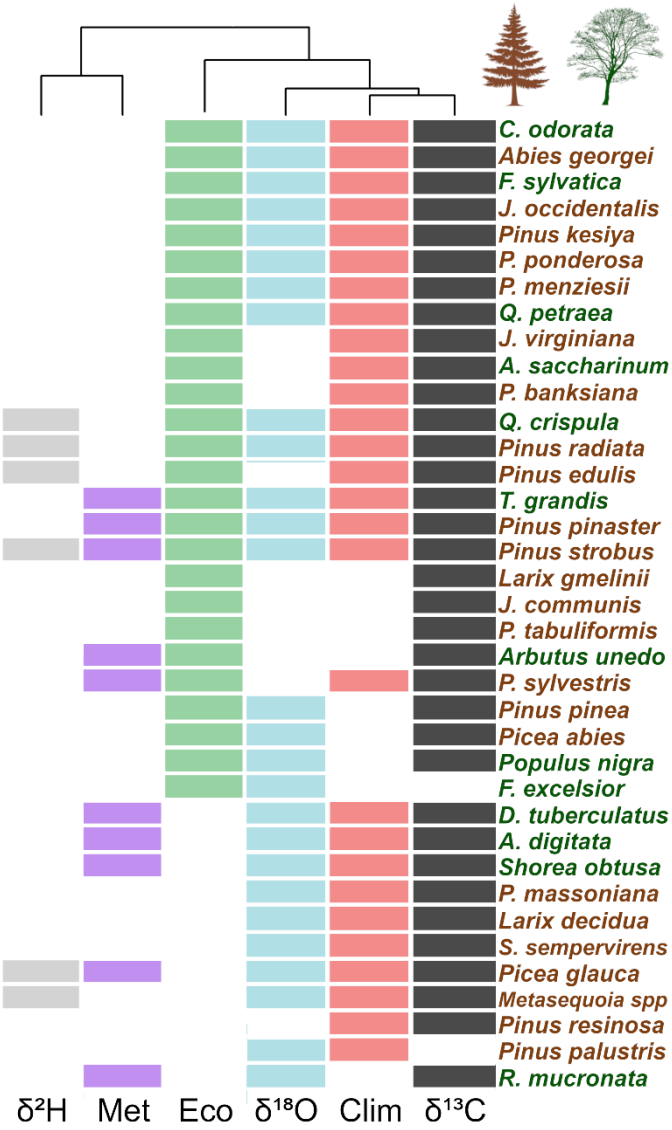

Figure S3: Conifer (brown) and broadleaf (green) species used in at least two studies for intra-annual stable isotope analyses. The dendrogram reveals the clusters of species sampled by study's goal and stable isotopes.

Table S1: Full list of the studies analyzed in this systematic review, categorized and subcategorized according to their applications, based on their main objectives and interpretation of the results.

Year	Reference	Category	Subcategory
1975	Wilson and Grinsted	Dendroclimatology	Climate signal
1977	Wilson and Grinsted	Dendroclimatology	Climate signal
1980	Tans and Mook	Dendroclimatology	Climate reconstruction
1991	Leavitt and Long	Dendroecology	Climate effect
1993	Kitagawa and Wada	Dendroclimatology	Climate signal
1993	Leavitt	Dendroecology	Climate effect
1994	White et al	Methodological Advances	Modelling
1994	Ogle and McCormac	Methodological Advances	Sample preparation
1995	Sheu et al	Dendroecology	Climate effect
1996	Livingston & Spittlehouse	Dendroecology	Climate effect
1996	Marshall and Monserud	Dendroecology	Climate effect
1998	Macfarlane and Adams	Dendroecology	Climate effect
1998	Brooks et al	Dendroecology	Climate effect
2000	Pendall	Dendroclimatology	Climate signal
2001	Takahashi et al	Dendroclimatology	Climate reconstruction
2002	Leavitt	Dendroclimatology	Climate signal
2002	Jäggi et al	Dendroecology	Biochemical effect
2002	Barbour et al	Dendroecology	Climate effect
2002	Leavitt and Wright	Dendroclimatology	Climate signal
2003	Kagawa et al	Dendroecology	Climate effect
2003	Jäggi et al	Dendroecology	Climate effect
2004	Tarhule and Leavitt	Dendroclimatology	Climate signal
2004	Verheyden	Methodological advances	Ringless
2004	Helle and Scheleser	Dendroecology	Biochemical effect
2004	Poussart et al	Methodological advances	Ringless
2004	Potts and Williams	Dendroecology	Climate effect
2004	Schulze et al	Methodological advances	Sample preparation
2004	Nakatsuka et al	Dendroclimatology	Climate signal
2004	Evans and Schrag	Methodological advances	Ringless
2005	Klein et al	Dendroecology	Environmental effect
2005	Li et al	Dendroecology	Environmental effect
2005	Poussart and Schrag	Dendroclimatology	Climate signal
2005	Roden et al	Dendroclimatology	Climate signal
2005	Verheyden et al	Methodological advances	Sample preparation
2006	Kagawa et al	Dendroecology	Biochemical effect

2006	Miller et al	Dendroclimatology	Climate signal
2006	Skomarkova et al	Dendroecology	Climate effect
2006	Verheyden et al	Dendroecology	Environmental effect
2007	Leavitt	Dendroclimatology	Climate signal
2007	de Micco et al	Dendroecology	Climate effect
2008	Dodd et al	Methodological advances	Sample preparation
2008	Weigl et al	Dendroclimatology	Climate signal
2008	Jahren and Sternberg	Dendroclimatology	Climate reconstruction
2008	Anchukaitis et al	Methodological Advances	Ringless
2009	Koretsune et al	Dendroecology	Climate effect
2009	Vaganov et al	Dendroecology	Biochemical effect
2009	Ogée et al	Methodological advances	Modelling
2009	Berkelhammer et al	Dendroclimatology	Climate signal
2009	Ohashi et al	Methodological advances	Ringless
2009	Roden et al	Dendroclimatology	Climate signal
2009	Gessler et al	Dendroecology	Biochemical effect
2009	Kress et al	Dendroclimatology	Climate signal
2010	Battipaglia et al	Dendroecology	Climate effect
2010	Eglin et al	Dendroecology	Biochemical effect
2010	Managave et al	Dendroclimatology	Climate signal
2010	Maunoury-Danger et al	Dendroecology	Biochemical effect
2010	Ballantyne et al	Methodological advances	Modelling
2010	Eilmann et al	Dendroclimatology	Climate effect
2010	Fichtler et al	Dendroclimatology	Climate signal
2011	Offermann et al	Dendroecology	Biochemical effect
2011	Li et al	Methodological advances	Sample preparation
2011	Pons and Helle	Methodological advances	Ringless
2011	Managave et al	Dendroclimatology	Climate signal
2011	Ballantyne et al	Dendroclimatology	Climate signal
2011	Michelot et al	Dendroecology	Biochemical effect
2012	De Micco et al	Methodological advances	Xylogenesis
2012	An et al	Dendroclimatology	Climate signal
2012a	Zhu et al	Dendroclimatology	Climate signal
2012b	Zhu et al	Dendroclimatology	Climate reconstruction
2013	Schollaen et al	Dendroclimatology	Climate signal
2013	Sarris et al	Dendroecology	Climate effect
2013	Johnstone et al	Dendroclimatology	Climate signal
2013	Krepkowski et al	Dendroecology	Biochemical effect

2013	Rossi et al	Dendroecology	Climate effect
2014	Boysen et al	Dendroclimatology	Climate signal
2014	Schollaen et al	Methodological advances	Sample preparation
2014	Battipaglia et al	Dendroecology	Climate effect
2014	Xu et al	Methodological advances	Ringless
2014	Treydte et al	Dendroclimatology	Climate signal
2014	Zeng et al	Dendroclimatology	Climate signal
2015	Schubert & Timmermann	Dendroclimatology	Climate reconstruction
2015	Schubert and Jahren	Dendroclimatology	Climate signal
2015	Rinne et al	Dendroecology	Biochemical effect
2015	Kimak and Leuenberger	Dendroecology	Biochemical effect
2016	Sargeant and Singer	Dendroecology	Climate effect
2016	Muangsong et al	Dendroclimatology	Climate signal
2016	Soudant et al	Methodological advances	Xylogenesis
2016	Szejner et al	Dendroecology	Climate effect
2016	Zeng et al	Dendroclimatology	Climate signal
2016a	Xu et al	Dendroclimatology	Climate signal
2016b	Xu et al	Dendroclimatology	Climate signal
2016	Ohashi et al	Methodological advances	Annuality
2016	Labotka et al	Dendroclimatology	Climate signal
2017	Zeng et al	Dendroecology	Climate effect
2017	Baton et al	Dendroclimatology	Climate signal
2017	Managave et al	Dendroecology	Climate effect
2017	Schollaen et al	Methodological advances	Sample preparation
2017	Kerhoulas et al	Dendroecology	Climate effect
2017	Harada et al	Dendroclimatology	Climate signal
2017	Fu et al	Dendroecology	Climate effect
2017	McCarroll et al	Dendroecology	Biochemical effect
2018	Nabeshima et al	Dendroecology	Biochemical effect
2018	Belmecheri et al	Dendroclimatology	Climate signal
2018	Szejner et al	Dendroecology	Climate effect
2018	Castagneri et al	Dendroecology	Climate effect
2018	Zalloni et al	Dendroecology	Climate effect
2018	Voelker et al	Dendroclimatology	Climate reconstruction
2018	Rebenack et al	Dendroclimatology	Climate signal
2018	McKenzie et al	Dendroecology	Climate effect
2018	Fonti et al	Dendroecology	Climate effect
2019	An et al	Dendroclimatology	Climate signal

2019	Michelot-Antalik et al	Dendroecology	Biochemical effect
2019	Cintra et al	Dendroecology	Climate effect
2019	Szymczak et al	Dendroclimatology	Climate signal
2020	Landshuter et al	Dendroclimatology	Climate signal
2020	Tepley et al	Dendroecology	Climate effect
2020	Locosselli et al	Dendroclimatology	Climate signal
2020	Xu et al	Dendroclimatology	Climate reconstruction
2020	Muangsong et al	Dendroclimatology	Climate signal
2020	Olson et al	Dendroclimatology	Climate reconstruction
2020a	Szejner et al	Dendroecology	Climate effect
2020b	Szejner et al	Dendroclimatology	Climate signal
2021	Xu et al	Dendroclimatology	Climate signal
2021	Miranda et al	Dendroecology	Climate effect
2021	Fan et al	Dendroclimatology	Climate signal
2021	Sargeant et al	Dendroecology	Climate effect
2021	Slotta et al	Dendroclimatology	Climate signal
2021	Vornlocher et al	Dendroclimatology	Climate reconstruction
2021	He et al	Dendroecology	Biochemical effect
2021	Szejner et al	Dendroclimatology	Climate signal
2021	Lukens et al	Dendroclimatology	Climate signal
2022	Giraldo et al	Dendroecology	Climate effect

Table S2: Categorization of physiological and environmental factors based on how they influence intra-ring stable isotope signatures, details of inclusion criteria and citation of the physiological and environmental influences for each category.

Type	Categories	Influences
Environmental	PDSI	PDSI
Environmental	Water	Relative humidity, vapor pressure deficit, precipitation, water availability, reservoir volume, atmospheric pressure.
Environmental	Source	Source water, typhoon, rooth depth, $\delta^{13}CO_2$.
Environmental	Temperature	Temperature
Environmental	Light	Fog, cloud cover, photoperiod, solar radiation
Physiological	Stomatal conductance	Stomatal conductance
Physiological	Carbon metabolism	Reserve mobilization, f-value, lignification, cellulose synthesis.
Physiological	Assimilation	Assimilation

Surveyed references

An, W., Liu, X., Leavitt, S., Ren, J., Sun, W., Wang, W., Wang, Y., Xu, G., Chen, T., & Qin, D. (2012). Specific climatic signals recorded in earlywood and latewood $\delta^{18}O$ of tree rings in southwestern China. *Tellus B: Chemical and Physical Meteorology*, 64(1), 18703.

Anchukaitis, K. J., Evans, M. N., Wheelwright, N. T., & Schrag, D. P. (2008). Stable isotope chronology and climate signal calibration in neotropical montane cloud forest trees. *Journal of Geophysical Research: Biogeosciences*, 113(G3).

Ballantyne, A. P., Miller, J. B., & Tans, P. P. (2010). Apparent seasonal cycle in isotopic discrimination of carbon in the atmosphere and biosphere due to vapor pressure deficit. *Global Biogeochemical Cycles*, 24(3).

Ballantyne, A. P., Baker, P. A., Chambers, J. Q., Villalba, R., & Argollo, J. (2011). Regional differences in South American monsoon precipitation inferred from the growth and isotopic composition of tropical trees. *Earth Interactions*, 15(5), 1-35.

Barbour, M. M., Walcroft, A. S., & Farquhar, G. D. (2002). Seasonal variation in $\delta^{13}C$ and $\delta^{18}O$ of cellulose from growth rings of *Pinus radiata*. *Plant, Cell & Environment*, 25(11), 1483-1499.

Baton, F., Tu, T. T. N., Derenne, S., Delorme, A., Delarue, F., & Dufraisse, A. (2017). Tree-ring $\delta^{13}C$ of archeological charcoals as indicator of past climatic seasonality. A case study from the Neolithic settlements of Lake Chalain (Jura, France). *Quaternary international*, 457, 50-59.

Battipaglia, G., De Micco, V., Brand, W. A., Linke, P., Aronne, G., Saurer, M., & Cherubini, P. (2010). Variations of vessel diameter and $\delta^{13}C$ in false rings of *Arbutus unedo* L. reflect different environmental conditions. *New Phytologist*, 188(4), 1099-1112.

Battipaglia, G., De Micco, V., Brand, W. A., Saurer, M., Aronne, G., Linke, P., & Cherubini, P. (2014). Drought impact on water use efficiency and intra-annual density fluctuations in *Erica arborea* on Elba (Italy). *Plant, Cell & Environment*, 37(2), 382-391.

Belmecheri, S., Wright, W. E., Szejner, P., Morino, K. A., & Monson, R. K. (2018). Carbon and oxygen isotope fractionations in tree rings reveal interactions between cambial phenology and seasonal climate. *Plant, Cell & Environment*, 41(12), 2758-2772.

Berkelhammer, M., & Stott, L. D. (2009). Modeled and observed intra-ring $\delta^{18}O$ cycles within late Holocene Bristlecone Pine tree samples. *Chemical Geology*, 264(1-4), 13-23.

Boysen, B. M., Evans, M. N., & Baker, P. J. (2014). $\delta^{18}O$ in the tropical conifer *Agathis robusta* records ENSO-related precipitation variations. *PLoS One*, 9(7), e102336.

Brooks, J. R., Flanagan, L. B., & Ehleringer, J. R. (1998). Responses of boreal conifers to climate fluctuations: indications from tree-ring widths and carbon isotope analyses. *Canadian Journal of Forest Research*, 28(4), 524-533.

Castagneri, D., Battipaglia, G., Von Arx, G., Pacheco, A., & Carrer, M. (2018). Tree-ring anatomy and carbon isotope ratio show both direct and legacy effects of climate on bimodal xylem formation in Pinus pinea. *Tree physiology*, 38(8), 1098-1109.

Cintra, B. B. L., Gloor, M., Boom, A., Schöngart, J., Locosselli, G. M., & Brienen, R. (2019). Contrasting controls on tree ring isotope variation for Amazon floodplain and terra firme trees. *Tree physiology*, 39(5), 845-860.

De Micco, V., Saurer, M., Aronne, G., Tognetti, R., & Cherubini, P. (2007). Variations of wood anatomy and $\delta^{13}C$ within-tree rings of coastal *Pinus pinaster* showing intra-annual density fluctuations. *Iawa Journal*, 28(1), 61-74.

De Micco, V., Battipaglia, G., Brand, W. A., Linke, P., Saurer, M., Aronne, G., & Cherubini, P. (2012). Discrete versus continuous analysis of anatomical and $\delta^{13}C$ variability in tree rings with intra-annual density fluctuations. *Trees*, 26, 513-524.

Dodd, J. P., Patterson, W. P., Holmden, C., & Brasseur, J. M. (2008). Robotic micromilling of tree-rings: a new tool for obtaining subseasonal environmental isotope records. *Chemical Geology*, 252(1-2), 21-30.

Eglin, T., Francois, C., Michelot, A., Delpierre, N., & Damesin, C. (2010). Linking intra-seasonal variations in climate and tree-ring $\delta^{13}C$: a functional modelling approach. *Ecological modelling*, 221(15), 1779-1797.

Eilmann, B., Buchmann, N., Siegwolf, R., Saurer, M., Cherubini, P., & Rigling, A. (2010). Fast response of Scots pine to improved water availability reflected in tree-ring width and $\delta^{13}C$. *Plant, Cell & Environment*, 33(8), 1351-1360.

Evans, M. N., & Schrag, D. P. (2004). A stable isotope-based approach to tropical dendroclimatology. *Geochimica et Cosmochimica Acta*, 68(16), 3295-3305.

Fan, R., Shimada, H., Tei, S., Maximov, T. C., & Sugimoto, A. (2021). Oxygen isotope compositions of cellulose in earlywood of *Larix cajanderi* determined by water source rather than leaf water enrichment in a permafrost ecosystem, Eastern Siberia. *Journal of Geophysical Research: Biogeosciences*, 126(9), e2020JG006125.

Fichtler, E., Helle, G., & Worbes, M. (2010). Stable-carbon isotope time series from tropical tree rings indicate a precipitation signal. *Tree-ring research*, 66(1), 35-49.

Fonti, M. V., Vaganov, E. A., Wirth, C., Shashkin, A. V., Astrakhantseva, N. V., & Schulze, E. D. (2018). Age-effect on intra-annual $\delta^{13}C$-variability within Scots pine tree-rings from Central Siberia. *Forests*, 9(6), 364.

Fu, P. L., Grießinger, J., Gebrekirstos, A., Fan, Z. X., & Bräuning, A. (2017). Earlywood and latewood stable carbon and oxygen isotope variations in two pine species in southwestern China during the recent decades. *Frontiers in plant science*, 7, 2050.

Gessler, A., Brandes, E., Buchmann, N., Helle, G., Rennenberg, H., & Barnard, R. L. (2009). Tracing carbon and oxygen isotope signals from newly assimilated sugars in the leaves to the tree-ring archive. *Plant, Cell & Environment*, 32(7), 780-795.

Giraldo, J. A., del Valle, J. I., González-Caro, S., & Sierra, C. A. (2022). Intra-annual isotope variations in tree rings reveal growth rhythms within the least rainy season of an ever-wet tropical forest. *Trees*, 36(3), 1039-1052.

Harada, M., Watanabe, Y., Nakatsuka, T., Tazuru-Mizuno, S., Horikawa, Y., Subiyanto, B., Sugiyama, J., Tsuda, T., & Tagami, T. (2017). Assessment of sungkai tree-ring $\delta^{18}O$ proxy for paleoclimate reconstruction in western Java, Indonesia. *Quaternary International*, 432, 33-38.

He, M., Bräuning, A., Rossi, S., Gebrekirstos, A., Grießinger, J., Mayr, C., Peng, C., & Yang, B. (2021). No evidence for carryover effect in tree rings based on a pulse-labelling experiment on *Juniperus communis* in South Germany. *Trees*, 35, 493-502.

Helle, G., & Schleser, G. H. (2004). Beyond CO_2-fixation by Rubisco–an interpretation of $^{13}C/^{12}C$ variations in tree rings from novel intra-seasonal studies on broad-leaf trees. *Plant, Cell & Environment*, 27(3), 367-380.

Jäggi, M., Saurer, M., Fuhrer, J., & Siegwolf, R. (2002). The relationship between the stable carbon isotope composition of needle bulk material, starch, and tree rings in *Picea abies*. *Oecologia*, 131, 325-332.

Jäggi, M., Saurer, M., Fuhrer, J., & Siegwolf, R. (2003). Seasonality of $\delta^{18}O$ in needles and wood of *Picea abies*. *New Phytologist*, 158(1), 51-59.

Jahren, A. H., & Sternberg, L. S. (2008). Annual patterns within tree rings of the Arctic middle Eocene (ca. 45 Ma): isotopic signatures of precipitation, relative humidity, and deciduousness. *Geology*, 36(2), 99-102.

Johnstone, J. A., Roden, J. S., & Dawson, T. E. (2013). Oxygen and carbon stable isotopes in coast redwood tree rings respond to spring and summer climate signals. *Journal of Geophysical Research: Biogeosciences*, 118(4), 1438-1450.

Kagawa, A., Naito, D., Sugimoto, A., & Maximov, T. C. (2003). Effects of spatial and temporal variability in soil moisture on widths and $\delta^{13}C$ values of eastern Siberian tree rings. *Journal of Geophysical Research: Atmospheres*, 108(D16).

Kagawa, A., Sugimoto, A., & Maximov, T. C. (2006). $^{13}CO_2$ pulse-labelling of photoassimilates reveals carbon allocation within and between tree rings. *Plant, Cell & Environment*, 29(8), 1571-1584.

Kerhoulas, L. P., Kolb, T. E., & Koch, G. W. (2017). The influence of monsoon climate on latewood growth of southwestern ponderosa pine. *Forests*, 8(5), 140.

Kimak, A., & Leuenberger, M. (2015). Are carbohydrate storage strategies of trees traceable by early–latewood carbon isotope differences? *Trees*, 29, 859-870.

Kitagawa, H., & Wada, H. (1993). Seasonal and secular $\delta^{13}C$ variations in annual growth rings of a Japanese cedar tree from Mt. Amagi, Izu Peninsula, Central Japan. *Geochemical Journal*, 27(6), 391-396.

Klein, T., Hemming, D., Lin, T., Grünzweig, J. M., Maseyk, K., Rotenberg, E., & Yakir, D. (2005). Association between tree-ring and needle $\delta^{13}C$ and leaf gas exchange in *Pinus halepensis* under semi-arid conditions. *Oecologia*, 144, 45-54.

Koretsune, S., Fukuda, K., Chang, Z., Shi, F., & Ishida, A. (2009). Effective rainfall seasons for interannual variation in $\delta^{13}C$ and tree-ring width in early and late wood of Chinese pine and black locust on the Loess Plateau, China. *Journal of forest research*, 14(2), 88-94.

Krepkowski, J., Gebrekirstos, A., Shibistova, O., & Bräuning, A. (2013). Stable carbon isotope labeling reveals different carry-over effects between functional types of tropical trees in an Ethiopian mountain forest. *New Phytologist*, 199(2), 431-440.

Kress, A., Young, G. H., Saurer, M., Loader, N. J., Siegwolf, R. T., & McCarroll, D. (2009). Stable isotope coherence in the earlywood and latewood of tree-line conifers. *Chemical Geology*, 268(1-2), 52-57.

Labotka, D. M., Grissino-Mayer, H. D., Mora, C. I., & Johnson, E. J. (2016). Patterns of moisture source and climate variability in the southeastern United States: a four-century seasonally resolved tree-ring oxygen-isotope record. *Climate dynamics*, 46, 2145-2154.

Landshuter, N., Mölg, T., Grießinger, J., Bräuning, A., & Peters, T. (2020). 10-year characteristics of moisture source regions and their potential effect on seasonal isotopic signatures of $\delta^{18}O$ in tropical trees of southern Ecuador. *Frontiers in Earth Science*, 8, 604804.

Leavitt, S. W. (1993). Seasonal $^{13}C/^{12}C$ changes in tree rings: species and site coherence, and a possible drought influence. *Canadian Journal of Forest Research*, 23(2), 210-218.

Leavitt, S. W. (2002). Prospects for reconstruction of seasonal environment from tree-ring $\delta^{13}C$: baseline findings from the Great Lakes area, USA. *Chemical Geology*, 192(1-2), 47-58.

Leavitt, S. W. (2007). Regional expression of the 1988 US Midwest drought in seasonal $\delta^{13}C$ of tree rings. *Journal of Geophysical Research: Atmospheres*, 112(D6).

Leavitt, S. W., & Lone, A. (1991). Seasonal stable-carbon isotope variability in tree rings: possible paleoenvironmental signals. *Chemical Geology: Isotope Geoscience section*, 87(1), 59-70.

Leavitt, S. W., Wright, W. E., & Long, A. (2002). Spatial expression of ENSO, drought, and summer monsoon in seasonal $\delta^{13}C$ of ponderosa pine tree rings in southern Arizona and New Mexico. *Journal of Geophysical Research: Atmospheres*, 107(D18), ACL-3.

Li, Z. H., Leavitt, S. W., Mora, C. I., & Liu, R. M. (2005). Influence of earlywood–latewood size and isotope differences on long-term tree-ring $\delta^{13}C$ trends. *Chemical geology*, 216(3-4), 191-201.

Li, Z. H., Labbé, N., Driese, S. G., & Grissino-Mayer, H. D. (2011). Micro-scale analysis of tree-ring $\delta^{18}O$ and $\delta^{13}C$ on α-cellulose spline reveals high-resolution intra-annual climate variability and tropical cyclone activity. *Chemical Geology*, 284(1-2), 138-147.

Livingston, N. J., & Spittlehouse, D. L. (1996). Carbon isotope fractionation in tree ring early and late wood in relation to intra-growing season water balance. *Plant, Cell & Environment*, 19(6), 768-774.

Locosselli, G. M., Brienen, R. J., de Souza Martins, V. T., Gloor, E., Boom, A., de Camargo, E. P., Saldiva, P. H. N., & Buckeridge, M. S. (2020). Intra-annual oxygen isotopes in the tree rings record precipitation extremes and water reservoir levels in the Metropolitan Area of São Paulo, Brazil. *Science of the Total Environment*, 743, 140798.

Lukens, W. E., Narmour, R. T., & Schubert, B. A. (2021). Seasonal hydroclimate recorded in high resolution $\delta^{18}O$ profiles across *Pinus palustris* growth rings. *Journal of Geophysical Research: Biogeosciences*, 126(12), e2021JG006505.

Macfarlane, C., & Adams, M. A. (1998). $\delta^{13}C$ of wood in growth-rings indicates cambial activity of drought-stressed trees of *Eucalyptus globulus*. *Functional Ecology*, 12(4), 655-664.

Managave, S. R., Sheshshayee, M. S., Borgaonkar, H. P., & Ramesh, R. (2010). Past break-monsoon conditions detectable by high resolution intra-annual $\delta^{18}O$ analysis of teak rings. *Geophysical Research Letters*, 37(5).

Managave, S. R., Sheshshayee, M. S., Bhattacharyya, A., & Ramesh, R. (2011). Intra-annual variations of teak cellulose $\delta^{18}O$ in Kerala, India: implications to the reconstruction of past summer and winter monsoon rains. *Climate dynamics*, 37, 555-567.

Managave, S. R., Shimla, P., Borgaonkar, H. P., Bhattacharyya, A., & Ramesh, R. (2017). Regional differences in the carbon isotopic compositions of teak from two monsoonal regimes of India. *Dendrochronologia*, 44, 203-210.

Marshall, J. D., & Monserud, R. A. (1996). Homeostatic gas-exchange parameters inferred from $^{13}C/^{12}C$ in tree rings of conifers. *Oecologia*, 105, 13-21.

Maunoury-Danger, F., Fresneau, C., Eglin, T., Berveiller, D., Francois, C., Lelarge-Trouverie, C., & Damesin, C. (2010). Impact of carbohydrate supply on stem growth, wood and respired CO_2 $\delta^{13}C$: assessment by experimental girdling. *Tree Physiology*, 30(7), 818-830.

McCarroll, D., Whitney, M., Young, G. H., Loader, N. J., & Gagen, M. H. (2017). A simple stable carbon isotope method for investigating changes in the use of recent versus old carbon in oak. *Tree Physiology*, 37(8), 1021-1027.

McKenzie, S. M., Slater, G., Kim, S. T., Pisaric, M. F., & Arain, M. A. (2018). Influence of seasonal temperature on tree-ring $\delta^{13}C$ in different-aged temperate pine forests. *Forest Ecology and Management*, 419, 197-205.

Michelot, A., Eglin, T., Dufrene, E., Lelarge-Trouverie, C., & Damesin, C. (2011). Comparison of seasonal variations in water-use efficiency calculated from the carbon isotope composition of tree rings and flux data in a temperate forest. *Plant, cell & environment*, 34(2), 230-244.

Michelot-Antalik, A., Granda, E., Fresneau, C., & Damesin, C. (2019). Evidence of a seasonal trade-off between growth and starch storage in declining beeches: assessment through stem radial increment, non-structural carbohydrates and intra-ring $\delta^{13}C$. *Tree Physiology*, 39(5), 831-844.

Miller, D. L., Mora, C. I., Grissino-Mayer, H. D., Mock, C. J., Uhle, M. E., & Sharp, Z. (2006). Tree-ring isotope records of tropical cyclone activity. *Proceedings of the National Academy of Sciences*, 103(39), 14294-14297.

Miranda, J. C., Lehmann, M. M., Saurer, M., Altman, J., & Treydte, K. (2021). Insight into Canary Island pine physiology provided by stable isotope patterns of water and plant tissues along an altitudinal gradient. *Tree Physiology*, 41(9), 1611-1626.

Muangsong, C., Cai, B., Pumijumnong, N., Hu, C., & Lei, G. (2016). Intra-seasonal variability of teak tree-ring cellulose $\delta^{18}O$ from northwestern Thailand: a potential proxy of Thailand summer monsoon rainfall. *The Holocene*, 26(9), 1397-1405.

Muangsong, C., Pumijumnong, N., Cai, B., Buajan, S., Lei, G., Wang, F., Li, M., & Payomrat, P. (2020). Effect of changes in precipitation amounts and moisture sources on inter-and intra-annual stable oxygen isotope ratios ($\delta^{18}O$) of teak trees from northern Thailand. *Agricultural and Forest Meteorology*, 281, 107820.

Nabeshima, E., Nakatsuka, T., Kagawa, A., Hiura, T., & Funada, R. (2018). Seasonal changes of δD and $\delta^{18}O$ in tree-ring cellulose of Quercus crispula suggest a change in post-photosynthetic processes during earlywood growth. *Tree Physiology*, 38(12), 1829-1840.

Nakatsuka, T., Ohnishi, K., Hara, T., Sumida, A., Mitsuishi, D., Kurita, N., & Uemura, S. (2004). Oxygen and carbon isotopic ratios of tree-ring cellulose in a conifer-hardwood mixed forest in northern Japan. *Geochemical Journal*, 38(1), 77-88.

Offermann, C., Ferrio, J. P., Holst, J., Grote, R., Siegwolf, R., Kayler, Z., & Gessler, A. (2011). The long way down—are carbon and oxygen isotope signals in the tree ring uncoupled from canopy physiological processes? *Tree Physiology*, 31(10), 1088-1102.

Ogée, J., Barbour, M. M., Wingate, L., Bert, D., Bosc, A., Stievenard, M., Lambrot, C., Pierre, M., Bariac, T., Loustau, D., & Dewar, R. C. (2009). A single-substrate model to interpret intra-annual stable isotope signals in tree-ring cellulose. *Plant, Cell & Environment*, 32(8), 1071-1090.

Ogle, N., & McCormac, F. G. (1994). High-resolution $\delta^{13}C$ measurements of oak show a previously unobserved spring depletion. *Geophysical Research Letters*, 21(22), 2373-2375.

Ohashi, S., Okada, N., Nobuchi, T., Siripatanadilok, S., & Veenin, T. (2009). Detecting invisible growth rings of trees in seasonally dry forests in Thailand: isotopic and wood anatomical approaches. *Trees*, 23, 813-822.

Ohashi, S., Durgante, F. M., Kagawa, A., Kajimoto, T., Trumbore, S. E., Xu, X., Ishizuka, M., & Higuchi, N. (2016). Seasonal variations in the stable oxygen isotope ratio of wood cellulose reveal annual rings of trees in a Central Amazon terra firme forest. *Oecologia*, 180, 685-696.

Olson, E. J., Dodd, J. P., & Rivera, M. A. (2020). Prosopis sp. tree-ring oxygen and carbon isotope record of regional-scale hydroclimate variability during the last 9500 years in the Atacama Desert. *Palaeogeography, Palaeoclimatology, Palaeoecology*, 538, 109408.

Pendall, E. (2000). Influence of precipitation seasonality on piñon pine cellulose δD values. *Global Change Biology*, 6(3), 287-301.

Pons, T. L., & Helle, G. (2011). Identification of anatomically non-distinct annual rings in tropical trees using stable isotopes. *Trees*, 25(1), 83-93.

Potts, D. L., & Williams, D. G. (2004). Response of tree ring holocellulose $\delta^{13}C$ to moisture availability in *Populus fremontii* at perennial and intermittent stream reaches. *Western North American Naturalist*, 27-37.

Poussart, P. F., Evans, M. N., & Schrag, D. P. (2004). Resolving seasonality in tropical trees: multi-decade, high-resolution oxygen and carbon isotope records from Indonesia and Thailand. *Earth and Planetary Science Letters*, 218(3-4), 301-316.

Poussart, P. F., & Schrag, D. P. (2005). Seasonally resolved stable isotope chronologies from northern Thailand deciduous trees. *Earth and Planetary Science Letters*, 235(3-4), 752-765.

Rebenack, C. E., Cherubini, P., & Anderson, W. T. (2018). Developing a carbon isotope chronology for a coastal subtropical tree species with variable subannual tree-ring growth. *Journal of Coastal Research*, 34(4), 828-842.

Rinne, K. T., Saurer, M., Kirdyanov, A. V., Loader, N. J., Bryukhanova, M. V., Werner, R. A., & Siegwolf, R. T. W. (2015). The relationship between needle sugar carbon isotope ratios and tree rings of larch in Siberia. *Tree Physiology*, 35(11), 1192-1205.

Roden, J. S., Bowling, D. R., McDowell, N. G., Bond, B. J., & Ehleringer, J. R. (2005). Carbon and oxygen isotope ratios of tree ring cellulose along a precipitation transect in Oregon, United States. *Journal of Geophysical Research: Biogeosciences*, 110(G2).

Roden, J. S., Johnstone, J. A., & Dawson, T. E. (2009). Intra-annual variation in the stable oxygen and carbon isotope ratios of cellulose in tree rings of coast redwood (*Sequoia sempervirens*). *The Holocene*, 19(2), 189-197.

Rossi, L., Sebastiani, L., Tognetti, R., d'Andria, R., Morelli, G., & Cherubini, P. (2013). Tree-ring wood anatomy and stable isotopes show structural and functional adjustments in Olive trees under different water availability. *Plant and Soil*, 372, 567-579.

Sargeant, C. I., & Singer, M. B. (2016). Sub-annual variability in historical water source use by Mediterranean riparian trees. *Ecohydrology*, 9(7), 1328-1345.

Sargeant, C. I., & Singer, M. B. (2021). Local and non-local controls on seasonal variations in water availability and use by riparian trees along a hydroclimatic gradient. *Environmental Research Letters*, 16(8), 084018.

Sarris, D., Siegwolf, R., & Körner, C. (2013). Inter-and intra-annual stable carbon and oxygen isotope signals in response to drought in Mediterranean pines. *Agricultural and Forest Meteorology*, 168, 59-68.

Schollaen, K., Heinrich, I., Neuwirth, B., Krusic, P. J., D'Arrigo, R. D., Karyanto, O., & Helle, G. (2013). Multiple tree-ring chronologies (ring width, $\delta^{13}C$ and $\delta^{18}O$) reveal dry and rainy season signals of rainfall in Indonesia. *Quaternary Science Reviews*, 73, 170-181.

Schollaen, K., Heinrich, I., & Helle, G. (2014). UV-laser-based microscopic dissection of tree rings–a novel sampling tool for $\delta^{13}C$ and $\delta^{18}O$ studies. *New Phytologist*, 201(3), 1045-1055.

Schollaen, K., Baschek, H., Heinrich, I., Slotta, F., Pauly, M., & Helle, G. (2017). A guideline for sample preparation in modern tree-ring stable isotope research. *Dendrochronologia*, 44, 133-145.

Schubert, B. A., & Jahren, A. H. (2015). Seasonal temperature and precipitation recorded in the intra-annual oxygen isotope pattern of meteoric water and tree-ring cellulose. *Quaternary Science Reviews*, 125, 1-14.

Schubert, B. A., & Timmermann, A. (2015). Reconstruction of seasonal precipitation in Hawai'i using high-resolution carbon isotope measurements across tree rings. *Chemical Geology*, 417, 273-278.

Schulze, B., Wirth, C., Linke, P., Brand, W. A., Kuhlmann, I., Horna, V., & Schulze, E. D. (2004). Laser ablation-combustion-GC-IRMS—a new method for online analysis of intra-annual variation of $\delta^{13}C$ in tree rings. *Tree Physiology*, 24(11), 1193-1201.

Sheu, D. D., Kou, P., Chiu, C. H., & Chen, M. J. (1996). Variability of tree-ring $\delta^{13}C$ in Taiwan fir: growth effect and response to May–October temperatures. *Geochimica et Cosmochimica Acta*, 60(1), 171-177.

Skomarkova, M. V., Vaganov, E. A., Mund, M., Knohl, A., Linke, P., Boerner, A., & Schulze, E. D. (2006). Inter-annual and seasonal variability of radial growth, wood density and carbon isotope ratios in tree rings of beech (*Fagus sylvatica*) growing in Germany and Italy. *Trees*, 20, 571-586.

Slotta, F., Wacker, L., Riedel, F., Heußner, K. U., Hartmann, K., & Helle, G. (2019). High resolution ^{14}C bomb-peak dating and climate response analyses of subseasonal stable isotope signals in wood of the African baobab—A case study from Oman. *Biogeosciences Discussions*, 2019, 1-37.

Soudant, A., Loader, N. J., Bäck, J., Levula, J., & Kljun, N. (2016). Intra-annual variability of wood formation and $\delta^{13}C$ in tree-rings at Hyytiälä, Finland. *Agricultural and Forest Meteorology*, 224, 17-29.

Szejner, P., Wright, W. E., Babst, F., Belmecheri, S., Trouet, V., Leavitt, S. W., Ehleringer, J. R., & Monson, R. K. (2016). Latitudinal gradients in tree ring stable carbon and oxygen isotopes

reveal differential climate influences of the North American Monsoon System. *Journal of Geophysical Research: Biogeosciences*, 121(7), 1978-1991.

Szejner, P., Wright, W. E., Belmecheri, S., Meko, D., Leavitt, S. W., Ehleringer, J. R., & Monson, R. K. (2018). Disentangling seasonal and interannual legacies from inferred patterns of forest water and carbon cycling using tree-ring stable isotopes. *Global change biology*, 24(11), 5332-5347.

Szejner, P., Belmecheri, S., Ehleringer, J. R., & Monson, R. K. (2020a). Recent increases in drought frequency cause observed multi-year drought legacies in the tree rings of semi-arid forests. *Oecologia*, 192, 241-259.

Szejner, P., Clute, T., Anderson, E., Evans, M. N., & Hu, J. (2020b). Reduction in lumen area is associated with the $\delta^{18}O$ exchange between sugars and source water during cellulose synthesis. *New Phytologist*, 226(6), 1583-1593.

Szejner, P., Belmecheri, S., Babst, F., Wright, W. E., Frank, D. C., Hu, J., & Monson, R. K. (2021). Stable isotopes of tree rings reveal seasonal-to-decadal patterns during the emergence of a megadrought in the Southwestern US. *Oecologia*, 197, 1079-1094.

Szymczak, S., Bräuning, A., Häusser, M., Garel, E., Huneau, F., & Santoni, S. (2019). The relationship between climate and the intra-annual oxygen isotope patterns from pine trees: a case study along an elevation gradient on Corsica, France. *Annals of Forest Science*, 76(3), 1-14.

Takahashi, H. A., Yonenobu, H., Nakamura, T., & Wada, H. (2001). Seasonal Fluctuation of Stable Carbon Isotopic Composition in Japanese Cypress Tree Rings from the Last Glacial Period–Possibility of Paleoenvironment Reconstruction. *Radiocarbon*, 43(2A), 433-438.

Tans, P. P., & Mook, W. G. (1980). Past atmospheric CO_2 levels and the $^{13}C/^{12}C$ ratios in tree rings. *Tellus*, 32(3), 268-283.

Tarhule, A., & Leavitt, S. W. (2004). Comparison of stable-carbon isotope composition in the growth rings of *Isorberlinia doka*, *Daniella oliveri*, and *Tamarindus indica* and West African climate. *Dendrochronologia*, 22(1), 61-70.

Tepley, A. J., Hood, S. M., Keyes, C. R., & Sala, A. (2020). Forest restoration treatments in a ponderosa pine forest enhance physiological activity and growth under climatic stress. *Ecological Applications*, 30(8), e02188.

Treydte, K., Boda, S., Graf Pannatier, E., Fonti, P., Frank, D., Ullrich, B., Saurer, M., Siegwolf, R., Battipaglia, G., Werner, W., & Gessler, A. (2014). Seasonal transfer of oxygen isotopes from

precipitation and soil to the tree ring: source water versus needle water enrichment. *New Phytologist*, 202(3), 772-783.

Vaganov, E. A., Schulze, E. D., Skomarkova, M. V., Knohl, A., Brand, W. A., & Roscher, C. (2009). Intra-annual variability of anatomical structure and $\delta^{13}C$ values within tree rings of spruce and pine in alpine, temperate and boreal Europe. *Oecologia*, 161, 729-745.

Verheyden, A., Helle, G., Schleser, G. H., Dehairs, F., Beeckman, H., & Koedam, N. (2004). Annual cyclicity in high-resolution stable carbon and oxygen isotope ratios in the wood of the mangrove tree *Rhizophora mucronata*. *Plant, Cell & Environment*, 27(12), 1525-1536.

Verheyden, A., Roggeman, M., Bouillon, S., Elskens, M., Beeckman, H., & Koedam, N. (2005). Comparison between $\delta^{13}C$ of α-cellulose and bulk wood in the mangrove tree *Rhizophora mucronata*: implications for dendrochemistry. *Chemical Geology*, 219(1-4), 275-282.

Verheyden, A., Helle, G., Schleser, G. H., & Beeckman, H. (2006). High-resolution carbon and oxygen isotope profiles of tropical and temperate liana species. *Schr Forsch Jülich Reihe Umw*, 61, 31-35.

Voelker, S. L., Roden, J. S., & Dawson, T. E. (2018). Millennial-scale tree-ring isotope chronologies from coast redwoods provide insights on controls over California hydroclimate variability. *Oecologia*, 187, 897-909.

Vornlocher, J. R., Lukens, W. E., Schubert, B. A., & Quan, C. (2021). Late Oligocene precipitation seasonality in East Asia based on $\delta^{13}C$ profiles in fossil wood. *Paleoceanography and Paleoclimatology*, 36(4), e2021PA004229.

Weigl, M., Grabner, M., Helle, G., Schleser, G. H., & Wimmer, R. (2008). Characteristics of radial growth and stable isotopes in a single oak tree to be used in climate studies. *Science of the Total Environment*, 393(1), 154-161.

White, J. W., Lawrence, J. R., & Broecker, W. S. (1994). Modeling and interpreting D/H ratios in tree rings: A test case of white pine in the northeastern United States. *Geochimica et cosmochimica acta*, 58(2), 851-862.

Wilson, A. T., & Grinsted, M. J. (1975). Palaeotemperatures from tree rings and the D/H ratio of cellulose as a biochemical thermometer. *Nature*, 257(5525), 387-388.

Wilson, A. T., & Grinsted, M. J. (1977). $^{12}C/^{13}C$ in cellulose and lignin as palaeothermometers. *Nature*, 265(5590), 133-135.

Xu, C., Sano, M., Yoshimura, K., & Nakatsuka, T. (2014). Oxygen isotopes as a valuable tool for measuring annual growth in tropical trees that lack distinct annual rings. *Geochemical Journal*, 48(4), 371-378.

Xu, C., Ge, J., Nakatsuka, T., Yi, L., Zheng, H., & Sano, M. (2016a). Potential utility of tree ring $\delta^{18}O$ series for reconstructing precipitation records from the lower reaches of the Yangtze River, southeast China. *Journal of Geophysical Research: Atmospheres*, 121(8), 3954-3968.

Xu, C., Zheng, H., Nakatsuka, T., Sano, M., Li, Z., & Ge, J. (2016b). Inter-and intra-annual tree-ring cellulose oxygen isotope variability in response to precipitation in Southeast China. *Trees*, 30, 785-794.

Xu, G., Liu, X., Sun, W., Szejner, P., Zeng, X., Yoshimura, K., & Trouet, V. (2020). Seasonal divergence between soil water availability and atmospheric moisture recorded in intra-annual tree-ring $\delta^{18}O$ extremes. *Environmental Research Letters*, 15(9), 094036.

Xu, C., Zhu, H., Wang, S. Y. S., Shi, F., An, W., Li, Z., Sano, M., Nakatsuka, T., & Guo, Z. (2021). Onset and maturation of Asian summer monsoon precipitation reconstructed from intra-annual tree-ring oxygen isotopes from the southeastern Tibetan Plateau. *Quaternary Research*, 103, 139-147.

Zalloni, E., Battipaglia, G., Cherubini, P., Saurer, M., & De Micco, V. (2018). Contrasting physiological responses to Mediterranean climate variability are revealed by intra-annual density fluctuations in tree rings of *Quercus ilex* L. and *Pinus pinea* L. *Tree physiology*, 38(8), 1213-1224.

Zeng, X., Liu, X., Wang, W., Xu, G., An, W., & Wu, G. (2014). No altitude-dependent effects of climatic signals are recorded in Smith fir tree-ring $\delta^{18}O$ on the southeastern Tibetan Plateau, despite a shift in tree growth. *Boreas*, 43(3), 588-599.

Zeng, X., Liu, X., Evans, M. N., Wang, W., An, W., Xu, G., & Wu, G. (2016). Seasonal incursion of Indian Monsoon humidity and precipitation into the southeastern Qinghai–Tibetan Plateau inferred from tree ring $\delta^{18}O$ values with intra-seasonal resolution. *Earth and Planetary Science Letters*, 443, 9-19.

Zeng, X., Liu, X., Treydte, K., Evans, M. N., Wang, W., An, W., Sun, W., Xu, G., Wu, G., & Zhang, X. (2017). Climate signals in tree-ring $\delta^{18}O$ and $\delta^{13}C$ from southeastern Tibet: insights from observations and forward modelling of intra-to interdecadal variability. *New Phytologist*, 216(4), 1104-1118.

Zhu, M., Stott, L., Buckley, B., Yoshimura, K., & Ra, K. (2012a). Indo-Pacific Warm Pool convection and ENSO since 1867 derived from Cambodian pine tree cellulose oxygen isotopes. *Journal of Geophysical Research: Atmospheres*, 117(D11).

Zhu, M., Stott, L., Buckley, B., & Yoshimura, K. (2012b). 20th century seasonal moisture balance in Southeast Asian montane forests from tree cellulose $\delta^{18}O$. *Climatic Change*, 115, 505-517.

Capítulo 3

Do drought tolerant trees benefit from irrigation? Insights from a multi-proxy tree-ring approach in Lisbon / Portugal

In collaboration with: Dra. Ana Paula Ramos, Filipa Maia, Ana Julia Francisco, Dra. Milena Godoy-Veiga, Dr. Mario Tomazello Filho, Dr. Francisco William da Cruz Júnior, Dr. Francisco J Escobedo, Dra. Laia Andreu-Hayles & Giulia Nunes de Aguiar Souto.

Manuscript submitted to *Urban Forestry & Urban Greening*

Abstract

Urban afforestation is a key strategy for mitigation and adaptation to climate change. However, many cities in semi-arid climates struggle to sustain tree growth, often relying on irrigation systems. It is well established that irrigation enhances non-drought-tolerant trees' growth and fosters ecosystem services, at the cost of physiological adjustments that lead to lower wood density, compromising trees' mechanical stability and pathogen resistance. Yet, the responses of drought-tolerant species are still overlooked by practitioners and decision-makers, questioning the possible costs and benefits of irrigation for these species. To investigate how drought-tolerant trees respond to long-term irrigation, we conducted a study with *Tipuana tipu* trees, a key species in Lisbon, Portugal, and other cities worldwide. Using a multi-proxy tree-ring approach, we examined even-sized and aged trees under similar conditions in the Duque de Saldanha Square but differing in irrigation regimes. The positive association between tree-ring width and stable oxygen isotopes confirms that these trees normally grow under water stress during the dry and hot summer seasons. The onset of irrigation in 2017 allowed trees to reduce the stomatal conductance limitations, as revealed by the significant decrease in stable carbon isotopes and the doubled basal-area increment. Notably, this growth enhancement did not result in significantly lower wood density, contrasting with the expected trade-off between wood density and growth rate. These findings question the assumption of wood density reduction associated with higher growth rates under irrigation and shed light on the adjustments in this common drought-tolerant species functioning in response to long-term irrigation.

Key-words: Street trees; *Tipuana tipu*; dendrochronology; wood density; stable isotopes.

Highlights

1.Irrigation systems are largely used in cities to support tree development.

2.Literature points to higher growth of irrigated trees but at the cost of wood density.

3.We probed the responses of *Tipuana tipu* to long-term irrigation in Lisbon / Portugal.

4.Tipuanas doubled the growth rate without significant reduction in wood density.

5. This response stems from a reduction in growth limitation by stomatal conductance.

1. Introduction

Climate change is one of the main challenges humanity faces this century, exposing billions of people to unsustainable living conditions (Fletcher et al., 2024), and threatening the lives of more than 50% of the world's population (United Nations, 2014). Urban populations are already grappling with heat islands, where temperatures significantly exceed the recorded rise in global average temperature (Han et al., 2023; Kim and Brown, 2021). Additionally, impervious surface combined with the increasing frequency and intensity of extreme climate events, exacerbates droughts and flooding – currently some of the most damaging natural hazards in cities worldwide – leveraging human mortality, morbidity, and economic vulnerability (Alves et al., 2024; Doocy et al., 2013). One of the most effective strategies to enhance urban resilience to climate change is the restoration of ecosystem functions, with urban trees playing a central role in providing long-term multifunctional ecosystem services (Elmqvist et al., 2015; Kong et al., 2021; United Nations, 2015). However, urban environments often impair tree functioning and subsequent ecosystem services provision by imposing physiological limitations on plant hydraulics and photosynthesis, particularly in cities with adverse climate conditions (Fini et al., 2022; López et al., 2021; Matsumoto et al., 2022). To better address these challenges, especially in dry regions, urban planners are increasingly investing in irrigation systems to decouple tree development from unfavourable growth conditions (Rambhia et al., 2023).

Trees can have limited access to groundwater in urban environments (Cregg, 1995; Smith et al., 2024), primarily due to impermeable and compacted urban soils (Bouma, 1991; Mullaney et al., 2015). Automated irrigation systems have become a common strategy to support urban tree development (Vico et al., 2014), ensuring adequate soil moisture during drought and sustaining sap flow even under challenging conditions. Thus, irrigation maintains canopy greenness, evapotranspiration, and carbon assimilation (Ibsen et al., 2023; López et al., 2021;

Luketich et al., 2019), enhancing tree growth (Vessella et al., 2010; Xi et al., 2021). These effects directly improve well-being through increased carbon sequestration, canopy shading, evaporative cooling, enchanced aesthetics, and other co-benefits (Daba and Dejene, 2018; Escobedo et al., 2011; Lafortezza and Chen, 2016; Wei et al., 2021).

Artificial water input through irrigation also brings challenges. The primary drawback is cost, not only financial (Parween et al., 2021; Spulber and Sabbaghi, 2012) but also environmental from the use of water itself in precipitation-scarce environments. Using water for irrigation raises bioethical concerns in arid regions or during drought events, as water scarcity requires prioritizing human needs over other uses (Sørup et al., 2020; United Nations, 2015). Conversely, discussions of these drawbacks often overlook the impacts of irrigation on urban tree functioning. Literature shows a trade-off between tree growth rates and wood density (Arsić et al., 2021). Fast growth is typically associated with greater investment in cell division and expansion – often resulting in wider vessels to support high evapotranspiration rates – and reduced allocation to secondary compounds and cell-wall thickening during xylogenesis. This combination can lead to lower wood density, making trees more vulnerable to mechanical failure and pathogens (Larjavaara and Muller-Landau, 2010; Niklas and Spatz, 2010; van Duong et al., 2023). Trees can only maintain optimal wood properties if leaf assimilation meets the higher xylogenesis carbon demands (Eckert et al., 2019). Therefore, while irrigation supports growth, it may also compromise tree's stability and long-term survival.

Most of these insights on irrigation effects on plants growth stem from relatively short-term laboratory and field experiments (de Luis et al., 2011; Rossi et al., 2013). Few studies have assessed the responses of mature trees under real conditions in cities (Vitali et al., 2024), particularly for drought-tolerant species, due to the inherent challenges of monitoring trees over prolonged periods. Long-term changes in tree growth rate and physiological response to environmental conditions can be accurately assessed by tree-ring studies. Measuring tree-ring width is the most common parameter used, as it reflects the radial increment of wood volume during each growing season (Babst et al., 2014; Metsaranta and Bhatti, 2016). Annual growth varies depending on the ontogenetic phase, climatic conditions, and disturbances that may either enhance or suppress growth for extended periods, known as growth release and suppression, respectively (Barton, 2024; Peltier and Ogle, 2020; Reed et al., 2020). Wood density also fluctuates in response to environmental factors, as trees adjust growth and hydraulic architecture (Waite et al., 2023). With a consistent water supply, trees can build wider vessels to maximize hydraulic efficiency, leading to reduced wood density. Conversely, under water-

limited conditions, trees produce narrow vessels increasing the hydraulic system's resilience, resulting into higher wood density (Fajardo et al., 2022).

Trees further adjust leaf physiological processes like assimilation rate and stomatal conductance. Both can be estimated via stable isotope measurements in tree rings (Cernusak and Ubierna, 2022; Miyahara and Locosselli, 2024; Song et al., 2022). For instance, C_3 plants discriminate the stable carbon isotopes during the CO_2 diffusion through the stomata and rubisco activity, both favouring ^{12}C to the detriment of ^{13}C (McCarroll and Loader, 2004). Thus, based on the ratio of ^{12}C and ^{13}C ($\delta^{13}C$) in the tree rings, one can infer the past physiological status of trees. A positive relationship between growth and $\delta^{13}C$ suggests growth limitations by assimilation, whereas negative relationships suggest limitation by stomatal conductance (Brienen et al., 2022). The oxygen isotope signature ($\delta^{18}O$) can also point to higher enrichment by the preferential evapotranspiration of the lighter isotope (McCarroll and Loader, 2004), and a positive association between $\delta^{18}O$ and growth evidence a limitation by stomatal conductance (Andreu-Hayles et al., 2022). However, distinct water sources, like that from irrigation, can dominate the tree-ring $\delta^{18}O$ values particularly if the water signature significantly differs between precipitation and cities' reservoirs (Dansgaard, 1964). Thus, a multiproxy approach improves results interpretation, requires a lower sample size (between 3 to 6 trees) for a site-representative series (Leavitt 2010), and holds a promising pathway to assess the growth strategies of trees under different treatments (Miyahara and Locosselli, 2024).

To better understand how trees coordinate xylogenesis and leaf-level physiology under different irrigation regimes in urban environments, we studied the drought-tolerant *Tipuana tipu* (Benth.) Kuntze (Fabaceae) in Lisbon, Portugal, which is becoming a model exotic species in cities worldwide (Miyahara et al., 2022). Using a multi-proxy tree-ring analysis – including tree-ring width, density, and stable carbon and oxygen isotopes – we tested the following hypotheses: I) Trees exhibit a significant increase in growth rate following the irrigation. II) The higher growth rate of irrigated trees is associated with reduced wood density. III) Irrigation increases stomatal conductance, resulting in lower $\delta^{13}C$ values. IV) Non-irrigated trees have more depleted $\delta^{18}O$ than irrigated trees for the additional input of reservoir water. By addressing these hypotheses, we aim to support improved decision-making regarding the implementation of irrigation systems in urban forestry management and planning.

2. Material and Methods

2.1. Species and Sampling Site

Tipuana tipu (Benth.) Kuntze is a native species to northern Argentina and southern Bolivia (Cattana et al., 2014), known for its drought tolerance in cities (Locosselli et al., 2024). This species became widely planted worldwide during the 20th century (Moreira et al., 2018) and is among the most common street trees in Lisbon, the capital of Portugal (Soares et al., 2011). *T. tipu* is a deciduous species (Zamproni et al., 2013), with clearly distinct semi-porous annual rings delimited by marginal parenchyma bands, successfully used in previous urban dendrochronological studies (Locosselli et al., 2019; 2024; Miyahara et al., 2022).

Sampling took place in Lisbon (Figure 1A). The city has a population of 507,220 people and a density of 5,070 inhabitants/km², as reported in 2018 by the Portuguese National Statistical Institute, with approximately 33,232 street trees within the municipality (Soares et al., 2011). Lisbon has a Mediterranean climate according to the Köppen classification (Köppen, 1931; Santos et al., 2023), characterized by wet winters and dry summers (Figure 1B). Sampling took place in the Duque de Saldanha Square (38°44'01.7"N; 9°08'41.4"W – Figure 1C), one of the main squares in the central axis of the city connecting key avenues, comprising a roundabout with two concentric tree lawns. The inner lawn relies solely on precipitation for water supply, while the outer lawn is irrigated using a drip-based automatic system (Figure 1D) implemented in the summer of 2017. It is based on a network of 16mm low density polyethylene pipes with maximum flow of 4 litres of water per hour, twice a day for 30 minutes. The soil is sandy, with medium organic matter content (4.62%), slightly alkaline pH (8.2), and low electrical conductivity (0.25 mS/cm). This specific site represents a unique condition to evaluate the response of comparable mature trees (Table 1) to the long-term effect of irrigation. It contrasts with other sites usually found in the city where trees differ in size, age and are either irrigated or not. Thus, having them together in the same site makes it a perfect study case to test the hypotheses of this study.

One or two increment cores per tree were sampled in May 2023 using 5mm diameter increment borers, from 12 trees – six irrigated and six non-irrigated – a standard number for dendroecological studies using stable isotopes in cities (Miyahara and Locosselli, 2024). Sampling injuries were plugged with natural cork. Samples were mounted on wooden supports and left to air-dry for one week (Locosselli et al., 2019; Locosselli et al., 2020). Data on DBH, height (TruePulse 200, Laser Technology Inc), crown base height, crown diameter (North–South and East–West, Model R, Richter Messwerkzeuge), and the geographical coordinates for

each tree were recorded in the field (see Table S1 in the supplementary material). A 2015 report from the Municipality of Lisbon recommended no pruning for the non-irrigated sampled trees and only a crown reduction for the irrigated trees (Núcleo de Arvoredo 2015). Nonetheless, there were no clear signs of different pruning among them in the field. The canopy projection area (PA) was calculated based on the two measured perpendicular directions North-South (D_{N-S}) and East-West (D_{E-W}), according to equation 1:

[1] $PA \approx \pi \times (D_{N-S} \div 2) \times (D_{E-W} \div 2)$

2.2. Tree-ring dating and chronology building

The transversal surface of all the samples was polished using sandpapers with progressively finer grits (120, 180, 220, 400, and 600 respectively). Compressed air was used to clean the polished surfaces, removing wood powder from the vessel lumen (Locosselli et al., 2019; Locosselli et al., 2020). The samples were then scanned with a high-resolution scanner (Epson Expression 12000XL) to obtain digital images with 2400 dpi (Godoy-Veiga et al., 2021). Tree rings were identified, marked, and measured for width, using CooRecorder software (Maxwell and Larsson, 2021). Visual cross-dating was performed by analysing the year-to-year tree-ring width patterns (Stokes and Smiley, 1996). First, we evaluated common growth patterns from different radii of the same tree to check for false or missing rings. Next, radii from different trees within the same group (irrigated or non-irrigated) were visually cross-dated to precisely date the formation of each tree ring. Mean series for each group were generated using CDendro software (Maxwell and Larsson, 2021). Dating quality was checked using COFECHA software (Holmes, 1983). The age of each tree was estimated by measuring the distance of the innermost ring to the estimated position of the pith based on the wood rays' extension and dividing this length by the mean width of the innermost five tree rings (Hietz, 2011).

We calculated the basal area increment (BAI) to calculate the mean tree-ring series using the Dendrochronology Program Library 'dplR' (Bunn, 2008), in R v.4.3.1 (R Core Team, 2023). To evaluate the common growth signal, non-climatic trends were removed using a 12-year cubic smoothing spline, preserving only high-frequency variability in the time series (Cook, 1987). Correlation among trees was quantified using the r-bar statistics (Briffa, 1995), calculated for the 12 studied years from 2011 to 2022, with six years before and six after the onset of irrigation.

2.3. Disturbance reconstruction and growth release detection

To statistically assess the impact of irrigation on tree growth, we conducted a Disturbance Analysis using the radial-growth averaging method (Nowacki and Abrams, 1997), chosen for suitability with populations of limited sample size (Carter et al., 2021; Altman et al., 2014). Given the short length of the tree-ring series, the relative change of growth rate was calculated based on 15 years preceding (M_1) and 6 years after (M_2) the potential growth release, following equation 2:

[2] $\%GC=[(M_2-M_1)\div M_1]\times 100$

where GC is the growth change, M_2 is the post-release period, and M_1 is the pre-release period (Nowacki and Abrams, 1997). We classified moderate growth release as ≥25%≤50%, while major growth release was defined as >50%. All analyses were performed using the package 'TRADER' (Altman et al., 2014) in R.

2.4. X-Ray Micro Densitometry

One radius from all sampled trees was selected based on the clearest visibility of tree rings for the micro density analysis. Thin transverse sections (~2mm thickness) were obtained using a circular saw (Proxxon KS 230, Locosselli et al., 2020). The thin sections were conditioned under controlled conditions (20 °C and 50% relative humidity) until reaching 12% moisture content (Ferreira and Tomazello Filho, 2009). The thickness of each section was measured with a digital calliper to calculate the mean thickness of each sample for the post-processing calculations. High-resolution wood density measurements were performed using an X-Ray densitometry chamber (Faxitron X-Ray) with a cellulose acetate wedge of known density (1.274 g/cm³) to create a standard curve for density calibration. Digital radiographs were analysed using WinDendro Density 2017a software (Regent Instruments Inc.) to determine high-resolution wood density profiles (Pompa-García et al., 2024). We characterized the wood density profiles using local regression (LOESS). Then, we compared radial density profiles, as well as maximum, mean, and minimum wood density values of each ring, and the mean wood density among the earlywood (intra-annual position 0-25%), middle (26-75%), and latewood (76-100%), between irrigated and non-irrigated trees, and before and after the irrigation. The

Wilcoxon Signed-Rank test, appropriate for paired non-parametric data, was used in R to assess differences within the same group of trees across the periods. Additionally, the Mann-Whitney test, a non-parametric method suitable for comparing two independent groups, was employed to evaluate differences between groups for the same periods.

2.5. Cellulose extraction and stable carbon isotopes analysis

We performed cellulose extraction adapted from Kagawa et al. (2015) and Schollaen et al. (2015) methods, and subsequently the stable carbon and oxygen isotope analyses for the 12 sampled trees at annual resolution from 2011 to 2022. Each transversal section of wood was placed inside supports made of perforated Teflon sheets, that were submerged twice in 5% NaOH solution within glass beakers, each immersion lasting 2 hours, in a water bath at 70 °C. Then, samples were washed four times with distilled water at room temperature for two minutes, except for the third wash at 60 °C. Subsequently, the samples were treated four times with a 7.5% $NaClO_2$ solution (pH 4 – 5), each treatment lasting 9 hours. Finally, the samples underwent four washes in distilled water, each lasting 2 minutes, with the last two washes conducted at 60 °C.

Samples were then frozen at -10 °C for 16 hours. Once frozen, the cellulose segments were freeze-dried for 72 hours. Tree rings were separated using a razor blade under a stereomicroscope and individually packed into microtubes of 2mL for cellulose homogenization. One mL of deionized water was added to each microtube, and the contents were homogenized twice using a Geno-Grinder for 5 minutes per run at 1200 RPM. The homogenized samples were then freeze-dried for three days. Between 95µg and 105µg of cellulose was precisely weighed and packed into tin capsules for $\delta^{13}C$ and silver capsules for $\delta^{18}O$, yielding one sample for each isotope per tree ring, with a total of 288 samples. The samples were combusted at 1020 °C for $\delta^{13}C$ and pyrolyzed at 1350 °C for $\delta^{18}O$, over glassy carbon in an EA-IRMS system, composed of a Delta V Advantage (ThermoScientific) Isotope Ration Mass Spectrometer (IRMS) coupled with a ConFlo IV and Element Analyser (EA; ThermoScientific).

We performed Principal Component Analyses (PCA) to evaluate the association between the tree-ring parameters and how they changed before and after the onset of the irrigation. We calculated the 95% confidence ellipses to test for differences between non-irrigated and irrigated periods.

3. Results

3.1. Chronology and tree growth

The mean estimated age of non-irrigated and irrigated trees is not statistically different and is close to 56 years old (Table 1). Also, tree height, canopy area, and crown base height are not statistically different between treatments (Table 1). Irrigated and non-irrigated trees also share clear common ontogenetic patterns of BAI before the implementation of the irrigation system (Figure 2A). The 12-years tree-ring series display a calculated r-bar of 0.517 and 0.483 for non-irrigated and irrigated trees, respectively (Table 1). The detrended mean series of both groups are also significantly correlated ($r = 0.67$, $p = 0.02$). Overall, trees display a growth decline between 1980 and 2000 related to the age-size trend. From 2000 onwards, trees share similar interannual tree-ring BAI patterns until 2017, the onset of irrigation. During the watering period, the irrigated trees exhibited an average growth rate 130.3% higher than that of the non-irrigated trees, and a 103% increase in the average BAI of irrigated trees compared to the six years before the irrigation (Table 1; Figure 2A). This significant increase in growth is visually evident in the tree rings in Figures 2B and 2C starting from 2017.

3.2. Disturbances and growth release

The disturbance analysis identified a growth release event in 2016, attributed to the sustained growth rate increase from 2017 onwards following irrigation (Figures 2D and 2E) only for the irrigated trees. No other growth release events in the tree-ring time series of the studied trees reached a comparable magnitude or involved such a high percentage of individuals.

3.3. X-Ray micro densitometry variations

The high-resolution wood density series (Figure 3A) illustrates the tree-ring wood density profile for the non-irrigated and irrigated trees. The Local Regression curves (LOESS) display the intra-annual trends in wood density for both groups of trees and for the tree rings before and after the onset of the irrigation. All trees exhibit a common intra-annual pattern of increasing wood density from the beginning to the end of tree rings. In irrigated trees, visible differences are apparent at the beginning and end of the tree rings, showing negligible lower density values

during the irrigated period. The Wilcoxon Signed-Rank Test results for minimum ring density (Figure 3B) and mean ring density (Figure 3C) between the different periods within the same group show no significant differences. The maximum ring density (Figure 3D) exhibits a minor but significant increase from before to after irrigation, in non-irrigated trees. However, the wood density in the earlywood (Figure 3E), middle (Figure 3F), and latewood (Figure 3G) showed no significant differences between treatments and periods.

3.4. Interannual variability in tree-ring stable carbon and oxygen isotope data

Figure 4 shows the average stable isotopic values for each ring from 2011 to 2022 for six non- and six irrigated trees. The $\delta^{13}C$ values of irrigated trees substantially decreased after 2017, whereas $\delta^{18}O$ signatures demonstrate a synchronicity between non-irrigated and irrigated populations before the onset of irrigation, and no change in the trends after the irrigation.

Based on the Principal Component Analyses (PCA – Figure 5), no significant difference was observed in the non-irrigated trees regarding BAI, density, $\delta^{13}C$, and $\delta^{18}O$, and the two periods of treatments (before and after the onset of irrigation) as revealed by the 95% confidence superimposed ellipses. The first and second components explain 81% of data variability, with the vectors indicating a significant positive association between the two stable isotopes, and between growth and $\delta^{18}O$ ($r = 0.58$, $r = 0.74$, $p < 0.05$, respectively, Tables S12, Figure S1). For the irrigated trees, the first and second components of the PCA explain 64.7% of the data variability, revealing a markedly different pattern of association among tree-ring parameters. A significant difference is evident between tree rings before and after irrigation, revealed by the 95% confidence non-superimposed ellipses. Under irrigation, tree rings exhibit higher BAI and lower $\delta^{13}C$ and $\delta^{18}O$, while wood density remains orthogonal to the axis of average tree-ring variability.

4. Discussion

The growth conditions of the trees sampled in the Duque de Saldanha Square, Lisbon / Portugal, were similar before the irrigation. This observation stems from the strong common growth signal between the groups of irrigated and non-irrigated trees, an expected result primarily due to the trees' similar dimensions, proximity, and exposure to similar micro-environmental conditions. These similarities likely trump any effect of the sample size, which, although

limited, is comparable to that in other urban dendroecological studies (Miyahara et al., 2022). The consistency of this synchronized tree growth pattern is further supported by the significant correlation between the detrended series for non-irrigated and irrigated trees for the period of interest (2011 to 2022). Notably, the mean BAI of irrigated trees increased over twofold than the non-irrigated trees.

The observed increase in BAI due to irrigation supports the first hypothesis of this study and aligns with findings from the literature, confirming that irrigation enhances the radial growth rate of urban trees even for drought-tolerant species like *T. tipu*. Our results are consistent with experimental observations on juvenile *Pinus halepensis* Mill. trees on the southeast coast of Spain (de Luis et al., 2011), and long-term experiments on mature trees of *Pinus sylvestris* L. conducted in southwestern Switzerland, from 2003 to 2019 (Vitali et al., 2024). The latter study describes a three-phase response to irrigation: an initial three-years phase, characterized by a progressive increase in growth rate peaking at 100% higher than non-irrigated trees; a second phase, from the fourth to the eleventh year, when growth rate declined but remained 50% higher than non-irrigated; and the third phase with a further reduction, stabilizing at 20% above the non-irrigated growth (Vitali et al., 2024). In contrast, *T. tipu* trees increased the growth rate by 100% immediately following irrigation in our study and sustained it during the six years of treatment. This result is surprising for a drought-tolerant species such as *T. tipu* (Locosselli et al., 2024), diverging from other drought-tolerant tree species like *Olea europaea* L. from the Mediterranean region, which showed positive growth trends limited to the first year of irrigation (Rossi et al., 2013).

While the increase in growth rate is well-supported by the literature, the absence of a significant reduction in wood density contradicts our second hypothesis. High growth rates are typically associated with thin-walled and wide conductive cells (Rathgeber, 2017), a strategy generally linked to reduced wood density (Zobel and Buijtenen, 2012). Water availability strongly influences this trade-off in urban and natural environments, allowing trees to adjust to environmental changes throughout their lifespan (Wimmer and Downes, 2003). Changes in wood density often reflect variations in the latewood-to-earlywood ratio, with drought affecting tree-ring growth patterns depending on its timing and intensity during the growing season (Torresan et al., 2024). Increased growth rates can potentially reduce mean wood density, thus compromising the structural integrity of the trunk and subsequently increasing susceptibility to decay, mechanical damage, and pathogen infection (Larjavaara and Muller-Landau, 2010; Niklas and Spatz, 2010; Rathgeber, 2017). However, in our study, *T. tipu* street trees in Lisbon

showed no significant decrease in minimum, average, maximum, or earlywood and latewood wood density.

The decoupling of $\delta^{13}C$ series between the two groups of trees after the onset of irrigation confirms our third hypothesis, and points to an increase in stomatal conductance with the surplus of water supply. Yet, the synchronized $\delta^{18}O$ patterns between non-irrigated and irrigated populations (Figure 4B) contradicts the expectation that the $\delta^{18}O$ signature of the water source would dominate the isotopic composition in tree rings, refuting our fourth hypothesis. This result is not entirely unexpected, given that the study site is a coastal city, and the nearby ocean is a large water reservoir enriched in ^{18}O (Gilfillan Jr, 1934). As a result, local precipitation at the study site is enriched in ^{18}O likely similar to the local water reservoirs used for irrigation. Conversely, the isotopic signals are dominated by the leaf physiology status, and the strong positive association between growth rate, $\delta^{18}O$ and $\delta^{13}C$ implies a growth limited by water stress (McCarroll and Loader 2004, Cintra et al., 2019). This observation is at odds with the positive association between $\delta^{13}C$ and the growth under the subtropical climate of the city of São Paulo, pointing to a photosynthetic limitation of growth during the wet summer (Locosselli et al 2014) but can be reconciled by the fact that trees are growing in the dry summer of the Mediterranean climate of Lisbon.

A key question remains: how do these trees coordinate their unique xylogenesis strategy with leaf-level physiological responses to irrigation? This is essential for understanding how trees integrate structural and functional responses under normal conditions. The PCA analysis revealed no change in BAI, wood density, $\delta^{13}C$, and $\delta^{18}O$ for non-irrigated trees before and after 2017. Conversely, irrigated trees shifted from a positive to a negative association between growth and isotope signatures, indicating a lower limitation by stomatal conductance, a must-needed strategy to cope with the higher carbon demands of the xylogenesis and water conductance under irrigation. Wood density remained orthogonal to the axis of growth, $\delta^{13}C$, and $\delta^{18}O$ variation, confirming consistent investment in similar wood tissue properties regardless of irrigation. Therefore, continuous irrigation using an automatic irrigation system proved beneficial and effective for the drought-tolerant *T. tipu* trees, likely enhancing the ecosystem services without increasing the risks associated with lower wood density.

5. Conclusion

This multi-proxy tree-ring analysis approach advanced our understanding of how urban trees respond to site characteristics, management regimes, and maintenance practices such as the automatic irrigation system, highlighting the integrated physiological and structural responses to increased water availability. By focusing on *Tipuana tipu*, a key drought-tolerant tree species for urban landscape worldwide and one of the most abundant in Lisbon, we demonstrated that a full-season automatic irrigation regime modulates tree physiology by enhancing stomatal conductance and assimilation rates. Consequently, biomass production increased, supporting higher growth rates without compromising average wood density. These findings question the assumption of the trade-off between growth and wood density in irrigated trees, suggesting that this species maintains wood resilience while benefiting from additional water resources. Normally, tree irrigation is a costly management tool in water-scarce cities. However, our results provide a robust basis for urban planners and decision-makers to adopt automated irrigation systems as a reliable and water-use effective strategy even for a drought tolerant species. Thus, increased tree growth via efficient irrigation systems can make for an efficient method to enhance ecosystem service provision – including carbon sequestration, shade, air cooling, and pollution interception – without necessarily increasing water-related costs and risks associated with structural instability or reduced wood durability.

Acknowledgement

The authors thank the Municipality of Lisbon for providing the sampling permits and supporting the fieldwork. Dr. Marcos Buckeridge and Dr. Gregório Ceccantini for grating access to equipment used in the sample preparation, and Dr. Jan Altman for the support on the growth release analyses. And FAPESP (2019/08783-0, 2023/17265-9), CNPq (311854/2022-2), CAPES (88887.715354/2022-00), FTC (UIDB/04129/2020 and UIDP/04129/2020), and DAFNE (J85F20000320005 and J83C23000270001) for financial support.

References

Altman, J., Fibich, P., Dolezal, J., & Aakala, T. (2014). TRADER: a package for tree ring analysis of disturbance events in R. *Dendrochronologia*, 32(2), 107-112.

Alves, R. A., Rudke, A. P., de Melo Souza, S. T., dos Santos, M. M., & Martins, J. A. (2024). Flood vulnerability mapping in an urban area with high levels of impermeable coverage in southern Brazil. *Regional Environmental Change*, 24(3), 96.

Andreu-Hayles, L., Lévesque, M., Guerrieri, R., Siegwolf, R. T., & Körner, C. (2022). Limits and strengths of tree-ring stable isotopes. In *Stable isotopes in tree rings: Inferring physiological, climatic and environmental responses* (pp. 399-428). Cham: Springer International Publishing.

Arsić, J., Stojanović, M., Petrovičová, L., Noyer, E., Milanović, S., Světlík, J., Horáček, P., & Krejza, J. (2021). Increased wood biomass growth is associated with lower wood density in *Quercus petraea* (Matt.) Liebl. saplings growing under elevated CO_2. *Plos one*, 16(10), e0259054.

Babst, F., Alexander, M. R., Szejner, P., Bouriaud, O., Klesse, S., Roden, J., Ciais, P., Poulter, B., Frank, D., Moore, D. J. P., & Trouet, V. (2014). A tree-ring perspective on the terrestrial carbon cycle. *Oecologia*, 176, 307-322.

Barton, K. E. (2024). The ontogenetic dimension of plant functional ecology. *Functional Ecology*, 38(1), 98-113.

Bouma, J. (1991). Influence of soil macroporosity on environmental quality. *Advances in agronomy*, 46, 1-37.

Briffa, K. R., & Jones, P. D. (1990). Basic chronology statistics and assessment. In: *Methods of Dendrochronology: Applications in the Environmental Sciences*. Kluwer Academic Publishers, pp. 137-152.

Briffa, K. R., Jones, P. D., Schweingruber, F. H., Shiyatov, S. G., & Cook, E. R. (1995). Unusual twentieth-century summer warmth in a 1000-year temperature record from Siberia. *Nature*, 376, 156–159.

Brienen, R., Helle, G., Pons, T., Boom, A., Gloor, M., Groenendijk, P., Clerici, S., Leng, M., & Jones, C. (2022). Paired analysis of tree ring width and carbon isotopes indicates when controls on tropical tree growth change from light to water limitations. *Tree Physiology*, 42(6), 1131-1148.

Bunn, A. G. (2008). A dendrochronology program library in R (dplR). *Dendrochronologia*, 26(2), 115-124.

Carter, D. R., Bialecki, M. B., Windmuller-Campione, M., Seymour, R. S., Weiskittel, A., & Altman, J. (2021). Detecting growth releases of mature retention trees in response to small-

scale gap disturbances of known dates in natural-disturbance-based silvicultural systems in Maine. *Forest Ecology and Management*, 502, 119721.

Cattana, M. E., de los Ángeles Sosa, M., Fernández, M., Rojas, F., Mangiaterra, M., & Giusiano, G. (2014). Native trees of the Northeast Argentine: Natural hosts of the *Cryptococcus neoformans–Cryptococcus gattii* species complex. *Revista iberoamericana de micología*, 31(3), 188-192.

Cernusak, L. A., & Ubierna, N. (2022). Carbon isotope effects in relation to CO_2 assimilation by tree canopies. In *Stable isotopes in tree rings: Inferring physiological, climatic and environmental responses* (pp. 291-310). Cham: Springer International Publishing.

Cook, E. R. (1987). The decomposition of tree-ring series for environmental studies. *Tree Ring Bulletin*, 47, 37–59

Cregg, B. M. (1995). Plant moisture stress of green ash trees in contrasting urban sites. *Journal of Arboriculture*, 21, 271-276.

Cunha, A. R., Soares, A. L., Catarino, S., Duarte, M. C., & Romeiras, M. M. (2025). Assessing the vulnerability of urban tree species to climate change: The case study of Lisbon gardens. *Urban Forestry & Urban Greening*, 104, 128664.

Daba, M. H., & Dejene, S. W. (2018). The role of biodiversity and ecosystem services in carbon sequestration and its implication for climate change mitigation. *Environmental Sciences and Natural Resources*, 11(2), 1-10.

Dansgaard, W. (1964). Stable isotopes in precipitation. *Tellus*, 16(4), 436-468.

de Luis, M., Novak, K., Raventós, J., Gričar, J., Prislan, P., & Čufar, K. (2011). Cambial activity, wood formation and sapling survival of *Pinus halepensis* exposed to different irrigation regimes. *Forest Ecology and Management*, 262(8), 1630-1638.

Dobbertin, M., Eilmann, B., Bleuler, P., Giuggiola, A., Graf Pannatier, E., Landolt, W., Schleppi, P., & Rigling, A. (2010). Effect of irrigation on needle morphology, shoot and stem growth in a drought-exposed *Pinus sylvestris* forest. *Tree Physiology*, 30(3), 346-360.

Doocy, S., Daniels, A., Murray, S., & Kirsch, T. D. (2013). The human impact of floods: a historical review of events 1980-2009 and systematic literature review. *PLoS currents*, 5.

Eckert, C., Sharmin, S., Kogel, A., Yu, D., Kins, L., Strijkstra, G. J., & Polle, A. (2019). What makes the wood? Exploring the molecular mechanisms of xylem acclimation in hardwoods to an ever-changing environment. *Forests*, 10(4), 358.

Elmqvist, T., Setälä, H., Handel, S. N., van der Ploeg, S., Aronson, J., Blignaut, J. N., Gómez-Baggethun, E., Nowak, D.J., Kronenberg, J., & de Groot, R. (2015). Benefits of restoring ecosystem services in urban areas. *Current opinion in environmental sustainability*, 14, 101-108.

Escobedo, F. J., Kroeger, T., & Wagner, J. E. (2011). Urban forests and pollution mitigation: Analyzing ecosystem services and disservices. *Environmental pollution*, 159(8-9), 2078-2087.

Fajardo, A., Piper, F. I., & García-Cervigón, A. I. (2022). The intraspecific relationship between wood density, vessel diameter and other traits across environmental gradients. *Functional Ecology*, 36(7), 1585-1598.

Ferreira, A. T. B., & Tomazello Filho, M. (2009). Characterization of tree-rings of *Pinus caribaea* var. *hondurensis* Barr. et Golf. trees by X-Ray densitometry. *Scientia Forestalis (Brazil)*, 37(83).

Fini, A., Frangi, P., Comin, S., Vigevani, I., Rettori, A. A., Brunetti, C., Moura, B. B., & Ferrini, F. (2022). Effects of pavements on established urban trees: Growth, physiology, ecosystem services and disservices. *Landscape and Urban Planning*, 226, 104501.

Fletcher, C., Ripple, W. J., Newsome, T., Barnard, P., Beamer, K., Behl, A., Bowen, J., Cooney, M., Crist, E., Field, C., Hiser, K., Karl, D. M., King, D. A., Mann, M. E., McGregor, D. P., Mora, C., Oreskes, N., & Wilson, M. (2024). Earth at risk: An urgent call to end the age of destruction and forge a just and sustainable future. *PNAS nexus*, 3(4), 106.

Fujiwara, S., & Yang, K. C. (2000). The relationship between cell length and ring width and circumferential growth rate in five Canadian species. *IAWA journal*, 21(3), 335-345.

Godoy-Veiga, M., Cintra, B. B. L., Stríkis, N. M., Cruz, F. W., Grohmann, C. H., Santos, M. S., Regev, L., Boaretto, E., Ceccantini, G., & Locosselli, G. M. (2021). The value of climate responses of individual trees to detect areas of climate-change refugia, a tree-ring study in the Brazilian seasonally dry tropical forests. *Forest ecology and management*, 488, 118971.

Han, D., Zhang, T., Qin, Y., Tan, Y., & Liu, J. (2023). A comparative review on the mitigation strategies of urban heat island (UHI): a pathway for sustainable urban development. *Climate and Development*, 15(5), 379-403.

Hietz, P. (2011). A simple program to measure and analyse tree rings using Excel, R and SigmaScan. *Dendrochronologia*, 29(4), 245-250.

Holmes, R. L. (1983). Computer-assisted quality control in tree-ring dating and measurement. *Tree-ring Bulletin*, 43. 69-78.

Ibsen, P. C., Santiago, L. S., Shiflett, S. A., Chandler, M., & Jenerette, G. D. (2023). Irrigated urban trees exhibit greater functional trait plasticity compared to natural stands. *Biology Letters*, 19(1), 20220448.

Kagawa, A., Sano, M., Nakatsuka, T., Ikeda, T., & Kubo, S. (2015). An optimized method for stable isotope analysis of tree rings by extracting cellulose from cross-sectional laths. *Chemical Geology*, 393–394, 16–25.

Kim, S. W., & Brown, R. D. (2021). Urban heat island (UHI) intensity and magnitude estimations: A systematic literature review. *Science of the Total Environment*, 779, 146389.

Kong, X., Zhang, X., Xu, C., & Hauer, R. J. (2021). Review on urban forests and trees as nature-based solutions over 5 years. *Forests*, 12(11), 1453.

Köppen, W. (1931). Grundriss der klimakunde. Berlin, Germany: W.

Lafortezza, R., & Chen, J. (2016). The provision of ecosystem services in response to global change: evidences and applications. *Environmental Research*, 147, 576-579.

Larjavaara, M., & Muller-Landau, H. C. (2010). Rethinking the value of high wood density. *Functional Ecology*, 701-705.

Locosselli, G. M., & Buckeridge, M. S. (2017). Dendrobiochemistry, a missing link to further understand carbon allocation during growth and decline of trees. *Trees*, 31(6), 1745-1758.

Locosselli, G. M., Camargo, E. P., Moreira, T. C. L., Todesco, E., Fátima Andrade, M., André, C. D. S., André, P. A., Singer, J. M., Ferreira, L. S., Saldiva, P. H. N., & Buckeridge, M. S. (2019). The role of air pollution and climate on the growth of urban trees. *Science of the Total Environment*, 666, 652-661.

Locosselli, G. M., Brienen, R. J., Souza Martins, V. T., Gloor, E., Boom, A., Camargo, E. P., Saldiva, P. H. N., & Buckeridge, M. S. (2020). Intra-annual oxygen isotopes in the tree rings record precipitation extremes and water reservoir levels in the Metropolitan Area of São Paulo, Brazil. *Science of the Total Environment*, 743, 140798.

Locosselli, G. M., Cintra, B. B. L., Ferreira, L. S., Silva-Luz, C. L., Miyahara, A. A. L., Brienen, R. J., Gloor, E., Boom, A., Grandis, A., & Buckeridge, M. S. (2024). Stress-tolerant trees for resilient cities: Tree-ring analysis reveals species suitable for a future climate. *Urban Climate*, 55, 101964.

López, J., Way, D. A., & Sadok, W. (2021). Systemic effects of rising atmospheric vapor pressure deficit on plant physiology and productivity. *Global Change Biology*, 27(9), 1704-1720.

Luketich, A. M., Papuga, S. A., & Crimmins, M. A. (2019). Ecohydrology of urban trees under passive and active irrigation in a semiarid city. *PloS one*, 14(11), e0224804.

Martinez-Meier, A., Sanchez, L., Pastorino, M., Gallo, L., & Rozenberg, P. (2008). What is hot in tree rings? The wood density of surviving Douglas-firs to the 2003 drought and heat wave. *Forest Ecology and Management*, 256(4), 837-843.

Matsumoto, M., Kiyomizu, T., Yamagishi, S., Kinoshita, T., Kumpitsch, L., Kume, A., & Hanba, Y. T. (2022). Responses of photosynthesis and long-term water use efficiency to ambient air pollution in urban roadside trees. *Urban Ecosystems*, 25(4), 1029-1042.

Maxwell, R. S., & Larsson, L. A. (2021). Measuring tree-ring widths using the CooRecorder software application. *Dendrochronologia*, 67, 125841.

McCarroll, D., & Loader, N. J. (2004). Stable isotopes in tree rings. *Quaternary Science Reviews*, 23(7-8), 771-801.

Medina, M., Flores, M. P., Ritter, L. J., Goya, J. F., Campanello, P. I., & Arturi, M. F. (2023). Wood density and leaf traits independently relate to growth rate of naturally regenerated tree species in *Araucaria angustifolia* plantations in the Atlantic Forest, Argentina. *Canadian Journal of Forest Research*, 54(1), 1-11.

Metsaranta, J. M., & Bhatti, J. S. (2016). Evaluation of whole tree growth increment derived from tree-ring series for use in assessments of changes in forest productivity across various spatial scales. *Forests*, 7(12), 303.

Miyahara, A. A. L., Paixão, C. P., Santos, D. R., Pagin-Cláudio, F., Silva, G. J., Bertoleti, I. A. F., Lima, J. S., Silva, J. L., Candido, L. F., Siqueira, M. C., Silva, R. P., Racanelli, Y. R. & Locosselli, G. M. (2022). Urban dendrochronology toolkit for evidence-based decision-making on climate risk, cultural heritage, environmental pollution, and tree management – A systematic review. *Environmental Science & Policy*, 137, 152-163.

Miyahara, A. A. L., & Locosselli, G. M. (2024). Challenges and advances in intra-annual tree-ring stable isotope research, a systematic review. *Dendrochronologia*, 126218.

Moreira, T. C., Amato-Lourenco, L. F., Silva, G. T., Andre, C. D. S., Andre, P. A., Barrozo, L. V., Singer, J. M., Saldiva, P. H. N., Saiki, M., & Locosselli, G. M. (2018). The use of tree barks to monitor traffic related air pollution: a case study in São Paulo–Brazil. *Frontiers in Environmental Science*, 6, 72.

Mullaney, J., Lucke, T., & Trueman, S. J. (2015). A review of benefits and challenges in growing street trees in paved urban environments. *Landscape and urban planning*, 134, 157-166.

Niemelä, J. (1999). Ecology and urban planning. *Biodiversity & Conservation*, 8, 119-131.

Niklas, K. J., & Spatz, H. C. (2010). Worldwide correlations of mechanical properties and green wood density. *American Journal of Botany*, 97(10), 1587-1594.

Nowacki, G. J., & Abrams, M. D. (1997). Radial-growth averaging criteria for reconstructing disturbance histories from presettlement-origin oaks. *Ecological monographs*, 67(2), 225-249.

Parween, F., Kumari, P., & Singh, A. (2021). Irrigation water pricing policies and water resources management. *Water Policy*, 23(1), 130-141.

Peltier, D. M., & Ogle, K. (2020). Tree growth sensitivity to climate is temporally variable. *Ecology Letters*, 23(11), 1561-1572.

Pompa-García, M., Vivar-Vivar, E. D., Hornink, B., Martínez-Rivas, J. A., Ortega-Rodriguez, D. R., & Tomazello Filho, M. (2024). Tree-ring wood density reveals differentiated hydroclimatic interactions in species along a bioclimatic gradient. *Dendrochronologia*, 85, 126208.

R version 4.3.1 (2023-06-16 ucrt) -- "Beagle Scouts" Copyright (C) 2023 *The R Foundation for Statistical Computing.*

Rambhia, M., Volk, R., Rismanchi, B., Winter, S., & Schultmann, F. (2023). Supporting decision-makers in estimating irrigation demand for urban street trees. *Urban Forestry & Urban Greening*, 82, 127868.

Rathgeber, C. B. (2017). Conifer tree-ring density interannual variability–anatomical, physiological and environmental determinants. *New Phytologist*, 216(3), 621-625.

Reed, K., Forster, J., Denman, S., Brown, N., Leather, S. R., & Inward, D. J. (2020). Novel dendrochronological modelling demonstrates that decades of reduced stem growth predispose trees to acute Oak decline. *Forest Ecology and Management*, 476, 118441.

Rossi, L., Sebastiani, L., Tognetti, R., d'Andria, R., Morelli, G., & Cherubini, P. (2013). Tree-ring wood anatomy and stable isotopes show structural and functional adjustments in Olive trees under different water availability. *Plant and Soil*, 372, 567-579.

Santos, M. L., Silva, C. M., Ferreira, F., Matos, J. S. (2023). Hydrological analysis of green roofs performance under a Mediterranean climate: A case study in Lisbon, Portugal. *Sustainability*, 15(2), 1064.

Schollaen, K., Baschek, H., Heirinch, I., & Helle, G., 2015. Technical note: an improved guideline for rapid and precise sample preparation of tree-ring stable isotope analysis. *Biogeosciences*, 12, 11587–11623.

Smith, I. A., Templer, P. H., & Hutyra, L. R. (2024). Water sources for street trees in mesic urban environments. *Science of The Total Environment*, 908, 168411.

Soares, A. L., Rego, F. C., McPherson, E. G., Simpson, J. R., Peper, P. J., & Xiao, Q. (2011). Benefits and costs of street trees in Lisbon, Portugal. *Urban Forestry & Urban Greening*, 10(2), 69-78.

Song, X., Lorrey, A., & Barbour, M. M. (2022). Environmental, physiological and biochemical processes determining the oxygen isotope ratio of tree-ring cellulose. In *Stable isotopes in tree rings: inferring physiological, climatic and environmental responses* (pp. 311-329). Cham: Springer International Publishing.

Sørup, H. J., Brudler, S., Godskesen, B., Dong, Y., Lerer, S. M., Rygaard, M., & Arnbjerg-Nielsen, K. (2020). Urban water management: can UN SDG 6 be met within the planetary boundaries?. *Environmental Science & Policy*, 106, 36-39.

Spulber, N., & Sabbaghi, A. (2012). *Economics of water resources: from regulation to privatization* (Vol. 13). Springer Science & Business Media.

Stokes, M. A., & Smiley, T. L. (1996). *An introduction to tree-ring dating*. University of Arizona Press.

Swaffield, S. R., & McWilliam, W. J. (2013). Landscape aesthetic experience and ecosystem services. *School of Landscape Architecture, Lincoln University*, (2.6), 349-362.

Torresan, C., Hilmers, T., Avdagić, A., Di Giuseppe, E., Klopčič, M., Lévesque, M., Motte, F., Uhl, E., Zlatanov, T., & Pretzsch, H. (2024). Changes in tree-ring wood density of European beech (*Fagus sylvatica* L.), silver fir (*Abies alba* Mill.), and Norway spruce (*Picea abies* (L.) H. Karst.) in European mountain forests between 1901 and 2016. *Annals of Forest Science*, 81(1), 49.

United Nations, U.N. *World Urbanization Prospects: The 2014 Revision: Highlights*; Department of Economic and Social Affairs, Population Division: New York, NY, USA, 2014.

United Nations, U.N. *Transforming Our World: The 2030 Agenda for Sustainable Development*; Department of Economic and Social Affairs, 1, 41: New York, NY, USA, 2015.

van Duong, D., Schimleck, L., & Lam Tran, D. (2023). Variation in wood density and mechanical properties of *Acacia mangium* provenances planted in Vietnam. *Journal of Sustainable Forestry*, 42(5), 518-532.

Vessella, F., Parlante, A., Schirone, A., Sandoletti, G., Bellarosa, R., Piovesan, G., Santi, L., & Schirone, B. (2010). Irrigation regime as a key factor to improve growth performance of *Quercus suber* L. *Scandinavian Journal of Forest Research*, 25(S8), 68-74.

Vico, G., Revelli, R., & Porporato, A. (2014). Ecohydrology of street trees: design and irrigation requirements for sustainable water use. *Ecohydrology*, 7(2), 508-523.

Vitali, V., Schuler, P., Holloway-Phillips, M., D'Odorico, P., Guidi, C., Klesse, S., Lehmann, M. M., Muesburger, K., Schaub, M., Zweifel, R., Gessler, A., & Saurer, M. (2024). Finding balance: Tree-ring isotopes differentiate between acclimation and stress-induced imbalance in a long-term irrigation experiment. *Global Change Biology*, 30(3), e17237.

Waite, P. A., Leuschner, C., Delzon, S., Triadiati, T., Saad, A., & Schuldt, B. (2023). Plasticity of wood and leaf traits related to hydraulic efficiency and safety is linked to evaporative demand and not soil moisture in rubber (*Hevea brasiliensis*). *Tree Physiology*, 43(12), 2131-2149.

Wei, J., Li, H., Wang, Y., & Xu, X. (2021). The cooling and humidifying effects and the thresholds of plant community structure parameters in urban aggregated green infrastructure. *Forests*, 12(2), 111.

Wimmer, R., & Downes, G. M. (2003). Temporal variation of the ring width–wood density relationship in Norway spruce grown under two levels of anthropogenic disturbance. *Iawa Journal*, 24(1), 53-61.

Xi, B., Clothier, B., Coleman, M., Duan, J., Hu, W., Li, D., Di, N., Liu, Y., Fu, J., Li, J., Jia, L., & Fernández, J.E. (2021). Irrigation management in Poplar (*Populus spp*.) plantations: A review. *Forest Ecology and Management*, 494, 119330.

Zamproni, K., Biondi, D., Lima Neto, E. M., & Martini, A. (2013). Weather effects on the phenology of *Tipuana tipu* (Benth.) Kuntze in the urban forest of Curitiba City, Paraná State, Brazil. *Revista da Sociedade Brasileira de Arborização Urbana*, 8(2), 9-22.

Zobel, B. J., & van Buijtenen, J. P. (2012). Wood variation: its causes and control. *Springer Science & Business Media*.

Table 1: Characterization of the sampled trees and their multi-proxy tree-ring series, with respective averages and standard errors for non-irrigated and irrigated trees. The letters represent the significance of variances between different periods and the same population (uppercase letters) obtained by the Wilcoxon Rank-Signed test; and variances between the same periods and different populations (lowercase letters) obtained by the Mann-Whitney test. See Tables S2 – S7 and Table S16 to access the detailed results of the statistical tests.

Parameter	Non-irrigated	Irrigated
N of trees (series)	6 (12)	6 (7)
Mean Diameter at Breast Height (cm)	$54.80^{A} \pm 4.04$	$55.33^{A} \pm 1.38$
Mean estimated tree age (years)	$55.66^{A} \pm 1.02$	$56.55^{A} \pm 3.51$
Mean Tree Height (m)	$14.95^{A} \pm 0.32$	$17.71^{A} \pm 1.20$
Mean Crown Base Height (m)	$3.45^{A} \pm 0.32$	$3.57^{A} \pm 0.47$
Mean Canopy Area Projection (m²)	$183.46^{A} \pm 28.11$	$250.39^{A} \pm 8.06$
r-bar	0.52	0.48
Mean Basal Area Increment (cm²) Before	$36.84^{Aa} \pm 5.20$	$45.63^{Aa} \pm 7.58$
Mean Basal Area Increment (cm²) After	$40.30^{Aa} \pm 7.96$	$92.81^{Bb} \pm 18.12$
Mean Ring Density (g/cm³) Before	$0.72^{Aa} \pm 0.01$	$0.76^{Aa} \pm 0.02$
Mean Ring Density (g/cm³) After	$0.75^{Aa} \pm 0.01$	$0.76^{Aa} \pm 0.02$
Mean Ring $\delta^{13}C$ (‰) Before	$-25.25^{Aa} \pm 0.13$	$-25.31^{Aa} \pm 0.20$
Mean Ring $\delta^{13}C$ (‰) After	$-25.60^{Ba} \pm 0.13$	$-26.28^{Bb} \pm 0.17$
Mean Ring $\delta^{18}O$ (‰) Before	$32.71^{Aa} \pm 0.22$	$32.88^{Aa} \pm 0.13$
Mean Ring $\delta^{18}O$ (‰) After	$32.43^{Aa} \pm 0.31$	$32.55^{Aa} \pm 0.13$

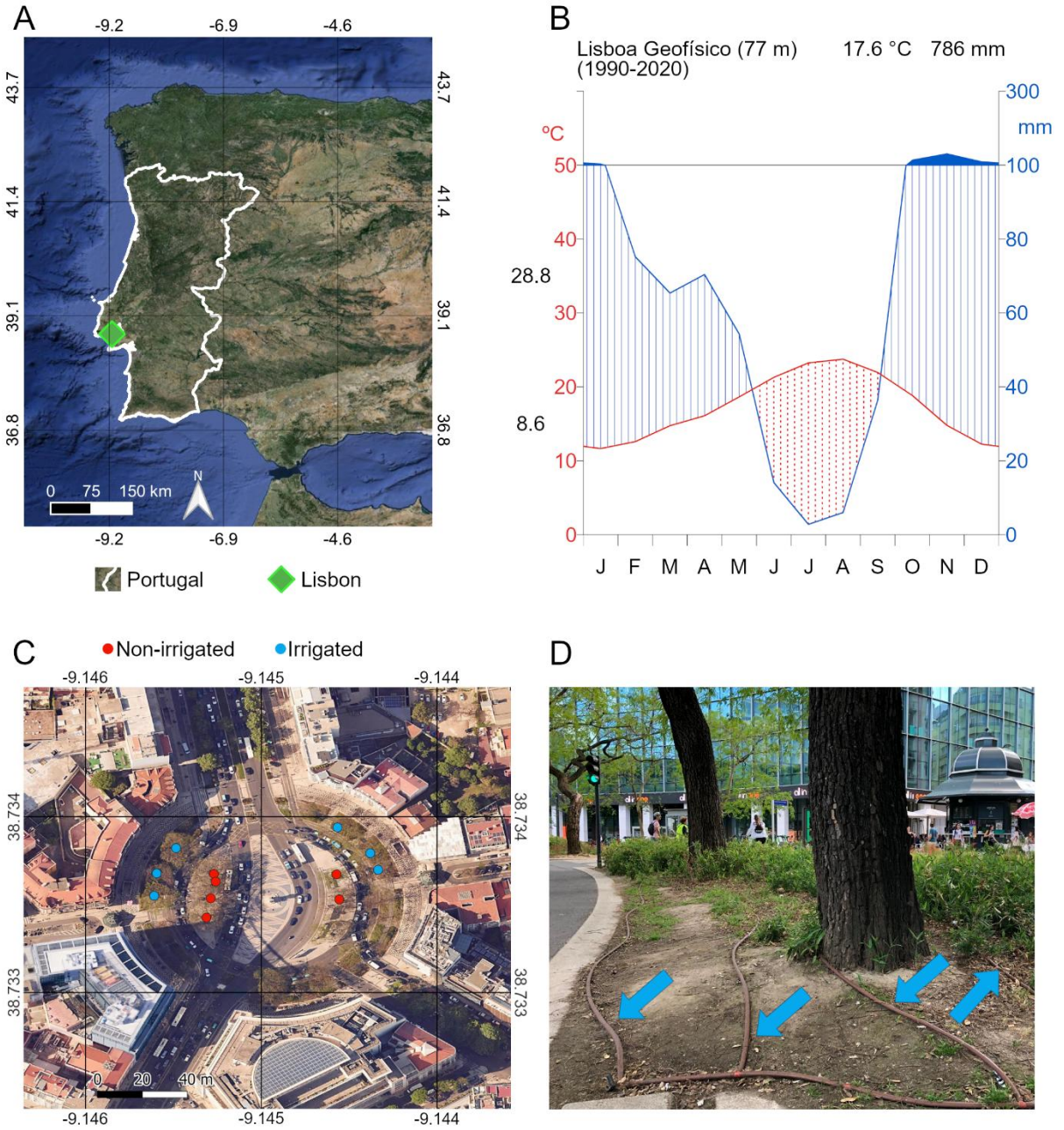

Figure 1: (A) Satellite image of the Iberian Peninsula, with the white line representing the border of continental Portugal and the green diamond marking the location of Lisbon. (B) Climate diagram for Lisbon, based on the data collected by the Portuguese Institute of Sea and Atmosphere (IPMA) at Lisboa Geofísico Station, from 1990 to 2020. (C) View of the Duque de Saldanha Square (38°44'01.7"N; 9°08'41.4"W) in Lisbon, with red dots indicating the locations of non-irrigated trees, and blue dots the locations of irrigated trees (see Table S1 in Supplementary Material for detailed information of each sampled tree). (D) *Tipuana tipu* trees supplied with water by an automatic irrigation system at the study site.

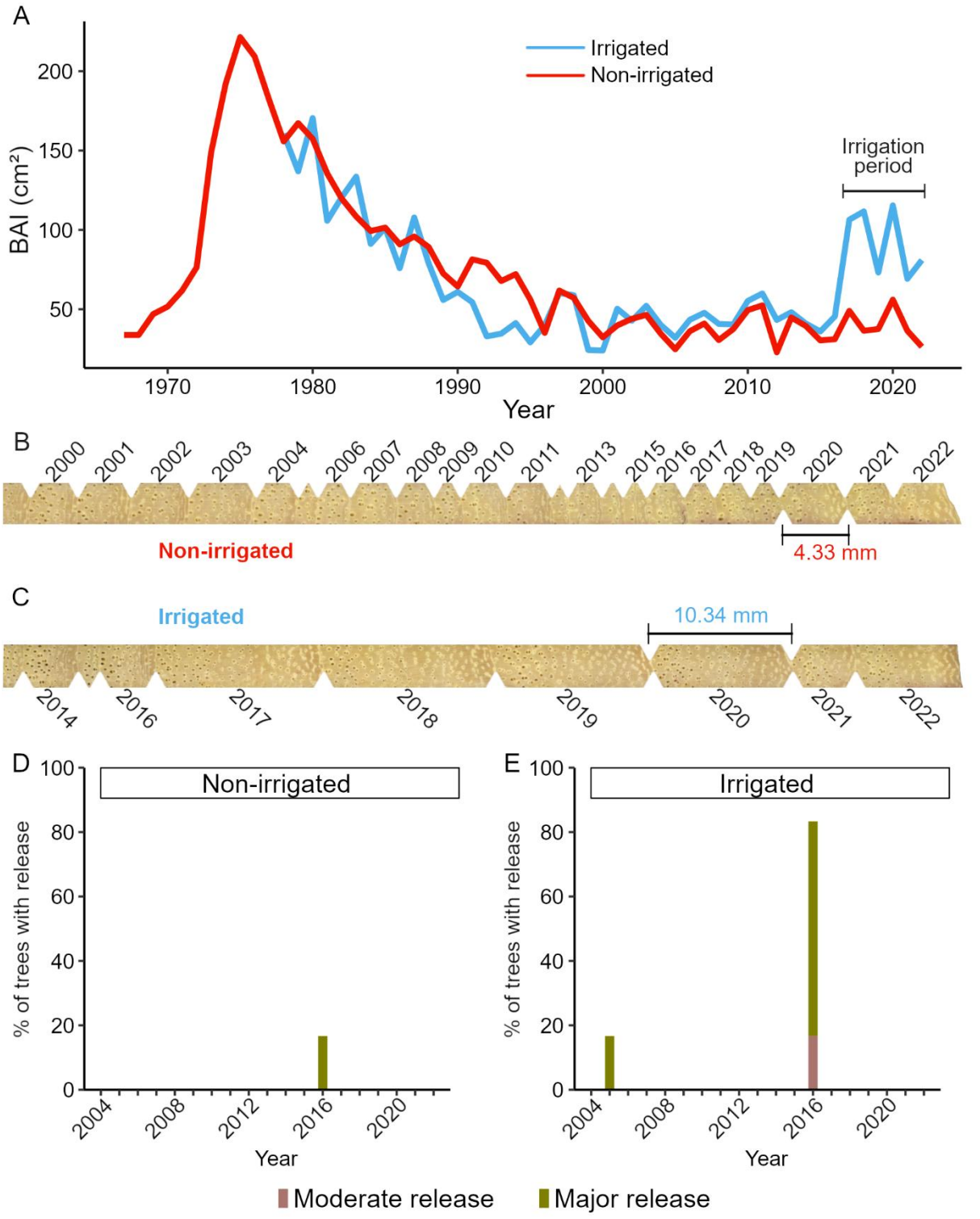

Figure 2: (A) Average basal area increment (BAI) values, in cm², of the two *Tipuana tipu* tree populations, illustrating the influence of the irrigation system since its implementation in 2017. (B, C) 2400 dpi resolution images of two sampled cores as examples of the non-irrigated and irrigated populations. The criteria used to select the exemplified samples was the clear visibility of the rings. (D) The percentage of non-irrigated population trees with growth release by year. Brown bars represent moderate release (≥25%≤50% of growth increase), and green bars represent major release (growth increase >50%). (E) The percentage of the irrigated population with moderate and major growth releases by year.

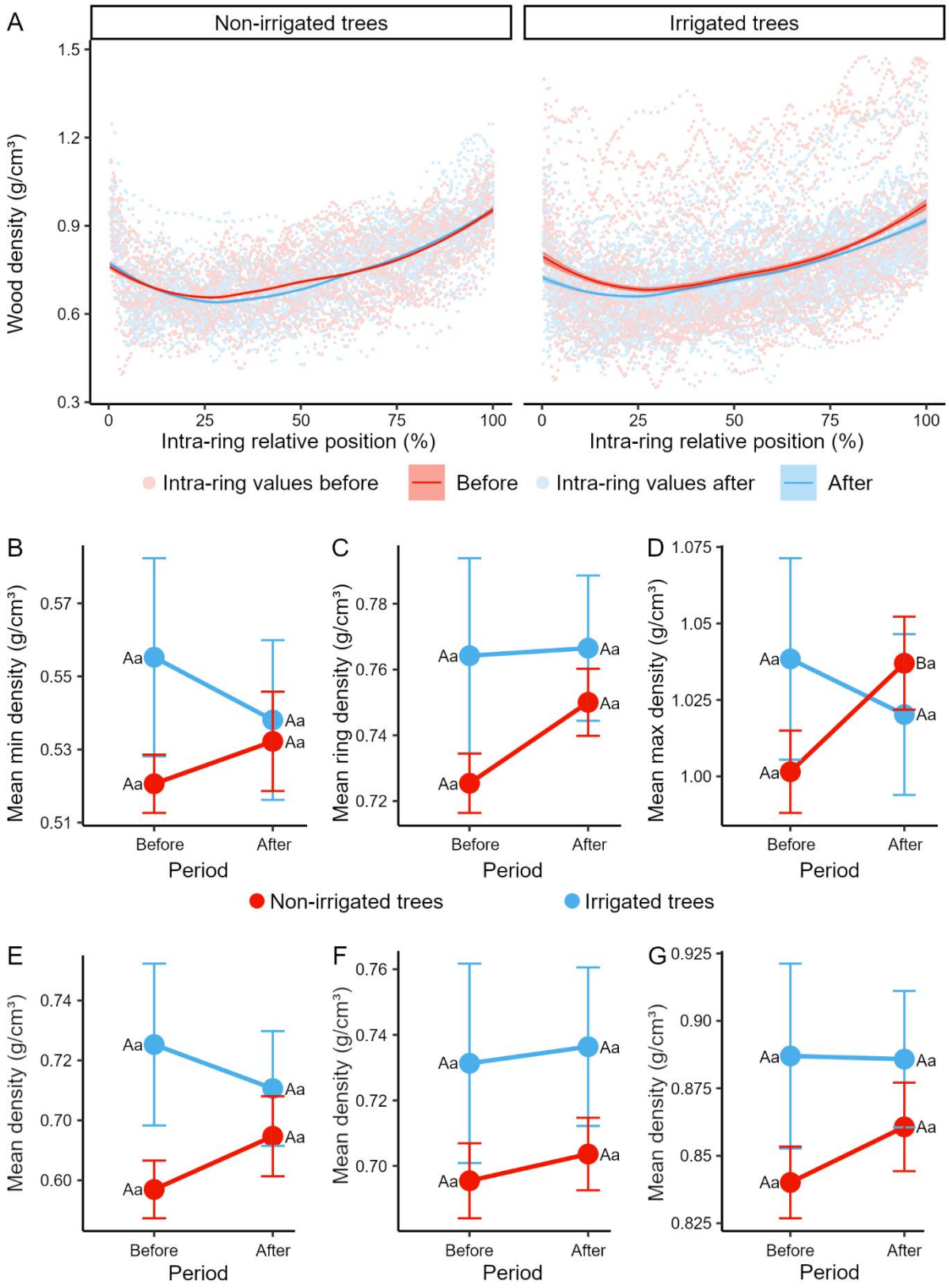

Figure 3: Measured wood density values comparing the two studied populations and the six-year-period before and after the implementation of irrigation. (A) High-resolution wood density of each sample, represented by grey dots, and the mean series (Local Regression LOESS curves) of the periods before (red) and after (blue) irrigation starts, for both studied populations of trees. The Wilcoxon Signed-Rank test was used to detect the significance of density

variations between the periods within the same population (uppercase letters), and the Mann-Whitney test for variations between the populations within same period (lowercase letters) for (B) minimum mean density; (C) total mean density; (D) maximum mean density; (E) earlywood mean density; (F) middle wood mean density; (G) latewood mean density. See Tables S4 and S5 in Supplementary Material to access the p-values and the effect size (r) with a 95% confidence of the statistics.

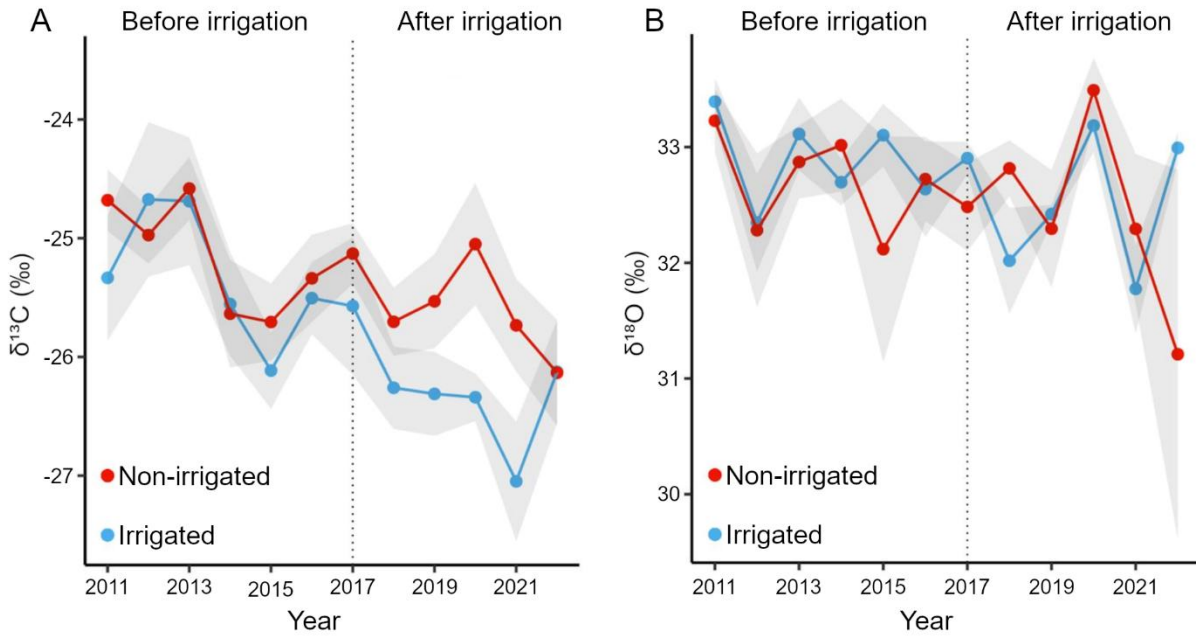

Figure 4: The dotted black vertical line in 2017 indicates the implementation of the irrigation system. Dots represent the interannual $\delta^{13}C$ and $\delta^{18}O$ values, and lines are the mean $\delta^{13}C$ and $\delta^{18}O$ temporal trends, with 95% confidence interval. (A) Stable carbon isotope signatures ($\delta^{13}C$) of *Tipuana tipu* from the two studied populations. (B) Stable oxygen isotope signatures ($\delta^{18}O$) of the studied trees.

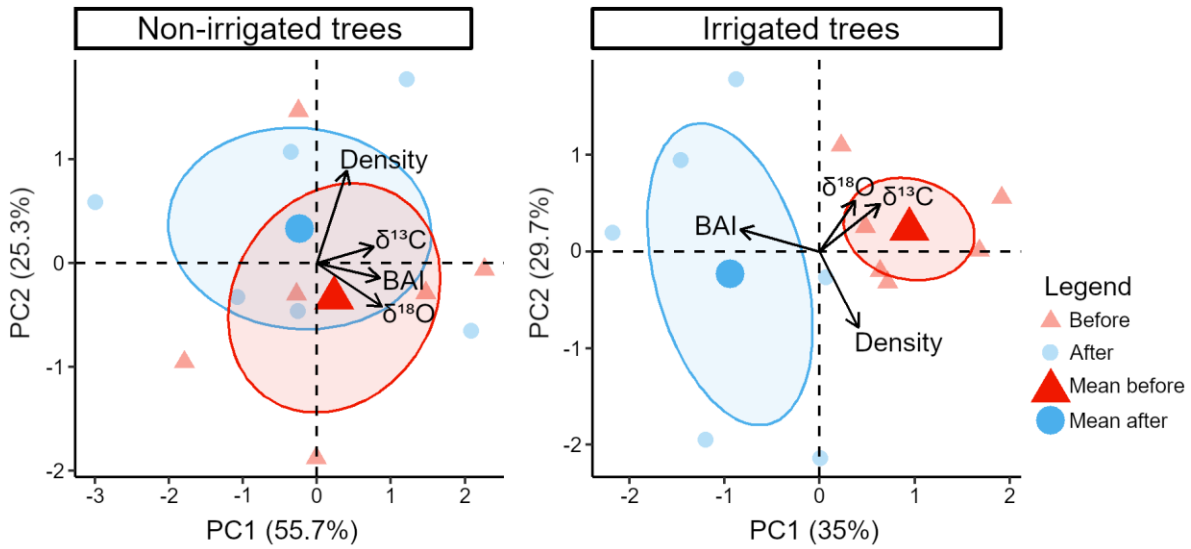

Figure 5: Principal Component Analysis (PCA) showing the influence of dendrochronological parameters (black vectors) on the proportion of six tree rings formed before (red dots) and six after (blue dots) the implementation of the irrigation system, for both irrigated and non-irrigated groups of trees. Refer to the Supplementary Materials for the PCA score matrix, eigenvalues, eigenvectors, and matrix correlations (Tables S8 – S13).

Supplementary material

Table S1: Municipality's ID, geographical coordinates and irrigation condition of each studied tree

ID	Coordinates (latitude; longitude)	Condition
2062	38.733782; -9.145159	Non-irrigated
2060	38.733907; -9.145143	Non-irrigated
2063	38.733684; -9.145181	Non-irrigated
2053	38.733868; -9.145134	Non-irrigated
2069	38.733905; -9.144515	Non-irrigated
2079	38.733777; -9.144501	Non-irrigated
2071	38.733928; -9.144302	Irrigated
2066	38.734013; -9.144342	Irrigated
2056	38.734145; -9.14451	Irrigated
2065	38.733461; -9.144445	Irrigated
2076	38.73391; -9.145436	Irrigated
2072	38.733795; -9.145449	Irrigated

Table S2: Wilcoxon Signed-Rank test p-values and the effect size (r) with a 95% confidence for mean BAI variations between different periods and same population. *Significant variance.

Population	p-value	r
Non-irrigated	0.54	0.10
Irrigated	1.46^{-6}*	0.73

Table S3: Mann-Whitney test p-values and the effect size (r) with a 95% confidence for mean BAI variations between same period and different populations. *Significant variance.

Period	p-value	r
Before	0.13	0.18
After	3.06^{-8}*	0.61

Table S4: Wilcoxon Signed-Rank test p-values and the effect size (r) with a 95% confidence for minimum, maximum, total ring, earlywood, middle wood, and latewood mean densities variations between different periods and same population. *Significant variance.

Population	Mean density	p-value	r
Non-irrigated	Minimum	0.68	0.07
Non-irrigated	Total (ring)	0.08	0.29
Non-irrigated	Maximum	0.048*	0.33
Non-irrigated	Earlywood	0.42	0.13
Non-irrigated	Middle wood	0.49	0.11
Non-irrigated	Latewood	0.59	0.09
Irrigated	Minimum	0.45	-0.13
Irrigated	Total (ring)	0.63	0.08
Irrigated	Maximum	0.25	-0.19
Irrigated	Earlywood	0.83	-0.04
Irrigated	Middle wood	0.68	0.07
Irrigated	Latewood	0.85	0.03

Table S5: Mann-Whitney test p-values and the effect size (r) with a 95% confidence for minimum, maximum, total ring, earlywood, middle wood, and latewood mean densities variations between same period and different populations.

Period	Mean density	p-value	r
Before	Minimum	0.69	-0.05
Before	Total (ring)	0.33	-0.12
Before	Maximum	0.83	-0.03
Before	Earlywood	0.55	0.07
Before	Middle wood	0.58	-0.07
Before	Latewood	0.94	0.01
After	Minimum	0.78	-0.03
After	Total (ring)	0.76	-0.04
After	Maximum	0.20	-0.15
After	Earlywood	0.66	0.05
After	Middle wood	0.52	0.07
After	Latewood	0.92	-0.01

Table S6: Wilcoxon Signed-Rank test p-values and the effect size (r) with a 95% confidence for mean $\delta^{13}C$ variations between different periods and same population. *Significant variance.

Population	p-value	r
Non-irrigated	0.01*	-0.42
Irrigated	5.99^{-5}*	0.68

Table S7: Mann-Whitney test p-values and the effect size (r) with a 95% confidence for mean $\delta^{13}C$ variations between same period and different populations. *Significant variance.

Period	p-value	r
Before	0.65	-0.05
After	0.007*	-0.32

Table S8: PCA scores of the non-irrigated trees.

Year	PC 1	PC 2	PC 3	PC 4
2022	-2.10	0.59	0.43	-0.52
2021	-1.08	-0.32	0.61	0.03
2020	2.08	-0.65	1.00	0.19
2019	-0.36	1.07	0.65	0.26
2018	-0.26	-0.46	0.30	0.57
2017	1.21	1.78	0.87	-0.16
2016	-0.28	-0.30	-0.67	0.43
2015	-1.79	-0.95	-0.09	-0.19
2014	-0.01	-1.88	-0.26	0.01
2013	1.47	-0.29	-1.01	-0.66
2012	-0.25	1.47	-1.77	0.33
2011	2.26	-0.06	-0.08	-0.29

Table S9: PCA scores of the irrigated trees.

Year	PC 1	PC 2	PC 3	PC 4
2022	0.07	-0.26	0.82	0.64
2021	-1.20	-1.94	-0.80	-0.51
2020	-1.46	0.95	1.20	0.44
2019	0.002	-2.13	0.47	0.80
2018	-2.18	0.20	-1.08	0.13
2017	-0.88	1.79	-0.25	0.57
2016	0.22	1.10	-0.89	-1.24
2015	0.64	-0.20	0.92	-1.24
2014	0.72	-0.32	-0.11	-0.65
2013	1.91	0.56	-0.06	0.72
2012	1.68	0.01	-1.62	0.66
2011	0.48	0.26	1.42	-0.34

Table S10: PCA eigenvalues and eigenvectors of the non-irrigated trees.

	Eigen value	Variance (%)	Variance (cumulative %)	$\delta^{13}C$	BAI	Density	$\delta^{18}O$
PC 1	2.23	55.74	55.74	0.77	0.85	0.40	0.87
PC 2	1.01	25.34	81.08	0.16	-0.14	0.89	-0.41
PC 3	0.62	15.63	96.71	-0.61	0.47	0.18	-0.01
PC 4	0.13	3.29	100	-0.13	-0.20	0.11	0.25

Table S11: PCA eigenvalues and eigenvectors of the irrigated trees.

	Eigen value	Variance (%)	Variance (cumulative %)	$\delta^{13}C$	BAI	Density	$\delta^{18}O$
PC 1	1.40	34.96	34.96	0.63	-0.83	0.40	0.37
PC 2	1.19	29.71	64.67	0.49	0.23	-0.78	0.52
PC 3	0.88	21.91	86.58	-0.46	0.11	0.26	0.76
PC 4	0.54	13.41	100.00	0.38	0.49	0.39	0.02

Table S12: Pearson correlation coefficient between the analysed tree-ring parameters of non-irrigated trees. * Statistically significant for $\alpha = 0.05$.

	$\delta^{13}C$	BAI	Density	$\delta^{18}O$
$\delta^{13}C$	1.00	0.36	0.33	0.58*
BAI	0.36	1.00	0.28	0.74*
Density	0.33	0.28	1.00	0.01
$\delta^{18}O$	0.58*	0.74*	0.01	1.00

Table S13: Pearson correlation coefficient between the analysed tree-ring parameters of irrigated trees. * Statistically significant for $\alpha = 0.05$.

	$\delta^{13}C$	BAI	Density	$\delta^{18}O$
$\delta^{13}C$	1.00	-0.28	-0.10	0.15
BAI	-0.28	1.00	-0.30	-0.09
Density	-0.10	-0.30	1.00	-0.06
$\delta^{18}O$	0.15	-0.09	-0.06	1.00

Table S14: Mann-Whitney test p-values and the effect size (r) with a 95% confidence for mean Diameter at Breast Height (DBH), Estimated Tree Age (ETA), Tree Height (TH), Crown Base Height (CBH), and Canopy Area Projection (CAP) variations between different populations. *Significant variance.

Variable	p-value	r
DBH	1.00	0
ETA	1.00	0
TH	0.12	0.46
CBH	0.52	-0.21
CAP	0.09	0.51

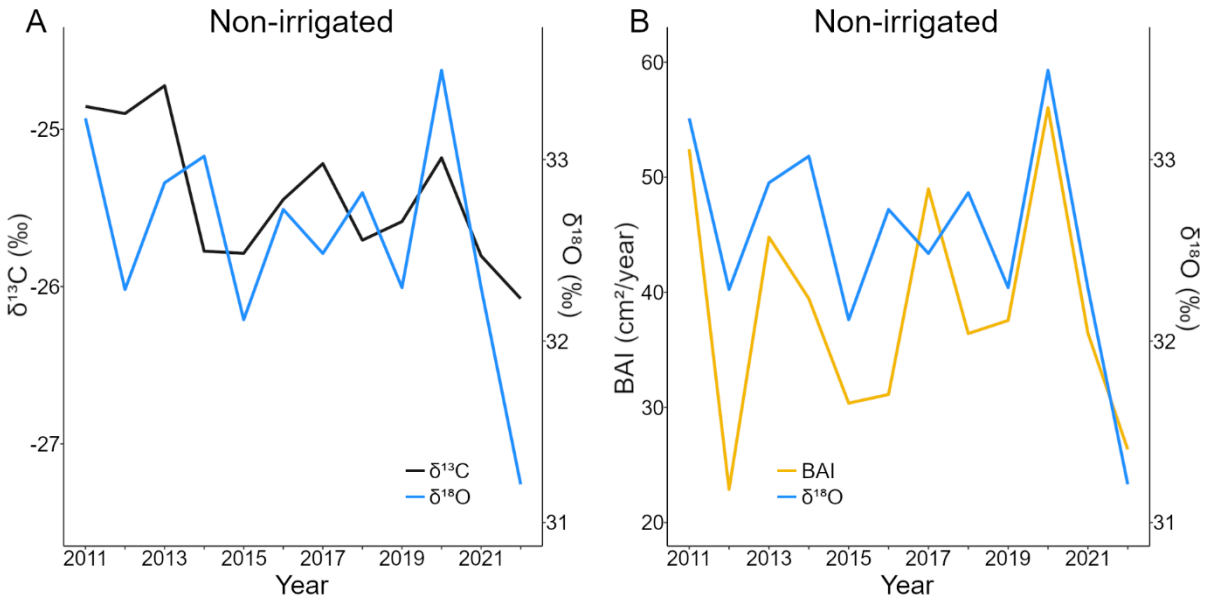

Figure S1: Mean temporal series for non-irrigated trees of (A) $\delta^{13}C$ and $\delta^{18}O$, and (B) BAI and $\delta^{18}O$.

Capítulo 4

Impacts of Air Pollution Reduction During COVID-19 Lockdowns on Urban Tree Development: An Intra-Annual Wood Density and Stable Carbon Isotope Approach

In collaboration with: Dr. Mario Tomazello Filho, Gabriela Morais Olmedo, Dr. Ariel Andrés Muñoz Navarro, Sebastián Alfredo Godoy Nuñez, Dr. Francisco Javier Fernandoy Pedredos and Dra. Milena Godoy-Veiga.

Manuscript to be submitted to *Dendrochronologia*

Abstract

The COVID-19 lockdowns created an event of abrupt reduction in atmospheric pollutants that can affect tree functioning. Despite the importance of trees to mitigate emissions in urban environments, the available assessments were performed with annual resolution, which do not record well such acute alterations in the atmosphere. This study assessed the impacts of air pollution reduction during the COVID-19 lockdown on the intra-annual growth of *Tipuana tipu* trees in São Paulo, Brazil, using high-resolution tree-ring analyses of wood density and stable carbon isotopes ($\delta^{13}C$). Trees sampled along a busy avenue exhibited higher wood density and significantly lower $\delta^{13}C$ values compared to those from a nearby park. The lockdown period during the 2020 / 2021 growing season coincided with a disruption in the typical intra-annual $\delta^{13}C$ trend observed in avenue trees in other growing seasons, shifting from a decreasing to an increasing pattern in the final tree-ring segments, a signal not observed in park trees. This isotopic shift is consistent with a reduction in fossil fuel emissions during the most restrictive phases of social distancing, suggesting that the studied avenue trees predominantly incorporate the $\delta^{13}C$ signature of their carbon source. Although the overall wood density trends remained consistent, a faster rate of density increase was observed in avenue trees during the lockdown year, potentially linked to changes in stomatal conductance and water-use efficiency under altered CO_2 conditions. These results demonstrate that intra-annual dendrochronological approaches, especially those in high-resolution such as by laser ablation, are sensitive enough to detect short-term atmospheric changes and provide valuable tools for monitoring urban environmental dynamics.

Keywords: High-resolution; stable carbon isotopes; wood density; air pollution; laser ablation.

1. Introduction

Air pollution is a major threat to the urban population worldwide. More than 50% of the urban population is exposed to levels above the recommendations by the World Health Organization (WHO, 2024), making it one of the main causes of premature death globally (Pozzer et al., 2023). Due to its role in public health, air pollution has long been at the core of environmental discussions in cities, and how public policies can aid in reducing concentrations to safe levels (Sofia et al., 2020). Urban forests are considered one of the measures to mitigate high levels of air pollution, as they offer potential adsorption of certain pollutants, such as particulate matter, on the surfaces of plants, primarily leaves and bark (Monaci and Baroni, 2025; Wang et al., 2024). There have been important advances in the understanding of the mechanisms behind this important ecosystem service provided by the urban trees (Anys and Weiler, 2024; Esfehankalateh et al., 2021; Zhang et al., 2022), which include carbon assimilation, rainfall interception, atmosphere cooling, and others (Berland et al., 2017; Moreno et al., 2024; Savo et al., 2025; Tan et al., 2016). Yet, the literature points to the impairments in tree functioning caused by air pollution (Winner and Atkinson, 1986) that could potentially disrupt the development of trees by up to 30% and curb their potential benefits (Locosselli et al., 2019). Most of what we know about the impact of air pollution comes from long-term changes in the urban air pollution trends (Pozzer et al., 2023), and there is a fundamental gap in how they respond to acute changes in the atmospheric levels, probably because such changes are rare and only associated with environmental disasters.

Recently, the world population has seen an unprecedented change in the air pollution levels in cities worldwide caused by the tragedy of the COVID-19 pandemic (Sannigrahi et al., 2021). Although changing in time and space, lockdowns were a status quo when facing the uncontrolled impacts of the pandemic as it unfolded in each country. The lockdowns caused significant changes in the concentrations of many air pollutants (Nakada and Urban, 2020; Siciliano et al., 2020) including those related to vehicular emissions like particulate matter, other sources in the city including resuspension, and more targeted pollutants like the nitrogen oxides (NOx) directly related to the fuel burning (Varella et al., 2017; Peel et al., 2013). As a matter of illustration, the reduction of NOx concentrations varied between 30-70% in São Paulo (Krecl et al., 2020), and similarly in other cities like 40-50% in Beijing (Zhang et al., 2020), and approximately 46% in Paris, 40% in Detroit, 37% in Milan, 36% in Frankfurt and 34% in London and Madrid (Sannigrahi et al., 2021). The question remains: did this decrease in air pollution result in any change in the functioning of urban trees?

This is a challenging question because, to our knowledge, no one was holding monitoring experiments with urban trees during the lockdowns, or were eventually allowed to hold these experiments due to the social distancing and mandatory quarantines. The only alternative to retrospectively assess the trees' responses lies in the tree-ring analyses. This environmental archive allows one to precisely assess the conditions by which trees lived in the past with high temporal accuracy (Esperon-Rodriguez et al., 2025; Lehmann et al., 2021; Miyahara and Locosselli, 2024; Savard, 2010). Tree-ring width is the main parameter measured in the tree rings to evaluate changes in the annual growth rate of trees. This has supported a vast literature on the responses of trees to environmental changes, including cities (Miyahara et al., 2022).

Tree rings are like a book written by trees using many layers of codes, and various proxies can be used to read and interpret recorded information (Rodriguez et al., 2023). This includes the assessment of wood density which is a measure of the actual biomass allocated in the tree rings as well as a measure of the hydraulic efficiency or safety (Locosselli and Buckeridge, 2017). In a situation of high growth and evapotranspiration rates, greater investment usually occurs in the development of wider vessels for water conduction, leading to lower wood density (Niklas and Spatz, 2010; Van Duong et al., 2023). In addition, carbon isotopes bring additional information on the source, the signature of the atmospheric CO_2, plus fractionation processes at the leaf level (Rodriguez-Caton et al., 2021; Miyahara and Locosselli, 2024). The ratio between ^{12}C and ^{13}C, denoted as $\delta^{13}C$, in atmospheric CO_2, has been gradually changing as it gets more depleted in the heavy ^{13}C due to the significant input from fossil fuel burning (Choi and Lee, 2012; Tans and Mook, 1980). On top of the source signature, CO_2 goes through two additional fractionation processes, namely the diffusion through the stomata and the Rubisco affinity during carboxylation, that discriminates the ^{12}C to the detriment of the ^{13}C (McCarroll and Loader, 2004). This intimate dependence on leaf physiological processes makes the $\delta^{13}C$ a source of insights into the changes in plants' functioning. When used together through a multi-proxy approach, these variables can provide a big picture of how trees respond to chronic (Jevšenak et al., 2024; Zhang et al., 2023) and acute disturbances (Favillier et al., 2023; Margolis et al., 2022).

Despite the long use of the multi-proxy approach in tree-ring research, there is little application in understanding the impacts of air pollution reduction during the COVID-19 lockdowns. To our knowledge, only one study decisively attempted to assess the impact of the lockdowns on the growth of urban trees, but with little success (Camarero et al., 2025). Partially, because of the temporal incompatibility between the standard tree-ring analysis and the duration of the lockdowns. The growing season, the period when trees are growing and recording the changes

in the environment, encompasses a few months depending on the local climate seasonality, whereas the most restrictive periods of the lockdowns lasted for a few weeks up to a few months. It is not impossible that a short-term event gets recorded in the tree rings, but it must be truly significant to have an impactful change in plant functioning to be assessed at an annual scale using standard dendrochronological methods. Alternatively, one can assess the changes along the growing season by analyzing the intra-annual variability, for instance, in wood density and stable isotopes. Tree rings can be divided manually with blades into more than 10 segments for a high-temporal resolution analysis that improves resolution from one growing season to weeks (Locosselli et al., 2020; Sarris et al., 2013). Another option is to use cutting-edge technologies, such as laser ablation – for instance *in continuum* along the same line every 150 µm (De Micco et al., 2012) – achieving a temporal resolution of less than a week. Bearing in mind that the lockdowns lasted for only a fraction of the growing season, the intra-annual analysis is likely mandatory to assess the impacts of air pollution reduction on the functioning of urban trees.

Having set the intra-annual analysis as the best methodological approach, one must then evaluate the possible responses of trees to air pollution changes. Although studies do show the direct impact on tree growth, defining the mechanisms behind the responses to vehicular emissions is tricky. Partially because air pollution is a complex mixture and it covaries with the emission of CO_2 from fossil fuel burning, enriched in ^{12}C. High concentrations of particulate matter can cover the leaf surface and reduce the photosynthetic radiation reaching the photosystem, increasing leaf temperature by absorbing long waves, and occluding the stomata (Li et al., 2019; Maher et al., 2013). These mechanisms can potentially reduce stomatal conductance increasing the $\delta^{13}C$ values in the tree rings (McCarroll and Loader, 2004). It can also result in higher wood density with a less efficient hydraulic system to cope with the lower leaf water demands. Yet, the high CO_2 concentrations can allow trees to have more access to carbon and increase their use in photosynthesis, with less water lost for photo-assimilated molecules of CO_2 (Silva and Anand, 2013). This would also increase the $\delta^{13}C$ values but without necessarily impairing tree development and growth (Groenendijk et al., 2015; Van Der Sleen et al., 2015). Conversely, the enrichment in atmospheric $^{12}CO_2$ due to higher vehicular emissions of fossil fuel burning solely would decrease the $\delta^{13}C$ signature of the tree ring, without necessarily affecting the leaf physiology. Thus, the response of trees to lower air pollution during the pandemic is an open question, as well as how it would be recorded in the tree rings, if it ever does.

In this study, we used state-of-art methods for intra-annual tree-ring analyses to assess the fine changes in tree functioning due to the changes in atmospheric concentrations of air pollution in the city of São Paulo, one of the largest urban conglomerates in the world, where two strict lockdowns were implemented in 2020 and 2021. To assess the impacts of air pollution reduction during the lockdowns on trees growing in an urban park and along a busy avenue, we employed high-resolution X-Ray wood densitometry and Laser Ablation-Combustion coupled with Isotope Ratio Mass Spectrometry (LA-C-IRMS) for high-resolution $\delta^{13}C$ determination. Both measurements were conducted at equidistant points along the surface of each target tree rings formed before (2018-2019), during (2020-2021), and after the pandemics (2022). Based on this approach, we tested the following hypotheses: I) The air pollution reduction during the COVID-19 lockdown events can be captured in high-resolution intra-annual tree-ring analyses; II) The reduction of air pollution during the lockdowns led to higher stomatal conductance and consequently the reduction of $\delta^{13}C$ values of the respective intra-annual segments; III) High-resolution wood density profiles capture the impact of reduced air pollution events on tree development; IV) The wood density corresponding to the periods of lockdown tend to decrease due to the higher growth and transpiration rates.

2. Material and Methods

2.1. Sampling site and species

Sampling took place in the city of São Paulo, Brazil, the fifth largest urban conglomerate in the world (United Nations, 2018), with an estimated population of 11.9 million people (IBGE, 2022) and an automotive fleet of approximately 34.3 million vehicles (SENATRAN, 2024). The climate is subtropical with a dry winter and wet summer according to Köppen's classification (Köppen, 1931), with an annual average temperature of 19.3 °C and 1536.2 mm of annual mean precipitation, calculated for the years between 1973 and 2023 (SMUL/SP, 2023).

We chose Ibirapuera Park as the control of this study for its substantial size, over 150 ha, and relative proximity to one of the main avenues in the city, named *Avenida 23 de Maio*, or 23rd of May Avenue (Figure 1A). This avenue is part of the North-South corridor that connects two extremes of the city. It has five lanes in the Northern direction and five towards the south. The outermost lanes, close to the tree lawns, are exclusively used by buses. It is 3.2 km long and connects the city center to Ibirapuera Park. The proximity between these two sampling areas

guarantees, to some extent, similar overall climate conditions, while differing significantly in exposure to vehicular pollution.

In these two sites (Figure 1B, C), we sampled trees of *Tipuana tipu* (Benth.) Kuntze (Fabaceae), an exotic but long-planted tree in the cities (Moreira et al., 2018), making it one of the three most common tree species found in São Paulo (Locosselli et al., 2024). This is a deciduous species from Northern Argentina and Southern Bolivia (Cattana et al., 2014) that produces distinct semi-porous rings delimited by marginal parenchyma bands (Locosselli et al., 2024). Based on tree-ring studies, this species is regarded as a drought-tolerant species but sensitive to elevated concentrations of air pollution, especially particulate matter of heavy metals (Locosselli et al., 2019). It has also been successfully assessed before in terms of intra-annual analyses and in urban environments (Ballikaya et al., 2023). These characteristics make it a target species for testing the proposed hypotheses of this study.

To characterize the environmental conditions of the sampled sites, climate data of precipitation and temperature obtained from the Vila Mariana station from the Emergency Management Center of São Paulo (CGE-SP, Figure 1D, E). Air pollution data of NOx were obtained from the Environmental Company of the State of São Paulo (CETESB, Figure 1F), the Ibirapuera Station (23°35’29.7”S 46°39’38.7”W), which is located inside the Park where these trees were collected, and the Cerqueira César Station (23°33’09”S 46°40’24.3”W), which is the one nearest the Avenue sample site.

2.2. Sampling and sample preparation

A total of 16 trees and 12 trees have been sampled, respectively, in the park and in the vicinity of the avenue. We took two 5 mm increment cores of each sampled tree. We also took notes in the field about the diameter of the breast height, the overall phytosanitary condition of the tree, and geographical coordinates (Table S1). Sampling holes were then plugged using natural cork to avoid exposure to pathogens. We fixed the samples in wooden holders and left them to air-dry for a couple of weeks. We then glued the samples and polished the transversal surface to reveal the tree rings using sandpaper with different grits (100 to 600) and used compressed air to remove the wood powder from the vessels (Locosselli et al., 2020). We scanned all samples at 2400 dpi (Godoy-Veiga et al., 2021), measured the tree-ring width using the CooRecorder software (Maxwell and Larsson, 2021), and visually cross-dated the tree rings. We assigned the calendar year of each tree ring formation using the Schulmann convention (Schulmann, 1956)

for trees sampled in the Southern Hemisphere (Andreu-Hayles et al., 2023). The growing season of the sampled trees occurs during the wet and warm period, starting in the austral Spring (approximately between September and November) and ending in the austral Fall of the subsequent year (approximately between April and June). The Basal Area Increment (BAI) was calculated for the target trees, and the mean BAI series for each sampling site was calculated (Figure S1).

Once samples were scanned and tree rings identified and marked, we chose the three individuals in each population with the best tree-ring delimitation and wide enough for a detailed intra-annual analysis. We produced 2mm thin sections of these samples using a circular saw (Proxxon KS 230, Locosselli et al., 2020). We then selected the target years in each sample, 2018 and 2019 corresponding to the year before the onset of the pandemic, 2020 and 2021 corresponding to the two years during the pandemic, and 2022 corresponding to the year after the pandemic.

2.3. X-Ray densitometry

One radius of each selected tree, a total of six radii, were conditioned under controlled conditions according to Ferreira and Tomazello Filho (2009) methods (20 °C and 50% relative humidity until the samples reach 12% moisture content). Then, using a digital calliper, the thickness of each sample was measured to obtain the mean thickness of each sample for the post-processing calculations. Using an X-Ray densitometry chamber (Faxitron X-Ray, Illinois, EUA) the high-resolution wood density was measured. A cellulose acetate wedge of known density (1.274g/cm^3) was used to create a standard curve for density calibration. The radiographies were then analysed by WinDendro Density 2017a software (Regent Instruments Inc., Canada) according to Pompa-García et al. (2024) methods to determine the high-resolution wood density profiles.

2.4 Cellulose extraction and stable carbon isotopes analysis

Cellulose extraction was performed for each selected sample, adapting the method from Kagawa et al. (2015) and Schollaen et al. (2015). Perforated Teflon sheets were tied with thread sealing tape to construct supports where the samples were conditioned for the extraction. Samples were submerged twice in a 5% NaOH solution inside glass beakers for two hours in a water bath at 70 °C. Then, the samples were submerged four times in room temperature distilled

water for two minutes (except for the third wash at 60 °C). Following, the samples were treated four times with 7.5% $NaClO_2$ solution at 70 °C, for 8h to 12h each. Finally, samples were washed in distilled water, two times at room temperature and two at 60 °C. Samples were frozen at -18 °C for 12 hours, then freeze-dried for 72 hours.

Using the digital images, each target year of each sample was identified by the anatomical traits, such as vessel caliber and arrangement, ring size, and marginal parenchyma bands. High-resolution stable carbon isotope analysis was conducted, using a laser ablation-combustion set-up (LA-C-IRMS), as described by Saurer et al. (2022). Samples were fragmented in the limit of the tree rings using a razor blade under a stereomicroscope, resulting in pieces with two rings each, to fit them in the 4 cm sealed sample of the LA-C-IRMS set-up. Using the high-definition video microscope, 15 transects with equal distances were marked in each ring for the laser shots to the subseasonal stable carbon isotope analysis. Each intra-annual transect was composed of three parallel spots with 50 μm diameter each, to better represent the respective section of the tree ring, and to reach the necessary amount of sample particles to be detected by the IRMS system. The laser setup was configured with a 70% output, fluence of 4.51 J/cm^2, repetition rate of 15 Hz, shot count of 30, dwell time of 1.33 seconds, Z depth of 1 μm, and an interaction count of 2. The $\delta^{13}C$ results were treated using the LIMS (Laboratory Information Management System) for Laser 2015 application (Coplen and Wassenaar, 2015), adapted for IRMS, for post-processing calculations.

2.5 Statistical analyses

The mean values of the high-resolution wood density and $\delta^{13}C$ for each one of the 15 intra-annual segments were calculated for each ring from each sample site. A local regression curve (LOESS) was employed in R software to characterize these data profiles (Figure 2). A box plot was created, using the package 'ggplot2' in R, and Student's T-test was conducted to evaluate the density distribution between the park and the avenue.

Principal Component Analyses (PCAs), using the 'FactoMineR' package in R, were conducted for each target year of ring formation to reduce the wood density and $\delta^{13}C$ data to their essential features, enabling the assessment of the importance of each tree-ring parameter and the differences among sampling sites.

3. Results

Tree rings from both avenue and park trees display similar wood density intra-annual trends, with increasing values from earlywood, or the initial segments, to the latewood, or the last segments (Figure 2). Although displaying similar trends as revealed by the Loess fits, the average wood density in the avenue trees (0.80 g/cm3) is significantly higher than in the park (0.77 g/cm3). Conversely, tree rings display distinct $\delta^{13}C$ trends between the two sampling sites. Avenue trees display a substantial decrease in $\delta^{13}C$ values from the earlywood to the latewood, whereas park trees display a flat to bell-shape trend in $\delta^{13}C$ values. Not only do the $\delta^{13}C$ trends differ between sites but also the $\delta^{13}C$ values are significantly lower in the avenue trees (-27.07 ‰) than in the park trees (-25.04 ‰).

When analyzed by growing years, there is no substantial visual difference in wood density among the soothing Loess curves for the park trees (Figure 2). In contrast, the wood density profiles display a consistent increasing values pattern from earlywood to latewood for all the years, except for 2020 / 2021, when values increase at a seemingly faster rate. The $\delta^{13}C$ values from 2020 / 2021 also stand out by not displaying the decreasing trend in the last third of the tree ring, shared by the other three growing years, but instead level off with an increasing trend towards the last segments.

These visual changes in the trends along the segments were further assessed by comparing the synchrony between the average wood density and $\delta^{13}C$ in each one of the 15 segments (Figure 3). The synchrony between the wood density values of the avenue and park trees is rather low in the first two-thirds of the tree rings and tends to strengthen in the last third of the tree ring. The synchrony is stronger in the two initial thirds of the tree ring for the $\delta^{13}C$ values (Figure 4), but tends to weaken towards the last third, when temporal variation tends to be in anti- phase, particularly for the growing year of 2020 / 2021. In this year, the $\delta^{13}C$ of the park trees decreased, whereas the $\delta^{13}C$ values of the avenue trees increased.

This offset is finally corroborated in the Principal Component Analysis (Figure 5). Overall, the first and second principal components explain a substantial share of the data variability, between 87.30% and 92.88% for 2021 / 2022 and 2018 / 2019 growing years, respectively. For all the growing years, the data from the first two-thirds of the tree-ring segments display negative PC1 scores, and the last third displays positive PC1 scores. This suggests a clear division in the tree ring characteristics along the segments. This variation along the PC1 axis is mostly driven by the differences in the wood density as it tends to increase from early wood to latewood, and partially by the stable carbon isotopes (Tables S2 to S5). For all the years but 2020 / 2021, stable

carbon isotopes values in the last segments were lower in the avenue trees as well as in the park trees. Nonetheless, 2020 / 2021 is the only year when values increase from segment 12 to 15 in the avenue trees.

4. Discussion

The impacts of air pollution on the development of urban trees are fundamental information to support evidence-based decision-making in urban forests and their performance in delivering ecosystem services. The recent tragedy of the COVID-19 pandemic and consequent social distancing and lockdowns turned out to be one of the few events that changed the atmosphere composition at a global scale, seconded by the industrial revolution, nuclear bomb test in the 1950s and 1960s and natural volcanic events (Horvatinčić et al., 2001; von Glasow et al., 2009; Yakir, 2011). The effects of these previous events were generally chronic and reasonably well detectable in tree-ring series worldwide (Dai and Fan, 1986; Pearson et al., 2005; Xing-Yun et al., 2006). However, the reduction in air pollution during the pandemic was rather acute and, although significant, only lasted for a few weeks to months. Detecting the impacts of these events would be unlikely to be captured using the standard annual approach (Camarero et al., 2025) in tree-ring research.

The intra-annual approach is likely the only alternative, aiming at sub-annual information ranging from months to a week, or even days, according to the number of intra-annual segments (Miyahara and Locosselli, 2024). Defining the equivalent period of the intra-annual segments is one of the main challenges of this approach (Miyahara and Locosselli, 2024) because one would need to know the exact growing season length for each analyzed year. Based on the precipitation distribution at our sampling site and the assumption that trees grow in the tropics when precipitation is higher than 60mm (Worbes, 1995), it is possible to estimate that the growing season lasts approximately six months. Thus, each segment would represent about 12 days. Still, higher precipitation volume at the end of the growing season could maintain high water table levels for longer periods supporting tree growth. This is a major uncertainty of this study that can limit the precise identification of the target events in the tree rings. Therefore, only trends were evaluated to extract evidence of air pollution reduction on the growth of the *T. tipu* trees in São Paulo.

The intra-annual wood density and stable carbon isotope values follow expected trends for this species in these two urban typologies (Locosselli et al., 2024). The increasing wood density results from the semi-porous wood anatomy that characterizes this species, with its wide

earlywood vessels gradually decreasing in diameter towards the latewood (Locosselli et al., 2020). Likewise, the overall intra-annual $\delta^{13}C$ trends follow similar trends observed in another park and street in São Paulo (Locosselli et al., 2024). Both populations growing in tree lawns along the street in Locosselli et al. (2024), or in the avenue of the present study, show a clear decreasing trend from the earlywood to the latewood, whereas the park trees show a stable to bell-like shape of the intra-annual $\delta^{13}C$ curve in both studies. These are the two most common intra-annual carbon isotope trends in broadleaf species (Miyahara and Locosselli, 2024). The bell shape is associated with temperature constraints in the middle of the growing season (Cintra et al., 2019; Olson et al., 2020; Zeng et al., 2017), and the decreasing trend results from the use of non-structural carbohydrates during the onset of the growing season (Krepkowski et al., 2013; Nabeshima et al., 2018; Rinne et al., 2015). Although trees show similar trends between studies' sampling sites as discussed above, it does not go unnoticed that the average tree-ring $\delta^{13}C$ values are higher in the street trees than in the park by 0.9 ‰, in the study by Locosselli et al. (2024). It is lower in the present study's avenue population by a magnitude of 2.02 ‰ compared to the park. There is a substantial difference between the two studied populations outside the parks. Lower values of $\delta^{13}C$ are usually regarded as a result of higher stomatal conductance for the discrimination during the CO_2 diffusion through the stomata (Brienen et al., 2022; Cernusak et al., 2013; Rodriguez-Caton et al., 2021). This assumption is at odds with the expected decrease in stomatal conductance under more stressful conditions like the ones found along big avenues (Lindén et al., 2023; Shekanino et al., 2023; Zhao et al., 2021). As an alternative explanation for this substantial decrease in average $\delta^{13}C$ values, the local atmosphere is depleted in the heavy carbon isotope due to vehicular CO_2 emissions from fossil fuel burning. The vehicular fleet on the studied avenue has buses, cars, and motorcycles mostly running either diesel or petrol. Thus, vehicular emissions are likely driving the stable carbon signature in the tree ring of trees growing along the avenue.

If the observation of a dominant vehicular CO_2 emission in the tree-rings signature is true, then one would expect an increase in the $\delta^{13}C$ during the social distancing periods and lockdowns. By substantially curbing the local vehicular emissions in the period corresponding to the end of the growing season, the decreasing trends in intra-annual $\delta^{13}C$ values would likely level off or reverse by a different mixture of CO_2 signatures. This is exactly what is observed in the avenue trees during the most restrictive lockdown in March and April of 2021, corresponding to the end of the growing season of the tree ring assigned to the year 2020. This result refutes our second hypothesis, as the predominant signal of the air pollution reduction effect on intra-annual tree-ring $\delta^{13}C$ originates from the carbon source rather than from the physiological responses of the trees.

Attributing this trend to the lockdown event is tricky as it could be associated with particular climate conditions during the end of the growing season affecting the two populations concomitantly. However, no significant change in climate conditions has been recorded in the climate data nor has it been also imprinted in the last segments of the 2020 tree ring in the park trees. This observation is further supported by the consistent synchrony between the avenue and park $\delta^{13}C$ series, along the segments up to two-thirds of the tree ring. From this point on, the $\delta^{13}C$ series starts to be in anti-phase, particularly for the year 2020, when the $\delta^{13}C$ value decreases in the park and increases in the avenue trees. This is the only year the PCA analysis showed that the $\delta^{13}C$ values increased from segment 12 to 15 in the street trees. Altogether, these pieces of evidence point to the atmospheric CO_2 signature change resulting from the lower vehicular CO_2 emission. This result corroborates our first hypothesis, demonstrating that the high-resolution intra-annual tree-ring analysis successfully captured the signal of the COVID-19 pandemics.

A question remains, did this change impact tree development? Evidence for any change in the growth or development of the avenue trees is tenuous based on the measured parameters. It is not possible to estimate any change in the actual growth rate, but some insights could arise from the intra-annual wood density profiles. The wood density increase trend from earlywood to latewood has not been disrupted during any of the years studied, the COVID-19 years included. There is also no clear change in the synchrony per segment between avenue and park trees. The only subtle change lies in the intra-annual profile, which shows an average increasing wood density trend similar to other years in the avenue trees but at an apparently higher rate during 2020, reinforcing our first hypothesis. If this increase in wood density rate is associated with the changes in CO_2 emissions from vehicles, the literature highlights the role of lower CO_2 concentrations in reducing the water-use efficiency of trees, which requires an increase in stomatal conductance to cope with the carbon demand (Mathias and Thomas, 2021; Zhao et al., 2022). Higher stomatal conductance can decrease leaf water potential and increase water tension in the xylem. As a consequence, this condition is often associated with higher water stress, to which trees typically respond by increasing wood density (Balzano et al., 2020; McCulloh et al., 2012; Searson et al., 2004; Torresan et al., 2024). These observations from previous studies could explain the higher wood density increase, especially in the late growing season, when water availability drops significantly before the beginning of the dry season. These findings refute our fourth hypothesis.

5. Conclusion

This is the first study to employ high-resolution, state-of-the-art measurements of density and stable carbon isotopes at the intra-annual scale, the only likely approach capable of detecting changes in tree development during the COVID-19 social distancing and lockdowns. These high-resolution methods suggest possible changes in the atmospheric CO_2 signature during the most restrictive phase of the lockdowns in the city of São Paulo, which resulted in a significant reduction in vehicular emissions on the avenue. The lower emission of CO_2 depleted in the heavy carbon isotope likely increased the values of the intra-annual segments, from 12 to 15, of the tree ring corresponding to the year 2020 / 2021. This change cannot be attributed to climate and was not replicated in the park trees series, which showed the opposite trend in $\delta^{13}C$ values. Despite these results suggesting that avenue trees recorded the impact of the restrictions of vehicle circulation, the pieces of evidence of changes in the growth and development of the trees are still weak and inconclusive. The tree ring corresponding to the year 2020 / 2021 shows the usual increasing wood density from the earlywood to the latewood in semi-ring porous wood, like the one from *T. tipu* trees, but it shows a distinctive and higher rate of increasing values. If this change is indeed associated with lower emissions, it could represent an adjustment under lower atmospheric CO_2 concentrations and likely water-use efficiency. It pushes the hydraulic system's risk of stress, requiring higher wood density according to the literature. Thus, rather than air pollution *per se*, CO_2 emissions play a role in the trees growing alongside the busy avenues.

References

Andreu-Hayles, L., Tejedor, E., D'arrigo, R., Locosselli, G. M., Rodríguez-Catón, M., Daux, V., Oelkers, R., Pacheco-Solana, A., Paredes-Villanueva, K., & Rodríguez-Morata, C. (2023). Dendrochronological advances in the tropical and subtropical Americas: Research priorities and future directions. *Dendrochronologia*, *81*, 126124.

Anys, M., & Weiler, M. (2024). Rainfall interception by urban trees: Event characteristics and tree morphological traits. *Hydrological Processes*, 38(4), e15146.

Ballikaya, P., Song, W., Bachmann, O., Guillong, M., Wang, X., & Cherubini, P. (2023). Chemical elements recorded by Quercus mongolica Fisch. ex Ledeb. tree rings reveal trends of pollution history in Harbin, China. *Forests*, 14(2), 187.

Balzano, A., Battipaglia, G., Cherubini, P., & De Micco, V. (2020). Xylem plasticity in *Pinus pinaster* and *Quercus ilex* growing at sites with different water availability in the Mediterranean region: relations between intra-annual density fluctuations and environmental conditions. *Forests*, 11(4), 379.

Berland, A., Shiflett, S. A., Shuster, W. D., Garmestani, A. S., Goddard, H. C., Herrmann, D. L., & Hopton, M. E. (2017). The role of trees in urban stormwater management. *Landscape and urban planning*, 162, 167-177.

Brienen, R., Helle, G., Pons, T., Boom, A., Gloor, M., Groenendijk, P., Clerici, S., Leng, M., & Jones, C. (2022). Paired analysis of tree ring width and carbon isotopes indicates when controls on tropical tree growth change from light to water limitations. *Tree Physiology*, *42*(6), 1131-1148.

Camarero, J. J., Rubio-Cuadrado, Á., de Andrés, E. G., Valeriano, C., Sánchez, P., & Querejeta, J. I. (2025). A tale of two cities: Impacts of the COVID-19 lockdown on growth and wood chemistry of urban trees. *Science of The Total Environment*, 974, 179252.

Cattana, M.E., de los Ángeles Sosa, M., Fernández, M., Rojas, F., Mangiaterra, M., Giusiano, G. (2014). Native trees of the Northeast Argentine: Natural hosts of the *Cryptococcus neoformans–Cryptococcus gattii* species complex. *Revista iberoamericana de micología*, 31(3), 188-192.

Cernusak, L. A., Ubierna, N., Winter, K., Holtum, J. A., Marshall, J. D., & Farquhar, G. D. (2013). Environmental and physiological determinants of carbon isotope discrimination in terrestrial plants. *New Phytologist*, 200(4), 950-965.

Choi, W. J., & Lee, K. H. (2012). A short overview on linking annual tree ring carbon isotopes to historical changes in atmospheric environment. *Forest Science and Technology*, *8*(2), 61-66.

Cintra, B. B. L., Gloor, M., Boom, A., Schöngart, J., Locosselli, G. M., & Brienen, R. (2019). Contrasting controls on tree ring isotope variation for Amazon floodplain and terra firme trees. *Tree Physiology*, *39*(5), 845-860.

Coplen, T. B., & Wassenaar, L. I. (2015). LIMS for Lasers 2015 for achieving long-term accuracy and precision of $\delta^{2}H$, $\delta^{17}O$, and $\delta^{18}O$ of waters using laser absorption spectrometry. *Rapid Communications in Mass Spectrometry*, *29*(22), 2122-2130.

Dai, K. M., & Fan, C. (1986). Bomb produced ^{14}C content in tree rings grown at different latitudes. *Radiocarbon*, 28(2A), 346-349.

De Micco, V., Battipaglia, G., Brand, W. A., Linke, P., Saurer, M., Aronne, G., & Cherubini, P. (2012). Discrete versus continuous analysis of anatomical and $\delta^{13}C$ variability in tree rings with intra-annual density fluctuations. *Trees*, *26*, 513-524.

Esfehankalateh, A., Ngarambe, J., & Yun, G. Y. (2021). Influence of tree canopy coverage and leaf area density on urban heat island mitigation. *Sustainability*, 13(13), 7496.

Esperon-Rodriguez, M., Brookhouse, M., Power, S. A., Avi, D., Baer, T., Rymer, P. D., & Tjoelker, M. G. (2025). Urban Tree Growth and Drought Responses Show Evidence of Climate Resilience. *Global Change Biology*, 31(6), e70281.

Favillier, A., Guillet, S., Lopez-Saez, J., Giacona, F., Eckert, N., Zenhäusern, G., Peiry, J. L., Stoffel, M., & Corona, C. (2023). Identifying and interpreting regional signals in tree-ring based reconstructions of snow avalanche activity in the Goms valley (Swiss Alps). *Quaternary Science Reviews*, *307*, 108063.

Ferreira, A.T.B., Tomazello Filho, M. (2009). Characterization of tree-rings of *Pinus caribaea* var. *hondurensis* Barr. et Golf. trees by X-Ray densitometry. *Scientia Forestalis (Brazil)*, 37(83).

Godoy-Veiga, M., Cintra, B.B.L., Stríkis, N.M., Cruz, F.W., Grohmann, C.H., Santos, M.S., Regev, L., Boaretto, E., Ceccantini, G., Locosselli, G.M. (2021). The value of climate responses of individual trees to detect areas of climate-change refugia, a tree-ring study in the Brazilian seasonally dry tropical forests. *Forest ecology and management*, 488, 118971.

Groenendijk, P., van der Sleen, P., Vlam, M., Bunyavejchewin, S., Bongers, F., & Zuidema, P. A. (2015). No evidence for consistent long-term growth stimulation of 13 tropical tree species: Results from tree-ring analysis. *Global Change Biology*, 21(10), 3762–3776.

Horvatinčić, N., Krajcar Bronić, I., & Obelić, B. (2001). Influence of the 14C and 3H global atmospheric contamination on the karst region of Croatia. In *World Correlation of Karst Ecosystem Newsletters, IGCP Project* 448 (p. 76).

IBGE. Brazilian Institute of Geography and Statistics. Available online: https://cidades.ibge.gov.br/brasil/sp/sao-paulo/panorama (accessed on 12 June 2025).

Jevšenak, J., Buras, A., & Babst, F. (2024). Shifting potential for high-resolution climate reconstructions under global warming. *Quaternary Science Reviews*, 325, 108486.

Kagawa, A., Sano, M., Nakatsuka, T., Ikeda, T., Kubo, S., (2015). An optimized method for stable isotope analysis of tree rings by extracting cellulose from cross-sectional laths. *Chemical Geology*, 393–394, 16–25.

Köppen, W. (1931). *Grundriss der klimakunde*. Berlin, Germany: W.

Krecl, P., Targino, A. C., Oukawa, G. Y., & Junior, R. P. C. (2020). Drop in urban air pollution from COVID-19 pandemic: Policy implications for the megacity of São Paulo. *Environmental Pollution (Barking, Essex: 1987)*, 265, 114883.

Krepkowski, J., Gebrekirstos, A., Shibistova, O., & Bräuning, A. (2013). Stable carbon isotope labeling reveals different carry-over effects between functional types of tropical trees in an Ethiopian mountain forest. *New Phytologist*, *199*(2), 431-440.

Lehmann, M. M., Vitali, V., Schuler, P., Leuenberger, M., & Saurer, M. (2021). More than climate: hydrogen isotope ratios in tree rings as novel plant physiological indicator for stress conditions. *Dendrochronologia*, *65*, 125788.

Li, Y., Wang, Y., Wang, B., Wang, Y., & Yu, W. (2019). The response of plant photosynthesis and stomatal conductance to fine particulate matter (PM 2.5) based on leaf factors analyzing. *Journal of Plant Biology*, 62, 120-128.

Linden, J., Gustafsson, M., Uddling, J., Watne, Å., & Pleijel, H. (2023). Air pollution removal through deposition on urban vegetation: The importance of vegetation characteristics. *Urban Forestry & Urban Greening*, *81*, 127843.

Locosselli, G. M., & Buckeridge, M. S. (2017). Dendrobiochemistry, a missing link to further understand carbon allocation during growth and decline of trees. *Trees*, *31*(6), 1745-1758.

Locosselli, G. M., de Camargo, E. P., Moreira, T. C. L., Todesco, E., de Fátima Andrade, M., de André, C. D. S., André, P. F., Singer, J. M., Ferreira, L. S., Saldiva, P. H. N., & Buckeridge, M. S. (2019). The role of air pollution and climate on the growth of urban trees. *Science of the Total Environment*, *666*, 652-661.

Locosselli, G. M., Brienen, R. J., de Souza Martins, V. T., Gloor, E., Boom, A., de Camargo, E. P., Saldiva, P. H. N., & Buckeridge, M. S. (2020). Intra-annual oxygen isotopes in the tree rings record precipitation extremes and water reservoir levels in the Metropolitan Area of São Paulo, Brazil. *Science of the Total Environment*, *743*, 140798.

Locosselli, G. M., Cintra, B. B. L., Ferreira, L. S., da Silva-Luz, C. L., Miyahara, A. A. L., Brienen, R. J., Gloor, E., Boom, A., Grandis, A., & Buckeridge, M. S. (2024). Stress-tolerant trees for resilient cities: tree-ring analysis reveals species suitable for a future climate. *Urban Climate*, *55*, 101964.

Maher, B. A., Ahmed, I. A., Davison, B., Karloukovski, V., & Clarke, R. (2013). Impact of roadside tree lines on indoor concentrations of traffic-derived particulate matter. *Environmental science & technology*, 47(23), 13737-13744.

Margolis, E. Q., Guiterman, C. H., Chavardès, R. D., Coop, J. D., Copes-Gerbitz, K., Dawe, D. A., Falk, D. A., Johnston, J. D., Larson, E., Li, H., Marschall, J. M., Naficy, C. E., Naito, A. T., Parisien, M.-A., Parks, S. A., Portier, J., Pulos, H. M., Robertson, K. M., Speer, J. H., Stambaugh, M., Swetnam, T. W., Tepley, A. J., Thapa, I., Allen, C. D., Bergeron, Y., Daniels, L. D., Fulé, P. Z., Gervais, D., Girardin, M. P., Harley, G. L., Harvey, J. E., Hoffman, K. M., Huffman, J. M., Hurteau, M. D., Johnson, L. B., Lafon, C. W., Lopez, M. K., Maxwell, R. S., Meunier, J., North, M., Rother, M. T., Schmidt, M. R., Sherriff, R. L., Stachowiak, L. A., Taylor, A., Tayloer, E. J., Trouet, V., Villarreal, M. L., Yocom, L. L., Arabas, K. B., Arizpe, A. H., Arseneault, D., Tarancón, A. A., Baisan, C., Bigio, E., Biondi, F., Cahalan, G. D., Caprio, A., Cerano-Paredes, J., Collins, B. M., Dey, D. C., Drobyshev, I., Farris, C., Fenwick, M. A., Flatley, W., Floyd, M. L., Gedalof, Z., Holz, A., Howard, L. F., Huffman, D. W., Iniguez, J., Kipfmueller, K. F., Kitchen, S. G., Lombardo, K., McKenzie, D., Merschel, A. G., Metlen, K. L., Minor, J., O'Connor, C. D., Platt, L., Platt, W. J., Saladyga, T., Stan, A. B., Stephens, S., Sutheimer, C., Touchan, R., & Weisberg, P. J. (2022). The North American tree-ring fire-scar network. *Ecosphere*, *13*(7), e4159.

Mathias, J. M., & Thomas, R. B. (2021). Global tree intrinsic water use efficiency is enhanced by increased atmospheric CO_2 and modulated by climate and plant functional types. *Proceedings of the National Academy of Sciences*, 118(7), e2014286118.

Maxwell, R.S., Larsson, L.A. (2021). Measuring tree-ring widths using the CooRecorder software application. *Dendrochronologia*, 67, 125841.

McCarroll, D., & Loader, N. J. (2004). Stable isotopes in tree rings. *Quaternary Science Reviews*, *23*(7-8), 771-801.

McCulloh, K. A., Johnson, D. M., Meinzer, F. C., Voelker, S. L., Lachenbruch, B., & Domec, J. C. (2012). Hydraulic architecture of two species differing in wood density: Opposing strategies in co-occurring tropical pioneer trees. *Plant, cell & environment*, 35(1), 116-125.

SENATRAN. Nacional Traffic Secretariat, Ministry of Transport, Brazil (2024).

Miyahara, A. A. L., Paixão, C. P., dos Santos, D. R., Pagin-Cláudio, F., da Silva, G. J., Bertoleti, I. A. F., Lima, J. S., Silva, J. L., Candido, L. F., Siqueira, M. C., Silva, R. P., Racanelli, Y. R., & Locosselli, G. M. (2022). Urban dendrochronology toolkit for evidence-based decision-making on climate risk, cultural heritage, environmental pollution, and tree management–A systematic review. *Environmental Science & Policy*, *137*, 152-163.

Miyahara, A. A. L., & Locosselli, G. M. (2024). Challenges and advances in intra-annual tree-ring stable isotope research, a systematic review. *Dendrochronologia*, 126218.

Monaci, F., & Baroni, D. (2025). Leaves and Tree Rings as Biomonitoring Archives of Atmospheric Mercury Deposition: An Ecophysiological Perspective. *Plants*, 14(9), 1275.

Moreira, T. C., Amato-Lourenco, L. F., da Silva G. T., Saldiva de Andre, C. D., de Andre, P. A., Barrozo. L. V., Singe, J., Saldiva, P. H. N., Saiki, M., & Locosselli, G. M. (2018). The use of tree barks to monitor traffic related air pollution: a case study in São Paulo–Brazil. *Frontiers in Environmental Science,* 6, 72.

Moreno, R., Nery, A., Zamora, R., Lora, Á., & Galán, C. (2024). Contribution of urban trees to carbon sequestration and reduction of air pollutants in Lima, Peru. *Ecosystem Services*, 67, 101618.

Nabeshima, E., Nakatsuka, T., Kagawa, A., Hiura, T., & Funada, R. (2018). Seasonal changes of δD and $\delta^{18}O$ in tree-ring cellulose of *Quercus crispula* suggest a change in post-photosynthetic processes during earlywood growth. *Tree Physiology*, *38*(12), 1829-1840.

Nakada, L. Y. K., & Urban, R. C. (2020). COVID-19 pandemic: Impacts on the air quality during the partial lockdown in São Paulo state, Brazil. *Science of the Total Environment*, *730*, 139087.

Olson, E. J., Dodd, J. P., & Rivera, M. A. (2020). Prosopis sp. tree-ring oxygen and carbon isotope record of regional-scale hydroclimate variability during the last 9500 years in the Atacama Desert. *Palaeogeography, Palaeoclimatology, Palaeoecology*, *538*, 109408.

Pearson, C., Manning, S. W., Coleman, M., & Jarvis, K. (2005). Can tree-ring chemistry reveal absolute dates for past volcanic eruptions?. *Journal of Archaeological Science*, 32(8), 1265-1274.

Peel, J. L., Haeuber, R., Garcia, V., Russell, A. G., & Neas, L. (2013). Impact of nitrogen and climate change interactions on ambient air pollution and human health. *Biogeochemistry*, 114, 121-134.

Pompa-García, M., Vivar-Vivar, E.D., Hornink, B., Martínez-Rivas, J.A., Ortega-Rodriguez, D.R., Tomazello Filho, M. (2024). Tree-ring wood density reveals differentiated hydroclimatic interactions in species along a bioclimatic gradient. *Dendrochronologia*, 85, 126208.

Pozzer, A., Anenberg, S. C., Dey, S., Haines, A., Lelieveld, J., & Chowdhury, S. (2023). Mortality attributable to ambient air pollution: A review of global estimates. *GeoHealth*, 7(1), e2022GH000711.

Rinne, K. T., Saurer, M., Kirdyanov, A. V., Loader, N. J., Bryukhanova, M. V., Werner, R. A., & Siegwolf, R. T. W. (2015). The relationship between needle sugar carbon isotope ratios and tree rings of larch in Siberia. *Tree Physiology*, *35*(11), 1192-1205.

Rodriguez, D. R. O., Sánchez-Salguero, R., Hevia, A., Granato-Souza, D., Cintra, B. B., Hornink, B., Andreu-Hayes, L., Assis-Pereira, G., Roig, F. A., & Tomazello-Filho, M. (2023). Climate variability of the southern Amazon inferred by a multi-proxy tree-ring approach using Cedrela fissilis Vell. *Science of the Total Environment*, *871*, 162064.

Rodriguez-Caton, M., Andreu-Hayles, L., Morales, M. S., Daux, V., Christie, D. A., Coopman, R. E., Alvarez, C., Rao, M. P., Aliste, D., Flores, F., & Villalba, R. (2021). Different climate sensitivity for radial growth, but uniform for tree-ring stable isotopes along an aridity gradient in Polylepis tarapacana, the world's highest elevation tree species. *Tree Physiology*, *41*(8), 1353-1371.

Sannigrahi, S., Kumar, P., Molter, A., Zhang, Q., Basu, B., Basu, A. S., & Pilla, F. (2021). Examining the status of improved air quality in world cities due to COVID-19 led temporary reduction in anthropogenic emissions. *Environmental research*, *196*, 110927.

Sarris, D., Siegwolf, R., & Körner, C. (2013). Inter-and intra-annual stable carbon and oxygen isotope signals in response to drought in Mediterranean pines. *Agricultural and Forest Meteorology*, *168*, 59-68.

Saurer, M., Sahlstedt, E., Rinne-Garmston, K. T., Lehmann, M. M., Oettli, M., Gessler, A., & Treydte, K. (2023). Progress in high-resolution isotope-ratio analysis of tree rings using laser ablation. *Tree physiology*, *43*(5), 694-705.

Savard, M. M. (2010). Tree-ring stable isotopes and historical perspectives on pollution–An overview. *Environmental Pollution*, *158*(6), 2007-2013.

Savo, V., D'Amato, L., Bartoli, F., Zappitelli, I., & Caneva, G. (2025). Evaluation of main regulating, provisioning, and supporting ecosystem services of urban street trees: A literature review. *Ecosystem Services*, 71, 101690.

Schollaen, K., Baschek, H., Heirinch, I., Helle, G., 2015. Technical note: an improved guideline for rapid and precise sample preparation of tree-ring stable isotope analysis. *Biogeosciences*. 12, 11587–11623.

Schulman, E. (1956). Dendroclimatic changes in semiarid America.

Searson, M. J., Thomas, D. S., Montagu, K. D., & Conroy, J. P. (2004). Wood density and anatomy of water-limited eucalypts. *Tree physiology*, 24(11), 1295-1302.

Siciliano, B., Carvalho, G., da Silva, C. M., & Arbilla, G. (2020). The impact of COVID-19 partial lockdown on primary pollutant concentrations in the atmosphere of Rio de Janeiro and São Paulo Megacities (Brazil). *Bulletin of Environmental Contamination and Toxicology*, *105*, 2-8.

Shekanino, A., Agustin, A., Aladefa, A., Amezquita, J., Gonzalez, D., Heldenbrand, E., Hernandez, A., May, M., Nuno, A., Ojeda, J., Ortiz, A., Puno, T., Quinones, J., Remillard, J., Reola, J., Rojo, J., Solis, I., Wang, J., Yepez, A., Zaragoza, C., & Carmona-Galindo, V. D. (2023). Differential stomatal responses to surface permeability by sympatric urban tree species advance novel mitigation strategy for urban heat islands. *Sustainability*, *15*(15), 11942.

Silva, L. C. R., & Anand, M. (2013). Probing for the influence of atmospheric CO_2 and climate change on forest ecosystems across biomes. *Global Ecology and Biogeography*, 22(1), 83–92.

SMUL/SP. Municipal Secretariat of Urban Planning and Licensing of the City of São Paulo São Paulo - Production and Information Analysis Coordination - Geoinfo (2023).

Sofia, D., Gioiella, F., Lotrecchiano, N., & Giuliano, A. (2020). Mitigation strategies for reducing air pollution. *Environmental Science and Pollution Research*, 27(16), 19226-19235.

Tan, Z., Lau, K. K. L., & Ng, E. (2016). Urban tree design approaches for mitigating daytime urban heat island effects in a high-density urban environment. *Energy and Buildings*, 114, 265-274.

Tans, P. P., & Mook, W. G. (1980). Past atmospheric CO_2 levels and the $^{13}C/^{12}C$ ratios in tree rings. *Tellus*, *32*(3), 268-283.

Torresan, C., Hilmers, T., Avdagić, A., Di Giuseppe, E., Klopčič, M., Lévesque, M., Motte, F., Uhl, E., Zlatanov, T., Pretzsch, H. (2024). Changes in tree-ring wood density of European beech (*Fagus sylvatica* L.), silver fir (*Abies alba* Mill.), and Norway spruce (*Picea abies* (L.) H. Karst.) in European mountain forests between 1901 and 2016. *Annals of Forest Science*, 81(1), 49.

United Nations, Department of Economic and Social Affairs, Population Division (2018). *The world's cities in 2018* – Data Booklet (ST/ESA SER.A/417).

Van Der Sleen, P., Groenendijk, P., Vlam, M., Anten, N. P. R., Boom, A., Bongers, F., Pons, T. L., Terburg, G., & Zuidema, P. A. (2015). No growth stimulation of tropical trees by 150 years of CO_2 fertilization but water-use efficiency increased. *Nature Geoscience*, 8(1), 24–28.

Varella, R. A., Duarte, G., Baptista, P., Villafuerte, P. M., & Sousa, L. (2017). Analysis of the influence of outdoor temperature in vehicle cold-start operation following EU real driving emission test procedure. *SAE International Journal of Commercial Vehicles*, *10*(2017-24-0140), 596-697.

von Glasow, R., Bobrowski, N., & Kern, C. (2009). The effects of volcanic eruptions on atmospheric chemistry. *Chemical Geology*, 263(1-4), 131-142.

Wang, M., Qin, M., Xu, P., Huang, D., Jin, X., Chen, J., Dong, D., & Ren, Y. (2024). Atmospheric particulate matter retention capacity of bark and leaves of urban tree species. *Environmental Pollution*, *342*, 123109.

Winner, W. E., & Atkinson, C. J. (1986). Absorption of air pollution by plants, and consequences for growth. *Trends in Ecology & Evolution*, *1*(1), 15-18.

Worbes, M. (1995). How to measure growth dynamics in tropical trees a review. *IAWA journal, 16(4), 337-351.*

World Health Organization. (2024). *World health statistics 2024: monitoring health for the SDGs, sustainable development goals*. World Health Organization.

Xing-Yun, Z., Jun-Long, Q., Jian, W., Qing-Yan, H., Zu-Liang, W., & Cheng-Zhong, C. (2006). Using a tree ring $\delta^{13}C$ annual series to reconstruct atmospheric CO_2 concentration over the past 300 years. *Pedosphere*, 16(3), 371-379.

Yakir, D. (2011). The paper trail of the 13C of atmospheric CO_2 since the industrial revolution period. *Environmental Research Letters*, 6(3), 034007.

Zeng, X., Liu, X., Treydte, K., Evans, M. N., Wang, W., An, W., Sun, W., Xu, G., Wu, G., & Zhang, X. (2017). Climate signals in tree-ring δ18O and δ13C from southeastern Tibet: insights from observations and forward modelling of intra-to interdecadal variability. *New Phytologist*, *216*(4), 1104-1118.

Zhang, R., Zhang, Y., Lin, H., Feng, X., Fu, T. M., & Wang, Y. (2020). NOx emission reduction and recovery during COVID-19 in East China. *Atmosphere*, 11(4), 433.

Zhang, W., Li, Y., Wang, Q., Zhang, T., Meng, H., Gong, J., & Zhang, Z. (2022). Particulate matter and trace metal retention capacities of six tree species: implications for improving urban air quality. *Sustainability*, 14(20), 13374.

Zhang, R., Hu, Z., Cherubini, P., Cooper, D. J., Zhu, L., & Lei, P. (2023). Tree-ring data reveal trees are suffering from severe drought stress in the humid subtropical forest. *Forest Ecology and Management*, 546, 121330.

Zhao, X., Guo, P., Yang, Y., & Peng, H. (2021). Effects of air pollution on physiological traits of *Ligustrum lucidum* Ait. leaves in Luoyang, China. *Environmental monitoring and assessment*, 193, 1-14.

Zhao, F., Wu, Y., Ma, S., Lei, X., & Liao, W. (2022). Increased water use efficiency in China and its drivers during 2000–2016. *Ecosystems*, 1-17.

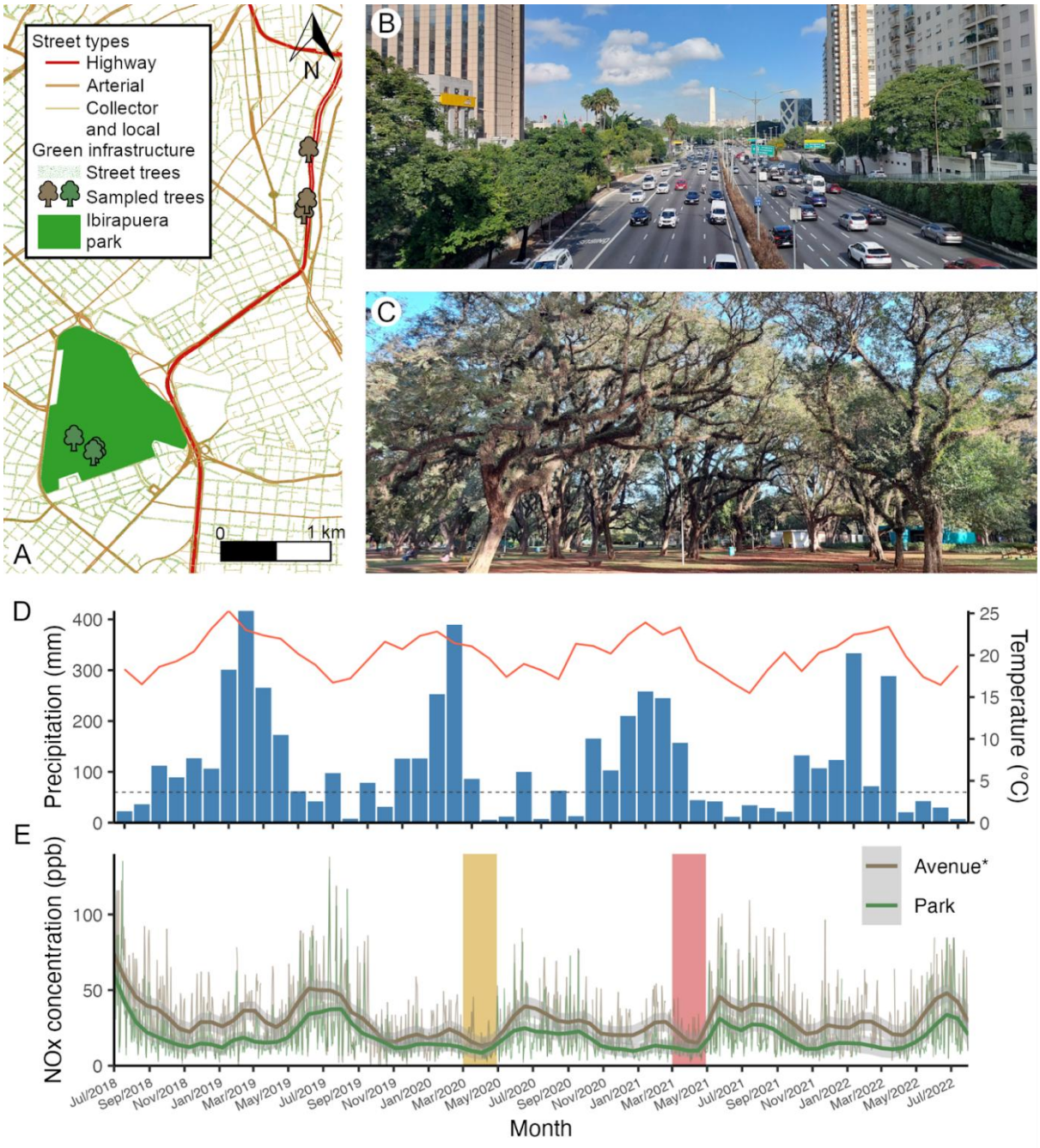

Figure 1: (A) Sampling sites in the city of São Paulo, (B) the 23rd of May Avenue, part of the North-South axis of the city, and (C) the Ibirapuera Park. (D) The monthly total precipitation and mean temperature of the sample sites, characterized by the Vila Mariana Station from the Emergency Management Center of São Paulo (CGE-SP), from the second semester of 2018 to the first semester of 2022. (E) The daily mean values of NOx air pollution during the four years analysed in this study. The yellow and red shaded areas represent the two main lockdowns and the most restrictive social distancing in the city. The LOESS smoothing curves represent the NOx trends in an Avenue *similar to that where the study took place, and the park trends are from data collected within the Ibirapuera park, both by the Environmental Company of the State of São Paulo (CETESB).

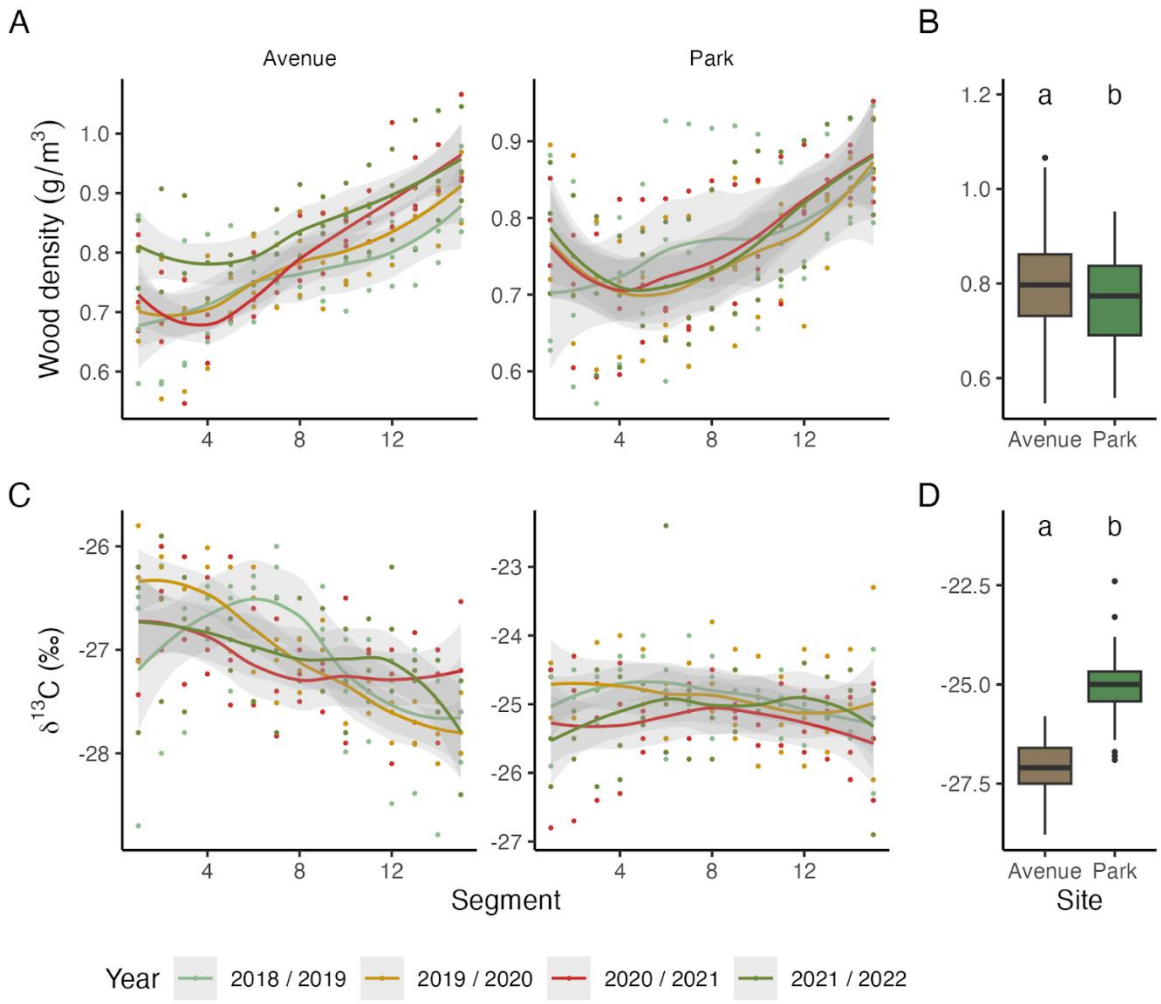

Figure 2: (A) Wood density and (C) stable carbon isotopes profiles represented by the LOESS smoothing curves along the 15 tree-ring segments for the four growing seasons. (B, D) Box plots representing the differences in wood density and stable carbon isotopes between the avenue and the park trees; different letters indicate a significant difference between sites according to the Student's T-test.

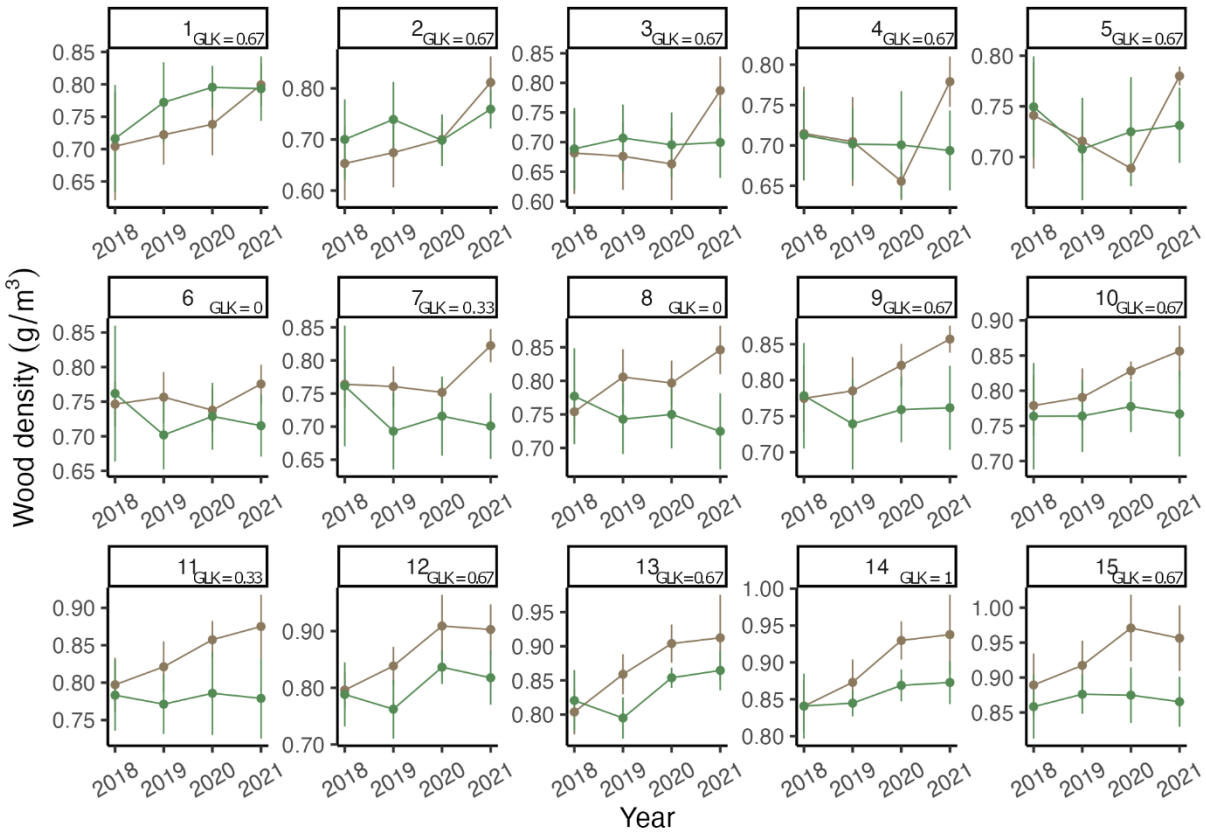

Figure 3: Average wood density series by segment in the tree rings of the trees from the avenue and the park. GLK values are a measure of synchrony between the two series. Bars represent the standard error.

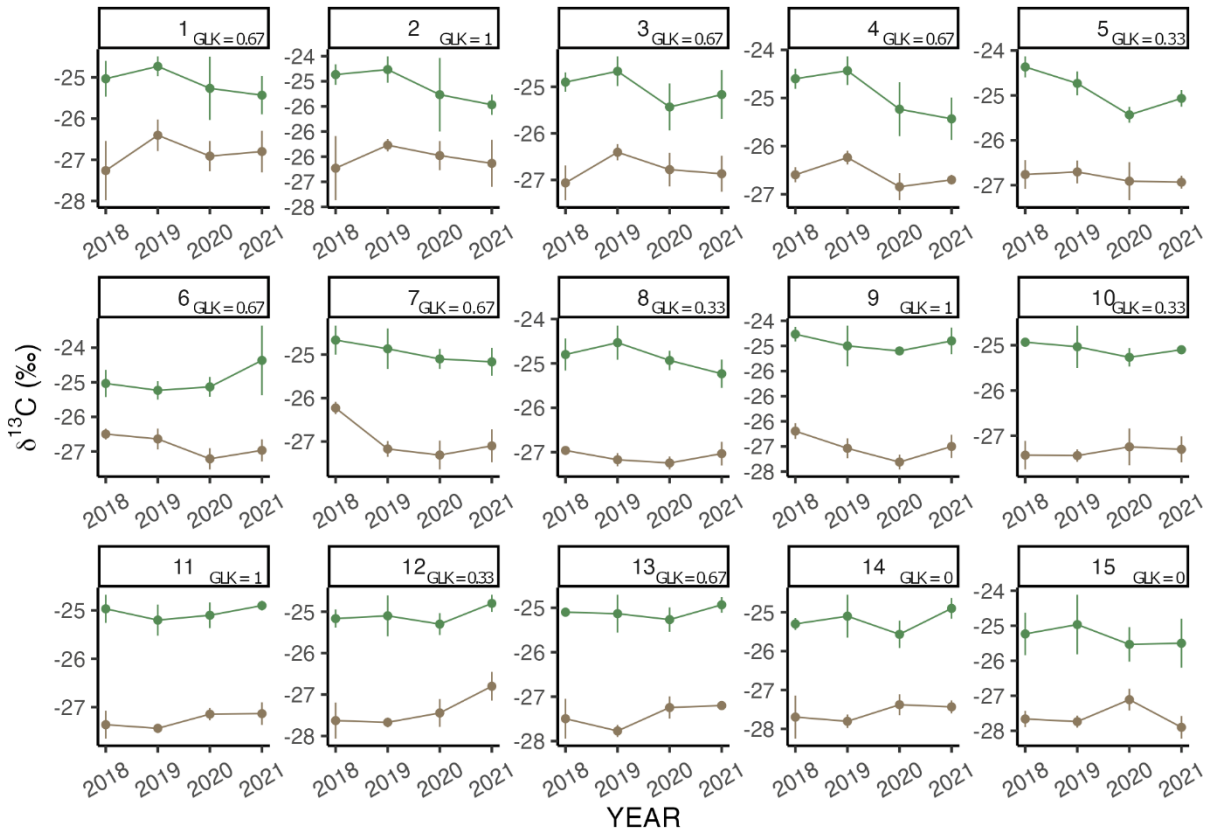

Figure 4: Average stable carbon isotope series by segment in the tree rings of the trees from the avenue and the park. GLK values are a measure of synchrony between the two series. Bars represent the standard error.

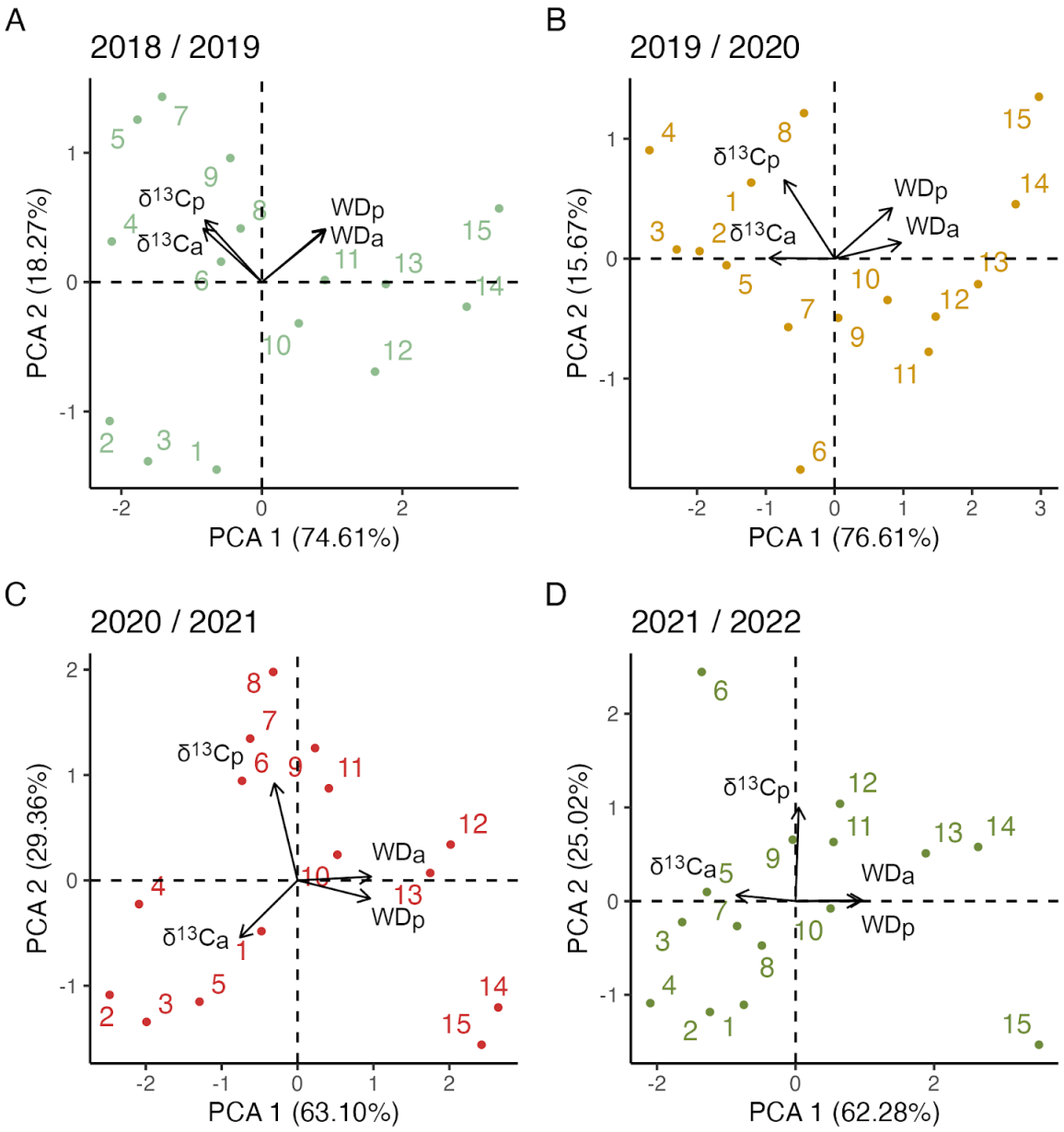

Figure 5: Principal component analysis of the carbon isotopes and wood density in the segments of the tree rings in the avenue ($\delta^{13}C_a$ and WD_a) and the park ($\delta^{13}C_p$ and WD_p) for the target growing seasons (A) before the pandemic, (B, C) during the pandemic, and (D) after the pandemic. Point labels represent each intra-annual segment, 1 as the first segment in earlywood, and 15 as the last one in latewood. Biplots represent the variability for each analysed growth year. See tables S2 to S5 to access the eigenvectors.

Supplementary Material

Table S1: Characteristics of all sampled trees. *Selected trees for wood density and $\delta^{13}C$ analyses.

ID	Coordinates	DBH (cm)	Sample site
aalm86	-23.5719; -46.6407	59.84	Avenue
aalm87	-23.5718; -46.6408	43.61	Avenue
aalm88	-23.5703; -46.6411	49.34	Avenue
aalm89	-23.5702; -46.6411	107.59	Avenue
aalm90*	-23.5699; -46.6413	67.80	Avenue
aalm91	-23.5640; -46.6404	64.30	Avenue
aalm92	-23.5638; -46.6406	76.39	Avenue
aalm93*	-23.5644; -46.6408	67.80	Avenue
aalm94	-23.5646; -46.6408	46.15	Avenue
aalm95	-23.5645; -46.6408	47.75	Avenue
aalm96	-23.5692; -46.6411	39.79	Avenue
aalm97*	-23.5690; -46.6410	69.07	Avenue
aalm76	-23.5910; -46.6601	63.66	Park
aalm77	-23.5915; -46.6600	73.85	Park
aalm78	-23.5912; -46.6603	87.53	Park
aalm79	-23.5912; -46.6510	87.53	Park
aalm80	-23.5912; -46.6601	76.71	Park
aalm81	-23.5913; -46.6599	44.24	Park
aalm82*	-23.5912; -46.6598	67.48	Park
aalm83*	-23.5915; -46.6601	68.12	Park
aalm84*	-23.5902; -46.6618	50.29	Park
aalm85	-23.5901; -46.6616	58.57	Park
aalm98	-23.5916; -46.6568	64.62	Park
aalm99	-23.5916; -46.6568	49.66	Park
aalm100	-23.5918; -46.6568	40.42	Park
aalm101	-23.5917; -46.6567	42.02	Park
aalm102	-23.5917; -46.6568	43.61	Park
aalm103	-23.5917; -46.6569	36.92	Park

Table S2: Eigenvectors of the PCA for the 2018 / 2019 growing season.

	PCA1	PCA2	PCA3	PCA4
WD_a	0.90	0.41	-0.03	-0.12
$\delta^{13}C_a$	-0.83	0.41	0.36	-0.01
WD_p	0.90	0.40	0.06	0.12
$\delta^{13}C_p$	-0.81	0.48	-0.34	0.01

Table S3: Eigenvectors of the PCA for the 2019 / 2020 growing season.

	PCA1	PCA2	PCA3	PCA4
WD_a	0.96	0.13	-0.15	0.16
$\delta^{13}C_a$	-0.95	0.004	0.30	0.13
WD_p	0.84	0.42	0.34	-0.04
$\delta^{13}C_p$	-0.73	0.65	-0.19	-0.006

Table S4: Eigenvectors of the PCA for the 2020 / 2021 growing season.

	PCA1	PCA2	PCA3	PCA4
WD_a	0.97	0.03	0.18	-0.15
$\delta^{13}C_a$	-0.76	-0.54	0.36	-0.01
WD_p	0.96	-0.17	0.18	0.15
$\delta^{13}C_p$	-0.30	0.92	0.24	0.03

Table S5: Eigenvectors of the PCA for the 2021 / 2022 growing season.

	PCA1	PCA2	PCA3	PCA4
WD_a	0.96	0.008	0.11	0.24
$\delta^{13}C_a$	-0.85	0.06	0.51	0.08
WD_p	0.91	-0.0006	0.37	-0.18
$\delta^{13}C_p$	0.05	0.10	-0.03	-0.007

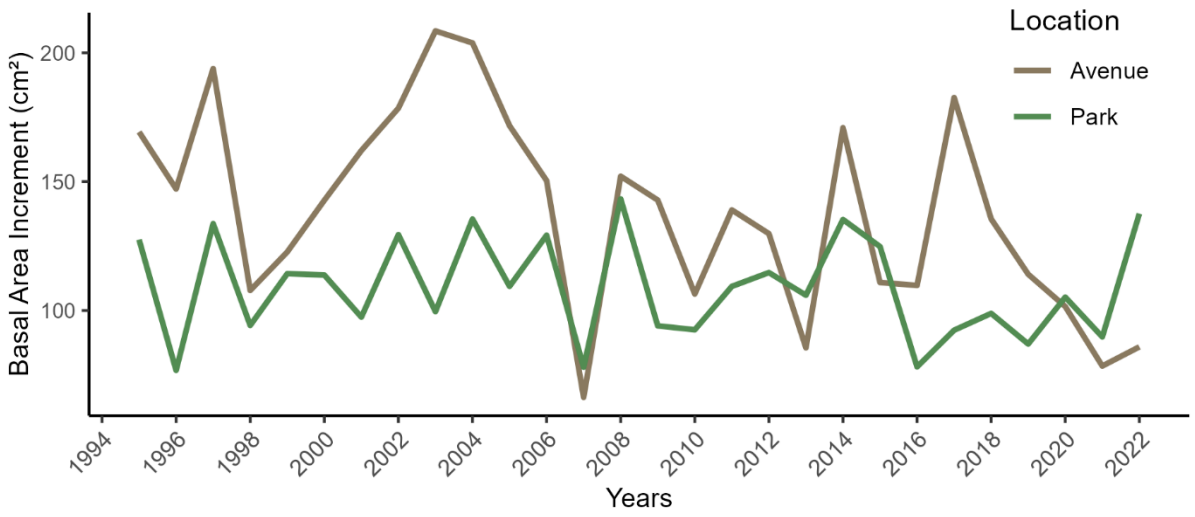

Figure S1: Mean basal area increment trends for the target trees from the 23rd of May Avenue and the Ibirapuera Park.

Discussão geral

A implementação de infraestruturas verdes e a promoção da biodiversidade ocupam posição de destaque nas estratégias de planejamento urbano voltadas para soluções baseadas na natureza. Essa estratégia busca resolver problemas ambientais, sociais e econômicos por meio de ações que incorporam elementos naturais, como as árvores, oferecendo grande potencial para a adaptação das cidades às mudanças climáticas globais. Contudo, tanto a seleção de espécies para compor a biodiversidade urbana quanto a avaliação das práticas de manejo dessas árvores demandam suporte técnico e científico, a fim de garantir a eficácia das soluções baseadas na natureza. Atualmente, as principais discussões sobre a seleção de espécies concentram-se na escolha entre nativas ou exóticas. Um dos argumentos mais frequentes é que as espécies nativas estariam mais bem adaptadas às condições ambientais locais. Entretanto, os ambientes urbanos passaram por intensas modificações na paisagem em função do uso e ocupação do solo decorrentes da atividade antrópica. Dessa forma, o planejamento das florestas urbanas deve ser integrado e adaptado à realidade de cada cidade, considerando a sua heterogeneidade ambiental.

Sistemas de classificação do ambiente urbano, como os Biotopos, já foram desenvolvidos em trabalhos anteriores (*e.g.* Sukkop & Weiler, 1988; Stewart et al., 2009; Yilmaz et al., 2010). O desenvolvimento desse conceito foi essencial para o avanço no conhecimento, mas é um sistema de classificação limitado apenas às características da estrutura da vegetação, que desconsidera a ampla variação climática dentro das cidades (Steenberg et al., 2015). O desenvolvimento de "biomas urbanos" representa um passo significativo ao integrar clima e vegetação, levando em consideração a heterogeneidade ambiental urbana (Miyahara et al., 2022a). Porém, a biodiversidade urbana também é composta por espécies exóticas que foram implementadas e, ao longo de décadas, vêm se naturalizando. Portanto, a escolha das espécies para a implementação de soluções baseadas na natureza em cidades deve ser baseada em evidências, para que tragam benefícios à população de forma eficiente, bem como tenham resiliência ao ambiente urbano.

O primeiro capítulo desta tese propôs um método para classificar a heterogeneidade ambiental do ambiente urbano, visando auxiliar na escolha de espécies adequadas para a arborização urbana. Foi construído um modelo de classificação, utilizando uma Análise Discriminante Linear que resultou em um modelo com 80% de acurácia, baseada em dados de clima e cobertura vegetal. Como resultado, a cidade de São Paulo foi classificada em quatro biomas urbanos, cujas condições encontram correspondência aos seguintes biomas naturais: Mata Atlântica, Mata Atlântica Sazonalmente Inundada, Cerrado, e Cerrado Sazonalmente Inundado.

Considerando que a provisão de serviços ecossistêmicos pelas árvores está diretamente associada ao seu bom desempenho (Moser-Reischl et al., 2019; Rahman et al., 2015), a escolha de espécies arbóreas eficientes para mitigar os efeitos das mudanças climáticas globais não precisa, necessariamente, restringir-se às espécies do bioma natural originalmente encontrado na área ocupada pela cidade de São Paulo, como por exemplo a Mata Atlântica. Os resultados obtidos no primeiro capítulo desta tese geraram conhecimento significativo para apoiar o poder público local na seleção de espécies adequadas para implementar em infraestruturas verdes da cidade (Miyahara et al., 2022a).

Além da escolha das espécies, é essencial desenvolver ferramentas que possibilitem avaliar o desempenho das árvores urbanas e verificar, com base em evidências, sua eficácia na provisão de serviços ecossistêmicos à população. Um campo de estudo com potencial para apoiar tomadores de decisões nas cidades, especialmente no planejamento e manejo da arborização urbana, é a dendrocronologia (Miyahara et al., 2022b). Estudar os anéis de crescimento, que são formados anualmente na madeira de algumas espécies, proporciona conhecimento preciso tanto sobre a árvore quanto sobre o ambiente em que está inserida. Os anéis de crescimento são registros históricos anuais, por exemplo, das respostas fisiológicas das árvores, das tendências de crescimento, e das condições ambientais e climáticas, tornando as árvores potenciais ferramentas vivas de monitoramento (Godoy-Veiga et al., 2021). Entre as aplicações já consolidadas da dendrocronologia em escala anual, destacam-se a reconstrução da temperatura e demonstração do atual aquecimento global (Mann et al., 1999), os registros de escassez hídrica (Morales et al., 2020; Stahle et al., 2016), o desenvolvimento de métodos sustentáveis para colheita de madeira em florestas tropicais (Schöngart, 2008), a avaliação de impactos urbanos em ecossistemas naturais (Resende et al., 2020), e o acesso a heranças culturais e transformações sociais (Andrade et al., 2019; Edvardsson et al., 2021).

A dendrocronologia também já foi aplicada a nível subanual, por meio do seccionamento transversal de cada anel de crescimento em múltiplas partes, o que permite aumentar a resolução temporal do estudo. A abordagem subanual, além de possibilitar a identificação de sinais climáticos mais fortes (Xu et al., 2016), contribui com a compreensão de sistemas climáticos complexos, como as monções asiáticas – permitindo identificar o volume de precipitação e origem da formação das chuvas (*e.g.* Muangsong et al., 2020; Wei et al., 2018) – ou do sistema desértico do Atacama durante o período Holoceno (*e.g.* Olson et al., 2020). Outras aplicações subanuais incluem a análise das respostas das árvores a anos secos e úmidos (Battipaglia et al., 2010), a comparação entre árvores saudáveis e em declínio (Michelot-Antalik et al., 2019), e o estudo da alocação e mobilização de reservas durante a estação de crescimento (Roden et al.,

2022). Ainda, a abordagem intra-anual é especialmente adequada para identificar os efeitos de práticas de manejo e de variações ambientais de curta duração no desenvolvimento das árvores. Visando avaliar o estado da arte no uso de informações a nível intra-anual, o segundo capítulo desta tese consistiu em uma revisão sistemática sobre a análises intra-anuais de isótopos estáveis. Foram revisados 132 artigos científicos, que demonstraram o surgimento dessa abordagem na década de 1970. Apesar da concentração de estudos no hemisfério norte (nos países mais desenvolvidos) devido à prevalência de espécies que formam anéis de crescimento e o alto custo associado à essa metodologia, a técnica intra-anual com isótopos estáveis demonstra ser eficaz para trazer novas evidências sobre as condições ambientais e as respostas fisiológicas das árvores a eventos de curta duração.

Além das aplicações já consolidadas, a dendrocronologia também apresenta potencial para avaliar o desempenho das infraestruturas verdes urbanas, permitindo investigar sua eficácia na provisão de serviços ecossistêmicos. A irrigação, por exemplo, é uma prática de manejo amplamente utilizada para promover o desenvolvimento de árvores urbanas (Livesley et al., 2021; Rambhia et al., 2023), pois favorece o funcionamento do sistema hidráulico e contribui para a manutenção das taxas de evapotranspiração e assimilação, promovendo o crescimento das árvores (Ibsen et al., 2023; López et al., 2021). No entanto, há evidências de que esse crescimento acentuado pode estar associado a reduções na densidade da madeira (Arsić et al., 2021; Medina et al., 2024), o que pode resultar em maior susceptibilidade a falhas mecânicas e infestação por patógenos (Niklas & Spatz, 2010; van Duong et al., 2023). A análise dos anéis de crescimento, por meio de uma abordagem *multiproxy*, é uma ferramenta robusta para trazer evidências sobre os impactos da irrigação no desenvolvimento de árvores, seja comparando o período anterior e posterior à irrigação, seja comparando árvores irrigadas e não irrigadas sob as mesmas condições climáticas em um mesmo local. Essa temática foi abordada no terceiro capítulo desta tese, no qual foram analisados a densidade da madeira e os isótopos estáveis de carbono e oxigênio, para verificar os efeitos da irrigação contínua em uma espécie de árvore tolerante à seca. A espécie estudada, *Tipuana tipu*, é protagonista na arborização urbana de muitas cidades do mundo. Em Lisboa (Portugal) foram encontrados indivíduos desta espécie em condições ideais para testar o efeito da irrigação. A pedido das autoridades locais, o estudo foi conduzido para fornecer evidências científicas sobre os impactos dessa prática de manejo no crescimento e nas respostas fisiológicas das árvores. Os resultados demonstraram que o suprimento hídrico promoveu o crescimento das árvores, principalmente devido ao aumento na condutância estomática, sem comprometer a densidade da madeira. Este estudo trouxe evidências concretas sobre o benefício da irrigação para a espécie *T. tipu*, destacando o potencial

da dendrocronologia como ferramenta de apoio à tomada de decisões sobre o manejo de infraestruturas verdes nas cidades.

Outro potencial de aplicação da dendrocronologia é a avaliação dos impactos da poluição atmosférica no desenvolvimento das árvores. A poluição do ar é um problema recorrente em áreas urbanas, afetando tanto a vegetação quanto a saúde humana. No entanto, a maioria dos estudos com anéis de crescimento sobre a poluição do ar concentram-se em análises de longo prazo, como investigações sobre os períodos após a revolução industrial (Graven et al., 2020; Yakir, 2011), ou em experimentos conduzidos sob condições controladas em laboratório (Chaudhary and Rathore, 2021; Han et al., 2022; Mukherjee et al., 2025). Esses enfoques, embora relevantes, limitam a compreensão dos efeitos de variações pontuais e abruptas na qualidade do ar em cenários urbanos reais. As restrições sociais impostas pela pandemia do COVID-19, por exemplo, configuram um evento global singular que resultou em reduções pontuais da poluição atmosférica, oferecendo uma oportunidade única para avaliar seus efeitos no desenvolvimento das árvores. Nesse contexto, a análise intra-anual de alta resolução dos anéis de crescimento emerge como uma ferramenta essencial para acessar os impactos da intensa e pontual redução de poluentes atmosféricos durante os *lockdowns* da pandemia do COVID-19 sobre as árvores. Demonstramos que durante os *lockdowns*, a redução do fluxo de automóveis reduziu a concentração de $^{12}CO_2$ atmosférico, registrado como um aumento significativo no $\delta^{13}C$ dos segmentos intra-anuais das árvores da Avenida 23 de maio, em São Paulo. Apesar de ainda não serem conclusivas, as análises de crescimento indicam alterações no perfil de densidade intra-anual que podem refletir um ajuste na eficiência do uso da água em resposta à redução das concentrações atmosféricas de CO_2. A abordagem *multiproxy* com alta resolução intra-anual, adotada no quarto capítulo desta tese, permitiu identificar as respostas fisiológicas das árvores a essas variações abruptas na qualidade do ar, fornecendo evidências sobre os efeitos da flutuação da composição atmosférica na vegetação urbana.

Conclusão geral

Esta tese contribuiu para o enriquecimento do conhecimento científico que oferece suporte ao planejamento e manejo das infraestruturas verdes urbanas, com ênfase na arborização como uma das principais ferramentas para adaptar as cidades frente às mudanças climáticas globais. Foi proposto um novo modelo de classificação de ambientes urbanos, que integra variáveis climáticas e de estruturas de vegetação, oferecendo suporte teórico para uma seleção mais criteriosa das espécies arbóreas, considerando a heterogeneidade ambiental das cidades. Essa abordagem amplia o debate sobre a seleção de espécies, superando a dicotomia entre nativas e exóticas, direcionando as decisões para contextos urbanos específicos.

O desenvolvimento de uma revisão sistemática focada na dendrocronologia em escala intra-anual, especificamente com análises de isótopos estáveis, compilou os avanços e lacunas atuais nessa área. Esse conhecimento proporcionou um panorama atualizado do estado da arte dessa abordagem, apontando para as principais perspectivas metodológicas, das quais algumas foram exploradas e desenvolvidas ao longo desta tese.

A dendrocronologia foi destacada como uma potencial ferramenta para monitorar o desempenho das árvores urbanas e avaliar a eficácia das infraestruturas verdes na provisão de serviços ecossistêmicos. Ao explorar a formação dos anéis de crescimento utilizando uma abordagem *multiproxy*, demonstrou-se que práticas de manejo, como a irrigação, podem promover significativamente o crescimento de árvores urbanas, sem comprometer, no caso estudado, a resistência da madeira. Esta evidência contribuiu com o poder público sobre a eficiência de suas práticas de manejo da arborização urbana.

O potencial da dendrocronologia foi expandido ao nível subanual para investigar os efeitos de eventos de curta duração sobre o funcionamento das árvores. A pandemia do COVID-19 proporcionou uma oportunidade ímpar para observar, em um cenário urbano real, como as variações abruptas na qualidade do ar - resultantes das restrições sociais impostas para conter a disseminação do Coronavírus - podem ser detectadas nos anéis de crescimento. A aplicação de tecnologias de alta resolução, como a análise de isótopos estáveis de carbono por ablação a laser, mostrou-se essencial para acessar essas respostas fisiológicas sutis, muitas vezes imperceptíveis em abordagens de menor resolução espaço-temporal.

De forma integrada, os resultados obtidos reforçam a relevância de utilizar metodologias inovadoras e promissoras para compreender o desenvolvimento das árvores urbanas em diferentes escalas temporais, e sob diferentes condições ambientais. Esse conhecimento gerado é relevante e com potencial para subsidiar políticas públicas e estratégias de implementação e

manejo de infraestruturas verdes eficazes, contribuindo com a resiliência e adaptação das cidades frente às mudanças climáticas globais.

Bibliografia

Andrade, C. V. L., Flores, B. M., Levis, C., Clement, C. R., Roberts, P., & Schöngart, J. (2019). Growth rings of Brazil nut trees (*Bertholletia excelsa*) as a living record of historical human disturbance in Central Amazonia. *PLoS One*, 14(4), e0214128.

Arsić, J., Stojanović, M., Petrovičová, L., Noyer, E., Milanović, S., Světlík, J., Horáček. P., & Krejza, J. (2021). Increased wood biomass growth is associated with lower wood density in *Quercus petraea* (Matt.) Liebl. saplings growing under elevated CO_2. *PloS One*, 16(10).

Battipaglia, G., De Micco, V., Brand, W. A., Linke, P., Aronne, G., Saurer, M., & Cherubini, P. (2010). Variations of vessel diameter and $\delta^{13}C$ in false rings of *Arbutus unedo* L. reflect different environmental conditions. *New Phytologist*, 188(4), 1099-1112.

Chaudhary, I. J., & Rathore, D. (2021). Assessment of dose–response relationship between ozone dose and groundnut (*Arachis hypogaea* L.) cultivars using Open Top Chamber (OTC) and Ethylenediurea (EDU). *Environmental Technology & Innovation*, 22, 101494.

Edvardsson, J., Almevik, G., Lindblad, L., Linderson, H., & Melin, K. M. (2021). How cultural heritage studies based on dendrochronology can be improved through two-way communication. *Forests*, 12(8), 1047.

Godoy-Veiga, M., Cintra, B.B.L., Stríkis, N.M., Cruz, F.W., Grohmann, C.H., Santos, M.S., Regev, L., Boaretto, E., Ceccantini, G., Locosselli, G.M. (2021). The value of climate responses of individual trees to detect areas of climate-change refugia, a tree-ring study in the Brazilian seasonally dry tropical forests. *Forest ecology and management*, 488, 118971.

Graven, H., Keeling, R. F., & Rogelj, J. (2020). Changes to carbon isotopes in atmospheric CO_2 over the industrial era and into the future. *Global biogeochemical cycles*, 34(11), e2019GB006170.

Han, Y., Lee, J., Haiping, G., Kim, K. H., Wanxi, P., Bhardwaj, N., Oh, J. M. & Brown, R. J. (2022). Plant-based remediation of air pollution: a review. *Journal of Environmental Management*, 301, 113860.

Ibsen, P. C., Santiago, L. S., Shiflett, S. A., Chandler, M., & Jenerette, G. D. (2023). Irrigated urban trees exhibit greater functional trait plasticity compared to natural stands. *Biology Letters*, 19(1), 20220448.

Livesley, S. J., Marchionni, V., Cheung, P. K., Daly, E., & Pataki, D. E. (2021). Water smart cities increase irrigation to provide cool refuge in a climate crisis. *Earth's Future*, 9(1), e2020EF001806.

López, J., Way, D. A., & Sadok, W. (2021). Systemic effects of rising atmospheric vapor pressure deficit on plant physiology and productivity. *Global Change Biology*, 27(9), 1704–1720.

Mann, M. E., Bradley, R. S., & Hughes, M. K. (1999). Northern hemisphere temperatures during the past millennium: Inferences, uncertainties, and limitations. *Geophysical research letters*, 26(6), 759-762.

Medina, M., Flores, M. P., Ritter, L. J., Goya, J. F., Campanello, P. I., & Arturi, M. F. (2024). Wood density and leaf traits independently relate to growth rate of naturally regenerated tree species in *Araucaria angustifolia* plantations in the Atlantic Forest, Argentina. *Canadian Journal of Forest Research*, 54(1), 1–11.

Michelot-Antalik, A., Granda, E., Fresneau, C., & Damesin, C. (2019). Evidence of a seasonal trade-off between growth and starch storage in declining beeches: assessment through stem radial increment, non-structural carbohydrates and intra-ring $\delta^{13}C$. *Tree Physiology*, 39(5), 831-844.

Miyahara, A. A. L., Wild, T., Sandre, A. A., Pellegrino, P. R. M., da Silva Filho, C. A., Buckeridge, M. S., & Locosselli, G. M. (2022a). Developing and classifying urban biomes as a basis for nature-based solutions. *Urban Climate*, 45, 101251.

Miyahara, A. A. L., Paixão, C. P., dos Santos, D. R., Pagin-Cláudio, F., da Silva, G. J., Bertoleti, I. A. F., de Lima, J. S., da Silva, J. L., Candido, L. F., & Siqueira, M. C. (2022b). Urban dendrochronology toolkit for evidence-based decision-making on climate risk, cultural heritage, environmental pollution, and tree management–A systematic review. *Environmental Science & Policy*, 137, 152–163.

Morales, M. S., Cook, E. R., Barichivich, J., Christie, D. A., Villalba, R., LeQuesne, C., Srur, A. M., Ferrero, M. E., Gonzáles-Reyes, A., Couvreux, F., Matskovsky, V., Aravena, J. C., Lara. A., Mundo, I. A., Rojas, F., Prieto, M. R., Smerdon, J. E., Bianchi, L. O., Masiokas, M. H., Urrutia-Jalabert, R., Rodriguez-Catón, M., Muñoz, A. A., Rokas-Badilla, M., Alvarez, C., Lopez, L., Luckman, B. H., Lister, D., Harris, I., Jones, P. D., Williams, A. P., Velazquez, G.,

Aliste, D., Aguilera-Betti, I., Marcotti, E., Flores, F., Muñoz, T., Cuq, E., & Boninsegna, J. A. (2020). Six hundred years of South American tree rings reveal an increase in severe hydroclimatic events since mid-20th century. *Proceedings of the National Academy of Sciences*, 117(29), 16816-16823.

Moser-Reischl, A., Rahman, M. A., Pauleit, S., Pretzsch, H., & Rötzer, T. (2019). Growth patterns and effects of urban micro-climate on two physiologically contrasting urban tree species. *Landscape and Urban Planning*, 183, 88-99.

Muangsong, C., Pumijumnong, N., Cai, B., Buajan, S., Lei, G., Wang, F., Li, M., & Payomrat, P. (2020). Effect of changes in precipitation amounts and moisture sources on inter-and intra-annual stable oxygen isotope ratios ($\delta^{18}O$) of teak trees from northern Thailand. *Agricultural and Forest Meteorology*, 281, 107820.

Mukherjee, S., Kalra, G., & Bhatla, S. C. (2025). Atmospheric nitrogen oxides (NOx), hydrogen sulphide (H_2S) and carbon monoxide (CO): Boon or Bane for plant metabolism and development?. *Environmental Pollution*, 125676.

Niklas, K. J., & Spatz, H.-C. (2010). Worldwide correlations of mechanical properties and green wood density. *American Journal of Botany*, 97(10), 1587–1594.

Olson, E. J., Dodd, J. P., & Rivera, M. A. (2020). *Prosopis sp*. tree-ring oxygen and carbon isotope record of regional-scale hydroclimate variability during the last 9500 years in the Atacama Desert. *Palaeogeography, Palaeoclimatology, Palaeoecology*, 538, 109408.

Rahman, M. A., Armson, D., & Ennos, A. R. (2015). A comparison of the growth and cooling effectiveness of five commonly planted urban tree species. *Urban Ecosystems*, 18, 371-389.

Rambhia, M., Volk, R., Rismanchi, B., Winter, S., & Schultmann, F. (2023). Supporting decision-makers in estimating irrigation demand for urban street trees. *Urban Forestry & Urban Greening*, 82, 127868.

Resende, A. F., Piedade, M. T., Feitosa, Y. O., Andrade, V. H. F., Trumbore, S. E., Durgante, F. M., Macedo, M. O., & Schöngart, J. (2020). Flood-pulse disturbances as a threat for long-living Amazonian trees. *New Phytologist*, 227(6), 1790-1803.

Roden, J., Saurer, M., & Siegwolf, R. T. (2022). Probing Tree Physiology Using the Dual-Isotope Approach. In *Stable Isotopes in Tree Rings: Inferring Physiological, Climatic and Environmental Responses* (pp. 463-479). Cham: Springer International Publishing.

Schöngart, J. (2008). Growth-Oriented Logging (GOL): A new concept towards sustainable forest management in Central Amazonian várzea floodplains. *Forest Ecology and Management*, 256(1-2), 46-58.

Stahle, D. W., Cook, E. R., Burnette, D. J., Villanueva, J., Cerano, J., Burns, J. N., Griffin, D., Cook, B. I., Acuña, R., Torberson, M. C. A., Szejner, P., & Howard, I. M. (2016). The Mexican Drought Atlas: Tree-ring reconstructions of the soil moisture balance during the late pre-Hispanic, colonial, and modern eras. *Quaternary Science Reviews*, 149, 34-60.

Steenberg, L. W. N., Millward, A. A., Duinker, P. N., Nowak, D. J., & Robinson, P. J. (2015). Neighborhood-scale urban forest ecosystem classification. *Journal of Environmental Management*, 163, 134-145.

Stewart, G. H., Meurk, C. D., Ignatieva, M. E., Buckley, H. L., Magueur, A., Case, B. S., Hudson, M., & Parker, M. (2009). Urban biotopes of Aotearoa New Zealand (URBANZ) II: Floristics, biodiversity and conservation values of urban residential and public woodlands, Christchurch. *Urban Forestry & Urban Greening*, 8, 149-162.

Sukopp, H., & Weiler, S. (1988). Biotope mapping and nature conservation strategies in urban areas of the Federal Republic of Germany. *Landscape and urban planning*, 15(1), 39-58.

van Duong, D., Schimleck, L., & Lam Tran, D. (2023). Variation in wood density and mechanical properties of Acacia mangium provenances planted in Vietnam. *Journal of Sustainable Forestry*, 42(5), 518-532.

Wei, Z., Lee, X., Liu, Z., Seeboonruang, U., Koike, M., & Yoshimura, K. (2018). Influences of large-scale convection and moisture source on monthly precipitation isotope ratios observed in Thailand, Southeast Asia. *Earth and Planetary Science Letters*, 488, 181-192.

Xu, C., Zheng, H., Nakatsuka, T., Sano, M., Li, Z., & Ge, J. (2016). Inter-and intra-annual tree-ring cellulose oxygen isotope variability in response to precipitation in Southeast China. *Trees*, 30, 785-794.

Yakir, D. (2011). The paper trail of the ^{13}C of atmospheric CO_2 since the industrial revolution period. *Environmental Research Letters*, 6(3), 034007.

Yilmaz, B., Gülez, S., Kaya, G. (2010). Mapping of biotopes in urban areas: a case study of the city of Bartin and its environs, Turkey. *Scientific Research & Essays*, 5(4), 352-365.